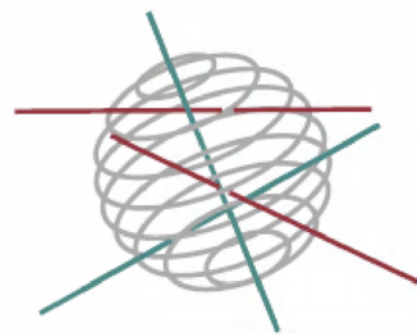# SSD

SCIENCE FOR A SUSTAINABLE DEVELOPMENT

"QUANTIFICATION OF EROSION/SEDIMENTATION TO TRACE THE NATURAL FROM THE ANTHROPOGENIC SEDIMENT DYNAMICS"

«QUEST4D»

Van Lancker V, Du Four I, Degraer S, Fettweis M, Francken F, Van den Eynde D, Devolder M, Luyten P, Monbaliu J, Toorman E, Portilla J, Ullmann A, Verwaest, T, Janssens J, Vanlede J, Vincx, M, Rabaut M, Houziaux J.-S, Mallaerts T, Vandenberghe H, Zeelmaekers, E, & Goffin A

ATMOSPHERE AND TERRESTRIAL AND MARINE ECOSYSTEMS

.be

SCIENCE FOR A SUSTAINABLE DEVELOPMENT (SSD)

North Sea

FINAL REPORT PHASE 1

QUANTIFICATION OF EROSION/SEDIMENTATION TO TRACE THE NATURAL FROM THE ANTHROPOGENIC SEDIMENT DYNAMICS "QUEST4D"

SD/NS/06A

Van Lancker V, Du Four I, Degraer S, Fettweis M, Francken F,

Van den Eynde D, Devolder M, Luyten P, Monbaliu J, Toorman E,

Portilla J, Ullmann A, Verwaest, T, Janssens J, Vanlede J, Vincx M,

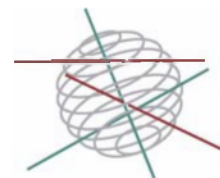Rabaut M, Houziaux J.-S, Mallaerts T, Vandenberghe H,

Zeelmaekers E, Goffin A

UNIVERSITEIT GENT — RCMG — KATHOLIEKE UNIVERSITEIT LEUVEN — flanders HYDRAULICS RESEARCH — Mariene Biologie Universiteit Gent — museum

Van Lancker V, Du Four I, Degraer S, Fettweis M, Francken F, Van den Eynde D, Devolder M, Luyten P, Monbaliu J, Toorman E, Portilla J, Ullmann A, Verwaest, T, Janssens J, Vanlede J, Vincx M, Rabaut M, Houziaux J.-S, Mallaerts T, Vandenberghe H, Zeelmaekers E, Goffin A, *QUantification of Erosion/Sedimentation patterns to Trace the natural versus anthropogenic sediment dynamics* "QUEST4D". Final Report Phase 1. Brussels : Belgian Science Policy 2009 – 135 p. (Research Programme Science for a Sustainable Development)

Table of content

Summary

Introduction

Sustainable development requires the quantification of human impacts, against the seafloor's ecological value. Recent impact studies have shown only localised effects, though indications of a longer-term and broader-scale degradation of the seafloor exist. This is due possibly to cumulative anthropogenically-induced effects, but the natural evolution and the response of the seafloor due to sea-level rise are poorly known. Nonetheless, it is likely that changing wave climate and an increased storminess induce different erosion/sedimentation patterns. Such evolution needs to be disentangled against the impact of dredging, aggregate extraction, fisheries and beach replenishment on the ecosystem's physical functioning.

The Belgian part of the North Sea (BPNS) is targeted for the reconstruction of seabed ecosystem changes over the past 150 years. Spatially and temporally extensive data sets have been compiled and allow studying various ecosystem components in the space, time and depth domain. Particularly, sediments and sediment transport processes have been studied, given their central role in ecosystem studies. Long-term ecosystem changes have been investigated, starting from a historical data-set on benthos and sediments, dating back to the first decade of the 20th century (the "Gilson collection"). Together with long-term datasets in the period 1866-2008, changes in bathymetry, sediments and macrobenthos were studied. Modelling tools have been refined with the aim of using them for dedicated case studies in phase 2 of the project. Natural changes were studied, based on observations and on climate change models. Quantification of human impact has been performed at sites, where long-term datasets were available.

The research strategy consisted of extensive GIS analyses, state-of-the-art observations/sampling (RV Belgica), experiments and advanced modelling, within the space, depth and time domain (4D). A multi-sensor tripod, a.o. measuring turbidity, currents and in-situ particle size is deployed on a quasi-permanent time-scale. Parameters are measured in function of model improvement, and observations are made to test hypotheses on seabed nature and dynamics, often in a multidisciplinary context.

The ecosystem in the space, time and depth domain

Generally, the BPNS is a typical sandbank-swale environment; though the coastal zone comprises large mud fields, often associated with highly turbid waters. Apart from hydrodynamics, origin of water masses, waves and bed composition, it has been shown that the occurrence of mixed sediments and their variability, the effects of waves on the failure of consolidated mud beds and the erosion effects of sand on top of consolidated mud are main drivers of sediment transport in the coastal zone. The formation of high concentration mud suspensions (HCMS), during storm periods has probably a major influence on the transport of suspended particulate matter (SPM) and on the deposition of mud in (mainly) navigation channels and harbours; hitherto never investigated.

Human activities are well-spread in the coastal zone (e.g. harbour extension works, dredging and disposal of dredged material, deepening of navigation channels, aggregate extraction); as such a good understanding is needed on non-cohesive and cohesive sediment dynamics and their interaction (deposition and erosion). Flocculation is an important process and still requires field-based measurements and calibration to improve numerical modelling of sediment transport. Sediment erodibility is a major issue, since the coastal zone comprises mud with variable degrees of consolidation that is eroded and deposited according to the prevailing hydro-meteorological agents. Measurements have shown that the critical shear stress for erosion increases rapidly with depth; hence mud erosion is mostly a surface phenomenon; however under storm conditions consolidated mud layers can be eroded.

The provenance of mud in the coastal zone has always been enigmatic. A turbidity maximum area extends roughly from the Westerschelde estuary to Ostend. Especially, in this area, several mud types exist of various ages and often Holocene to older mud layers are outcropping. Mud provenance was studied using detailed qualitative and quantitative analyses of the bulk and clay mineralogy of mud and their potential source areas. The results show that the clay mineralogy of the Holocene, modern and recent mud and SPM is identical. A very similar clay assemblage is found in the Scheldt river (Estuary and further upstream) and the Rupel river. These results indicate a close provenance relationship between the BPNS and sediments transported by the Scheldt. On the other hand, potential source areas that could be excluded as major sources of BPNS mud include the Dover Strait coasts, the Eocene and Pleistocene glacial deposits, currently exposed on the BPNS sea floor and suspension from the Atlantic Ocean. A similar to almost identical clay mineralogy was determined, respectively, for Holocene salt marsh deposits and Eemian interglacial deposits, sampled near the present-day coastline; this suggests that a provenance relationship between BPNS mud and the Scheldt river system has existed on and off since the Late Pleistocene.

Sedimentation/erosion patterns have been studied also, on the basis of time-series of very-high resolution multibeam bathymetry and sonar imagery. Especially, near the main disposal ground of dredged material, complex sediment transport processes occur. Important bedload transport rates and sand dune migration are identified, completely opposite to the residual currents and suspension transport. These observations are important in view of recirculation of dredged material, hence will allow future optimisation of dredging/disposal activities. Nearby the disposal ground, hotspots of biodiversity are found, in the troughs of sand dunes. Aggregations of the polychaet 'Owenia fusiformis' here occur; in these areas bedforms do not migrate, whilst outside of these patchy areas, a dune migration rate of 20m is observed. It is not clear yet whether these patches are associated with the disposal ground or with higher nutrient supply from the Westerschelde estuary.

Long-term ecosystem changes

The Gilson collection (1899-1908) provided a unique opportunity to investigate how physical and biological processes have changed over the whole 20th century. Sediment and benthos data were obtained with dedicated sampling gears, operated sequentially within dense sampling grids. The dataset has been reconstructed enabling investigation of baseline relationships between benthic communities and seafloor composition. Sampling procedures and data quality issues were clearly identified, providing robust data for further analysis.

Historic sediment type maps were constructed, based on Gilson's sediment sample descriptions. Further to prior digitizations, Gilson's benthos archive was now completed with bivalves, polychaetes and amphipods. "Baseline maps" of benthos composition (species richness, total abundances) were drawn and provide a coherent picture of the former distribution of benthic biodiversity alongside the Belgian and Dutch coastal zone and in the surroundings of the Westhinder sand bank. Linking macrobenthic and sediment data will further enable to determine whether some ecological structure can be found in this century-old "new" sub-regional species assemblage.

The distribution of bivalves was further explored and compared to the present-day distribution (1994-2008, UG-ILVO database). Changes were attributed to long-term patterns in the North Atlantic Oscillation (NAO), since the bulk of both data-set had indeed been collected under opposite winter NAO conditions. All observed species distribution shifts match the expectations of altered physiographic conditions, due to NAO. On the BPNS, processes related to turbidity and sedimentation/re-suspension are important, and the very coastal waters to the West experience contrasting patterns of salinity, under prolonged episodes of positive or negative NAO conditions. The latter effect, clearly tracked in euryhaline benthos data, reflects increased river runoffs (due to NAO-induced increased precipitations over NW Europe). Both effects are

imposed by highly positive NAO values, especially since the regime shift of 1988. The very different pattern displayed by the historic data, prior to 1903, seems to mirror 30 years of sustained negative NAO conditions. Results urge for a re-examination of variations in datasets, due to NAO cyclicity and their shifts. Especially, the overall turbidity and siltation increase of Belgian coastal waters needs verification against varying river discharges, resulting from NAO cyclicity.

Long-term analyses were performed on bathymetry datasets in the period 1866-2007. No significant movement of the sandbanks could be demonstrated, though some banks had variable patterns of erosion and deposition, with the Flemish Banks showing accretion along their SW extremity, and erosion along their NE part. The troughs in-between banks experienced erosion mainly, resulting in steeper slopes of the banks. In the coastal zone, a sedimentation trend seems to dominate, with particular accretion of sediments in the Grote Rede swale, landward of the Wenduine Bank. From the analyses of long-term sediment changes, this would correspond with mud deposition. Apart from human-induced, localised, sediment changes (e.g. disposal grounds of dredged material), no wide-spread changes in median grain-size could be deduced. However, a major change is seen in the sorting of the sandy sediments over the past 100 yrs. All of the Gilson samples that were re-analysed, were well-sorted, whilst recent samples are predominantly moderate to poorly-sorted. The cause of this worsening in sorting is associated with enrichment of fine sandy sediments, as shown by the skewness value of the recent sediments. Their spatial occurrence is mostly linked to harbour areas, disposal grounds, and aggregate extraction sites; though the trend is also observed in the so-called 'natural systems'. A possible link with NAO or other cyclicity should be investigated.

Modelling of processes

For predictions and more integral impact assessments, modelling is a prerequisite. However, the complexity of the BPNS seabed nature and dynamics requires refined modelling, ideally calibrated and validated with observations and measurements. Improved bed models are being designed to account for erosion of old sediments (Holocene and outcropping Tertiary clays) distinguishing between active layers and more passive buffer or parent layers. It has been shown that classical flocculation models, based on an empirical approach, are not able to satisfactorilly reproduce measurement data and required a better understanding of SPM dynamics. To study its implications in coastal morphodynamics, both the mineral, as well as the microbial fraction needs consideration. Since, these are strongly site-specific, this information should be acquired at the same moment.

A major issue remains the influence of the Westerschelde estuary on the sediment- and morphodynamics of the BPNS and vice versa. Especially, cross-border mud transport is highly sensitive internationally and has led to numerous studies. Mud balances, computed by modelling, result in a yearly net export of 2 Mton from the Scheldt estuary, being still one order of magnitude larger than the net import, following from mud balances, based on observations. Exact numbers from observations remain associated with large uncertainties and are not well known; estimates range from 0.05 to 0.35 Mton yearly net import. Since it appears that the model's concentration gradient between the inner and outer estuary of the Scheldt is realistic, the computed export might be due to an underestimation of the estuarine circulation and the observed phase error of the M4 tidal component. The latter influences the tidal asymmetry and thus also the residual sediment transport. Further verifications are needed.

Finally, wave turbulence and wave energy dissipation, and their importance in the turbulence part of hydrodynamic models are being modelled. Therefore a coupled wave-current model has been implemented and tested on High Performance Computer facilities. This will enable a more sound modelling and interpretation of current field (including turbulence) measurements and its consequences for SPM modelling. The model suite will later be used for specific case studies.

Natural evolution and climate change

To interpret changes in the marine environment or to assess human impacts adequately, knowledge on the natural variability of seabed processes is needed. Especially sandbank areas are prone to variation and storms can have major impacts on sediment volume changes. This was investigated for a sandbank area, without human impact, where a series of bathymetric data were available. From a correlation of sediment volume changes with the directionality and strength of winds, waves and currents, it was shown that prolonged northeastern conditions are associated with the lowest sediment budgets, whilst those from the southwest are clearly associated with a sediment input. The spatial validity of these findings needs further investigation, though useful repetitive bathymetric time series are generally very scarce.

The influence of storms on SPM concentration has been studied also. Here, the direction of wind, wave height and availability of erodible cohesive sediments are crucial. It is argued that local mud sources, such as mud in sandy beds or consolidated mud layers, have to exist, besides the well-known and generally accepted English Channel, as major source of SPM.

For the study of the influence of climate change on seabed processes, a dedicated investigation was set-up. It has been shown that high sea surges along the Belgian coast occur when a low pressure system remains stationary over the Baltic Sea and is associated with a reinforced Azores high. This sea-level pressure (SLP) pattern shows a strong Southwest-Northeast pressure gradient leading to onshore winds along the Belgian coast. Wintertime highest sea surges (99th percentile) at Ostend have increased at a rate of + 1 mm/yr from 1925 to 2000. This increase is associated with the SLP rise over the Azores leading to an increase of the frequency of strong surge-related pressure gradient. A statistical downscaling method is used to set-up a model to relate SLP to sea surge at Ostend. A multiple linear regression is designed to relate the daily surge height at Ostend with (i) the daily SLP over the Baltic Sea; and (ii) the daily value of the pressure gradient between the Baltic Sea and the Azores. This regression robustly reproduces the interannual to long-term variability of high surges at Ostend. The regression is then used with SLP time series simulated until 2100 under climate change scenarios. High surges are expected to stay stationary during the 21st century, associated with no significant changes in SLP conditions over the Baltic Sea and over the Azores. It is not expected that climate change for the 21st century would significantly modify surge and wave-related atmospheric circulation. Nevertheless, the mean sea-level rise, associated thermal dilatation and ice melting, will ineluctably increase the amplitude of sea level peaks during storm events. Possible links between hydro-meteorological parameters (storm-surges, waves) and beach and foreshore sediment volumes for the Belgian coast will be investigated.

Impact of human activities

Finally, case studies were selected where the impact of human activities is known, however now attempting to quantify changes on the long-term.

A good example is the long-term effect of the harbour extension works of Zeebrugge, which has impacted the area just east of it, the 'Bay of Heist'. A strong sedimentation trend (in the form of a sandbank) was revealed in the bay itself, but also in a zone parallel to and some 100m away from the eastern groyne of the harbour. The former results from low flow velocities, due to the sheltering effect of the eastern groyne; whilst the latter sedimentation pattern is due possibly to the wave attenuation effect of the eastern groyne. Sedimentation trends are predicted aiding future management of the area.

Natural from anthropogenically-induced sedimentation was studied on the main disposal ground of dredged material (Vlakte van de Raan, B&W S1). A clear difference is observed in sedimentation patterns between the old and present disposal site of dredged material, respectively on a sand shoal and in a gully. This shows the importance of morphological setting

for the final estimation of impacts; however, also the type of disposed material will determine recovery rates after cessation of activities. Sediment transport processes in this area are complex, and need further investigation to get a better insight in the consequences of the long-term disposal of dredged material in near coastal areas.

On a larger scale, long-term changes in the cohesive sediment distribution of the Belgian–Dutch nearshore zone have been correlated with the increase of maritime access works. Conclusions were made on the basis of changes in the distribution of fresh mud and increase of suspended sediment during the last 100 years. The possible fingerprint of NAO cyclicity needs further investigation.

Finally, the need emerged to quantify the extent of beam trawling activities on the BPNS. Fisheries activities remain the most frequent disturbers of the seafloor, yet hitherto their spatial extent is never investigated. Generally, fishing activities occur in the swales of sandbanks mainly, with highest concentration towards the foot of the steep slope of the sandbanks. For the first time, this disturbance is quantified and demonstrated along two sandbank areas. A methodology is now in place to evaluate the impact of beam trawling on a large-scale; this can be applied whenever new high-resolution and good quality multibeam backscatter data are available. These data are crucial in the evaluation of long-term changes in soft-substrata habitats.

1.   INTRODUCTION

1.1   Context

Seabed, living and non-living resources are exploited increasingly: sand and gravel is needed for beach nourishment and for construction purposes, the accessibility of harbours requires regular dredging and disposal operations, offshore windmills contribute to our future energy supply and pipelines and cables transport gas and electricity to the mainland. The interaction of these activities with the seabed nature and processes needs careful consideration. However, present-day impact studies remain often inconclusive because of: the lack of a 'non-disturbed' reference situation, the interference of both naturally and anthropogenically-induced changes and, the hitherto unknown, role of climate change on seabed processes. Moreover, the range of human activities may result in cumulative effects affecting the magnitude and extent of the impact on the seabed. A sustainable management, based on an overall marine environmental status and its possible degradation, is therefore needed. Setting-up environmental targets and well-balanced monitoring programs have become timely. These will help in protecting and preserving the marine environment and safeguard our seas for future generations.

1.2   Objectives and expected outcomes

Quest4D targets the Belgian part of the North Sea (BPNS) to reconstruct seabed ecosystem changes in the past 100 years. This becomes feasible since extensive data have become available on the seabed nature and processes. The datasets are unique in Europe and allow going beyond traditional research. Throughout the reconstruction, case studies will be built and impacts will be modelled, relating seabed changes to both naturally and anthropogenically-induced sediment dynamics. Furthermore, climate change scenarios will be modelled and their consequences on the management of the seabed will be estimated. A significant increase in knowledge on the sediment and sediment transport system is thus expected, which is key to any ecosystem or impact study. Final results will contribute to the development of more sustainable exploitation strategies of non-living seabed resources.

Expected outcome:
A Geographic Information System and **databases** containing multidisciplinary information on the seabed of the Belgian Continental Shelf, including various human impacts of the last 100 years and a historic reference situation of 1900.
Models, in which the nearshore-shelf is coupled to the coast and Scheldt-estuary to address the sand and mud balance and idealised models to be used in impact assessments;
Parameters to be used in climate change studies;
Case studies on the effect of fisheries, aggregate extraction and long-term disposal of dredged material on the seabed;
Management tools (e.g. indicators) for a sustainable development / exploitation, including recommendations.
Publication of the main results in peer-reviewed journals and presentations at dedicated fora; for the public at large, leaflets, a set of animations and posters will be produced.

2. THE ECOSYSTEM IN THE SPACE, TIME, DEPTH DOMAIN

2.1 Sediments and sediment transport

2.1.1 Cohesive, non-cohesive and mixed sediments on the BPNS

Assessing the effects of anthropogenic impacts, such as harbour extension, dredging and disposal works, deepening of navigation channels and aggregate extraction, is becoming important increasingly and more accurate means of predicting the consequences are needed. An important aspect is the influence of mud content on the transition between cohesive and non-cohesive behaviour of sediments and thus on the erosion and transport of them. The mutual interaction of cohesive and non-cohesive sediments on the erosion behaviour occurs in different ways: sand movement on top of a cohesive substrate; failure of cohesive sediment bed due to wave action, this may result in the formation of mud pebbles (Jacinto & Le Hir, 2001),; and erosion of mixed sediments. Fine sediments (mud, clay) are found frequently in the Belgian nearshore zone. They are of different age and have thus a different consolidation, ranging from fluid mud to Tertiary clays. Mixed sediments, mud pebbles and thin layers of sand on top of consolidated mud occur frequently (Fettweis et al., 2007b, Fettweis et al., 2009). This, together with the observation of high concentration mud suspensions (HCMS, see long-term measurements below), indicates that these three types of erosion of mixed sediments are of importance on the BPNS. Up to now only few transport models have been set-up which have implemented sand-mud processes, using separate equations for sand and mud and include mutual interactions between both sediment types, see Van Ledden (2002) and Waeles et al. (2007). Both models treat mixed sediments, but they do not include erosion processes, induced by sand on consolidated mud or massive failure of consolidated beds, due to wave erosion. The latter processes could possibly explain the very high suspended sediment concentration, which have been measured during storm conditions.

Figure 1 gives an overview of site-specific measurements.

2.1.2 Erodibility measurements

Measurements of the critical shear stress for erosion $\tau_{e,crit}$ were carried out with the SETEG-system, a unique erosion flume developed at the University of Stuttgart and with a CSM (cohesive strength meter).

A typical result from the SETEG measurements is shown in Figure 2. From the variation of the wet bulk density and of $\tau_{e,crit}$ with depth, mostly a similar pattern can be derived: at the surface, $\tau_{e,crit}$ is rather low (typical values between 0.3-1.0 Pa), but increases rapidly after a few cm, up to values of several Pa (max of 13 Pa); suggesting that the underlying layers are more consolidated. For comparison: a typical value of $\tau_{e,crit}$ for mud, used in numerical models of the BPNS, is 0.5 Pa. Some cores also exhibit a large variation of both $\tau_{e,crit}$ and bulk density, indicating the presence of different layers in the sample. Some samples seem to indicate a positive correlation between the bulk density and $\tau_{e,crit}$, although some show no correlation at all, indicating that other parameters (e.g. grain-size, POC) might influence the results. When only recent mud is considered (categorization was made on a visually and on a density value below 1.5 g/cm³ (Fettweis et al., 2007b), an average bulk density of 1.3 ± 0.1 g/cm³ is found, and an average $\tau_{e,crit}$ of 1.9 ± 0.9 Pa, showing that recent mud can be resuspended easiliy. The SETEG flume is capable also of measuring the erosion rate $\dot{M}$ (kg/m²/s): a system of laser lines monitors the volume of the eroding sediment, out of which mass erosion rates can be calculated, in combination with the density profile.
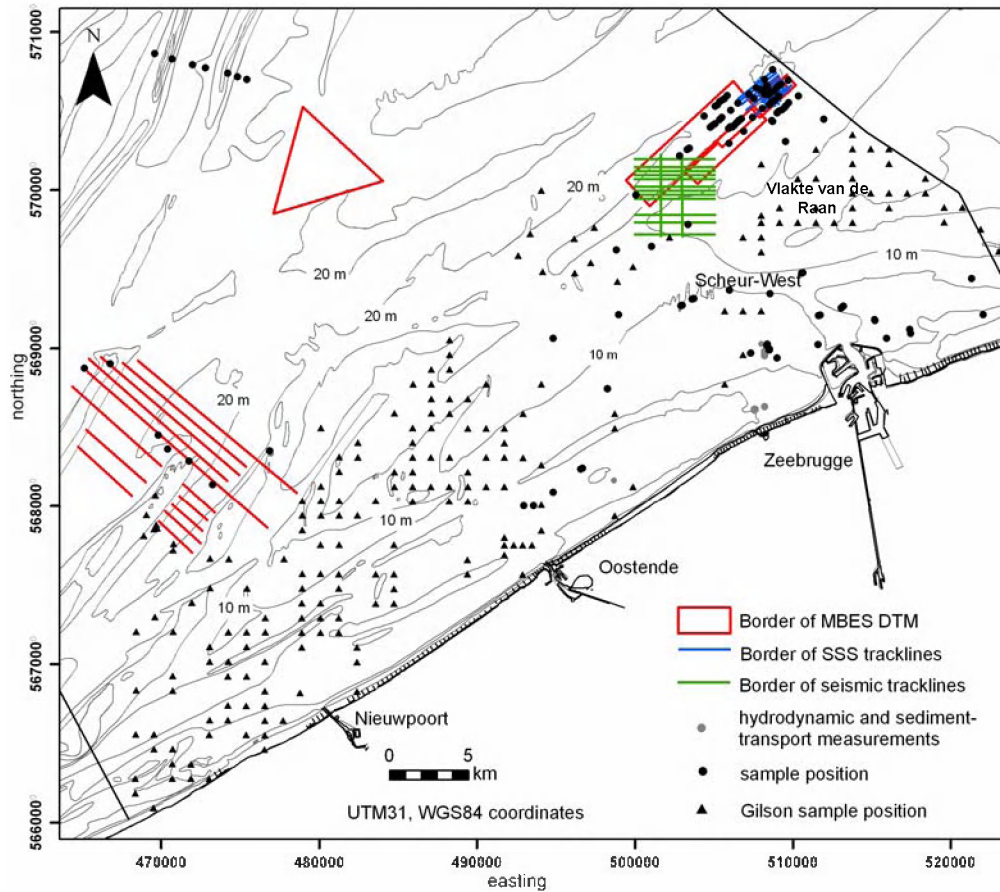
Figure 1.   Overview of the QUEST4D retrieved/analysed data.
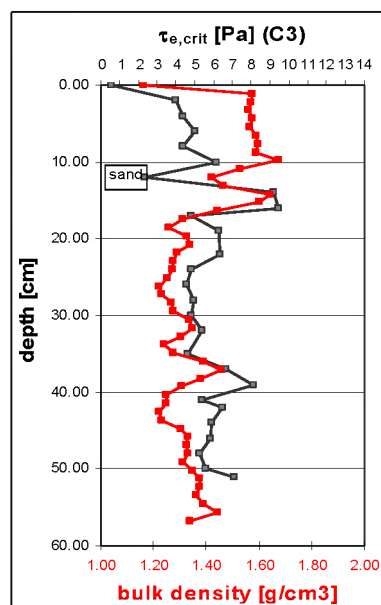

Figure 2.   Bulk density and the critical shear stress for erosion using the SETEG system.

Erosion rate measurements have been performed at certain depths in several subsamples (see Figure 3). Note that many numerical models use a linear dependency of the erosion rate on the shear stress exerted by the flow:

$$\dot{M} = E \cdot \frac{\tau - \tau_{e,crit}}{\tau_{e,crit}}$$ in which E is the erosion rate, M the eroded mass, □ the bed stress. Following this linear dependency, erosion rates should be on a straight line, with a slope equal to $E/\tau_{e,crit}$. It is observed that some sets of data points seem to exhibit this linear behaviour, although others seem to exhibit no trend at all. The latter is on the one hand due to uncertainties, inherent in measuring the erosion rates; on the other hand to the premise of linear behaviour, which is not always a valid approximation.
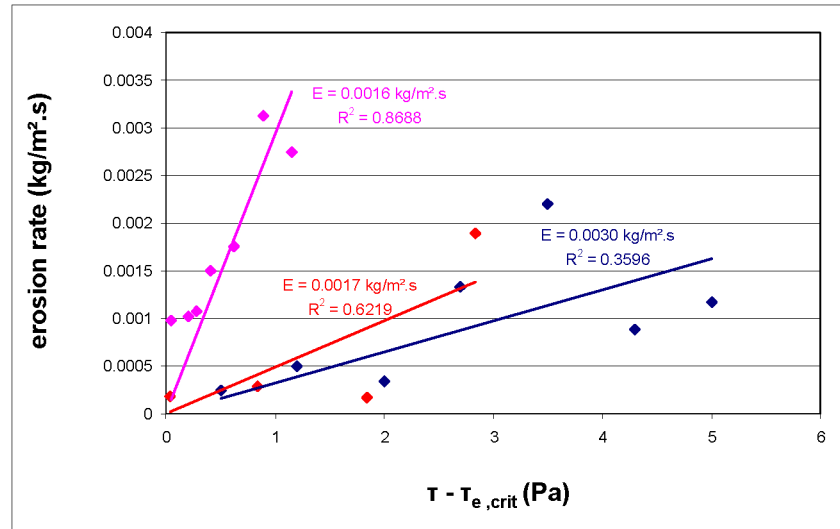
Figure 3.   Some results of the erosion rate measurements.

Additional sedimentological parameters were measured (WL): wet bulk density, critical shear stress for erosion $\tau_{e,crit}$ with the CSM, grain size distribution, and total organic carbon content (TOC). The fact that the WL and Stuttgart measurements were performed on parallel, but not on the same subsamples and given the relatively large changes of the sedimentological parameters with depth makes it difficult to exactly correlate the parameters measured on both subsamples. Nevertheless, parameters measured on parallel subsamples can be plotted on the same graph to visually inspect possible correlations. An example is presented in Figure 4, which shows the wet bulk density of two parallel subsamples. In general bulk density profiles of subsamples show an overall good agreement, although at certain depths some small differences can appear. Figure 4 shows also the depth profiles of $\tau_{e,crit}$ of two parallel subsamples, determined with the CSM at WL and with the SETEG flume in Stuttgart. In general, there is very little or no similarity between $\tau_{e,crit}$ (CSM) and $\tau_{e,crit}$ (SETEG) depth profiles. The CSM, which has a working principle totally different from that of the SETEG flume (a water jet pulse is vertically fired onto the sediment surface with increasing pressure until the onset of erosion is observed) and has a much smaller footprint than the SETEG flume (a few cm2 for the CSM, ~ 100 cm2 for the flume) is probably not suitable for the measurement of $\tau_{e,crit}$ of North Sea mud, and probably not even suitable to provide relative measures of the erosion stability.

Correlations between sedimentological parameters have been set-up between grain-size distribution, wet bulk density and TOC. Only one strong relation was observed, namely between the mud fraction and TOC (determined through measurement of loss-on-ignition, see Borovec, 1996). A strong correlation was found between the logarithm of the TOC and mud fraction (R^2 = 0.80, Figure 5). A weak correlation was found between mud fraction and bulk density (R^2 = 0.44, Figure 6). Because of the strong relation between TOC and the mud fraction, a weak correlation could consequently also be found between TOC and bulk density (R^2 = 0.42).
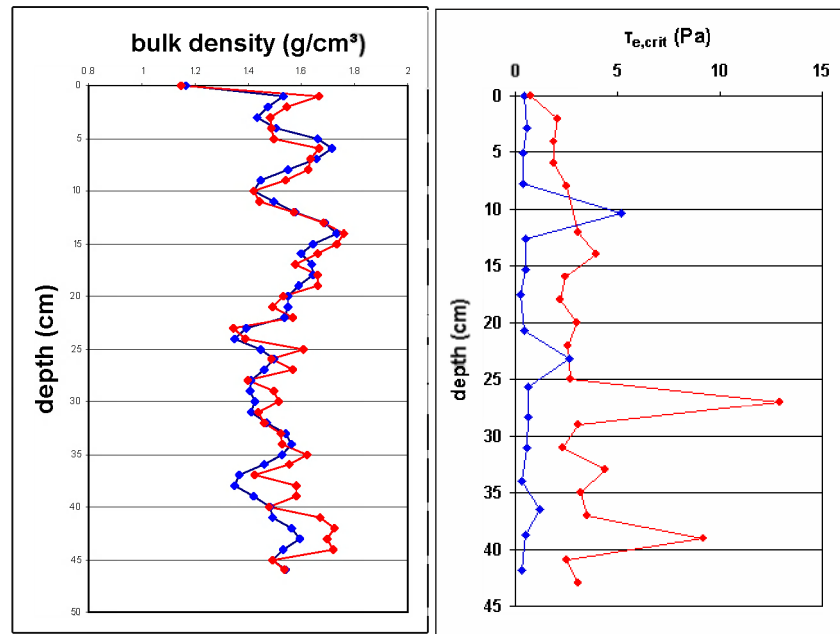
Figure 4.   Bulk density profiles (left) and critical shear stress for erosion (right)of 2 subsamples from the same boxcore. Blue: measured at WL ($\tau_{e,crit}$: CSM); red: University of Stuttgart ($\tau_{e,crit}$:.SETEG).
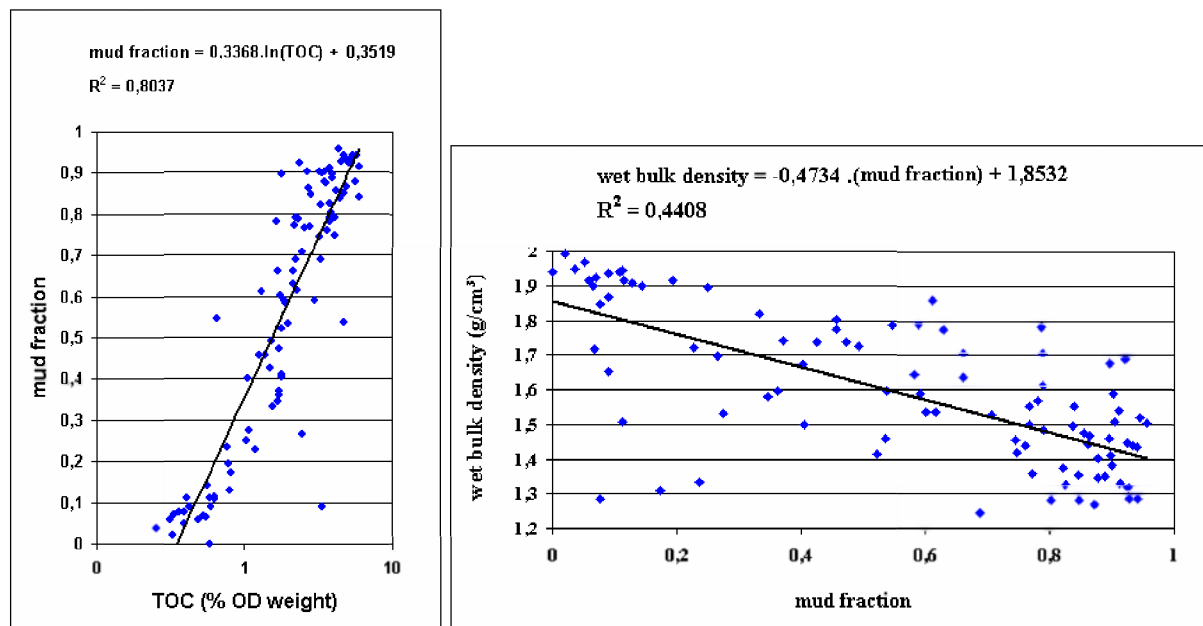
Figure 5.   Correlation between TOC and mud fraction (left) and mud fraction and wet bulk density (right) for all box-cores.

2.1.3   Provenance of BPNS mud

Clay minerals are a significant component of the mineralogy of BPNS mud and SPM. Therefore the provenance of BPNS mud was studied by detailed qualitative and quantitative analyses of the clay and bulk mineralogy of mud and compared to the same analyses on sediments of their potential source areas.

In a previous study (Fettweis et al., 2007b), an initial characterization of 120 BPNS bottom and suspension samples was undertaken. To validate the results of this study, an additional 38 bottom and suspension samples were analyzed (sampling by RV Belgica). Key information to be

derived from the current study is the determination of spatial patterns, present in the clay mineral distribution. Therefore all potential major source areas were extensively sampled (overview in Fontaine, 2004). For the Scheldt river, 18 bottom and suspension samples were taken between the harbour of Antwerp and its mouth. Further upstream, up to St. Amands, and from the Rupel tributary, 16 riverbank mud samples were taken. For the Dover Strait coasts, the sampling of beach sediments was deemed more important than outcrop sampling; the beach sediments representing the mixing of all locally available eroded sediments. A total of 28 beach and outcrop sediments were sampled along the French coast (between Dunkirk and the Somme Estuary) and along the English Coast (between Folkestone and Portsmouth). One suspension sample taken near the English coast (Thames Estuary) was analyzed. To evaluate the clay minerals transported to the BPNS from the Atlantic Ocean, four suspension samples from the Gulf of Biscay and The Channel were analyzed. To estimate the variation in clay mineralogical composition of marine bottom and suspension samples, also 6 samples from more distant locations (up to Norway and Portugal) were collected.

As detrital clay mineral associations can be expected to vary with changing palaeogeography and even because of human-induced changes in historical times (Brockamp & Zuther, 2004), clay mineral associations were determined for some major palaeogeographic situations during the Quaternary evolution of the North Sea and the Scheldt river system. This analysis allows for framing the mineralogy of the most recent BPNS sediments in a better perspective and for the evaluation of eventual reworking of older deposits as a source for the present-day BPNS mud. For the Holocene, 14 samples from salt marshes and intertidal flats were taken from cores, drilled in the present-day coastal area. Equivalents for Pleistocene deposits, outcropping on the BPNS seafloor, were taken in the Campine Basin (13 samples), the Roer Valley in the Netherlands (18 samples) and from various cover sands in Flanders (five samples). Also eight samples from intertidal flats from the Eemian interglacial were sampled in the near coastal area. Below the Quaternary seafloor cover, also Eocene and some Oligocene strata can be eroded; their clay mineralogy was evaluated, based on 95 samples taken from drill cores and quarries on land. In total 265 samples were analyzed.

The analyses are based on state-of-the-art standardized techniques and allow for the detection of mineralogical differences well below the resolution of other techniques. (Srodon et al, 2001; Omotoso et al, 2006). Bulk mineralogical analyses, combined with Cation Exchange Capacity (CEC) analyses, were carried out to determine absolute quantities of clay mineral groups. To determine the detailed clay mineralogy of the samples, the fractions $<2\mu$m and $<0.2\mu$m were extracted by high speed centrifugation after extensive pre-treatments (Jackson, 1975), removing cementing agents, such as carbonates, organic matter and Fe-(hydr)oxides. Oriented slides were made of these fractions in Ca-form and recorded by X-Ray Diffraction (XRD) in air-dry, glycolated and heated ($550°^C$/1h) state. Oriented slides were also made of K, Mg and Li saturated fractions and recorded under specific states ($300°^C$/1h and glycerol solvated). XRD powder scans were used to evaluate the clay mineral polytypes, using diagnostic peaks of their three dimensional diffraction patterns and the Al versus Fe content, using the 060 reflections (Moore & Reynolds, 1997). This set of analyses provides a detailed mineralogical (bulk and clay) 'fingerprint' of the analyzed samples. More details about the samples, the analysis techniques and the qualitative and quantitative results can be found in Annex I and the PhD of Zeelmaekers (available end of 2009).

The results show that the clay mineralogy of Holocene and recent mud is identical and consists of randomly interstratified (R0) mixed-layered illite-smectite, discrete illite, discrete smectite, kaolinite and minor amounts of chlorite and vermiculite. The clay mineralogy of suspension samples taken at or near the location of BPNS mud is identical. A very similar clay assemblage is found in the Scheldt river (Estuary and further upstream) and the Rupel river. These results indicate a close provenance relationship between the BPNS and Scheldt transported sediments. On the other hand, several potential sources areas could be excluded as major sources of BPNS

mud: (1) beach sediments of the British coasts were found to be distinctly different (more smectite and kaolinite, almost no chlorite and vermiculite); (2) beach sediments of the French coasts were found to be much more similar, but seem to differ in their detailed mineralogical features; (3) major contributions from Eocene (extremely smectitic) and most Pleistocene deposits (very variable clay mineralogy), currently exposed on the BPNS sea floor, can be excluded; and (4) the same conclusion holds for suspensions from the Atlantic Ocean (almost no smectite and mixed-layered illite-smectite).

Finally, a similar to almost identical clay mineralogy was determined, respectively for Holocene salt marsh deposits and Eemian interglacial deposits sampled near the current coastline; this suggests that a provenance relationship between BPNS mud and the Scheldt river system has existed on and off since the Late Pleistocene.

Theoretically, the large-scale mixing of some of the excluded potential source areas cannot be excluded without geochemical analyses, but the strong similarity in clay mineralogy between BPNS mud and the Scheldt river system, in present and past, suggests that the mixing hypothesis is unlikely.

2.1.4 Sedimentation/erosion patterns

Sedimentation/erosion patterns have been studied in the area north of the Vlakte van de Raan; including the disposal ground B&W S1, one of the main sedimentation areas on the BPNS (Figure 1). Side-scan sonar, multibeam and chrono-sequential single-beam echosounding data, together with Van Veen grab samples have been collected, processed and analysed in GIS. acoustic data revealed different sedimentation and erosion patterns, originating from natural processes and human-induced activities. Sedimentation is evident on the disposal ground itself, however, sediments also accumulate in a SW direction, backwards to the navigation channel. Bedload transport processes are consistently opposite to the NE directed residual currents and SPM transport. Results have been published and can be found in Du Four & Van Lancker (2008).

Towards the Dutch border, extensive small-scale sedimentation patches, formed by *O. fusiformis*, are present (Figure 6). This tube-building polychaet occurs in aggregations of up to 6000 tubes per m². They occupy areas of up to 12 km². The patches occur in-between large to very large dunes; which form sheltered conditions to the tubeworms. In contrast to other dunes in the area, devoid of dense aggregations, an overall stability of the bedforms is observed (Figure 7). Multibeam time series show that the patches are very stable, regardless the extensive fishing activities in the area. The results are submitted for publication (Rabaut et al., subm.).
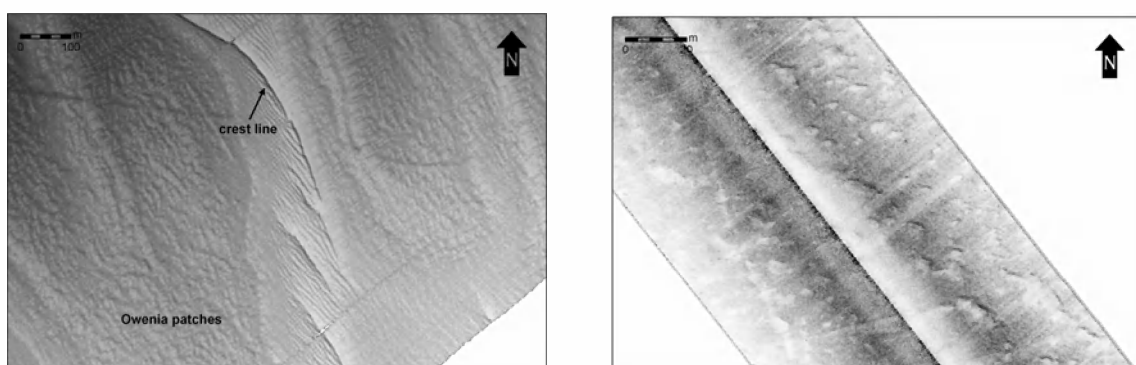
Figure 6.   (left) Detailed shaded relief map of an area with very large dunes; in the troughs extensive fields of *O. fusiformis* are present; and (right) detailed SSS mosaic showing individual *Owenia* patches.
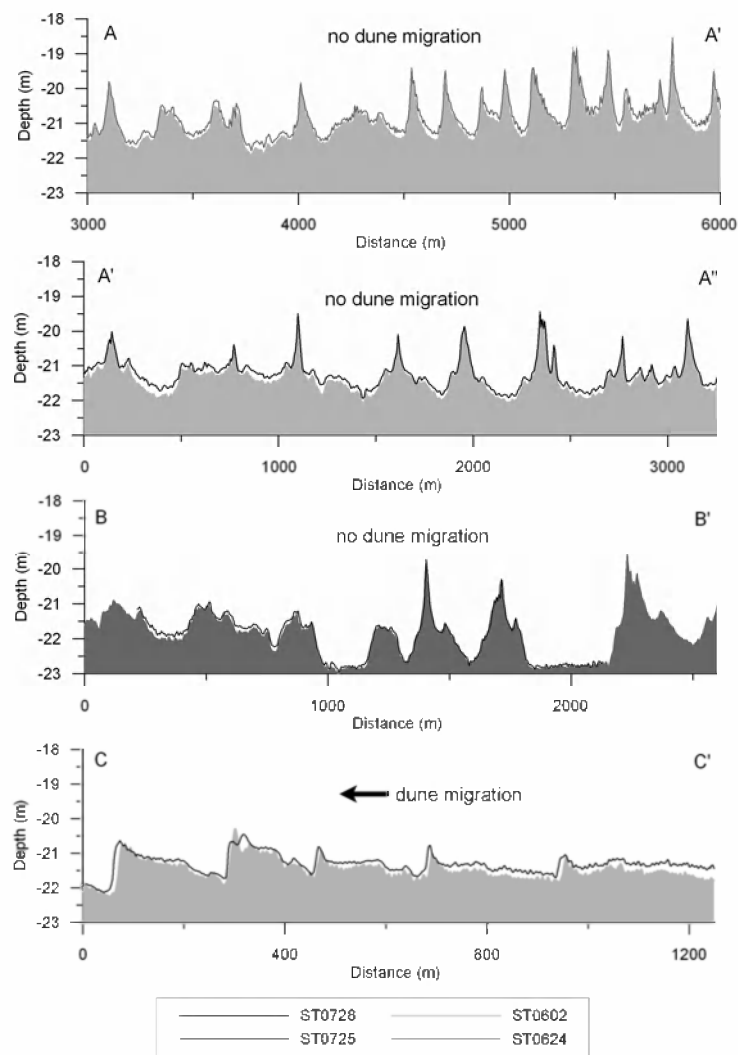
Figure 7. Cross-sections based on the DTMs of successive bathymetric surveys aligned transversally to the dunes. No dune migration is observed for the dunes stabilised by O. fusiformis bioherms, while the dunes which are not stabilised by O. fusiformis do migrate in a SW direction (up to 20m). Vertical scale x30 exaggeration.

2.2 Long-term ecosystem changes

2.2.1 Historic reference framework

The composition of benthic communities is dependent upon environmental conditions, of which sediment composition is an important factor. It is hypothesized that long-term changes in the composition of benthic communities will mirror changes in sediment composition and transport patterns. In the absence of historical data, such long-term trends can only be inferred, based on present-day knowledge and know-how. Uniquely for the BPNS, a historical baseline can be considered, based on the extensive collection of sediment and benthic invertebrates, collected by G. Gilson in the first decade of the 20th century. These data are digitized and verified at RBINS since 2001 (van Loen et al., 2002 and Houziaux et al., 2008). In QUEST4D, the investigation of soft sediment invertebrates were aimed at; these are well-sampled since the 1970s, whilst Houziaux et al (2008) studied hard substrate species on the basis of the same historic data-set.

1. Re-building a baseline reference sediment map for the period 1899-1910

The quality of the description-derived sediment parameters was controlled by grain-size analyses, of which results enabled to create baseline maps for major sediment types. The robust data, resulting from this quality-check, were plotted in an integrative map of sediment types (Figure 8). Details on these procedures and more information can be found in Annex II.
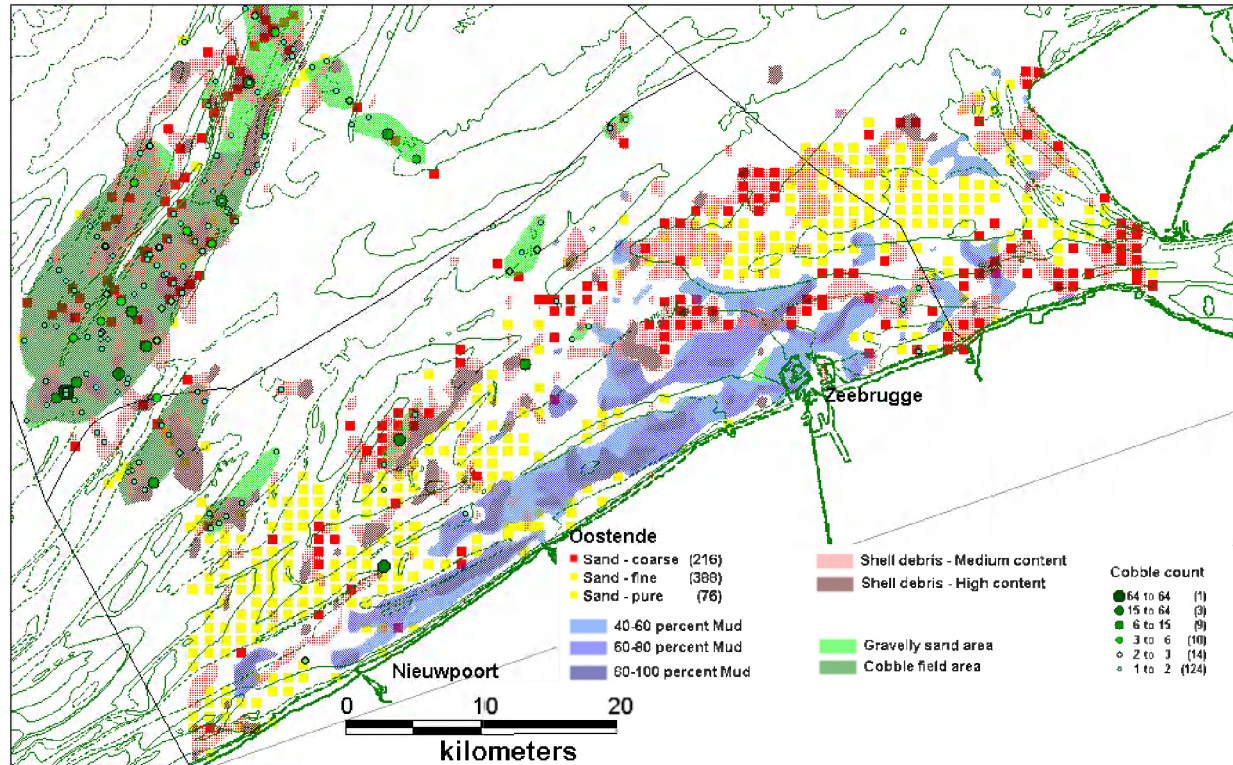
Figure 8.   Integrated sediment type map, based on Gilson's validated historic information on the seafloor of the BPNS (1899-1908, mainly).

2. Re-building the historic reference baseline for soft-bottom macrobenthos, ~1899-1910

The distribution of species richness and overall specimen abundance was mapped (Figure 9) following strict data selection criteria (Annex II). All species collected alive are taken into account at accurately geo-referenced sampling stations (suspect stations eliminated from the data-set to avoid interpolation bias). For colonial organisms (e.g. hydrozoans or bryozoans), abundances are replaced by presence/absence counts.

Overall species richness and specimen abundance show drastically differing patterns which only partly match the recent general descriptions of benthic biodiversity in the BPNS. In agreement with formerly obtained results (Houziaux et al, 2008), the Westhinder area hosts highest levels of benthic species richness, especially in the western and eastern gullies south to the kink area of the sandbank and the scarp in the gullies; here maximum amounts of cobbles were gathered as well. These stations appear as the core of the pebble community of gravels in the BPNS. Levels of species richness are minimum values that are likely to increase, if determinations at genus and family levels would be included. True species richness is thus expected to surpass the maximum value of 60 species, so far obtained.

High levels of richness are found also in patches along the northern tip of the 'Westhinder', around the 'Oosthinder' and southern (the Buyten ratel – Oostdijck gully) adjacent areas. Although much lower amounts of samples are available from the gullies located south to the Thornton, Goote and Akkaert banks, they also host high species richness, comparable with that

measured along the westernmost part of the coastal waters. To the East, some high values of species richness are also found along the Dutch coast of Walcheren (Deurloo and West-Kappelle channels).

Maximum amounts of benthic specimens were gathered at large, distinct patches at some 8-12 km off the coast from Ostend to the Dutch coast of Walcheren. At 2 stations, more than 10,000 living animals were found, being exceptional cases indicative of larger high density patches for the bivalves *Abra alba* (Off Zeebrugge) or *Donax vittatus* (off Ostend). The *A. alba* patch was located in an area that is nowadays regularly dredged, ensuring passage for large ships (navigation channel "Scheur"). However, these much higher values can be induced by e.g. a particularly high recruitment during one year. This phenomenon is likely to explain the exceptional value obtained for *D. vittatus* at one station off Ostend. On the contrary, the *A. alba* patch is widespread, with decreasing abundances along its border. This area is thus particularly favourable for this species. Given its position along the northern border of the turbidity maximum area of the BPNS (Fettweis et al, 2006), its low species richness, and the fact that this deposit-feeding species is tolerant to siltation and high mud contents, the historical data point to an area where higher siltation rates occurred, compared to the rest of the sampling grid. However, the morphological analysis of Fettweis et al (2009) did reveal accumulation of muddy sediments between 1866 and 1911 only landward and, to a lesser extent, seawards of the Wenduyne bank.

To the West of Ostend, only few coastal stations contain more than hundred individuals, among which the areas of highest species richness along the Westhinder sand bank. By contrast, extremely low amounts of animals were found in the coastal waters between Ostend and Blankenberge, landward of the Wenduyne bank, i.e. the Grote Rede. The quasi absence of macrobenthic species (apart from *Diastylis rathkei*) is in agreement with the determined accretional trend of this area (see Annex II), result section: mud content). To the East of Blankenberge, abundance values remain low, but locally increase to more than 10 specimens of very few species.

Overview figures of frequency of occurrence and total abundance in Gilson's dredge data-set provide a first indicator on the relative importance of species within the considered area (see Annex II). Shallow infaunal bivalves clearly dominate the samples, with *D. vittatus, S. subtruncata, A. alba* and *M. bidentata* recorded at more than 100 stations. *A. alba* is the most abundantly collected species, immediately followed by *D. vitattus*, but at a much lower number of stations. This is explained by the very patchy distribution of *A. alba*, as compared to the widespread *D. vittatus* (Figure 9). *S. subtruncata* was always gathered in low abundances. The numerically dominant polychaete species (Nephtys spp, Ophelia limacina) are much under-represented, as compared to contemporary relative abundances (see Van Hoey et al, 2004). The soft bottom macrobenthos, sampled by Gilson, was dominated by bivalves.
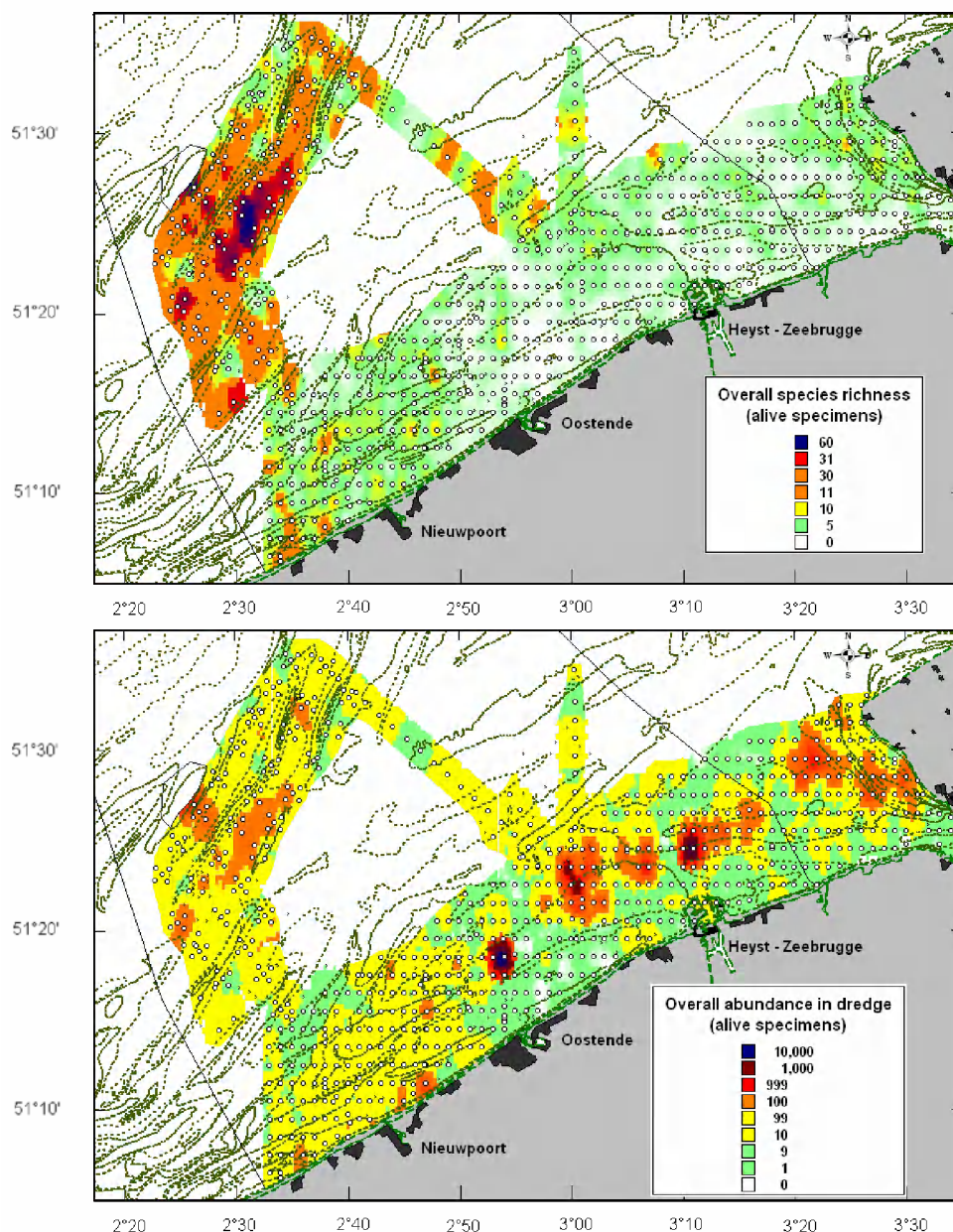
Figure 9. Total species richness (above) and total specimen abundance (below) at accurately geo-positioned dredge stations (suspect stations eliminated), for the period **1899-1911**. Background: present-day bathymetry and coastline. See Annex II for details on data selection and processing.
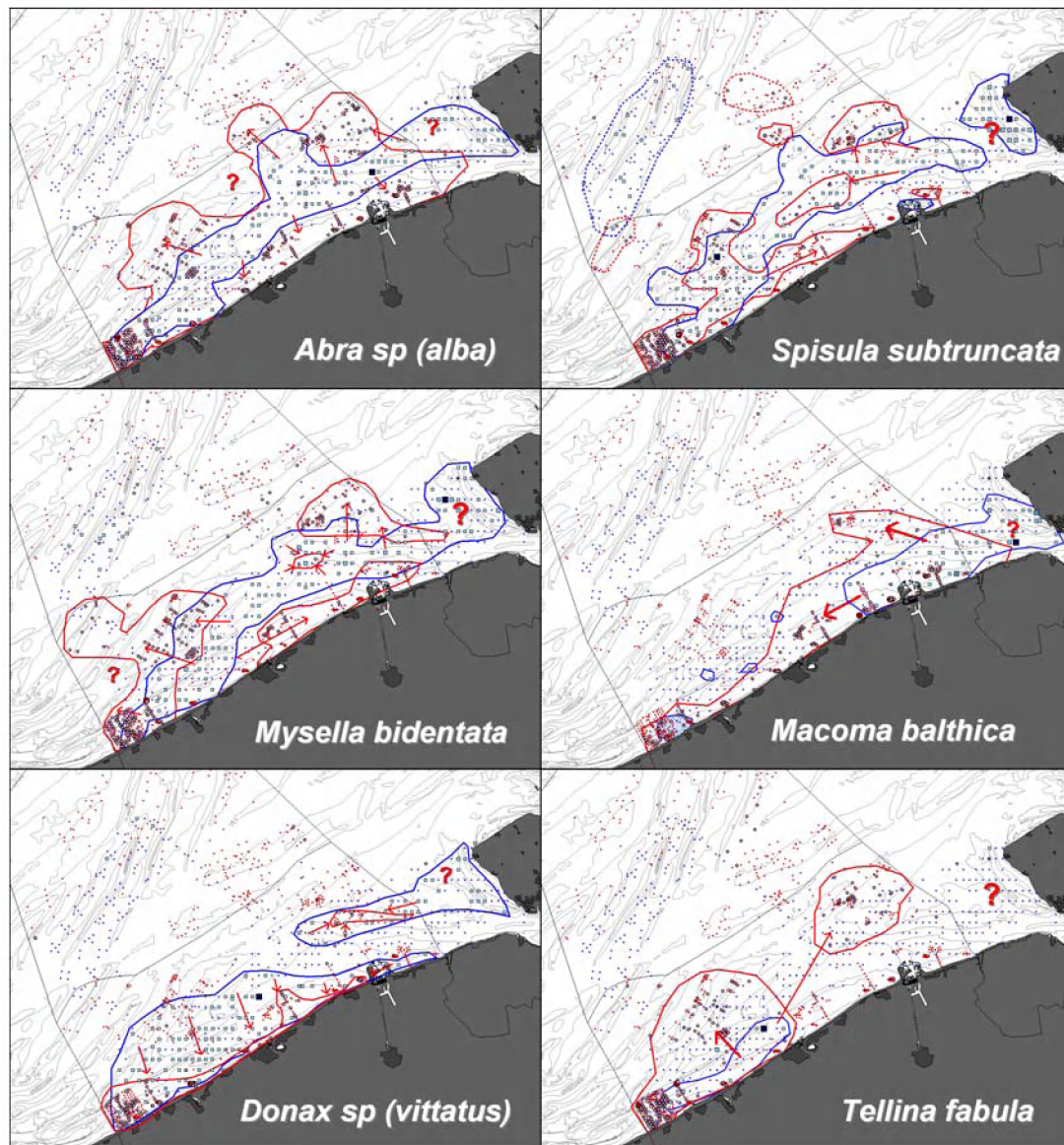
Figure 10.   General distribution maps of the 5 most abundant shared species and *T. fabula* in the periods 1899-1911 (blue scaled squares) and 1994-2008 (red scaled circles). Contours of distributions were roughly drawn around station patches (blue: historic extent; red: contemporary extent). Arrows point at apparent directions of shifts. Question marks indicate areas were no recent data is available. See Annex II for grid-based maps of distribution of 16 bivalve species in areas where historical and contemporary data were acquired.

Major shifts were noted, the most important being related to resistance to siltation (mud-tolerant species *A. alba, M. bidentata, T. fabula* expanded their distribution range; contrary to the mud intolerant species *D. vittatus*) and lower salinities (the eurytherm, estuarine *Macoma balthica extends much further along the western coast*). Results of the data-gridding approach indicate that observed shifts in mud-tolerant species are statistically significant. Increased SPM concentrations and tidal sedimentation rates thus now occur over the whole coastal area, and the main continental river runoff signal (Macoma) shows clear westward expansion along and close to the coastline.

When the time-windows of our respective benthic data-sets are superimposed on the long-term trend in the North Atlantic Oscillation (NAO; http://www.cgd.ucar.edu/cas/jhurrell/ indices.html), they appear to have been predominantly collected under two opposite episodes: prior to 1903, Gilson's data are representative of the former period of 30 years of mainly negative NAO displaying high year-to-year variability. To the contrary, the contemporary data

from 1994 to the early 2000s depict conditions where NAO has been very high, with unprecedented peaks since 1988, signaling global climatic change (Weijerman et al, 2004).
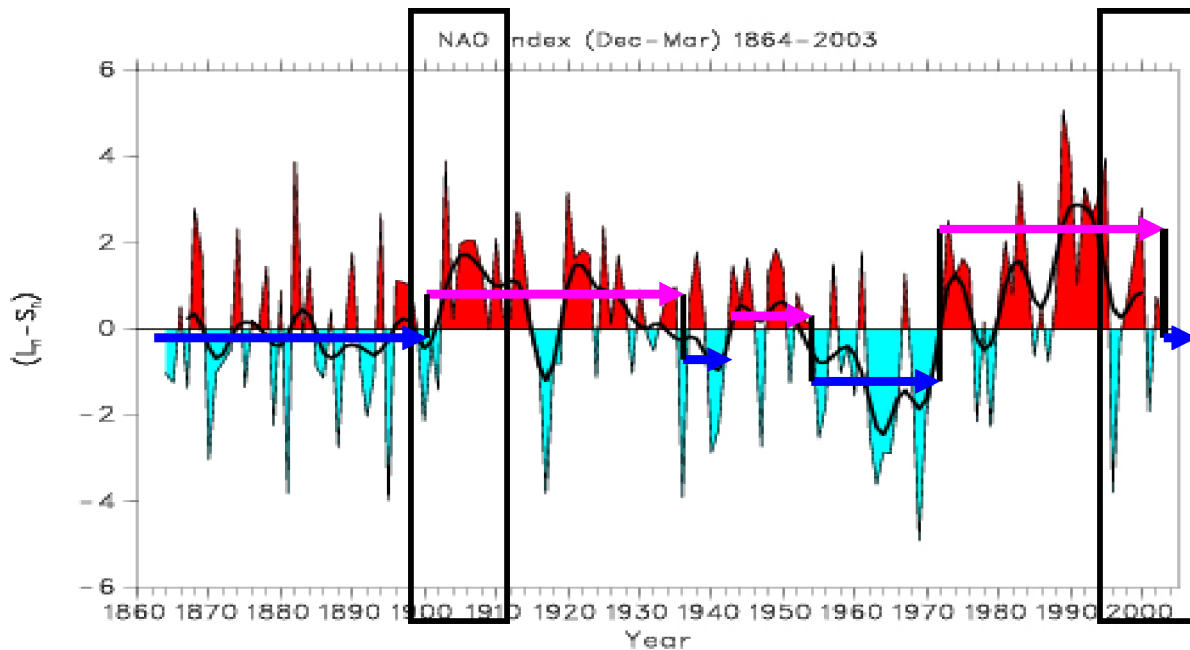
Figure 11.   Long-term change in NAO values since 1866 (http://www.cgd.ucar.edu/cas/jhurrell/indices.html), The time-frames of our data-sets (1899-1911; 1994-2008) are indicated. Indicative average value of NAO is graphically done. I WILL RE-DO it with the data

Examination of expected influence of the North Atlantic Oscillation on the local physiographic references clearly revealed that all observed changes match expectations according to known effects of the prevalent NAO conditions in the considered periods (Figure 11). Seven to eight distinct periods can be identified on the NAO time-series, with the 1914-1918 period in balance (short). It appears that pre-1903 Gilson's data (the bulk of coastal bivalve data) were gathered at the end of a 30-years time-span of predominantly negative NAO with high year-to-year fluctuations, while the post-1988 situation coincides with unprecedented increase in the NAO positive values, due to ongoing climatic change and referred to as a "regime shift" by Weijerman et al (2005). Observed "long-term" shifts thus mirror two different states of the coastal ecosystem.

The major effects of high NAO conditions, resulting from increased westerly winds over the North Atlantic bringing warmer and moister air to the continent, are to increase continental river runoffs resulting from increased precipitations, increase intensity and frequency of northerly winds and gales, and increased entrance of Channel waters in the Southern Bight. During negative NAO conditions, river runoffs are restricted, as also the influence of Channel water and northerly gale activity in the NE Atlantic. The main effects of positive NAO conditions at the BPNS are thus: (1) increased trends to siltation; and (2) increased influence of continental rivers (including the Schelde) which is fully mirrored by the observed distribution shifts (Figure 12). As such, strong changes in ecosystem functioning trigger a numerical dominance of siltation-resistant species. From a human point of view, this represents a "degradation" of the local "ecological quality", as compared to the former situation which was more favourable to species-rich benthic communities. The results show that the long-term signal of increased levels of human disturbance is, alongside the coast (up to about ten to twelve miles offshore in the eastern BPNS), masked by NAO-induced trend to increased siltation, probably due to increased river runoffs in conjunction with expected increase of northern gales (so far not detected for the BPNS). The results confirm that the NAO acts through two main ways: (1) abrupt yearly changes

in the sign of the NAO, which is expected to have impacts on temperature and salinity sensitive species; and (2) influence of average NAO conditions over longer periods, since the expected effects on increased turbidity and river runoffs act with a time-lag of probably a year.

Given the regime shift established since 1988, the measured amplitude of change is most probably larger than formerly. The long-term trends in macrobenthic bivalves do not enable us to support the view that navigation channel dredging is the primary agent responsible for larger SPM concentrations in the BPNS. Contrary, riverine inputs (Schelde and other continental rivers; see Lacroix et al, 2004), linked to high NAO conditions seem to provide a better candidate, as demonstrated by the recent extension of the euryhaline, estuarine (and thus siltation-resistant) *M. balthica*. Increased southwesterly winds thus paradoxically co-occur with increased river runoffs, which are indeed good candidates to explain the recent increase of SPM concentrations. The "smothering effect" of benthos, resulting from sustained onset of high positive NAO values, does not occur off the Flemish banks, off the Western coast, and it is deduced that NAO alters the Hinderbanken area more slightly through slight eastward extension of Channel waters off the Belgian coast.

The results match some recent short-term observations on brief and sudden NAO reversal (e.g. BPNS: Van Hoey, 2007; German bight: Kröncke et al, 2001) and suggest that most "regime shifts", observed so far, coincide with a reversal or significant change in NAO winter conditions. However, the effects might vary locally; since the German bight changes were ascribed mainly to SST and food availability to suspension- and deposit-feeders, while in the turbid BPNS a strong smothering effect dominates.

The findings are potentially important for the understanding of long-term trends in coastal marine biodiversity. They call for sound revision of previous data, paying attention to yearly NAO evolution. We predict that data mining for the period 1930-1973, dominated by negative NAO values, will result in findings of a situation comparable to that of Gilson, with however a less marked influence of yearly variation, inducing more pronounced negative physiographic effects. Consequently, SPM concentrations and benthic species smothering can be expected to have been much lower during that period.

If our interpretation is confirmed, the historical data of Gilson thus represent a baseline situation for median- to low NAO conditions. Obviously (Figure 11), the 1935-1973 period is characterized by a much lower NAO average value. Data from this period need investigation to check agreement with expectation that more marked NAO effects occur during that period, as compared to Gilson's sampling period (changes in physiographic conditions should be even more dramatic between 1935-1973 and 1994-2003).

The lower variability displayed by the offshore communities, suggests less variable environmental conditions there, with more prominent impact of sea surface temperatures, because these areas are hardly influenced by the increased riverine discharges, due to concomitant eastward move of Atlantic waters into the Eastern Channel and through the Straight of Dover.
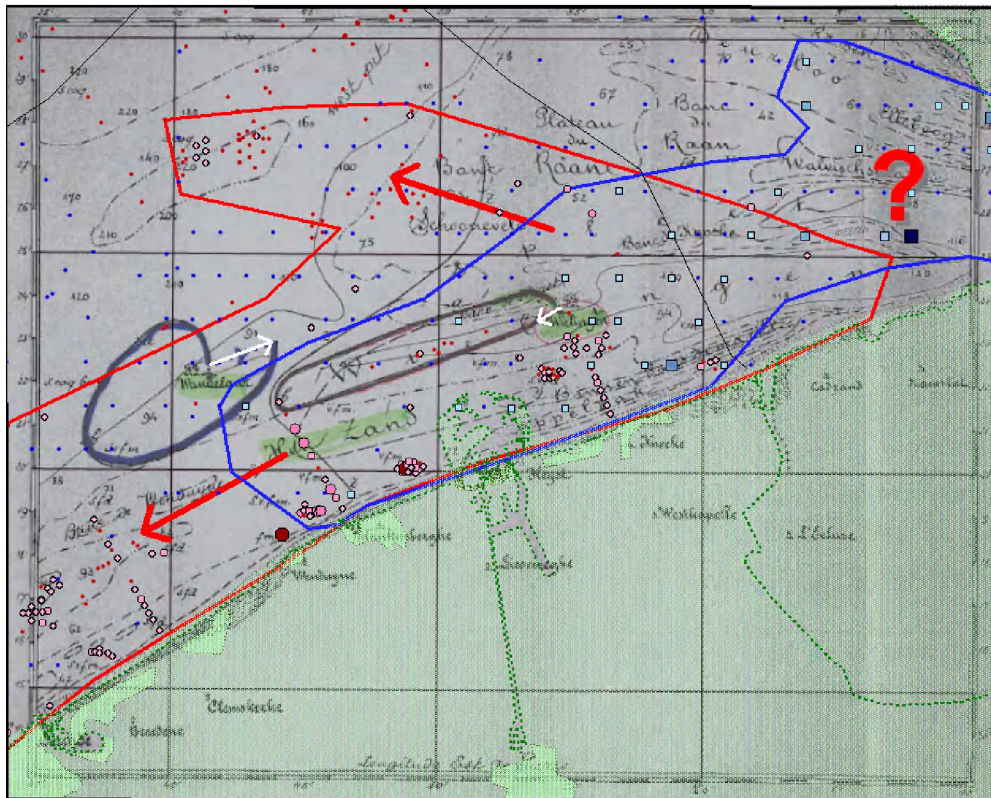
Figure 12.   Detail of the distribution of *M. balthica* (historic: scaled blue squares; contemporary scaled red dots) along the Belgian East coast, superimposed on the map of currents of Van Mierlo (1899). Blue dots: historical sampling stations. Red dots: contemporary sampling stations. Van Mierlo mapped the trajectory of two bottles released for one tidal cycle at the lightships Wandelaar (dark blue line) and Wielingen (dark red line). The residual current direction is indicated by the white arrows. The present-day coastline (including Zeebrugge harbour), administrative boundaries and cities are superimposed in green nuances and dashed lines.

Our observations most probably explain the "counter-intuitive" higher resistance to severe winters of coastal communities, observed by Reiss et al (2006) in the German Bight, as compared to offshore communities.

On the long-term, our results show that Belgian coastal waters typically experience two different states of benthic communities depending on NAO sign, whilst more stable community compositions characterize offshore areas. This further indicates that offshore areas are more sensitive to disturbance and recover more slowly after a perturbation. All these observations must now be confronted to a re-examination of available data-sets taking into account different NAO periods.

2.2.3   Long-term bathymetric changes

Based on historical navigation charts (~150 years ago up till now), the morphological evolution of the BPNS is studied. A selection of charts spanning a large spatial (a large part of the BPNS) and time (last centuries) domain, is being digitized. Table 1 presents the selected navigation charts that have been digitized (the most recent chart is a compilation of different datasets, digitally available).

Table 1.   Details of the digitized charts (Flemish Authorities, Division Hydrography)

Date	Title of chart	Surveyed
1866	Carte Générale de Bancs de Flandres compris entre Gravelines et l'embouchure de l'Escaut	?
1908	Mer du Nord Dunquerque – Flessingue	1901 - 1908
1938	Noordzee – Vlaamsche Banken	?
1969	Noordzee – Vlaamse Banken	1959 - 1969
2007	(composed from different recent charts)	1997 - 2007

ArcGIS is used to interpolate the digitized charts to grids with a spatial resolution of 20m x 20m, making it possible to study the morphological evolution by visualisation of depth lines and chart differencing. For the interpolation, a special methodology was used in order to create grids with smoothly varying depth values. In this methodology, a chart of a specific year is not only based on the interpolation of data points of that year, but also on the chart of 2007, which had a much higher data point density. By doing so, the derived charts not only are the result of an interpolation in space, but also in time, and it is implicitly assumed that the basic morphologic patterns (such as presence of sandbanks) on the BPNS are approximately stable, which is confirmed by earlier studies (Van Cauwenberghe, 1971). The application of this methodology results from the observation that straightforward interpolation of the chart data points into a grid using one of the algorithms provided by ArcGIS would result in the artificial creation of pits and peaks on the location of some data points, making it impossible to compare the different grids, since different charts have data points on different locations.

It must still be noted that –given the large uncertainties on the water depths of the data points, especially on the older charts, results of the analysis of the grids must be handled with great care (a quantitative uncertainty analysis was not carried out).

Figure 13 shows an example of the visualization of a time series of depth lines, in this case the 8m depth lines (reference level: TAW) of the Middelkerke sandbank. The depth lines indicate that there was no significant movement of the Middelkerkebank during the last 150 years, though it seems that the northeastern part of the bank has undergone erosion, while the southwestern part has accreted. This is confirmed by the sedimentation trend map, which is shown in Figure 14, as also in literature (e.g. De Moor, 2002). The latter is the result of a linear least squares fitting of the time series of bathymetric data, listed in Table 1. Locations with no significant trend ($R^2 < 0.5$) are left out.

Similar analyses of depth lines, together with the sedimentation map of Figure 14, reveals that many significant morphological changes are the result of human activity: deepening due to dredging of the navigation channels towards the harbour of Antwerp (Scheur) and Zeebrugge (Pas van het Zand) and towards Ostend, where the navigation channel cuts through the Stroombank; accretion due to dredge disposal on the locations S1, ZBO (near Paardenmarkt bank), and OOS (near Ostend, on the southwestern tip of the Wenduinebank). A clear sedimentation trend can also be observed in the shelter of the breakwaters of the outer harbour of Zeebrugge.

The study also indicates that there is no significant movement of the sandbanks during the last 150 years, though some banks (especially the Coastal Banks: Smalbank, Nieuwpoortbank, Ostendbank and Wenduinebank) seem to be prone to erosion at the seawards side and to sedimentation at the coastal side, which could indicate minor movement towards the coast. However, taking into account the relatively large uncertainties on both position and depth

values of the original data points, this movement cannot be considered significant, though it must be noted that none of the banks showed the opposite effect (movement towards the sea).
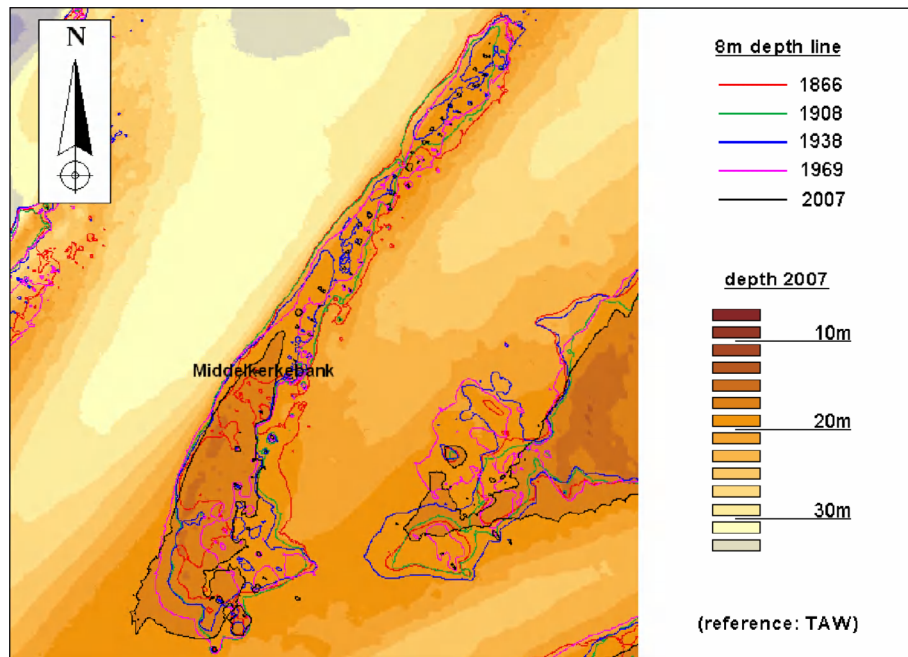
Figure 13.   Time series of the 8m depth lines of the Middelkerke sandbank.
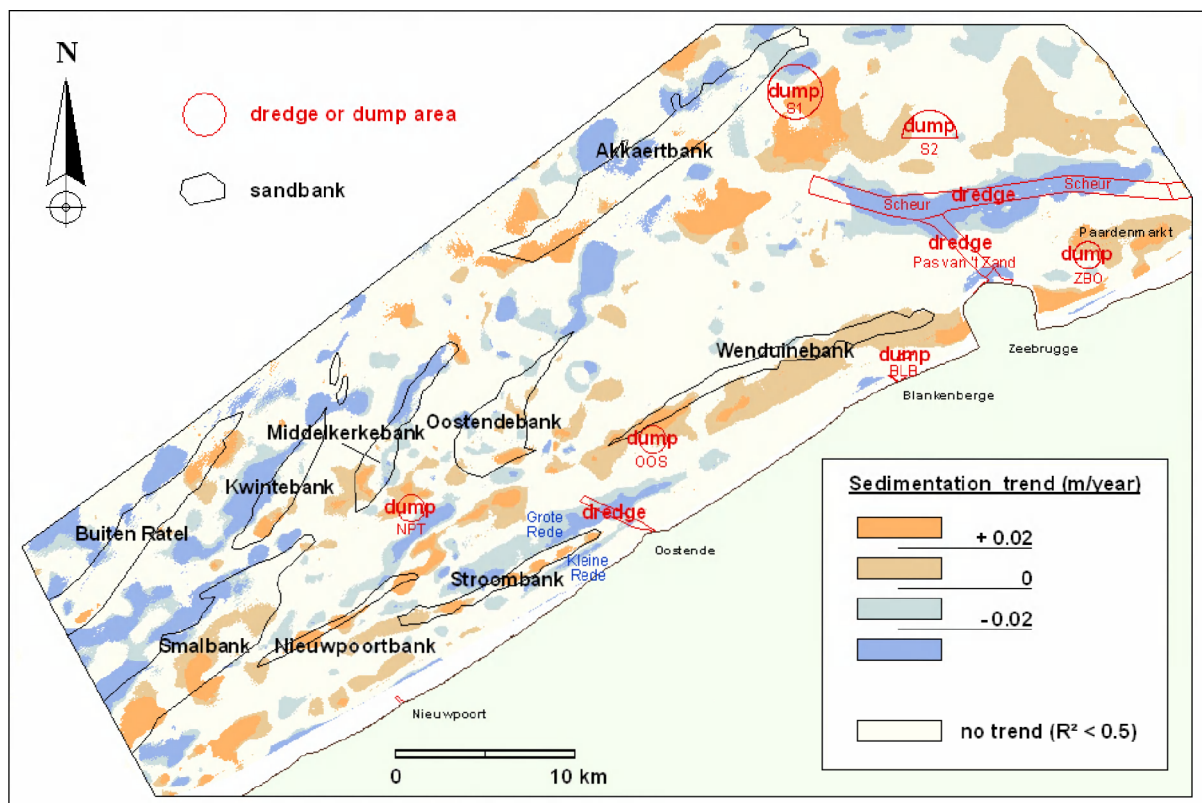
Figure 14.   Sedimentation trend along the southwestern part of the BPNS, based on the bathymetric chart differences in the period 1866-2007.

Nevertheless, the Coastal Banks are the most naturally dynamic zones: significant sedimentation trends are observed for the Nieuwpoortbank, the Wenduinebank and the Stroombank, while erosion occurred in the troughs between the Stroombank and the coast (Kleine Rede) and at the

seawards side of the Stroombank (Grote Rede). The sandbanks of the Hinderbanks (located further in sea, not shown in Figure 14) could not be studied, since the errors on the position of the data points in that area was too large, mainly due to erroneous positioning of the lightship Noordhinder on the older charts.

2.2.4 Long-term sediment changes

Mud

Detailed investigation of Figure 8 (see also Annex I), combined with an analysis of bathymetric changes in the former 40 years (1866-1911), revealed interesting historical patterns in the coastal plain between Ostend and Heist (nowadays Zeebrugge harbour area). Even then, the whole area was subject to high siltation rates and an overall depth shallowing. Gilson's "soft" muds (interpreted as freshly deposited) were reported in the western part, while "hard" muds (interpreted as consolidated ancient mud) were reported in the eastern part, probably indicating different sediment dynamics. Comparing nautical charts, much less shallowing was noticed for the western Westdiep and the Zeebrugge muddy areas, whilst no change was detected at the mud patches of the western West Diep and seawards of the Wenduyne sand bank. The area where Zeebrugge harbour was built, was already undergoing siltation, before harbour construction. This is likely the reason of constant siltation in recent navigation channels, implying regular dredging to maintain navigable fairways.

Gilson's field descriptions (consolidation, thickness), together with bathymetric maps of 1866–1911, indicate further that the distribution of fresh mud and suspended sediment have changed during the last 100 years. Nowadays, thick layers of fresh mud (>30 cm) are attributed to anthropogenic causes and indicate that erosion of older Holocene mud has increased in recent times. Further readings see Fettweis et al. (in press).

Sand

The SediCURVE@SEA database (1899-2008, Van Lancker, Annex IV) was used to compare sediment changes in the sand fraction in the period ~1900-2009. For the median grain-size (d50), no major or consistent changes were found over large areas. However, striking differences were found when evaluating the sorting and skewness of the sediments. Figure 16a shows the sorting of all sediments of the Gilson collection: except for some locations where gravel or shell hash prevails (e.g. Westhinder area or areas with bedforms), all sediments are well-sorted. This is not the case for the recent sediment samples, now showing an overall worsening in sorting over vast areas. For clarity, Figure 16b shows only the distribution of the moderate to poorly sorted sediments. Noteworthy, is the observation that this trend only occurs in the coastal zone; though also along the newly implanted windmills, offshore. To explain the cause of the wide-spread worsening of sorting, the skewness was evaluated for these locations. Figure 16c shows that the poorer sorting seems solely due to an enrichment of (very) fine sands.
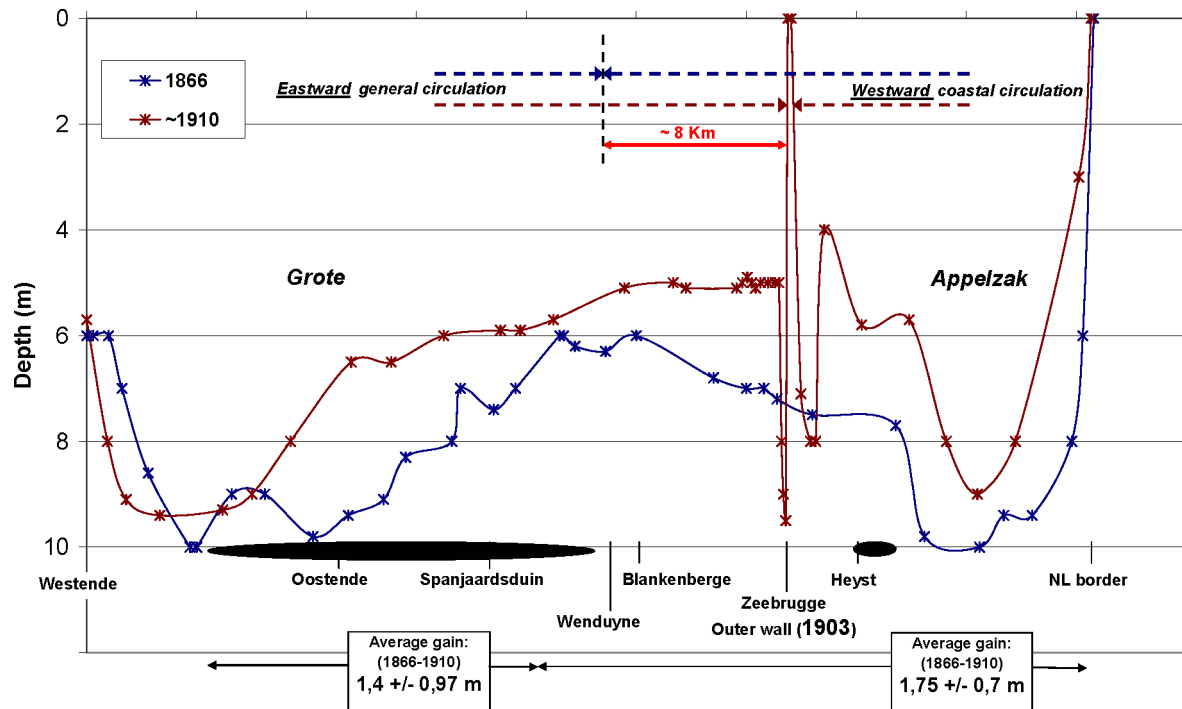
Figure 15. Bathymetric profiles in the Grote Rede and Appelzak gully (transect between Westende and the Dutch border), recorded by Stessels (1866; blue) and Urbain (1911 – with measurements up to 1908; red). Upper arrows indicate the theoretical meeting point of general North-eastward and coastal (Appelzak) westward residual circulations in both periods (see text). The black-filled areas at the basis of the figure represent the areas where pure mud samples were gathered, in the vicinity of the transect by Gilson (1900s). Average seafloor rising trends (decreased depth) were calculated.

Although, more consistent patterns occur around harbours, near disposal grounds and aggregate extraction sites, the trend is widespread and also occurs in so-called 'natural systems', such as the Westdiep-Broersbank system. Further analyses are needed to investigate other causes of change, such as NAO cyclicity (see below).

For all sampling locations, see Annex IV (SediCURVE@SEA). The analyses were performed on the sand fraction only. Using the bulk sediment grain-size information would induce too much bias on the results.
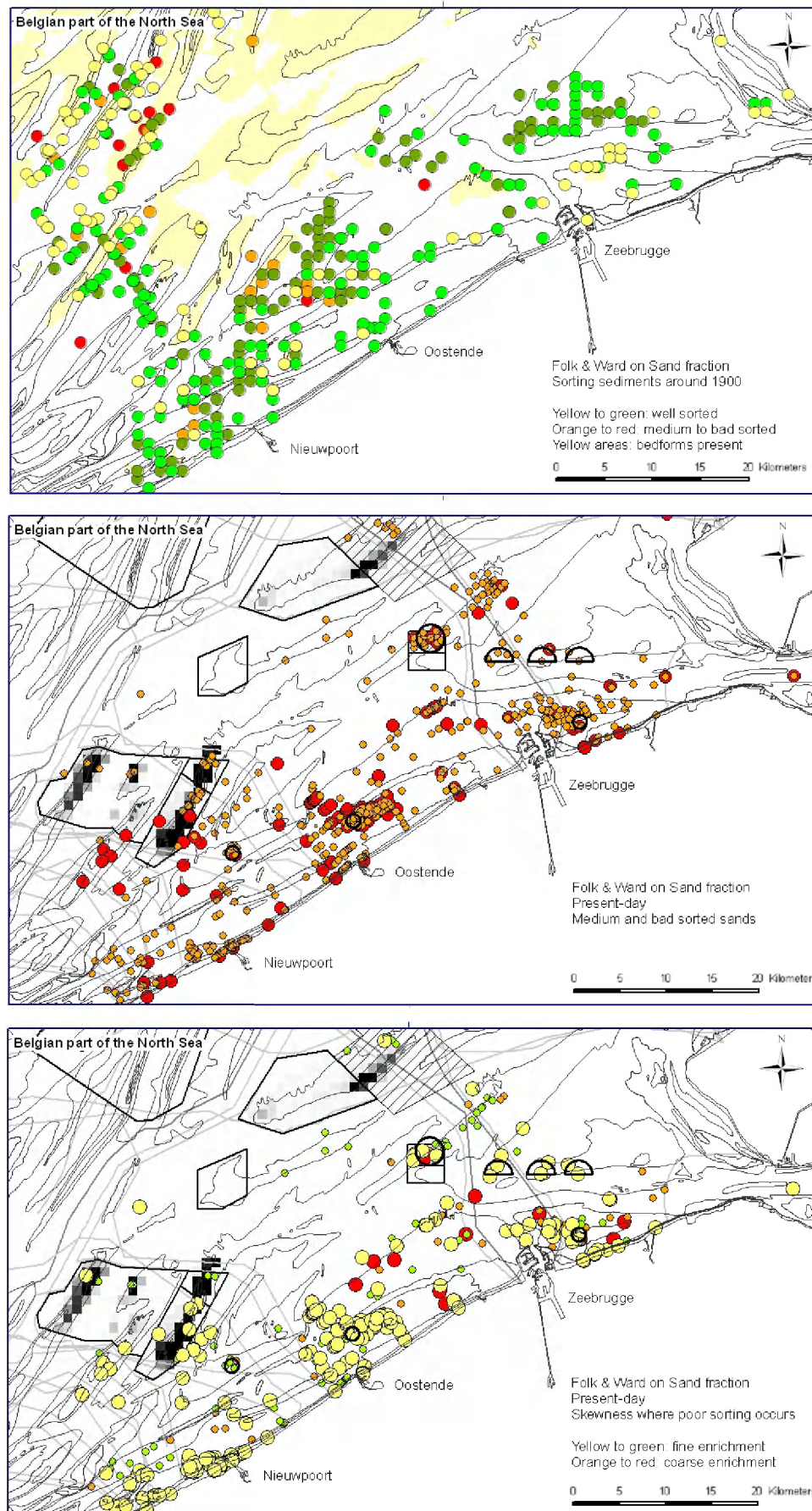
Figure 16.   (a) Sorting of all re-analysed Gilson samples; (b) spatial distribution of recent sand samples having a moderate to poorly sorting; and (c) skewness of the nowadays moderate to poorly sorting sands. Analysis based on SediCURVE v.1 database.

3.   MODELLING OF PROCESSES

3.1   Sediment transport model - BPNS

3.1.1   Bed model

To account for erosion of old sediments (Holocene and outcropping Tertiary clays), a distinction between an active layer and a parent bed is needed. From the erodibility measurements (see above), a 4 Pa critical erosion shear stress (τ_{ce}) was considered to distinguish the active from the parent bed layers. For sandy sediments the active and parent bed layers are equal. The active layer consists of different sub-layers allowing consolidation of mud, pore filling of sandy sediments, by mud and segregation between sand and mud layers.

Both the active and parent bed layer are characterised by 15 variables, resulting in 30 variables on every sampling location. These variables include erosion characteristics, e.g. τ_{ce} at surface, τ_{ce} averaged over a depth interval, bulk density averaged over a depth interval, mass in a depth interval and critical erosion rate averaged over depth interval, as also sediment characteristics, such as grain sizes in 8 classes from gravel to clay. The definition of clay ($< 8 \mu$m) is based on the difference between sortable silts and aggregated particles (Chang et al. 2007), and the discrimination between a cohesive and non-cohesive behaviour is based on van Ledden et al., 2004 (Figure 17). The results are afterwards interpolated on a 250 m grid. Sedimentological maps of sand, silt and clay percentages are constructed, together with a spatial map of the van Ledden classes. Data were extracted from the SediCURVE@SEA database (Van Lancker, Annex IV).
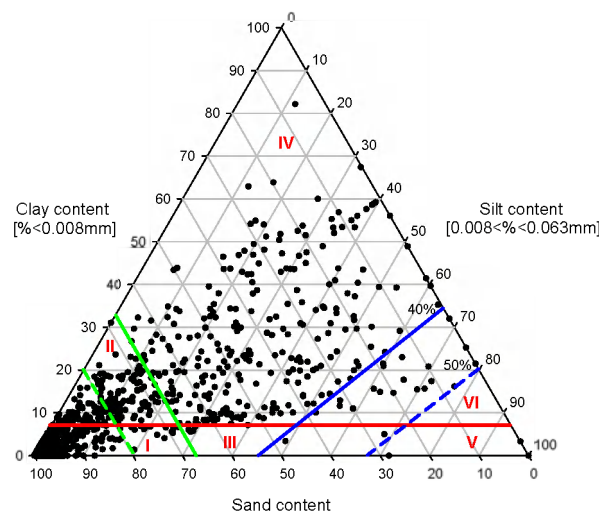
Figure 17.   Ternary diagram of BPNS sediment samples, considered for the bed model with transitions for cohesion and network structure. I = non-cohesive sand-dominated, II = cohesive sand-dominated and IV = cohesive clay-dominated network structure.

3.1.2 Flocculation modelling

Settling of mud flocs is controlled by flocculation and determines by large the transport of cohesive sediments. Flocculation is the process of floc formation and break-up and has a direct impact on settling velocity. Through its influence on deposition, a direct link with formation of mud or sand-mud deposits and thus erosion behaviour exists.

Many flocculation models calculate the settling velocity of mud flocs in an empirical, theoretical or heuristic way. Maggi (in press) developed a mechanistic model of floc formation and break up, following simultaneous flocculation of organic and mineral SPM particles. The suspended matter is split into a mineral (1-ϑ) and an organic fraction (ϑ). Both fraction are cohesive and influence the growth and the break up of flocs. The volume of particles in a floc can be written as the sum of the volume of the mineral (Vm) and the organic constituents (Vb):

$$V = V_M + V_B = (1 - \zeta)V + \zeta V \qquad (3.1)$$

with ϑ = V_b/V the fraction of organic constituents. The changes of V as a function of time can then be written as:

$$\frac{dV}{dt} = \frac{dV_M}{dt} + \frac{dV_B}{dt} \qquad (3.2)$$

dV_m/dt is solved using the flocculation model of Winterwerp (1998). dV_b/dt is based on Winterwerp's model extended with terms to describe the growth of aggregate-attached micro-organisms under nutrient-rich conditions. If fractal geometry is assumed for the flocs, then V can be written as:

$$V = D_f^{nf} \big/ D_p^{nf-3} \qquad (3.3)$$

with D_f the flocsize, D_p the size of the primary particles and nf the fractal dimension. Equation 3.2 can be solved numerically for the floc size D_f using an explicite finite difference method. If the effective density of flocs is written as (Winterwerp, 1998):

$$\Delta \rho = (\rho - \rho_w) \left(\frac{D_p}{D_f} \right)^{3-nf} \qquad (3.4)$$

then the settling velocity of the flocs, w_s, is calulated as:

$$w_s = \frac{a}{18b} \frac{(\rho - \rho_w)}{\mu} g D_p^{3-nf} \frac{D_f^{nf-1}}{1 + 0.15 \, \mathrm{Re}^{0.687}} \qquad (3.5)$$

with g the gravitational acceleration, Re the floc Reynolds number (= $w_s D_f \vartheta^{-1}$) and a and b form parameters of the floc.

The flocculation model has been calibrated for a 1D application (Maggi, in press) for floc size using measurements of particle size and SPM concentration near Zeebrugge (MOW1: tidal cycle measurements 8-9/09/2003) and on the Kwintebank (tripod, 2-11/03/2004), see Fig 2.1 and Fettweis et al. (2006). The turbulent shear stress was calculated using the 3D application of the COHERENS hydrodynamic model for the Belgian Continental Shelf (OPTOS-BCP). The results are shown in Fig 1.

The settling velocity and effective density, calculated using equations 3.4 and 3.5, are presented in Fig 2 and 3. Maggi (in press) used an averaged fractal dimension of 2 in the flocculation model. Based on measurements, a fractal dimension of 2.59 for the Kwintebank time series has been derived. By using this value, instead of a fractal dimension of 2, much higher settling

velocities are obtained. Small variations in parameter values can lead to significant changes in settling velocity. This underlines the importance to accurately estimate the fractal dimension.
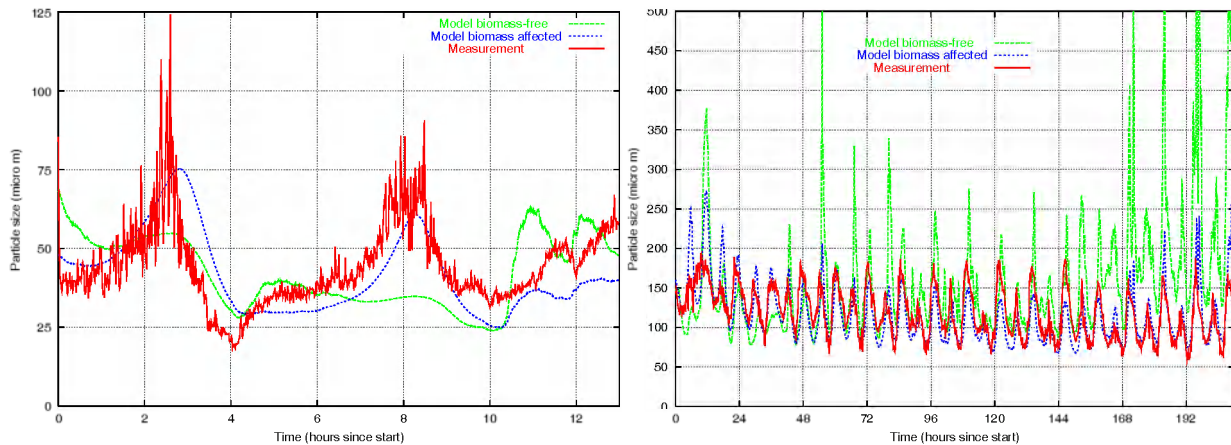
Figure 18. Comparison between measured and simulated floc size (with and without biomass). (left) MOW1 (8-9/09/2003 and (right) Kwintebank (2-11/03/2004). Zero on the x-axis corresponds with the start of the measurements.
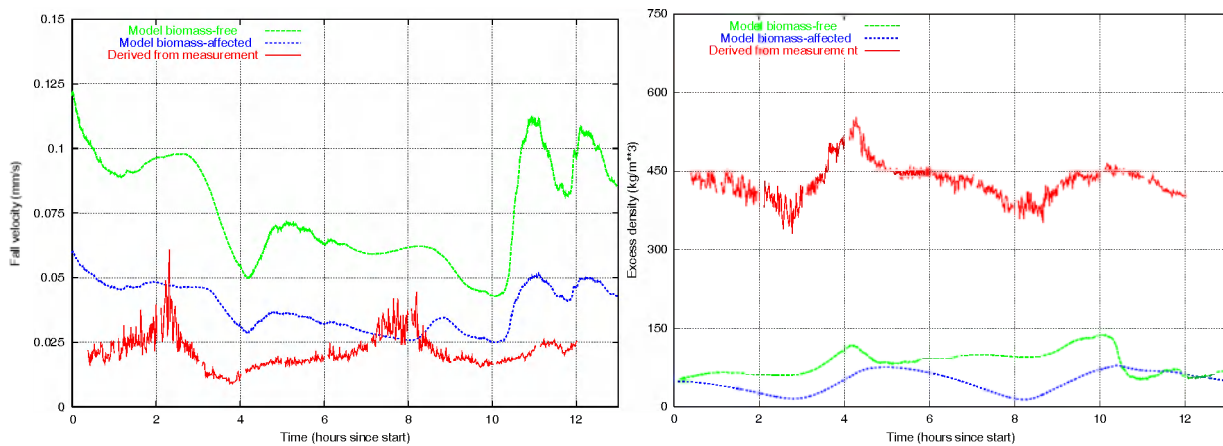
Figure 19. MOW1 (8-9/09/2003, 2003-22). Settling velocity and effective density calculated with the 1D floc model and derived from measurements. The settling velocity and the effective density have been calculated using a fractal dimension of 2. Zero on the x-axis corresponds with the start of the measurements.
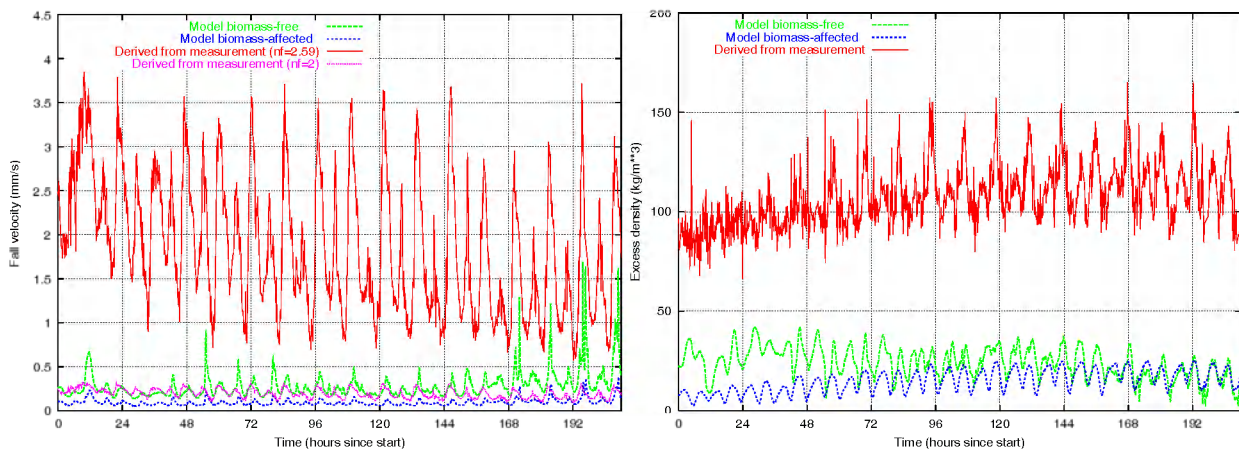
Figure 20. Kwintebank (2-11/03/2004). Settling velocity and effective density calculated with the 1D floc model and derived from measurements. The settling velocity and the effective density have been calculated using a fractal dimension of 2. Zero on the x-axis corresponds with the start of the measurements.

Implementation into a 2D sediment transport model

The 1D calibration has clearly shown that the parameters of the flocculation model are site specific. In order to implement the flocculation model into a 2D (and 3D) numerical sediment transport model, the geographical variation of the parameters has to be included. Previous research has shown that parameters, such as the organic content and the primary particle size have a geographical variation. Analysis of suspension samples show that the percentage of organic matter is between 5-12%. The POC and PON concentration has been measured since 2004 during tidal cycle measurements. The POC concentration varies between 0.1 and 25 mg/l, the PON concentration between 0.05 and 3.3 mg/l and the SPM concentration between 2 and 758 mg/l. If it is assumed that the sum of POC and PON concentration represents the organic matter content, then a relation between SPM and the POC+PON fraction of the SPM can be derived. The data from the turbidity maximum show that the POC and PON percentage is non-linearly linked with the SPM concentration. This indicates that during deposition relative more mineral particles (or flocs with higher mineral fraction) are settling and deposited than flocs with a lower mineral content or biological particles.

The primary particle size (D_p) has been measured on 5 suspension samples from 3 different locations (Fettweis, 2008). The D_p on the Hinderbanken is 7.2±3.0 μm, on the Kwintebank 2.1±1.5 μm and near Ostend 1.1±3.7 μm. The grain size data also show that the mineral fraction of the SPM from the Kwintebank is slightly higher than from samples taken in the turbidity maximum.

The parameters of the flocculation model are calculated in the 2D model as a function of SPM concentration.

Results 2D simulations

The period February – March 2004 has been simulated using a hydrodynamic and sediment transport model. The results from the 1D and 2D simulations are similar, nevertheless an underestimation of the SPM concentration in the 2D results is observed. The latter is the most important reason for the difference in particle size and settling velocity. The underestimation of SPM concentration is probably caused by on the one hand the fact that the measurements have been carried out at 1.4 m above the bed, whereas the 2D model calculates depth averaged values, and on the other hand that the model uses a seasonally-averaged boundary condition of SPM concentration.

3.2 Sediment transport model – Scheldt estuary

A mud transport model for the Scheldt estuary is being developed in collaboration with Deltares/Rijkswaterstaat. The model domain ranges from the tidal boundary at Gent, down to Nieuwpoort and Zeebrugge, the grid counts 5 vertical layers and has a resolution ranging from 30 m in the tributaries to 400 m at the North Sea boundaries.

In order to assess the model performance with respect to seasonal dynamics, a full year was simulated. Simulating the year 2006 enabled a comparison with remote sensing data. From these data, it is observed that there is a fairly good agreement in spatial distribution and temporal changes of the TSM (total suspended matter) in the surface layer between the mud model results and the remote sensing measurements, though it must be noted that an absolute comparison is difficult, due to the fact that satellite data usually represent a much thinner layer than the top layer of the model's vertical grid (41% of the total water depth). On the contrary, the observed seasonal dynamics in mud fraction on the plates are not reproduced by the model. In the model, mud content in summer is not significantly higher than in winter, as is observed, suggesting that seasonal mud dynamics are not only driven by external forces (such as the variable sediment input), but also have internal causes. At present, the only internal forcing with

seasonal variation in the model is wind-generated surface waves; other possible internal causes include changed sediment properties (settling velocity, critical shear stress for erosion) due to biological influences.

Mud balances computed by the model result in a yearly net export of 2 Mton, which is the same magnitude of order, as computed by a previous version of the mode (3Mton), but still one order of magnitude larger than the net import following from mud balances. Exact numbers from observations involve large uncertainties and are not well known, but estimates range from 0.05 to 0.35 Mton yearly net import. Since it appears that the model's concentration gradient between inner and outer estuary is realistic, the computed export is probably due to an underestimation of the estuarine circulation (estuarine turbidity maximum concentration levels are too low, especially near the bed) and the observed phase error of the M4 tidal component. The latter influences the tidal asymmetry and thus also the residual sediment transport.

In summary, the developed mud transport model reproduces qualitatively many features of fine sediment dynamics of the Scheldt river, but in a quantitative sense some aspects (seasonal dynamics, estuarine circulation) can still be improved.

Results from a simple semi-empirical model, able to represent the essence of coastal mud dynamics on a time scale of years, can be found in Annex V. This model is based on a mass balance and on the present state of knowledge on large scale mud processes in the Belgian coastal zone (plus the mouth of the Schelde river).

3.3   Coupling of a wave model and hydrodynamic model

For the coupling of waves and currents, the COHERENS flow model (MUMM), the parallel version of WAM (version 451; semi-open source, courtesy of H. Guenther of GKSS) and the parallel version of SWAN (version 40.72; open source code T.U.Delft) have been implemented and tested on the High Performance Computer facilities of K.U.Leuven.

Water level results from the (still experimental) parallel version of the COHERENS model (from the 2D module) compare well with measurements; therefore it is believed that the code has been implemented successfully.

The WAM model is particularly well suited for ocean and shelf sea applications and extensive experience is available with the WAM Cycle 4 (WAM-PRO version, Monbaliu et al., 2000). After writing and including a new routine for meteo-input (UKMO winds provided by MUMM), the results of WAM 451 are (nearly) identical to results from the 'old' sequential code. As an illustration of the model performance, a time series plot for significant wave height and for mean period Tm02 (Figure 21) are shown below.
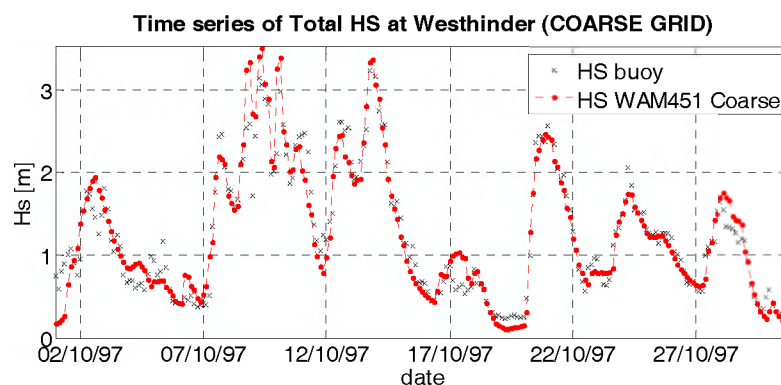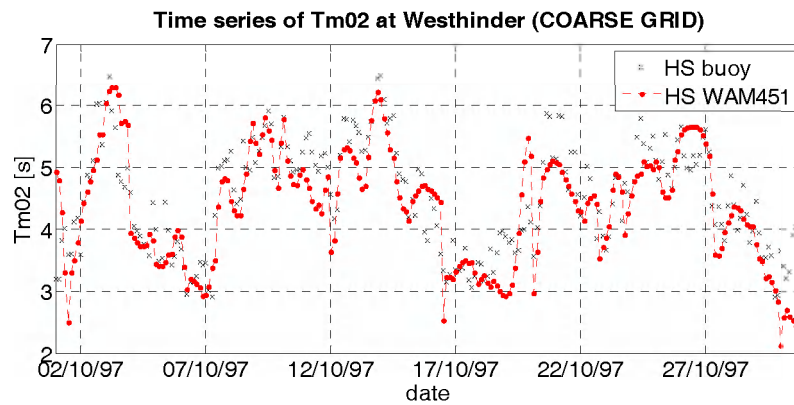
Figure 11.   Time series for significant wave height (upper figure) and mean period T_{m02}.

It was opted to use the SWAN model for applications on the Belgian Continental Shelf. This model is specifically adapted for coastal applications and code development for new insights in shallow water physics is very active. Moreover the model allows for dynamic updating of water levels and current fields and can output several parameters essential for shallow water application (e.g. wave orbital velocities, radiation stress fields). It is therefore well suited for coupling with a hydrodynamic model.

The SWAN model is less suitable for large scale applications, such as simulating waves in the North Sea. In order to provide the necessary boundary conditions to the SWAN model for applications on the Belgian Continental Shelf, a new routine was added to the WAM451 model code. This routine creates boundary condition files for subsequent SWAN model runs without restriction of the modelling domain, used in SWAN (spherical, cartesian, curvilinear). Some additional modifications to the main code of WAM were necessary to limit (optimize) the size of these boundary files.

All individual components have been tested on the High Performance Computer facilities. Off-line coupling between waves (SWAN model) and the hydrodynamic model is operational. The model suite can thus be used for specific studies in Phase 2. However, some additional work will also be done in Phase 2 to optimize full dynamic coupling of the individual model components.

4. NATURAL AND ANTHROPOGENIC IMPACT

4.1 Natural evolution and climate change

4.1.1 Natural evolution

Hydro-meteorological data from the Flemish Hydrography (1987-2007) are analysed statistically against sediment volume changes. For a case study of the near coastal sandbank Baland Bank, a principal component analysis allowed to differentiate sediment budgets of 8 consecutive bathymetric soundings against the directionality and strength of the sand transporting agents: winds, waves and currents. Generally, northeastern conditions are associated with the lowest sediment budgets, whilst winds blowing from the southwest are clearly associated with a sediment input. From the temporal observations, the consistency and hence duration of the prevailing hydro-meteorological conditions seems more important than the strength of the process. Due to the natural cyclicity in erosion/sedimentation, the area recovered fairly quickly from stormy periods. A publication of the results is underway (Van Lancker).

During the long-term measurements, different storms have been registered. The influence of storms on SPM concentration depends on the direction of wind, on wave height and on the availability of erodible cohesive sediments. As such, the effect of every storm is different, because the meteorological and sedimentological history determines the SPM concentration. It is argued that local mud sources, such as mud in sandy beds or consolidated mud layers, have to exist besides the well-known and generally accepted English Channel as major source of SPM (Fettweis et al., 2007a). Local sources are probably only effective during extreme conditions, such as high wave induced bottom stress. In the coastal area consolidated mud layers exist that cannot erode under normal conditions (critical erosion stress > 10Pa). Wave forcing may result in failure of the consolidated bed and in the formation of mud pebbles (Silva-Jacinto & Le Hir, 2001). Mud pebbles have been found frequently in the area (Fettweis et al. 2007b). The results are extensively reported in Annex VI (Fettweis et al., Annex VI).

4.1.2 Climate change

Atmospheric forcing of storm surges and waves for the Belgian coast

The daily seal-level pressure field (SLP from NCAR reanalysis gridded dataset) has been correlated with (i) daily surge height at Ostend for the period 1925-2000, and (ii) daily maximum wave height at Westhinder for the period 1994-2001. At daily time scale, surge height at Ostend and wave height at Westhinder are both correlated with sea-level pressure (SLP) over the Baltic Sea ([15°-20°E], [50°-55°N]) (Figure 22).
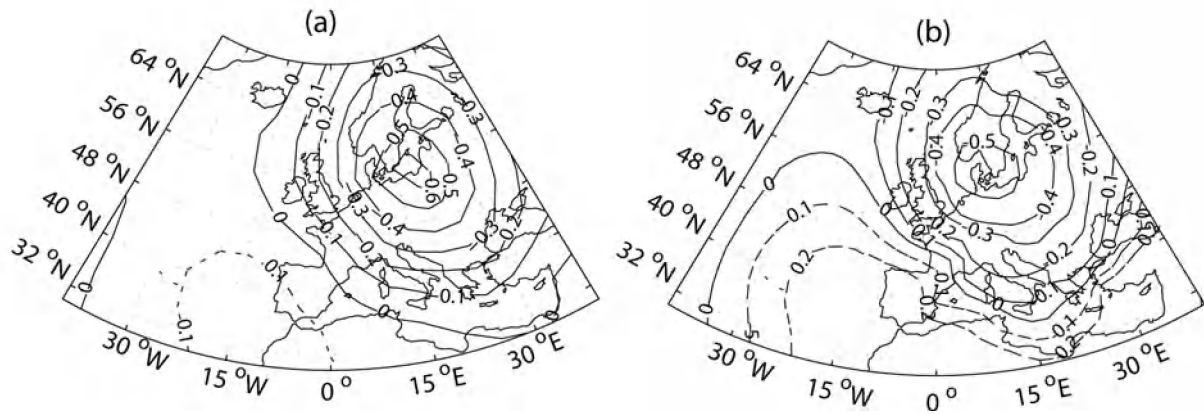
Figure 22.   Correlation between daily sea-level pressure field (NCAR dataset) and (a) the daily surge height at Ostend for the period 1925-2000 and (b) the daily maximum wave height at Westhinder for the period 1994-2001. Positive (negative) correlations are drawn as dashed (full) lines.

Mean daily SLP field has been computed for sea surges at Ostend > 35 cm (i.e. the 90th percentile of daily surge height at Ostend for the period 1925-2000) and for daily maximum wave height Hs at Westhinder > 2.5 m (i.e. the 90th percentile of daily wave height at Westhinder for the period 1994-2001). Highest surges and waves are associated with a deep low pressure system over the Baltic Sea (Figure 23). Associated with a reinforced Azores high, the Northeast-Southwest gradient across the North Sea is rather strong. This SLP pattern favours strong onshore winds, from Northwest sectors in the southern part of the North Sea, with as a consequence piling up of and the generation of considerable waves along the Belgian coast.
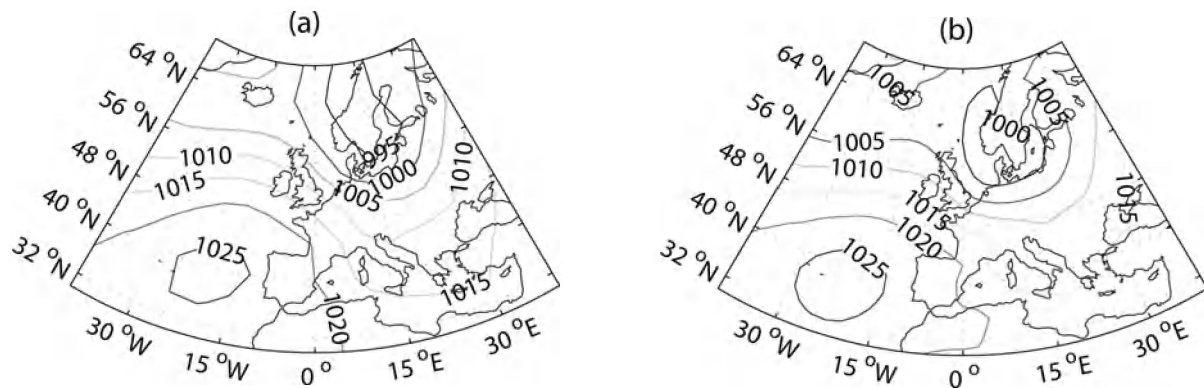
Figure 23.   Mean of daily sea-level pressure field (in hPa) computed for (a) daily surge at Ostend > 35 cm for the period 1925-2000, and (b) for daily maximum wave height at Westhinder > 2.5 m for the period 1994-2001.

20th century climate variability and impact on surge and wave height for the Belgian coast

The wintertime (October to March) 99th percentile (P99) of daily sea level and of sea surge has been computed at Ostend for the period 1925-2000. Wintertime P99 of sea level shows an increasing trend of +3 mm/yr (Figure 24a). During the same period, the wintertime P99 of sea surge has increased at a rate of +1 mm/yr, but especially from ~1960 to 1980 (Figure 24). Surge height then tends to slightly decrease until the beginning of the 21st century. During the 20th century, the mean sea level has risen at a rate of +2 mm/yr (Van den Eynde et al., 2008). To summarize, long-term increase in wintertime P99 of sea level (i.e. extreme sea levels) during the 20th century could be explained by the superposition of (1) the increase in wintertime P99 of sea surge, partly associated with increase in onshore NW winds and storminess in the Southern North Sea, especially between 1960 and 1980 (Alexandersson et al., 2000; Weisse et al., 2005), and of (2) the slow mean sea-level rise, mostly linked with thermal expansion (Nerem & Mirchum, 2001; Cazenaves & Nerem, 2004).

In the CLIMAR project (Belgian Science Policy) the longest available wave-height time series have been analyzed for the Belgian and Dutch coast. A clear statistically significant long-term trend is not visible for the period 1980-2007. Nevertheless, for most stations along the Belgian coast, a small decrease is found in extreme wave height (CLIMAR, 2007). This variability of wave height is consistent with: (i) the decrease in surge height observed at Ostend from ~1980 (Figure 26b) and (ii) the slight decrease in wind speed in the southern North Sea during the last two decades (CLIMAR, 2007; Van den Eynde et al., 2008). To summarize, daily to multi-decadal surge and wave height variability are strongly correlated to each other.
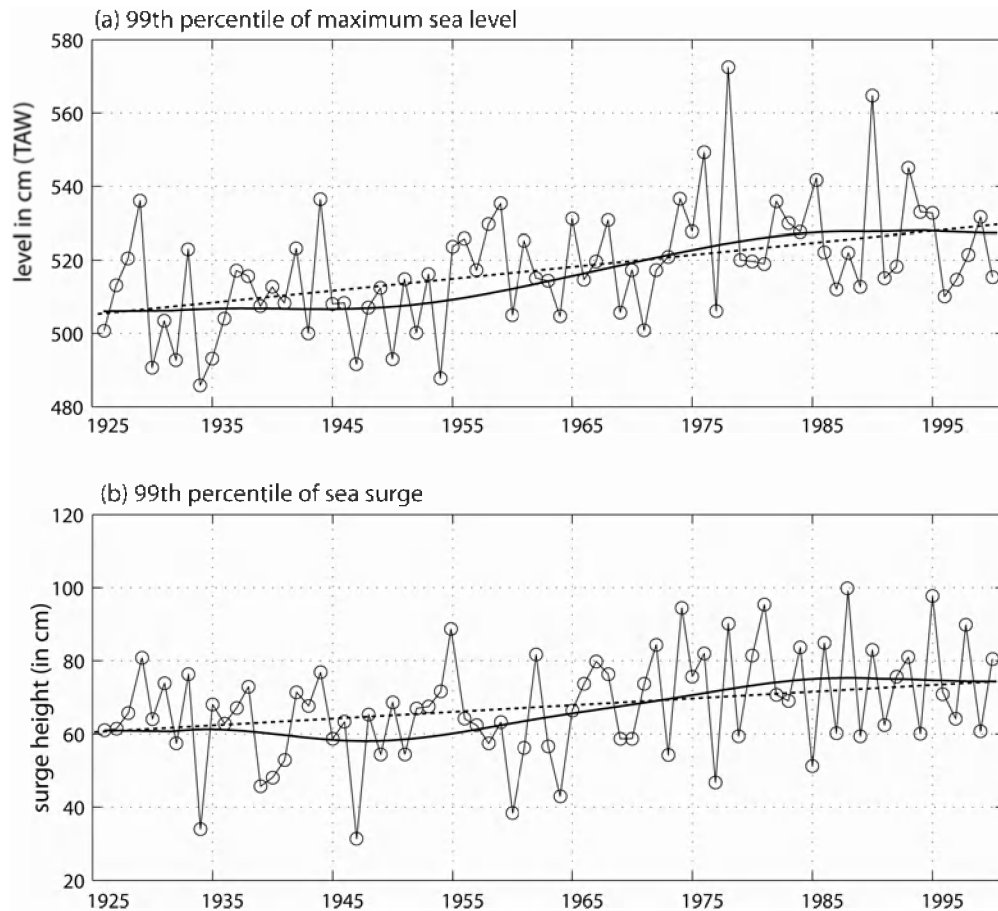
Figure 24.   (a) Wintertime (October-March) 99th percentile of daily sea-level at Ostend for the period 1925-2000. (b) Wintertime 99th percentile of daily surge at Ostend for the period 1925-2000. In superimposed bold curve: low-pass filtered variations retaining only periods longer than 30 years. Superimposed dashed line gives the linear trend.
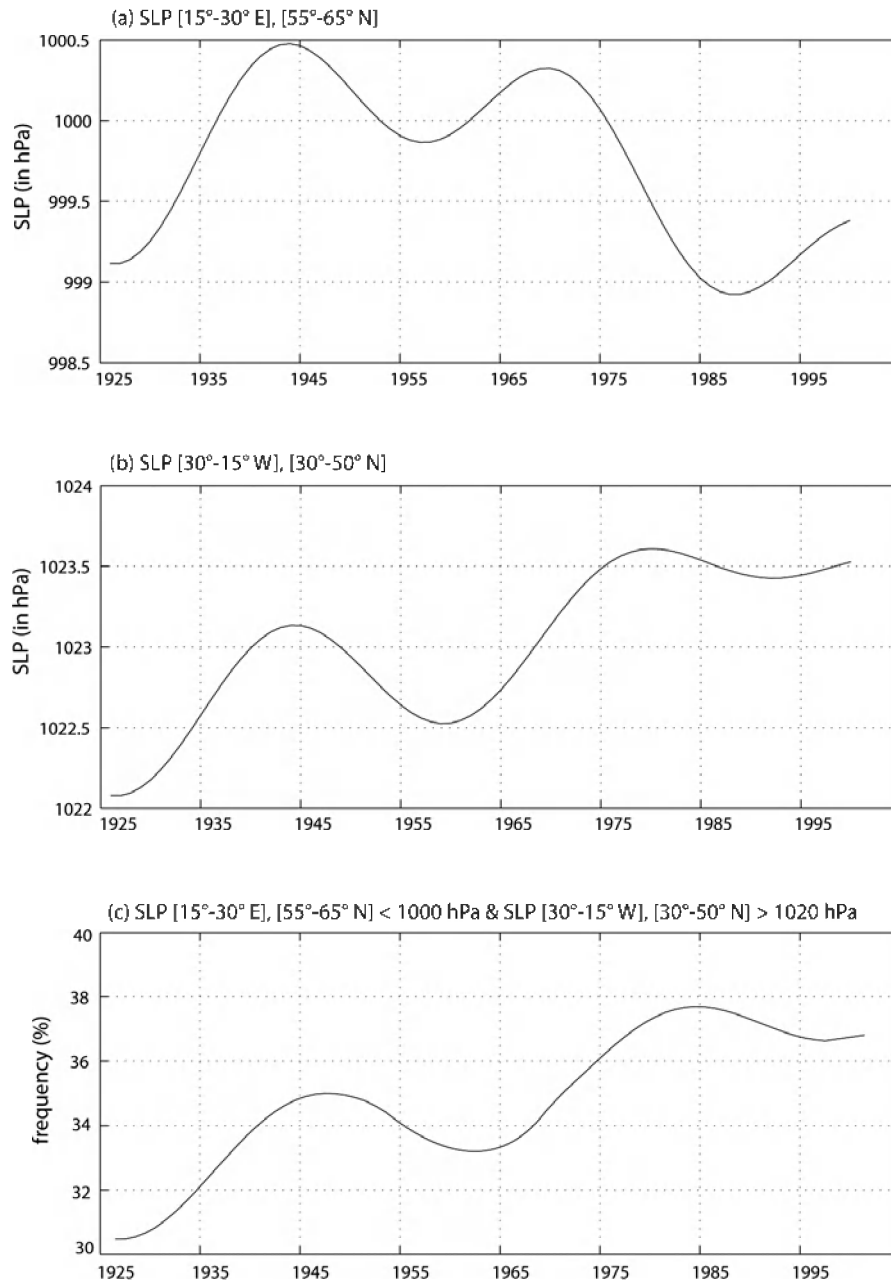
Figure 25.   (a) Low-pass filtered (retaining periods longer than 30 years) wintertime (October-March) mean sea-level pressure (SLP) averaged over [15°-30°E], [55°-65°N] and over (b) [30°-15°W], [30°-50°N] on the period 1925-2000. (c) Low-pass filtered wintertime frequency of days with SLP > 1020 hPa over (30°-15°W], [30°-50°N] associated with SLP < 990 hPa over [15°-30°E], [55°-65°N].

The highest sea surges and waves are associated with a strong southwest-northeast pressure gradient between high pressure around the Azores [30°-0°W], [35°-45°N] and low pressure over the Baltic Sea ([15°-20°E], [50°-55°N]). Figure 23 displays the low-pass filtered variability (only periods longer than 1/30 cycle-per-year) of the yearly mean SLP averaged over these two area. Figure 25b shows a clear increase of the SLP over the Atlantic, between 35°N and 45°N, particularly from ~1960 to 1980, consistent with the increase of the Azores high and the positive deviation of the North-Atlantic Oscillation shown in previous studies (Hurell & Van Loon, 1997; Machel et al., 1998). The behaviour of the SLP over the Baltic Sea is less monotonous and shows clear multi-decadal oscillations (Figure 23a). Nevertheless, over the whole available period the linear trend is not significant (Figure 23a). The yearly frequency of strong daily barometric gradient between low pressure < 990 hPa over the Baltic Sea and high

pressure < 1020 hPa over the Azores increased during the 20th century and particularly between 1960 and 1980 (Figure 27), synchronous with the SLP rise over the Azores (Figure 23b). This increase is consistent with the increase in sea-surge height and wind speed during the same period (Alexandersson et al., 2000; Weisse et al., 2005). Then, the yearly frequency of such daily barometric gradient slightly decreases until the beginning of the 21st century (Figure 23c) consistent with the weak decrease of surge height, wave height and wind speed in the southern part of the North Sea during the last two decades of the 20th century (CLIMAR, 2007).

<u>Statistical downscaling: model set-up for surge and wave height simulation</u>

There has been considerable interest and concern regarding the interannual and long-term variation of the amplitude of sea surges and waves and their dependence on SLP variability. Many studies, focusing on the German Bight have demonstrated the strong link between the intramonthly percentiles of sea surges and the seasonal SLP over the eastern North Atlantic (i.e. Heyen et al., 1996; von Storch & Reichardt, 1997; Langenberg et al., 1999). Following results presented in previous section, two SLP indexes are designed as predictors of surge and wave height along the Belgian coast:

> The first one is the daily SLP averaged over the Baltic Sea ([15°E-20°E], [50°N-55°N]) which is quasi-linearly correlated with the daily surge height at Ostend;

> The second one is the daily value of the pressure gradient between the SLP, averaged over the Baltic Sea ([15°E-20°E], [50°N-55°N]) and over the Azores ([30°W-0°W], [35°N-45°N]), corresponding to the difference between the highest and the lowest SLP area observed during highest surges and waves at Ostend. Moreover, this pressure gradient is clearly linked with the direction and strength of the Northwesterly atmospheric flow. This gradient has been empirically fitted in order to find the best correlation with the daily surge and wave height at Ostend.

A multiple linear regression was designed for the period 1950-2000 to relate daily surge height at Ostend to: (1) daily SLP averaged over the Baltic Sea and (2) daily value of the pressure gradient between the SLP averaged over the Baltic Sea and the Azores. A multiple linear regression has also been tested with daily wave-height anomalies for the period 1994-2001 (for each year, daily wave-height anomalies are computed as the difference between the daily maximum wave height minus the yearly mean wave height).

$$DH = (a * BS) + (b * GRA) + cst \qquad (4.1)$$

With coefficients a, b and cst (i.e. constant value), coefficients of the regression (Table 2) and with DH, hindcast daily wave-height anomaly / surge height (in cm), BS the daily sea-level pressure (in hPa) average over the Baltic Sea and GRA, the daily value of the pressure gradient (in hPa) between SLP averaged over the Baltic Sea and the Azores for the period 1950-2000. In many applications, the predictor does not completely specify the prediction (von Storch & Zwiers, 1999). In a prediction perspective, hindcast time series need to have the same standard deviation as the observations. To meet this requirement, it has been proposed to inflate the hindcast by setting a coefficient of inflation (Karl et al., 1990). For the daily surge-height and daily wave-height anomaly time series, a coefficient of inflation has been computed as the ratio between the standard deviation of observations and hindcast. This technique has been used in the downscaling literature to some extent (e.g. Huth, 1999).

Table 2. Coefficient of the regression (*a*, *b* and *cst*) and coefficient of inflation (*IF*) for the regression using daily SLP averaged over the Baltic Sea and the daily value of the pressure gradient between the Baltic Sea and the Azores as predictors of daily surge height at Ostend (second line) and of daily surge-height anomaly at Westhinder (third line).

	a	b	cst	IF
Surge (1950-2000)	-0.96	-0.22	968.3	1.65
Wave (1994-2002)	-1.4	-1.6	1457.6	2.2

At daily time scale, correlation between hindcasts and *in situ* observations is significant (r = 0.60 for surge height, r = 0.58 for wave-height anomaly) over 99% level of confidence according to a Student t-test. Monthly 90th percentiles have then been extracted from the inflated daily surge-height (wave-height anomaly) time series computed by the regression and compared with *in situ* observations at Ostend (Westhinder) for the period 1950-2000 (1994-2001) (Figure 24 and Table 3). The agreement between observed and hindcast monthly 90th percentile is very strong (Figure 24 and Table 3). In fact, the intra-seasonal and intra-annual variability is correctly reproduced by these statistical models. Moderate root-mean-squared error (RMSE) indicates weak uncertainties about the individual hindcasts (Table 3).
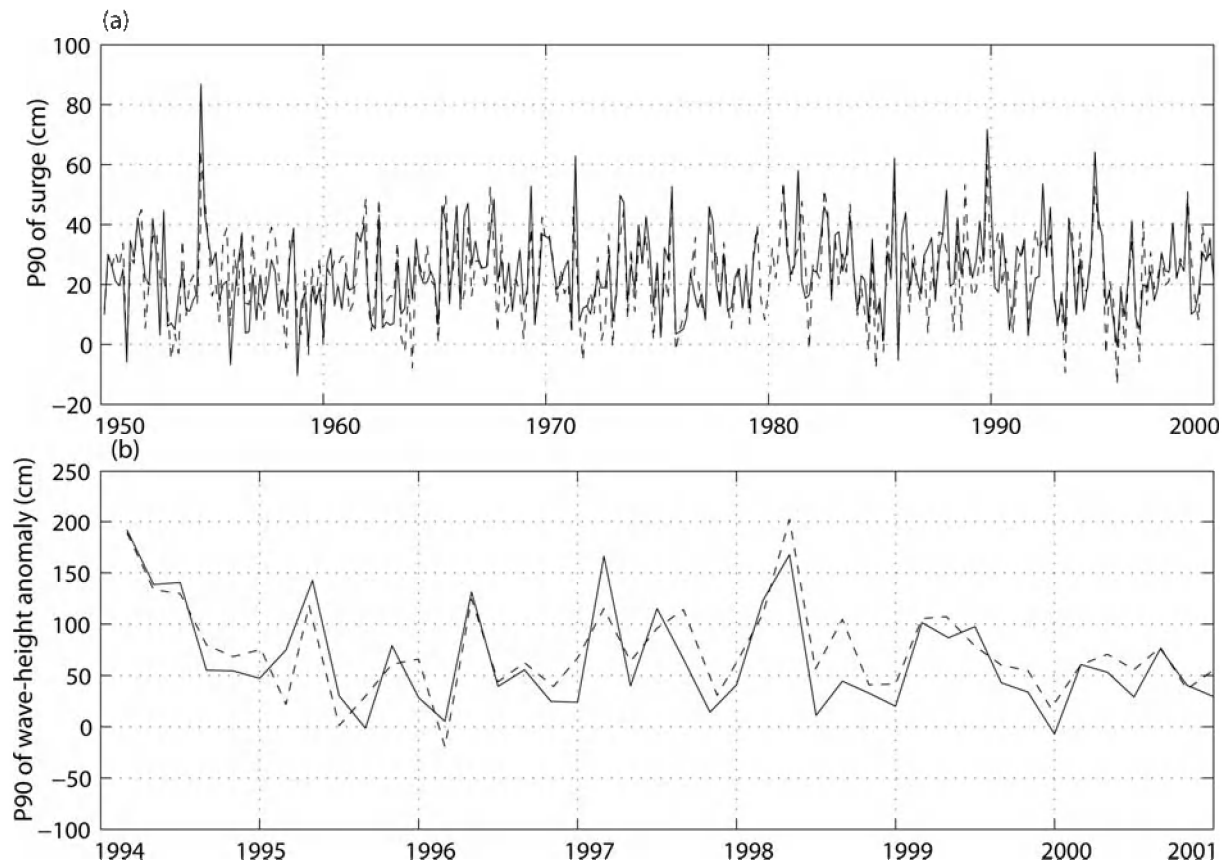
Figure 26. Time series of the monthly 90th percentile: (a) of surge at Ostend station for the period 1950-2000, and (b) of wave-height anomaly at Westhinder for the period 1994-2001. *In situ* observation (blue line) and estimated (red line) with the linear regression, using daily SLP averaged over the Baltic Sea, and the daily value of the pressure gradient between the Baltic Sea and the Azores as predictors.

Table 3.   Goodness-of-fit statistics of the monthly 90th percentile of surge (second line) and of wave-height anomaly (third line) estimated with the linear regression using daily SLP averaged over the Baltic Sea and daily value of the pressure gradient between the Baltic Sea and Azores as predictors and after inflation. With the linear correlation, the roots mean square error (RMSE) and the standard deviation (Std). Three stars indicate the two-sided 99% level of significance according to a random-phase test.

	Correlation (obs. vs hind.)	RMSE (cm)	Mean (cm)		Std. (cm)	
			Obs.	Sim.	Obs .	Sim.
Surge P90 (1950-2000)	0.76***	7.9	32.1	30.2	14.2	14.8
Wave P90 (1994-2002)	0.72***	8.1	68.1	71.3	50	47.3

21st century surge and wave height variability

The two linear regressions designed in the previous section have been applied to a 17-member ensemble run of SLP simulated by ECHAM-MPI/OM Global circulation model for the period 1950-2100 under A1b climate change scenario (ESSENCE project, Sterl et al., 2008). The yearly 90th percentiles of surge and of wave-height anomaly are then computed from all resulting daily surge-height time series simulated for the period 1950-2100. First of all, on the historical period (1950-2000), simulations and observations show the same statistical skills (not shown). Then, over the 21st century, the yearly 90th percentile of surge and waveheight anomaly appear stationary along the Belgian coast under A1b climate change scenario, despite a weak multi-decadal variability (Figure 25). Moreover, results are similar when using two single run of SLP simulated by ARPEGE (Royer et al., 2002) under A2 and B2 climate change scenarios (not shown). To summarize, future climate change, in an optimistic (B2), median (A1b) and pessimistic scenario (A2), would not significantly modify surge and wave height characteristics along the Belgian coast (Ullmann et al., 2009) during the 21st century.

During the 21st century, the yearly mean SLP over the Baltic Sea stays almost stationary (Figure 26). Even if the daily to interannual variability of surge and wave along the Belgian coast are quasi exclusively associated with SLP variability over the Baltic Sea, the SLP variability over the Azores could play a role over the long-term by modifying the strength of the pressure gradient between the Azores and the Baltic Sea. In other words, the SLP variability over the Azores could change the strength and direction of the atmospheric circulation over Western Europe and affect surges at local scale (Ullmann & Monbaliu, 2009). It is therefore important to have a large-scale view to analyze long-term changes in surges and waves at local and regional scale. The behaviour of SLP near the Azores stays almost stationary in each of 17-ensembles runs under A1b SRES scenario (Figure 26b). The yearly frequency of days associated with a strong pressure gradient between low pressure > 990 hPa over the Baltic Sea and high pressure > 1020 hPa over the Azores stays logically stationary during the same period (Figure 26c). No significant long-term trend has been found within the 17-ensembles runs. The same results are observed when considering the two single runs A2 and B2 (not shown). It means that in each storyline for the future climate considered in this study, i.e. B2, A2 and A1b, climate change (i.e. external forcing as GHG) would not significantly modify the strength and the frequency of high surge and high wave-related North-Westerly atmospheric flow in the southern part of the North Sea.
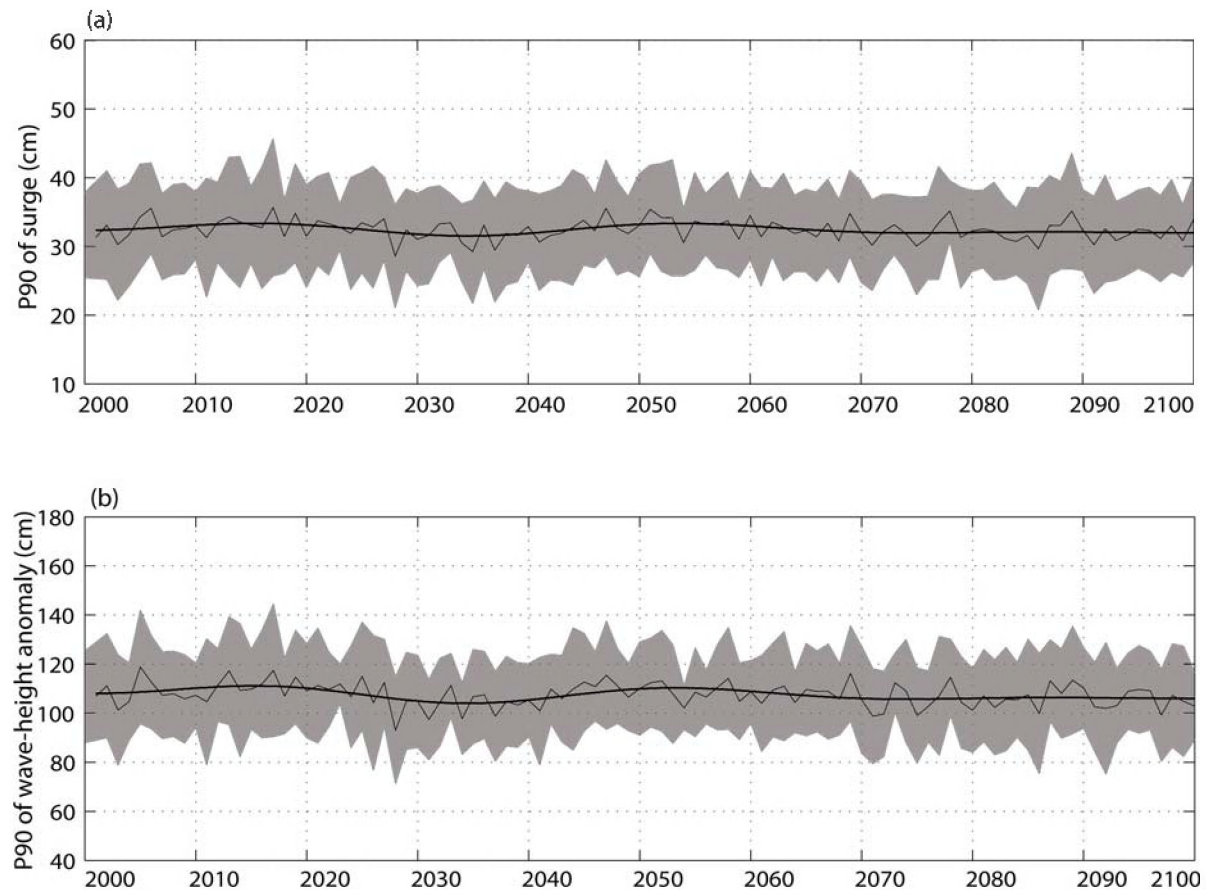
Figure 27.   (a) Thin line: mean of the 17-ensembles time series (A1b) of wintertime 90th percentile of sea surges for the period 2000-2100. Bold line: 30 year low-pass variations using a recursive low-pass Butterworth filter (Butterworth, 1930). The gray shading represents the variability within the 17-ensembles time series in each winter (i.e. the yearly mean +/- one standard deviation). (b) The same for wintertime 90th percentile of wave-height anomaly.

Conclusion

From this study, one can conclude that climate change for the 21st century would not significantly modify surge and wave-related atmospheric circulation. Nevertheless, the mean sea-level rise, associated thermal dilatation and ice melting, will ineluctably increase the amplitude of sea level peaks during storm events. Following the different climate change scenarios for the 21st century, proposed by CLIMAR, and interpreting the results from this study, it is logical to retain the two most likely scenarios for the Belgian coast: (1) a medium scenario (M), with no changes in storminess and storm-related surges and waves, and with a medium rate of sea-level rise of +6.0 mm/year (i.e. +60 cm until 2100); and (2) a warm scenario (W), with still no changes in storminess, but with an accelerated mean sea-level rise, with a mean rate of +9.3 mm/year (i.e. +93 cm until 2100); this corresponds to the upper rate of the IPCC's estimations (IPCC, 2007).
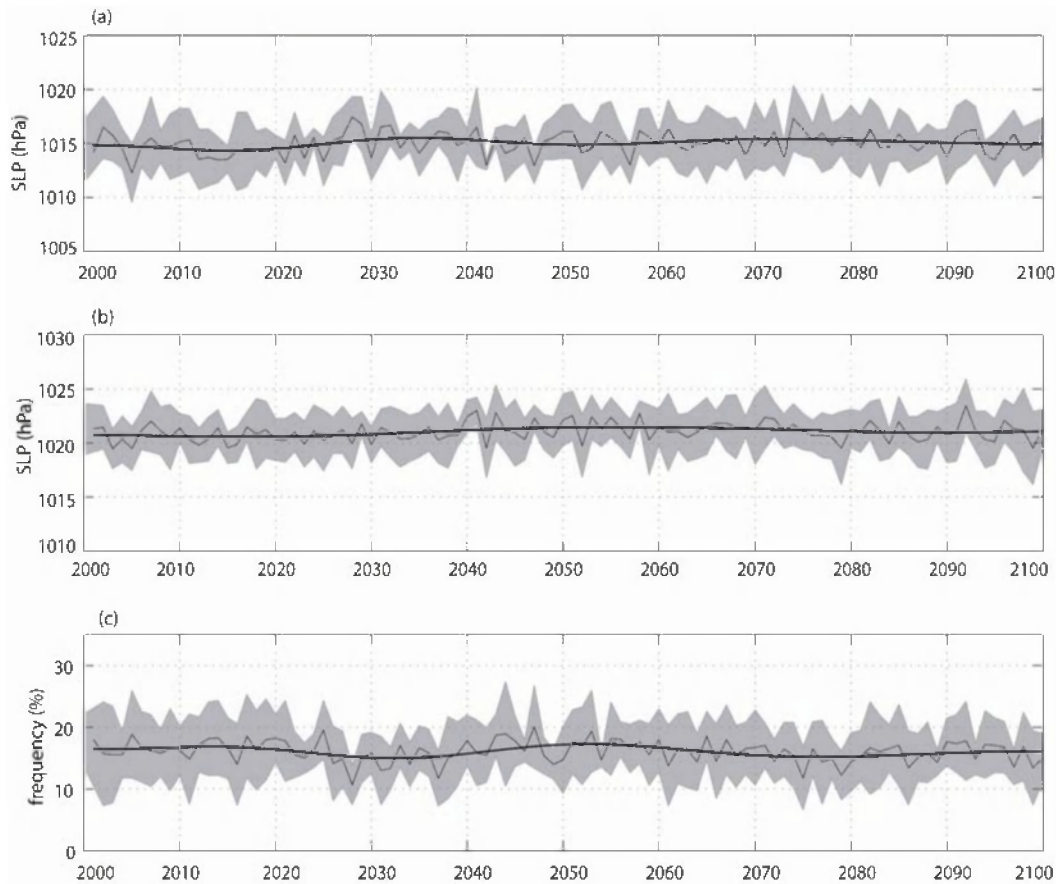
Figure 28. Thin line: average of the 17-ensembles time series of wintertime mean SLP (a) over the Baltic Sea ([15°E-20°E], [50°N-55°N]), (b) over the Azores ([30°W-0°W], [35°N-45°N]) and (c) of the frequency of daily SLP over the Baltic Sea < 990 associated with SLP > 1020 over the Azores (2000-2100). Bold line: 30 year low-pass variations using a recursive low-pass Butterworth filter (Butterworth, 1930). The gray shading represents the variability within the 17-ensembles time series in each year (i.e. the yearly mean +/- one standard deviation).

4.2 Impact of human activities

4.2.1 Long-term effect of harbour extension works

East of Zeebrugge Harbour, in the Bay of Heist, a sandbank has formed which has emerged recently. Based on a trend analysis of a time series of bathymetric data, erosion and sedimentation patterns were investigated, since the construction of the groynes of the outer harbour of Zeebrugge (1977-1986). 7 bathymetric charts (years: 1987, 1990, 1993, 1995, 1997, 1999 and 2003) were used with a grid cell resolution of 20x20m. For each grid cell, a linear least squares fit is performed on the time series of the 7 depth values. The slope of the resulting straight line gives the erosion trend for that particular grid cell, while the coefficient of determination R^2 gives an indication of the significance of the erosion trend. Some results of the linear least squares fit are shown in Figure 29: the chart gives the space-dependent erosion rate in the Bay of Heist. Negative values of the erosion rate are to be interpreted as sedimentation rates, and locations where $R^2 < 0.5$ are left out because the significance of the erosion/sedimentation trend is too low for these locations.
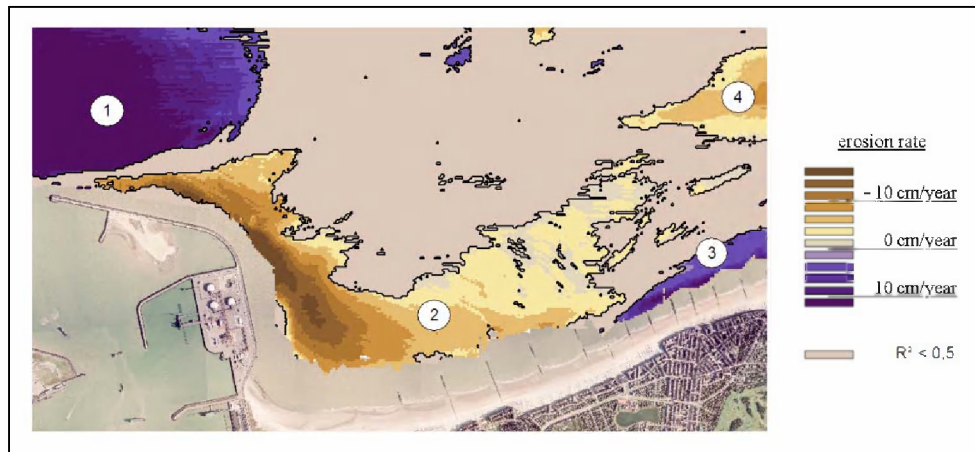
Figure 29.   Erosion rates in the Bay of Heist.

Four regions can be distinguished: (1) the entrance of the outer harbour of Zeebrugge. A clear erosion trend can be observed, due to the high flow velocities resulting from the contraction of the stream lines, caused by the groynes of the Zeebrugge harbour; (2) Bay of Heist: this region is prone to sedimentation, due to low flow velocities, resulting from the sheltering effect of the eastern groyne; (3) the Appelzak, a tidal gully; and (4) a shoal, called Paardenmarkt, located close to a dredge disposal site.

Sedimentation seems to be the consequence of two mechanisms, qualitatively depicted in Figure 19. Green: sedimentation is the result of the low flow velocities, due to the sheltering effect of the eastern groyne. Light blue: sedimentation parallel to the eastern groyne; the mechanism for this preferential sedimentation zone is not clear, but is possibly the result of the wave attenuation effect of the eastern groyne. Dark blue: remarkable is that the overlap between these two preferential sedimentation zones corresponds to the location of the new emerging sandbank.

Figure 29. Qualitative representation of the sedimentation patterns in the Bay of Heist.

4.2.2   Long-term effect of the disposal of dredged material

Sedimentation patterns were investigated along a disposal ground of dredged material (B&W S1), based on chrono-sequential multibeam and single-beam echosounding data, together with disposal intensity data and the analysis of vibrocores. Part of the data is reported under Task 1.1.1 and has been published in Du Four & Van Lancker (2008). Extensive reporting on the vibrocore analysis can be found in Dezeure (2007) and Veys (2008). Here, only a summary is given with emphasis on the coupling of the observations with disposal intensity data and the results from the vibrocore analysis.

Difference maps of chrono-sequential single-beam data from 1976 till 2006 demonstrate that the disposal of dredged material has strongly altered the former morphology of the area. Sediments have not only accumulated on the disposal site B&W S1, but also far outside, mainly towards the navigation channels, more specific to the SW. This SW-directed bedload transport is further confirmed by the consistent ebb-dominated asymmetry of the very large dunes and their SW migration. These findings contrast the overall flood dominated residual current transport

direction. The disposal efficiency has been estimated as 30-40%, based on a comparison between the actual disposed amount of dredge spoil and the sediment volume changes.
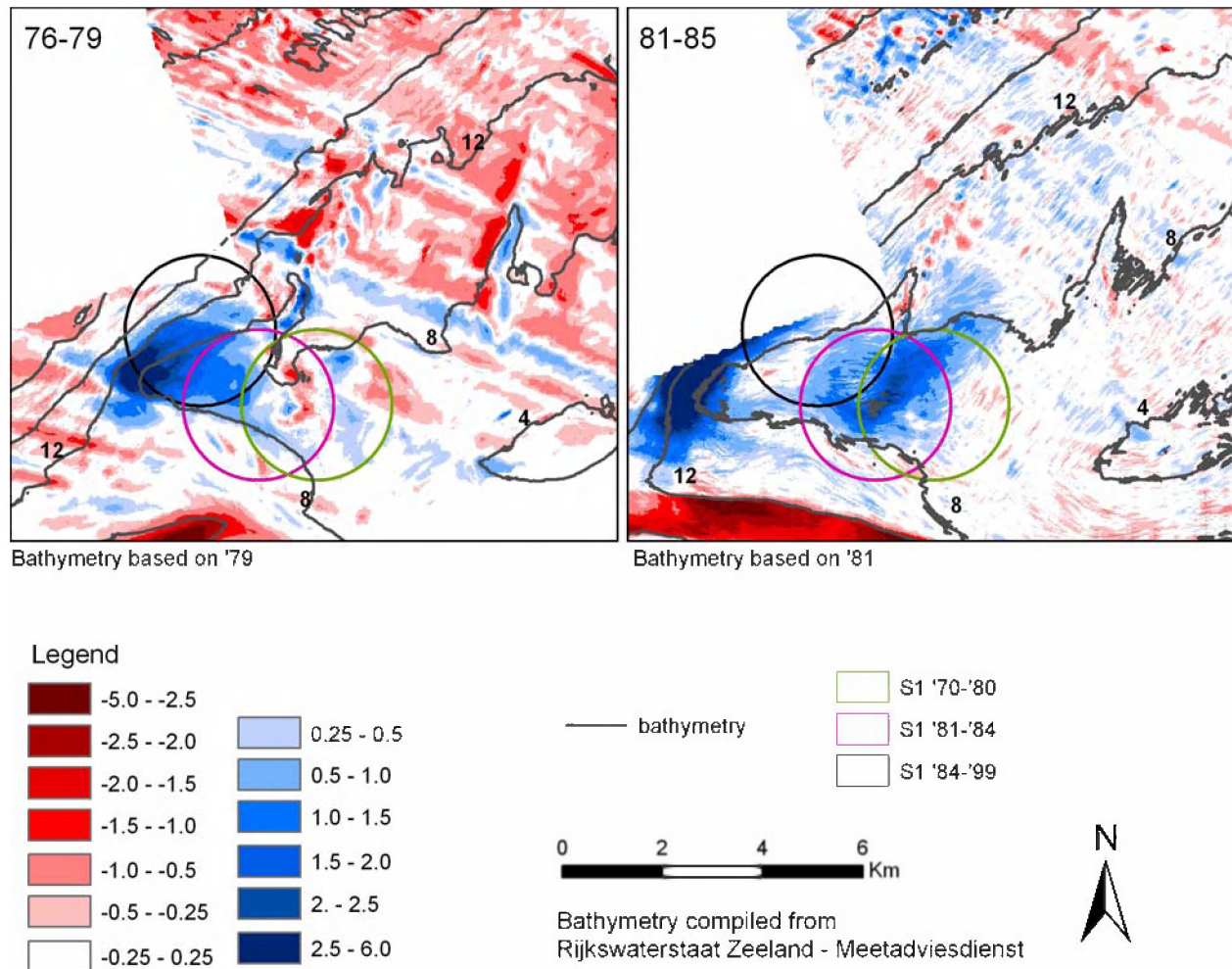
Figure 30.   Examples of depth difference maps in the Vlakte van de Raan region. Blue sedimentation; Red erosion.

Vibrocore analyses (density profiles, lithological descriptions, photographs, sediment subsampling) and integration with depth evolution and disposal intensity data allowed to differentiate natural from anthropogenically-induced sedimentation. The latter is particularly demonstrated along the old and new disposal sites, though each having different sedimentation patterns, because of their difference in morphological setting (Figure 31). On the old disposal site, mainly sandy sediments are found, whilst on the new one, the mud fraction is higher. As the old disposal site is located on a sandy shoal, the sediments will be winnowed and reworked more by waves than in a tidal gully. However, if hard clay from Tertiary or Holocene origin, originating from deepening works, is disposed, it remains in-situ, both on the new disposal site, as well as on the old one.
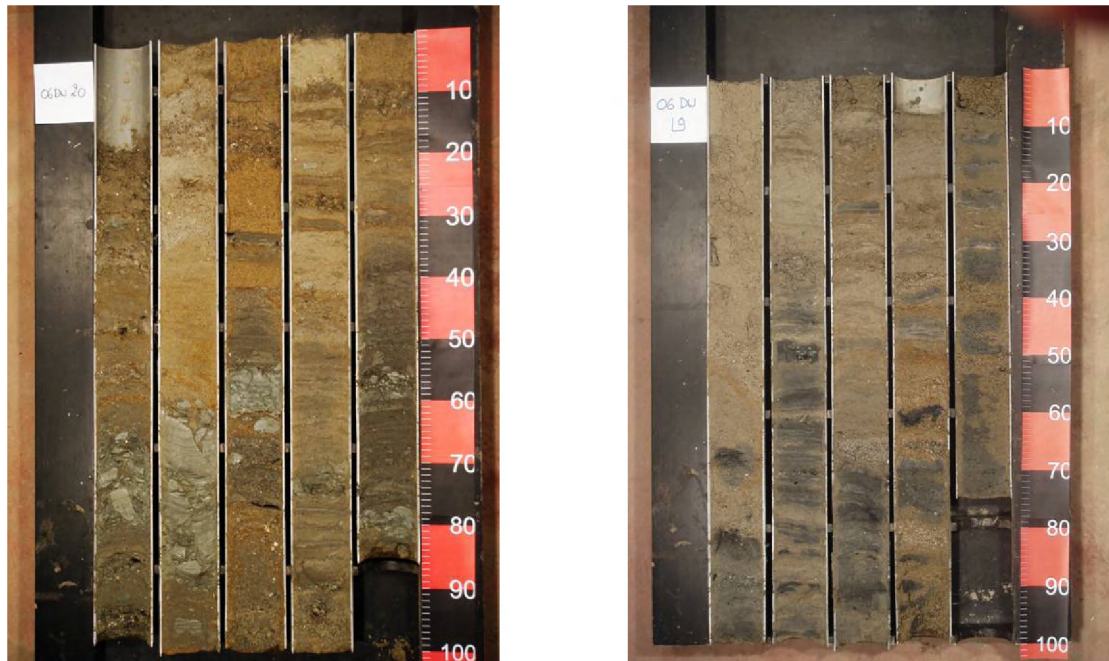
Figure 31.   Photograph of 2 vibrocores taken on: a) the present disposal site; and b) the old disposal site.

To assess the natural sedimentation, difference maps, showing an alternation of erosion and accretion were compared over 30-yrs. From this, the dynamical character of the region was demonstrated, both at present and in the past. The latter emerged from a rather complex subsurface deposition, comprising Holocene sands, silty tidal flat deposits and Tertiary clays.

4.2.3   Long-term influence of maritime access works on the distribution of cohesive sediments

Long-term changes in the cohesive sediment distribution of the BPNS nearshore zone are related to human activities (port construction, deepening of navigation channels, disposal of dredged sediments) and to natural variability, due to tides and meteorological effects. Results are based on the combined analyses of recent and historic (100 years ago) sediment sample information and bathymetric maps. Data processing was based mainly on field descriptions of the samples (consolidation, thickness) and on bathymetric maps of 1866–1911. Results indicate that the distribution of fresh mud and suspended sediment has changed during the last 100 years, due mainly to maritime access works. Most of the present deposition of thick layers of fresh mud (> 30 cm) has anthropogenic causes. The results further indicate that erosion of older Holocene mud has increased in recent times and, as a consequence, higher amounts of fine-grained sediments are being released into the southern North Sea today. Further readings see Fettweis et al. (in press).

4.2.4   Impact of beam trawling on the BPNS

Beam trawling on the seabed can be revealed from very-high resolution sonar imagery (Van Lancker et al., 2007). However, to evaluate the spatial extent of impacts and to extrapolate some of the findings, data are needed over wide areas. Datasets from various sources (e.g. from UG-RCMG and FPS Economy, SME's and Energy) have been merged (ArcGIS), and multibeam tracklines were sailed additionally to bridge some of the most important gaps. From the datasets, the spatial extent of fishing activities was estimated, hitherto never done before. The analyses required a careful processing of the data, as also advanced filtering techniques to remove noise and artefacts (i.e. spatial frequency filtering and spatial directional filtering). Results are

extensively reported in Janssens (2009). Figure 32a/b shows the results for the Thornton Bank. The final results show the beam trawling disturbance of the seafloor, calculated per 250m grid cell. Generally, fishing activities are concentrated mainly in the swales of sandbanks, with highest disturbance towards the foot of the steep slope of the sandbanks. For the Thornton Bank (Figure 32), it is clear that its swale to the southwest is trawled most heavily. The percentage of disturbance easily reaches 30%, with maximum values up to 73%. Comparison of these areas with other datasets shows that these areas: (1) are mostly flat (BPI analysis, Verfailie et al., 2007); (2) have a higher amount of gravel (sediment maps (Van Lancker et al., 2007) and high multibeam backscatter values); (3) have higher percentages of silt and clay (sediment maps (Van Lancker et al., 2007)); (4) have higher predicted values of the *A. alba* community (Degraer et al., 2008); and (5) are hydrodynamically less energetic (maps Van Lancker et al., 2007). Results for the Oostdijck sandbank show similar disturbance values, in both swales adjacent to the sandbank, though towards the steep slope the values are somewhat higher. The disturbance is calculated as 16% maximally. A methodology is now in place to evaluate fisheries activities on a large-scale, whenever new high-resolution and good quality multibeam data are available. These data are crucial in the evaluation of long-term changes in soft-substrata habitats.
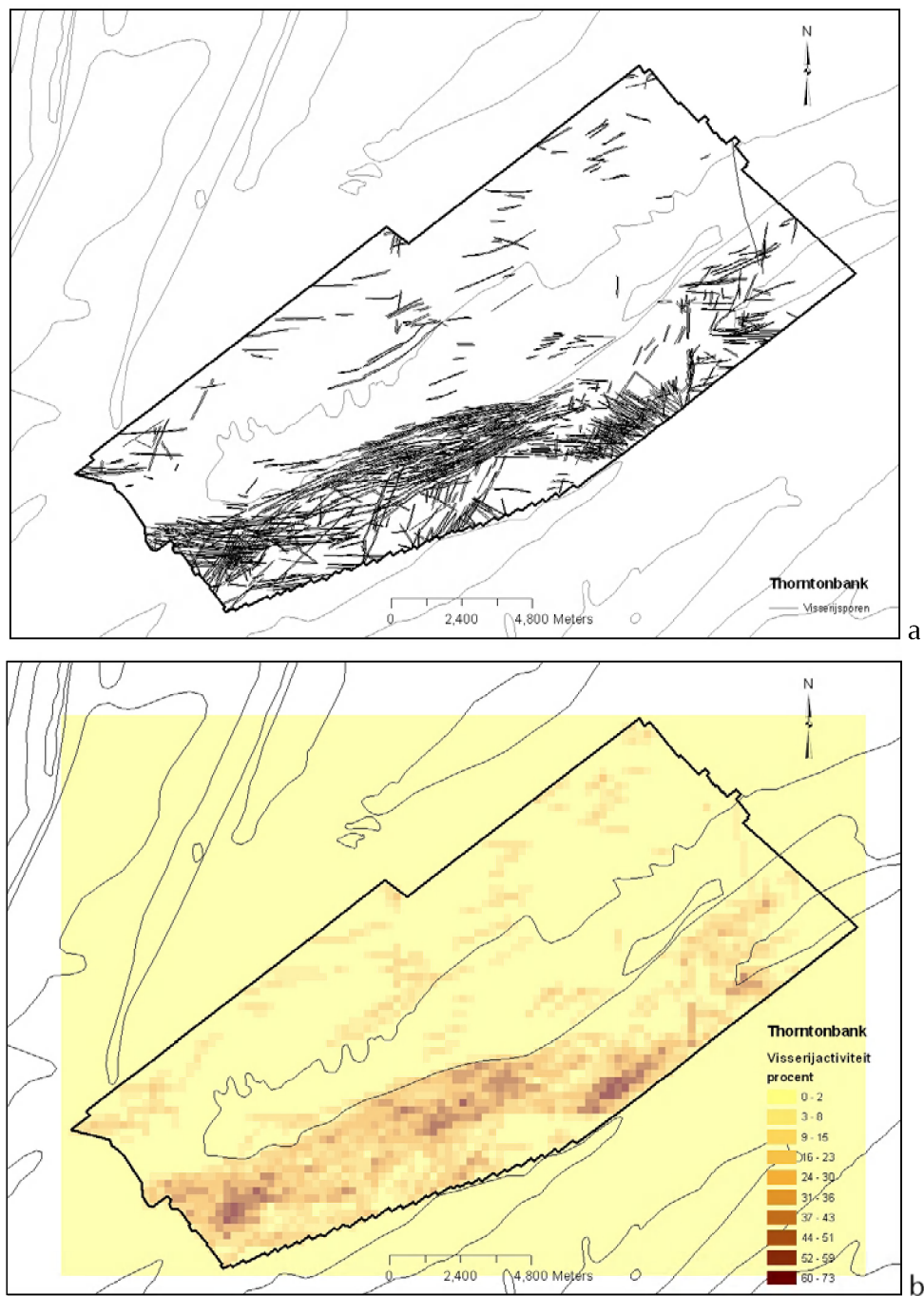
Figure 32. (a) Identification of beam trawling marks, on the basis of very-high resolution multibeam backscatter data (2m data resolution within the delineated area); (b) quantification of the marks on a 250m grid. A maximum of 73% disturbance of a grid cell was calculated; on the Oostdijck sandbank, a maximum of 16% only was obtained.

5.   DATA MANAGEMENT AND VALORISATION

Information on sample, hydrodynamic, sediment transport and acoustic data is compiled in GIS. The basis is the GIS@SEA Information System (Van Lancker et al., 2007). Information on the field campaigns, including cruise reports, can be found on the Q4D website: http://www.vliz.be/projects/quest4D/news.php#field. GIS models are built to incorporate the data in an efficient way. Datasets, received so far, are imported in the database (http://www.mumm.ac.be/datacentre/Databases/QUEST4D/index.php): erosion rates at different excess shear stress values, bulk densities and grain size parameters. They can be downloaded by the project partners using the online query interface. Currently the adaptation of the database and the development of the specific query module for data series are being finalized. This query module will enable the download of series of measurements based on selection criteria. The preparatory work for data import of the historical Gilson datasets on sediment and benthos has started. For sediment data, a part of the samples (59 until now) is already imported in the QUEST4D database. For benthos, information from Darwin, as well as the digitized information from Gilson's list is considered.

Valorisation of results is done on a regular basis. A project website with a public and restricted area is available (http://www.vliz.be/projects/quest4D) and can be adjusted according to the needs of the Quest4D consortium. The restricted area gives access to restricted documents and publications, but also to an FTP server and a message board. The Quest4D leaflet (http://www.vliz.be/projects/quest4D/docs/folder%202008.pdf) is distributed at national and international fora. Publication is also made at the foundation "SeaOnScreen" (http://www.seaonscreen.org, with i.e. posters, 'newspaper', animations) with the aim of showing the public and politicians the value of the North Sea. A series of posters was created, highlighting exploration and characterization of the seafloor. The posters were used during the "Wetenschapsfeest" (17-19/10/2008), an initiative of the Flemish Government and Technopolis.

On May, 14th 2009, an international discussion workshop was organised entitled 'Sediment dynamics and increasing anthropogenic pressure: ways forward? (Conveners: Van Lancker, Fettweis & Vanlede). The maximum of participants was reached (50). 5 invitees from abroad successfully added value to the discussions.

Valorisation also takes place during meetings with a follow-up committee, consisting of governmental organisations (Flemish/Federal), industrial groups and the main users of the EEZ (see 7). An overall kick-off meeting took place in Brussels on 26/03/07. Targeted end-users meetings were held at 19/11/07, 27/06/08 and 14/05/09 (together with Quest4D workshop). Ad hoc technical meetings took place with most of the end-users, to ensure exchange of data or equipment. (http://www.vliz.be/projects/quest4D/news.php#oral).

A1 Publications, based on results within Quest4d

Du Four, I. and Van Lancker, V. 2008. Changes of sedimentological patterns and morphological features due to the disposal of dredge spoil and the regeneration after cessation of the disposal activities. Marine Geology 255, 15-29.

Fettweis, M. 2008. Uncertainty of effective density and settling velocity of mud flocs derived from in-situ measurements. Estuarine, Coastal and Shelf Science, 78, 426-436.

Fettweis M, Houziaux J-S, Du Four I, Van Lancker V, Baeteman C, Mathys M, Van den Eynde D, Francken F, Wartel S., in press. Long-term influence of maritime access works on the distribution of cohesive sediment: Analysis of historical and recent data from the Belgian nearshore area (southern North Sea). Geo-Marine Letters.

Fettweis, M., Francken, F., Van den Eynde, D., Verwaest, T., Janssens, J. and Van Lancker, V., subm.. Storm influence on SPM concentrations in a coastal turbidity maximum area (southern North Sea) with high anthropogenic impact. Continental Shelf Research.

Rabaut, M., Du Four, I., Van Lancker, V., Degraer, S. and Vincx, M., subm. Ecosystem engineers stabilize sand bank systems: investigating valuable *Owenia fusiformis* microhabitats using multibeam and side-scan sonar. Remote Sensing of the Environment.

Ullmann A., Monbaliu J., 2009. Changes in atmospheric circulation over the North Atlantic and sea surge variations along the Belgian coast during the 20th century. International Journal of Climatology. Doi: 10.1002/joc.1904

Ullmann A., Sterl A., Van den Eynde D., Monbaliu J., subm. Atmospheric pressure and sea surges along the Belgian coast during the 20th century and changes in sea-surge height under climate change. Continental Shelf Reseach.

6.   CONCLUSIONS AND RECOMMENDATIONS

The ecosystem in the space, time, depth domain

Sediments and sediment transport

● Apart from hydrodynamics, origin of water masses, waves and bed composition, it has been shown that the occurrence of mixed sediments and their variability, the effects of waves on the failure of consolidated mud beds and the erosion effects of sand on top of consolidated mud are main drivers of sediment transport in the Belgian coastal zone.

● Long-term measurements with the tripod have shown that a high SPM concentration layer (> 3g/l) is formed regularly near the bed and can often be related to the occurrence of high SPM concentration during previous stormy periods. The knowledge of occurrence of persistent near-bottom high SPM concentration layer in the Belgian near-shore area is new. Further research has to be carried out in order to understand its dynamics and its influence on the high siltation rate in the 'Pas van het Zand' navigation channel and in the port of Zeebrugge.

● From in-situ measurements on sediment erodibility, crucial for adequate model input, it has been shown that mud erosion is mostly a surface phenomenon; the critical shear stress for erosion increases rapidly with depth.

● Results from clay mineralogy show a provenance relationship between BPNS mud and the Scheldt river system that existed on and off since the Late Pleistocene. These results would benefit from extending the clay mineralogy analyses to the entire North Sea area, in particular the Netherlands and France. Future analyses should include, ideally, information based on e.g. geochemistry, heavy minerals, microfossils.

● The measurements and observations in the area north of the Vlakte van de Raan show the importance of bedload transport. The sand transport is directed towards the SW, while residual currents are in a NE direction. This is contrary to what would be expected from the 'general' intuitive believe that long-term sediment transport is either in the direction of the residual currents or in the direction of the strongest (usually) flood currents. In view of predicting long-term trends, using numerical sediment transport models, a better understanding of these processes is necessary. The latter could be an illustration of the effect of waves that can alter the direction of sediment transport or density-driven currents should be better modelled in the area of the Westerschelde estuary. Systematic simulation of currents and waves is recommended, as also a dedicated measurement campaign, if feasible.

● The effect of biota on bedform stability is shown clearly and needs further investigation. In particular, the causes of high biodiversity patches should be further investigated.

Long-term ecosystem changes

● The historical data indicate that environmental changes can indeed be traced to verify assumptions on the effect of human impact at sea. However, in coastal waters, the signal is seemingly weaker than in the offshore, most probably due to the fact that climatic variability affects greater amount of physiographic forcing conditions than in the offshore. Offshore areas are thus apparently more sensitive to direct impacts at sea, hence deserve more attention on the irreversibility of certain subsequent losses in the benthic compartment.

● It is hypothesised that the composition of coastal macrobenthic communities undergoes NAO-mediated changes. The high NAO conditions prevailing since 20 years, together with certain human activities, create conditions of turbidity which favour opportunistic

siltation-resistant species, of which polychaetes are prominent. As such, tidal siltation rates, rather than sediment silt content may influence macrobenthos in the coastal zone. Indeed, the high turbidity area does not match exactly the distribution of surface muddy sediments, a part of which is consolidated and ancient, at a given moment. Predictability of community composition seems to be driven primarily by prevailing NAO conditions and should be accounted for in future habitat suitability modelling studies. To that purpose, re-investigation of data available in the period 1955-1973 should provide insight into the cyclic pattern of benthic composition.

● No significant movement of the sandbanks on the BPNS could be demonstrated, during the last 150yrs. Some banks (especially the Coastal Banks seem to be prone to erosion at the seawards side and to sedimentation at the coastal side, which could indicate minor movement towards the coast. The Grote Rede swale, landward of the Wenduine Bank has clearly accreted. The Flemish Banks show accretion along their SW extremity, and erosion along their NE part. The troughs in-between the banks experienced erosion, resulting in steeper slopes of the banks.

● In the Belgian coastal zone, an enrichment of fine sandy sediments is found, inducing more poorly sorted sediments than 100yrs ago; spatially these changes are mostly linked to harbour areas, disposal grounds, and aggregate extraction sites; though the shallowing trend and enrichment of fine sands is confirmed, both along anthropogenically-steered, as well as along 'natural' systems, based on high resolution short- to medium-term observations and sampling.

Modelling of processes

● To account for erosion of old sediments (Holocene and outcropping Tertiary clays), improved bed models, distinguishing between active and parent layers, are needed to simulate the BPNS sediment transport.

● Classical flocculation models, based on an empirical approach, are not able to satisfactory reproduce the measurement data. A comprehensive understanding of SPM dynamics and its implications in coastal morphodynamics must include the mineral, as well as the microbial fraction. Because the mineral and organic constituents are strongly correlated to the site, a calibration of a flocculation model will be largely site specific. It is therefore important to have data on the suspended matter and the organic concentration at the same moment.

● An important part of our understanding of flocculation and cohesive sediment dynamics (deposition and erosion) is based on measurements. The uncertainties associated with indirect (or direct) settling velocity measurements are very high due to their statistical nature; the total error will be even higher because systematic errors due to a lack of accuracy of the measuring instruments have not been included. Our results underline that the statistical nature of flocculation processes and settling velocity must be taken into account when modelling cohesive sediment transport by at least a standard deviation of settling velocity based on measurements or by introducing a floc size (and settling velocity) distribution in numerical model.

● Mud balances computed by modelling result in a yearly net export of 2 Mton from the Scheldt estuary, being still one order of magnitude larger than the net import following from traditional mud balances. Exact numbers from observations involve large uncertainties and are not well known, but estimates range from 0.05 to 0.35 Mton yearly net import. Since it appears that the model's concentration gradient between inner and outer estuary is realistic, the computed export is probably due to an underestimation of the estuarine circulation and the observed phase error of the M4 tidal component. The latter influences the tidal asymmetry and thus also the residual sediment transport.

● Wave turbulence and wave energy dissipation and their importance in the turbulence part of hydrodynamic models need further attention in the modelling and interpretation of current field (including turbulence) measurements and its consequences for SPM modelling.

Natural and anthropogenic impact

Natural evolution and climate change

● For a sandbank area, a correlation was found between sediment volume changes and the directionality and strength of sand transporting agents: winds, waves and currents. Generally, northeastern conditions are associated with the lowest sediment budgets, whilst winds blowing from the southwest are clearly associated with a sediment input.

● The influence of storms on SPM concentration depends on the direction of wind, on wave height and on the availability of erodible cohesive sediments. It is argued that local mud sources, such as mud in sandy beds or consolidated mud layers, have to exist besides the well-known and generally accepted English Channel as major source of SPM.

● It is not expected that climate change for the 21st century would significantly modify surge and wave-related atmospheric circulation. Nevertheless, the mean sea-level rise, associated thermal dilatation and ice melting, will ineluctably increase the amplitude of sea level peaks during storm events. Possible links between hydro-meteorological parameters (storm-surges, waves) and beach and foreshore volumes for the Belgian coast will be investigated further. A downscaling approach will be then used to design statistical models to simulate interannual to multi-decadal variability of beach's volume with as input large-scale atmospheric features (atmospheric pressure, weather regimes), which are well resolved by climate models. The final aim is to use these statistical models with climate models outputs to forecast possible beach's volume variations along the Belgian coast due to future climate change.

Impact of human activities

● The long-term effect of harbour extension works has been demonstrated with the case study 'Bay of Heist'. A strong sedimentation trend was revealed in the bay itself and in a zone parallel to and some 100m away from the eastern groyne of Zeebrugge harbour. The former results from low flow velocities, due to the sheltering effect of the eastern groyne; whilst the latter sedimentation pattern is due possibly to the wave attenuation effect of the eastern groyne.

● The regional impact assessment of long-term disposal of dredged material in area of the Vlakte van de Raan (B&W S1) showed a clear difference in sedimentation patterns between the old and the present disposal site of dredged material. A difference in morphological setting is important, but also the type of material that has been dumped. Natural from anthropogenically-induced sedimentation could be distinguished. Still, sediment transport processes of this area need further investigation to get a better insight in the consequences of the disposal of dredged material in near coastal areas.

● The study of long-term changes in the cohesive sediment distribution of the Belgian–Dutch nearshore zone, has shown that the distribution of fresh mud and suspended sediment has changed during the last 100 years. This is thought to be due mainly to maritime access works, though the effect of NAO cyclicity needs further investigation.

● A methodology is now in place to quantify the spatial distribution of beam trawling activities on the BPNS. Generally, fishing activities are concentrated mainly in the swales of sandbanks, with highest disturbance towards the foot of the steep slope of the sandbanks. These data are crucial in the evaluation of long-term changes in soft-substrata habitats.

REFERENCES

Alexandersson H., Tuomenvirta H., Schmith T., Iden K., 2000. Trends of storms in NW Europe derived from an updated pressure data set. Clim. Res., 14: 71-73.

Andersen, T. J., Fredsoe, J., Pejrup, M. 2007. In-situ estimation of erosion and deposition thresholds by Acoustic Doppler Velocimeter (ADV). Estuarine, Coastal and Shelf Science, 75, 327-336.

Borovec, Z. 1996. The relationship between the content of organic carbon and total organic matter in the stream sediments of Czech rivers. European Water Pollution Control, 6(4), 15-20.

Brockamp, O., Zuther, M., 2004. Changes in clay mineral content of tidal flats sediments resulting from dike construction along the Lower Saxony coast of the North Sea, Germany. Sedimentology, **51**, 591-600.

Cazenave A., Nerem R.S., 2004. Present-day sea level change: observations and causes. Rev. Geophys., 42, RG3001, doi: 10.1029/2003RG00139.

Chang, T.S., B.W. Flemming and A. Bartholomä, 2007. Distinction between sortable silts and aggregated particles in muddy intertidal sediments of the East Frisian Wadden Sea, southern North Sea. Sedimentary Geology, 202, 3, 453-463.

CLIMAR. 2007: Impact of climate change on the physical and chemical parameters of the North Sea. Literature study. 70pp.

Degraer, S., Verfaillie, E., Willems, W., Adriaens, E. Vincx, M. Van Lancker, V. 2008. Habitat suitability modelling as a mapping tool for macrobenthic communities: An example from the Belgian part of the North Sea. Continental Shelf Research, 28(3):369-379. doi: 10.1016/j.csr.2007.09.001.

Degraer, S., U. Braeckman, J. Haelters, K. Hostens, T. Jacques, F. Kerckhof, B. Merckx, M. Rabaut, E. Stienen, G. Van Hoey, V. Van Lancker & M. Vincx (2009). *Studie betreffende het opstellen van een lijst met potentiële Habitatrichtlijn gebieden in het Belgische deel van de Noordzee*. Eindrapport in opdracht van de Federale Overheidsdienst Volksgezondheid, Veiligheid van de Voedselketen en Leefmilieu, Directoraat-generaal Leefmilieu. Brussel, België. 93 pp.

Dezeure, B., 2007. Sedimentation rates at dumpsites of dredged material. Thesis submitted to obtain the degree of Master in Science in Advanced Studies in Marine and Lacustrine Sciences. Unpublished Msc Thesis, Gent (B): Universiteit Gent (Renard Centre of Marine Geology), 38 pp.

Du Four, I., Van Lancker, V. 2008. Changes of sedimentological patterns and morphological features due to the disposal of dredge spoil and the regeneration after cessation of the disposal activities. Marine Geology, 255, 15-29. doi:10.1016/j.margeo.2008.04.011.

Fettweis, M., Van den Eynde, D. 2003. The mud deposits and the high turbidity in the Belgian-Dutch coastal zone, Southern bight of the North Sea. Continental Shelf Research, 23, 669-691.

Fettweis, M., Francken, F., Pison, V., Van den Eynde, D. 2006. Suspended particulate matter dynamics and aggregate sizes in a high turbidity area. Marine Geology, 235, 63-74.

Fettweis, M., Nechad, B., Van den Eynde, D. 2007a. An estimate of the suspended particulate matter (SPM) transport in the southern North Sea using SeaWiFS images, in-situ measurements and numerical model results. Continental Shelf Research, 27, 1568-1583.

Fettweis, M., Du Four, I., Zeelmaekers, E., Baeteman, C., Francken, F., Houziaux, J.-S., Mathys, M., Nechad, B., Pison, V., Vandenberghe, N., Van den Eynde, D., Van Lancker, V., Wartel, S. 2007b. Mud Origin, Characterisation and Human Activities (MOCHA). Belgian Science Policy, EV/35, 59pp. http://www.belspo.be/belspo/home/publ/pub_ostc/EV/rappEV35_en.pdf

Fettweis, M. 2008. Uncertainty of effective density and settling velocity of mud flocs derived from in-situ measurements. Estuarine, Coastal and Shelf Science, 78, 426-436.

Fettweis M, Houziaux J-S, Du Four I, Van Lancker V, Baeteman C, Mathys M, Van den Eynde D, Francken F, Wartel S., in press. Long-term influence of maritime access works on the distribution of cohesive sediment: Analysis of historical and recent data from the Belgian nearshore area (southern North Sea). Geo-Marine Letters.

Fontaine, K., 2004. Waar komt het slib voor de Belgische kust vandaan? Een kleimineralogische benadering, Licentiaatsthesis, KULeuven, 118pp.

Heyen H., Zorita E., von Storch H., 1996. Statistical downscaling of monthly mean North-Atlantic air pressure to sea level anomalies in the Baltic sea. Tellus, 48A: 312-323.

Houziaux, J.-S., Kerckhof, F., Degrendele, K., Roche, M., Norro A., 2008. "The Hinder banks : yet an important region for the Belgian marine biodiversity?" ('HINDERS'). Belgian Science Policy Office, Final report. 123 pp. + 131 pp. Annexes.

Hurrell, J.W. (1995) Decadal trends in the North Atlantic Oscillation: regional temperatures and precipitations. Science, 269: p. 676-679.

Hurrell, J.W., and R.R. Dickson, 2004: Climate variability over the North Atlantic. In: N.C. Stenseth, G. Ottersen, J.W. Hurrell, and A. Belgrano (Eds.). *Marine Ecosystems and Climate Variation - the North Atlantic*. Oxford University Press, pp. 15-31.

Hurrell J.W., Van Loon H., 1997. Decadal variations in Climate associated with the north Atlantic deviation. Climatic change, 36: 301-326.

Huth, R., 1999: Statistical downscaling in central Europe: Evaluation of methods and potential predictors. Climate Res.,13: 91-101.

IPCC, 2007. Climate Change 2007. The Physical Science Basis. Cambridge University Press, Cambridge, 940 p.

Jackson, M.L., 1975. Soil chemical analysis – Advanced course, 2de editie. Published by the author, Madison, Wisconsin, 895pp.

Janssens, R., 2009. Optimalisering van sediment- en morfodynamische analyses van zandige substraten, Belgische deel van de Noordzee. Thesis to submit to obtain the degree of Master in Geology. Gent (B): Universiteit Gent (Renard Centre of Marine Geology), 126p.

Karl T.R., Wang W.C., Schlesinger M.E., Knight R.W. Portman D., 1990. A method of relating general circulation model simulated climate to observed local climate. Part I: Seasonal statistics. Journal of Climate, 3, 1053-1079

Kröncke, I., Zeiss B. and Rensing P., 2001. Long-term variability in macrofauna species composition off the island of Nordeney (East Frisia, Germany) in relation to changes in climatic and environmental conditions. Senckenbergiana maritima, 31, 1. p. 65-82.

Lacroix, G., Ruddick, K., Ozer, J. and Lancelot, C., 2004. Modelling the impact of the Scheldt and Rhine/Meuse plumes on the salinity distribution in Belgian waters (southern North Sea). Journal of Sea Research, 52. p. 149-153.

Langenberg H., Pfizenmayer A., Von Storch H., Sundermann J., 1999. Storm-related sea level variations along the North Sea coast: natural variability and anthropogenic change. Cont. Shelf Res., 19: 821-842.

Le Hir, P., Monbet, Y., Orvain, F. 2007. Sediment erodability in sediment transport modelling: Can we account for biota effects? Continental Shelf Research, 27, 1116-1142.

Luyten, P. J., Jones, J. E., Proctor, R., Tabor, A., Tett, P., Wild-Allen, K. 1999. COHERENS A Coupled Hydrodynamical-Ecological Model for Regional and Shelf Seas: User Documentation. MUMM, Brussels. 914pp.

Machel H., Kappla A., Flohn H., 1998. Behaviour of the centres of action above the Atlantic since 1881, Part 1, characteristics of seasonal and interannual variability. Int J. Climatol, 18: 1-22.

Maggi, F. In press. Bioflocculation of suspended particles in nutrient-rich aqueous ecosystems. Journal of Hydrology.

Moore, D.M., Reynolds, R.C., 1997. X-ray diffraction and the identification and analysis of clay minerals. Oxford University Press, Oxford-New York, 371pp.

Nerem R.S., Mitchum G.T., 2001. Observations of sea level change from satellite atltimetry. Sea level rise: history and consequence, Academic press, San Diego, 121-163.

Omotoso, O., McCarty, D.K., Hillier, S., Kleeberg, R., 2006. Some successful approaches to quantitative mineral analysis as revealed by the 3rd Reynolds Cup Contest. Clays and Clay Minerals, 54, 748-760.

Royer J.F., Cariolle D., Chauvin F., Déqué M., Douville H., Hu R.M, Planton S., Rascol A., Ricard J.L., Melia D.S.Y., Sevault F., Simon P., Somot S., Tyteca S., Terray L., Valcke S. (2002). Simulation des changements climatiques au cours du XXIème siècle incluant l'ozone stratosphérique. Compte Rendus Geoscience, 334: 147-154.

Silva-Jacinto, R. Le Hir, P. 2001. Response of stratified muddy beds to water waves. In: Coastal and Estuarine Fine Sediment Processes (McAnally, W.H., Mahta, A.J., eds.). Proceedings in Marine Science, 3, 95-108.

Środoń, J., Drits, V.A., McCarty, D.K., Hsieh, J.C.C, Eberl, D.D. 2001. Quantitative XRD analysis of clay-rich rocks from random preparations. Clays and Clay Minerals, 49, 514-528.

Sterl A., Severijns C., van Oldenborgh G.J., Dijkstra H., Hazeleger W., van den Broeke M., Burgers G., van den Hurk B., van Leeuwen P.J., van Velthoven P., 2008. When can we expect extremely high surface temperatures? Geophys. Res. Lett., 35, (2008), L14703 doi: 10.1029/2008GL034071

Ullmann A., Monbaliu J., 2009. Changes in atmospheric circulation over the North Atlantic and sea surge variations along the Belgian coast during the 20th century. International Journal of Climatology. Doi: 10.1002/joc.1904

Ullmann A., Sterl A., Van den Eynde D., Monbaliu J., 2009. Atmospheric pressure and sea surges along the Belgian coast during the 20th century and changes in sea-surge height under climate change. Continental Shelf Reseach. Submitted.

Van den Eynde, D., F. Francken, S. Ponsar en J. Ozer, 2008. Bepaling van de primaire impacten van klimaatsverandering: statistische analyse van metingen van golven, windsnelheid en –richting en van zeewatertemperatuur. Technisch Rapport CLIMAR/X/DVDE/200807/ NL/TR4, Rapport voorbereid in het kader van het CLIMAR project, uitgevoerd voor Federaal Wetenschapsbeleid, Contract SD/NS/01A, Beheerseenheid van het Mathematisch Model van de Noordzee, 40 pp. (Annex 1-04).

Van Cauwenberghe, C. 1971. Hydrografische analyse van de Vlaamse banken langs de Belgisch-Franse kust. Het Ingenieursblad, 1971, No. 19, p. 563-571

Van Hoey, G., Vincx, M., Degraer, S., 2007. Temporal variability in the Abra alba community determined by global and local events. Journal of Sea Research 58, 144-155.

Van Lancker, V., Du Four, I., Verfaillie, E., Deleu, S., Schelfaut, K., Fettweis, M., Van den Eynde, D., Francken, F., Monbaliu, J., Giardino, A., Portilla, J., Lanckneus, J., Moerkerke, G., Degraer, S., 2007. Management, research and budgetting of aggregates in shelf seas related to end-users (Marebasse). Final Scientific Report. Belgian Science Policy, 125pp.

van Ledden, M. 2002. A process-based sand-mud model. In: Fine Sediment Dynamics in the Marine Environment (Winterwerp, J.C., Kranenburg, C., eds.), Proceedings in Marine Science, 577-594.

van Ledden, M., van Kesteren, W.G.M., Winterwerp, J. 2004. A conceptual framework for the erosion behaviour of sand-mud mixtures. Continental Shelf Research, 24, 1-11.

Van Mierlo, C.-J., 1899. La carte lithologique de la partie méridionale de la mer du Nord. Bulletin de la Société Belge de Geologie, Paléontologie et Hydrologie, XII, 2nde série (tome III) : p. 219 – 265.

Veys, K., 2008. Natural versus Anthropogenically-induced sedimentation, North of the Vlakte van de Raan (Belgian part of the North Sea). Thesis to obtain the degree of Master in Science in Advanced Studies in Marine and Lacustrine Sciences. Gent (B): Universiteit Gent (Renard Centre of Marine Geology), 29 pp + Annex.

Von Storch H., Reichardt H., 1997. A scenario of storm surge statistics for the German bight at the expected time of doubled atmospheric Carbon Dioxide concentration. Journal of Climate, 10: 2653-2662.

Von Storch H., Zwiers F.W., 1999. Statistical analysis in climate research. Cambridge Univ. Press. 494 p.

Waeles, B., Le Hir, P., Lesueur, P., Delsinne, N. 2007. Modelling sand/mud transport and morphodynamics in the Seine river mouth (France): an attempt using a process-based approach. Hydrobiologia, 588, 69-82.

Weijerman, M., Lindeboom, H., Zuur, A.F., 2005. Regime shifts in marine ecosystems of the North Sea and Wadden Sea. Mar. Ecol., Prog. Ser. 298, 21–39.

Weisse R., Von Storch H., Feser F., 2005. Northeast Atlantic and North Sea storminess as simulated by regional climate model 1958-2001 and comparison with observations. J. Climate, 18: 465-479.

Westrich, B., Jancke, T. 2007. Report on erosion behaviour measurements of undisturbed sediment cores from the Belgian North Sea bed. University of Stuttgart, Institute of Hydraulic Engineering,

Winterwerp, J.C. 1998. A simple model for turbulence induced flocculation of cohesive sediment. Journal of Hydraulic Research, 36, 309-326.

Winterwerp, J. 1999. On the dynamics of high-concentrated mud suspensions. PhD thesis, TU Delft, The Netherlands, 172pp.

Winterwerp, J. 2001. Stratification effects by cohesive and non-cohesive sediment. Journal of Geophysical Research, 106(C10), 22559-22574.

SSD

SCIENCE FOR A SUSTAINABLE DEVELOPMENT
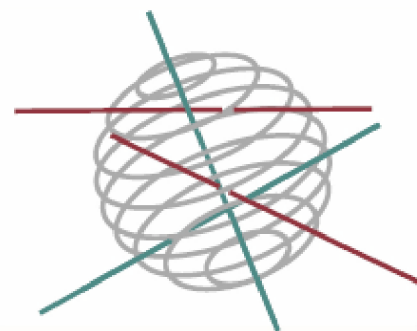
ANNEXES

**"QUANTIFICATION OF EROSION/SEDIMENTATION TO
TRACE THE NATURAL FROM THE ANTHROPOGENIC
SEDIMENT DYNAMICS"
«QUEST4D»**

Van Lancker V, (Editor)
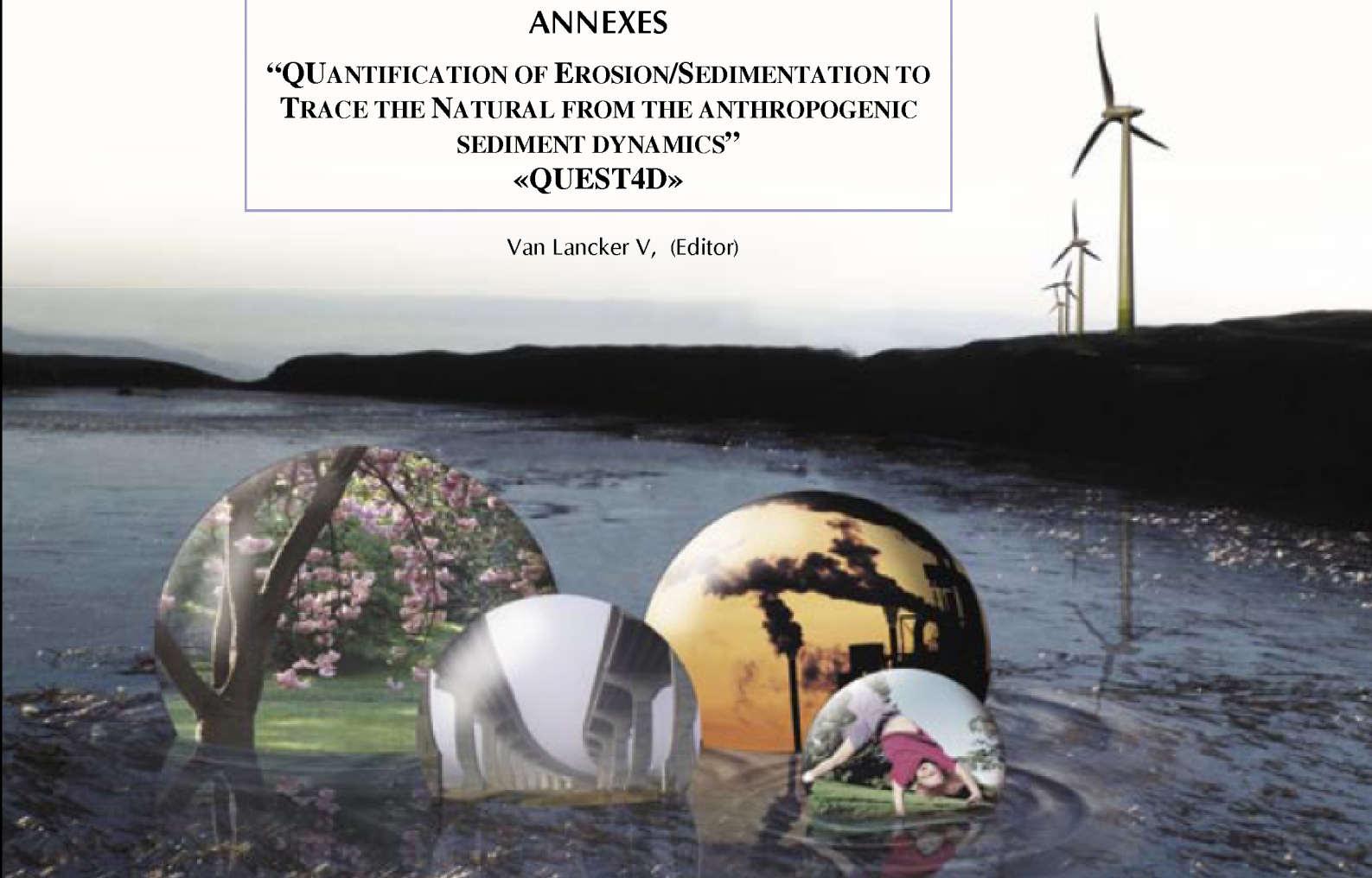
ATMOSPHERE AND TERRESTRIAL AND MARINE ECOSYSTEMS

.be

SCIENCE FOR A SUSTAINABLE DEVELOPMENT
(SSD)
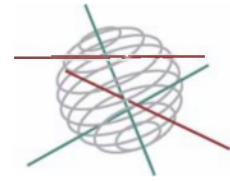
North Sea

FINAL REPORT - ANNEXES

QUANTIFICATION OF EROSION/SEDIMENTATION TO TRACE THE NATURAL FROM THE ANTHROPOGENIC SEDIMENT DYNAMICS "QUEST4D"

SD/NS/06A

Editor
Vera Van Lancker

BELGIAN SCIENCE POLICY
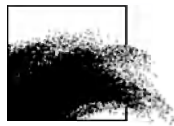
Rue de la Science 8
Wetenschapsstraat 8
B-1000 Brussels
Belgium
Tel: +32 (0)2 238 34 11 – Fax: +32 (0)2 230 59 12
http://www.belspo.be

Contact person: XXXXXXXX
+32 (0)2 238 3X XX

Table of content Annexes

Annex I. Clay mineralogy as provenance indicator for BPNS mud

Edwin Zeelmaekers[1] & Noël Vandenberghe[1]

[1]Laboratory for Applied Geology and Mineralogy, KULeuven, Celestijnenlaan 200E, 3001 Heverlee, Belgium

1. Introduction and Methodology

1.1 Strategy

Clay minerals are a considerable part of the mineralogical content of the BPNS muds (up to 40wt%, cfr. below). Their defective structure, their small crystal size and unique properties make them an extremely variable mineral group and therefore at the same time potentially also a very diagnostic group when used in provenance studies of clay rich sediments. Following this reasoning this study was undertaken to characterize the clay mineralogy of the BPNS muds and their potential sources areas in detail to be able to draw provenance conclusions, either by excluding potential source areas or by finding very convincing clay mineralogical matches between the muds and one or more potential source areas.

This study was possible because of the application of a state-of-the-art methodology, enabling detailed qualitative and quantitative analyses of the bulk and clay mineralogy.

1.2 Methodology

The analysis of the (clay) mineralogy is based on (i) a quantitative bulk analysis and CEC analysis and (ii) a clay extraction for qualitative analyses, both depending on X-ray diffraction (XRD) measurements.

All samples were first dried at $60°^C$, crushed, sieved to pass through a < 0.5mm screen and thoroughly homogenized to ensure representative splits were used in the different analyses.

1.2.1 Bulk analysis

2.7g of a crushed and homogenized sample was mixed with 300mg of a zincite internal standard in a McCrone Micronizing Mill and reduced to a grain size < 10 ꭎm. Of the obtained mixtures an X-ray diffraction (XRD) pattern of the hkl-reflections was recorded (Cu-anode / 5-65°2ꭎ / step size 0.02° / 2s counting time).

This sample preparation and the used data analysis are based on the techniques described by Środoń et al. (2001). The QUANTA software was used for data analysis (Chevron proprietary software; Mystkowski et al., 2002). This is currently the most accurate way to determine the overall quantitative composition of clay-bearing sediments (accuracy report: Omotoso et al., 2006). It allows for a very accurate determination of the quantitative mineralogical composition of a bulk rock for all non-clay minerals (including amorphous phases) and clay minerals in groups. For the examined samples, these groups are:

- Kaolinite

- Chlorite & Vermiculite

- 2:1 dioctahedral clays & micas (illite, smectite, illite-smectite,

  muscovite, glauconite, …)

The accuracy and precision are similar and are estimated at about 0.5wt% to 1.0wt% for small amounts (<5%; depending on the mineral) and about 1.0% to 2.5% for large amounts (>15%). The error for amorphous phases is assumed to be the highest. The individual errors are not cumulative for the Sum Clay and Sum Non-Clay values, which have a similar accuracy and precision as described above.

1.2.2 CEC measurements

Since illite(/muscovite) and smectite ('swelling layers') are quantified together in the group "2:1 dioctahedral clays & micas", a Cation Exchange Capacity ('CEC') measurement was carried out using the Co-hexamine technique (after Bardon et al., 1993), to distinguish between them. Generally the CEC of a sample can be considered as originating entirely from the smectite in the sample. Therefore a CEC-measurement allows for splitting up the group "2:1 dioctahedral clays & micas" into separate weight percentages for 'equivalents' of illite(/muscovite) and smectite in the sample.

CEC results are expressed in milli-equivalent per 100g (meq/100g). Assuming an average smectite layer charge of 110meq/100g (cfr. Šrodoń et al., 2009) the meq/100g value can easily be recalculated in % smectite equivalent in the sample, using equation:

% smectite equivalent = CEC/1.1   (1)

The margin of error is about 3 meq/100g (so about 3% smectite)

1.2.3 Qualitative and quantitative analysis of the extracted clay fraction

To obtain more detailed information about the clay minerals they were extracted from the bulk sediment. Hereto all cementing agents (carbonates, organic matter and Fe-oxides) were removed following the procedure of Jackson (1975). After these treatments the fractions $<0.2\mu$m and $<2\mu$m were separated by centrifugation. Oriented sedimentation slides were made of these fractions and registered using XRD in different states (air-dry, ethylene glycol saturated, heated to 550°C/1h) to permit standard clay identification techniques (e.g. Moore & Reynolds, 1997). Oriented slides were also made of K, Mg and Li saturated fractions and recorded under specific conditions (300°C/1h and glycerol solvated). XRD powder scans were used to evaluate the clay mineral polytypes using diagnostic peaks of their three dimensional diffraction patterns and the Al versus Fe content using the 060.

1.3 Notes on reporting and presentation of the results

1.3.1 Bulk analysis & CEC results

All results are reported in wt% and are normalized to 100%, a large majority of the unnormalized results ranges between 97 and 103wt%. Using equation (1) the "2:1 dioctahedral clays & micas" group was split up in "smectite" and "illite" equivalents, these values are added to the tables in **illitics**. Using Sum Clay and Sum "2:1 dioctahedral clays & micas" and the calculated smectite and illite equivalents the relative proportions of the different clay minerals within the clay fraction was calculated, the same was done only for relative proportions of smectite and illite equivalents in the "2:1 dioctahedral clays & micas" group. The results of both these calculations are always shown in a separate table "in clay fraction".

For low values of CEC and Sum "2:1 dioctahedral clays & micas" the relative error for the calculations above is very high because of the absolute error of about 3meq/100g for the CEC

measurements. Therefore the results of the calculations should be considered with caution. To draw attention to this fact such results are underlined.

When CEC measurements could not be done the "2:1 dioctahedral clays & micas" group could not be split into smectite and illite equivalents.

Qtz = Quartz; Kspar = K feldspar; Plag = Plagioclase; ☐Carb = Sum carbonates (calcite + Mg-calcite + aragonite + dolomite + ankerite); Pyr = pyrite; Hal = halite; Gyp = gypsum; Ana = anatase; Am = amorphous; ☐NC = Sum Non Clays; Kaol = Kaolinte; ☐2:1 = Sum 2:1 dioctahedral clays & micas; Chl = chlorite (and traces of vermiculite); ☐Clay = Sum Clays

1.3.2 Concept of data interpretation

All analyses described above require a certain amount of sample. Often not enough sample was available to do all analyses or not enough clay could be extracted (e.g. for suspension samples, beach sands respectively). For this reason not all the samples that are mentioned in the sample lists have their bulk results reported.

When interpreting the clay mineralogy of a potential source area versus the BPNS muds all analyses – if possible - were taken into account as they each contribute part of the information. Sometimes conclusions had to be based on partial information. Some potential source areas could be rejected based only on the results from the smectite and illlite proportions determined by the bulk and CEC analyses. Other potential source areas did not require bulk + CEC analyses as the detailed clay mineralogy was distinctly different from the BPNS muds. For every potential source area only one Figure comparing a diffraction pattern of the source area versus the BPNS muds is included, always a diffraction pattern most representative of the entire group is used.

Figures: displayed values are d-spacings in ☐ngstrom; 17☐ = smectite 001 / 10☐ = illite 001 / 7☐ = kaolinite 001, higher order peaks and mixed-layered mineral peaks are not labeled. Peaks for chlorite and vermiculite are generally too small to be clearly labeled.

Except for the initial figure of the BPNS muds, all displayed diffraction patterns are of glycolated oriented slides of the $<2\mu m$ fraction, registered using Cu radiation. The BPNS diffraction pattern displayed for comparison is always from the same sample.

Detailed explanations of the used methodology, its accuracy, precision and limitations, and more extended results reports, together with in dept discussions of the results and a focus on the bulk results can be found in the PhD work of Edwin Zeelmaekers, funded by IWT Flanders (available end of 2009).

1.4 References

Bardon, C., Bieber, M.T, Cuiec, L., Jacquin, C., Courbot, A., Deneuville, G., Simon, J.M., Voirin, J.M., Espy., M., Nectoux, A., and Pellerin, A., 1993. Recommandations pour la détermination expérimentale de la capacité d'échange de cations des milieux argileux. *Revue de L' Institut Francais Du Pétrole* 38, 5, 621-626.

Jackson, M.L., 1975. *Soil chemical analysis – Advanced course, 2nd edition*. Published by the author, Madison, Wisconsin, 895pp.

Moore, D.M., Reynolds, R.C., Jr., 1997. *X-ray diffraction and the identification and analysis of clay minerals*. Oxford University Press, Oxford-New York, 371pp

Mystkowski, K., Środoń, J., McCarty, D.K., 2002. Application of evolutionary programming to automatic XRD quantitative analysis of clay-bearing rocks: The Clay Minerals Society 39th Annual Meeting, abstract, Boulder, Colorado.

Omotoso, O., McCarty, D.K., Hillier, S., Kleeberg, R., 2006. Some successful approaches to quantitative mineral analysis as revealed by the 3rd Reynolds Cup Contest. *Clays and Clay Minerals* 54, 748-760

Środoń, J., Drits, V.A., McCarty, D.K., Hsieh, J.C.C., Eberl, D.D., 2001. Quantitative XRD analysis of clay-rich rocks from random preparations. *Clays and Clay Minerals* 49, 514-528.

Środoń, J., Zeelmaekers, E., Derkowski, A., 2009. The charge of component layers of illite-smectite in bentonites and the nature of end-member illite, *Clays and Clay Minerals* accepted.

2. Results

2.1 Characterization of the BPNS muds

2.1.1 BPNS bottom sediments

Samples

Sample	Description	Location
EZS 1	Holocene mud from core (2-4cm depth)	Sampling station "700" - near Zeebrugge
EZS 2	Holocene mud from core (12-4cm depth)	Sampling station "700" - near Zeebrugge
EZS 3	Holocene mud from core (24-26cm depth)	Sampling station "700" - near Zeebrugge
EZS 4	Holocene mud from core (34-36cm depth)	Sampling station "700" - near Zeebrugge
EZS 15	Holocene mud from core (1.35-1.43m depth)	Coring location "SWB" - near Zeebrugge
EZS 92	Recent mud	Sampling station "702" - near Zeebrugge
EZN 7	Recent mud	Sampling station "115b" - near Nieuwpoort
EZN 8	Recent mud	Sampling station "250" - near Scheldt mouth
KFT 9	Holocene mud	Sampling station "700" - near Zeebrugge
KFT 26	Recent mud	Sampling station "130" - near Ostend
LGT 52	Recent mud	Sampling station "130" - near Ostend
LGT 53	Recent mud	Sampling station "OE17" - near Ostend
LGT 58	Recent mud	Sampling station "OE13" - near Ostend
LGT 60	Recent mud	Sampling station "702" - near Zeebrugge
LGT 61	Recent mud	Sampling station "OE14" - near Ostend
LGT 62	Recent mud	Sampling station "230" - near Ostend
LGT 25	Recent mud	Near sampling station "435" - offshore east BPNS
LGT 30	Recent mud	East BPNS - 20km offshore Scheldt mouth
LGT 34	Holocene mud	East BPNS - 20km offshore Zeebrugge
LGT 38a	Sandy mud	East BPNS - 15km offshore Zeebrugge
LGT 39	Recent mud	East BPNS - 15km offshore Zeebrugge
LGT 43	Recent mud	Zeebrugge harbour
LGT 44	Recent mud	Zeebrugge harbour

Quantitative bulk & clay mineralogy

Sample	Qtz	Kspar	Plag	ΣCarb	Pyr	Hal	Gyp	Ana	Am	ΣNC	Kaol	Σ2:1	(eq.) Smect	(eq.) Illite	Chl	Σclay	Total
EZS1	28	5	4	27	0	2	1	0.5	1	68	2	26	16.2	9.5	3	31	100
EZS2	43	7	5	25	0	0.8	0.5	0.2	0.2	82	2	15	9.0	5.9	2	19	100
EZS3	33	6	5	29	0.2	0.8	0.5	0.5	0.4	75	2	20	13.8	5.9	3	25	100
EZS4	28	5	4	27	0.1	1	0.9	0.5	1	68	1	26	16.6	9.2	4	31	100
EZS15	24	3	4	28	0.2	0.6	2	0.4	1	64	1	29			5	35	100
EZS92	63	4	3	12	0	0.9	0	0	0.6	84	0.4	13	9.4	4.0	2	16	100
EZN7	76	5	4	9	0	0	0	0	0.0	94	0	4	4.0	-	0.6	5	100
EZN8	79	5	3	8	0	0.3	0	0	0.1	95	0.5	3	3.0	-	1	5	100
KFT26	67	8	9	2	0	0.5	0	1	0.2	88	1	10	3.7	6.0	2	13	100
KFT9	40	5	6	23	0.3	2	1	0	0.7	78	2	20	13.1	7.0	1	23	100
LGT52	84	6	6	0.5	0	0	0	0	0.0	97	0.2	2	2.0	-	1	3	100
LGT62	86	4	6	0.2	0	0	0	0.2	0.0	96	0.4	3	3.0	-	0.7	4	100
LGT30	58	4	2	16	0.6	0.5	0.4	0.1	0.1	81	2	15	11.4	3.2	2	19	100
LGT34	29	4	5	23	1	0	0.7	0	0.5	63	5	29	18.4	11.0	2	36	100
LGT38a	82	5	2	8	0	0.4	0	0	0.0	97	0.2	1	1.0		0.6	2	100
LGT39	28	3	5	29	0.3	2	0.5	0.2	1	69	3	27	16.4	10.8	1	31	100
LGT43	20	2	3	29	0.3	2	0.5	0.4	1	59	3	32	22.4	9.4	5	40	100

Sample	In clay fraction						
	%smect	%illite	%2:1	%kaol	%chl	%S in 2:1	%I in 2:1
EZS1	52.9	30.8	83.7	6.5	9.8	63.2	36.8
EZS2	47.7	31.1	78.8	10.6	10.6	60.6	39.4
EZS3	55.8	24.0	79.8	8.1	12.1	70.0	30.0
EZS4	53.8	29.9	83.8	3.2	13.0	64.3	35.7
EZS15			82.6	2.9	14.5		
EZS92	59.4	25.4	84.8	2.5	12.7	70.0	30.0
EZN7	88.0	-	88.0	0.0	12.0	100.0	-
EZN8	67.4	-	67.4	10.9	21.7	100.0	-
KFT26	29.1	47.3	76.4	7.9	15.7	38.0	62.0
KFT9	56.6	30.4	87.0	8.7	4.3	65.0	35.0
LGT52	61.3		61.3	6.5	32.3	100.0	

LGT62	_70.3_		70.3	10.8	18.9	100.0	
LGT30	_61.2_	_17.3_	78.5	10.8	10.8	78.0	_22.0_
LGT34	50.4	30.4	_80.8_	13.7	5.5	62.4	37.6
LGT38a	_60.0_		_60.0_	10.0	30.0	100.0	
LGT39	52.4	34.7	_87.2_	9.6	3.2	60.2	39.8
LGT43	56.4	23.5	_79.9_	7.5	12.6	70.6	29.4

Qualitative detailed clay mineralogy
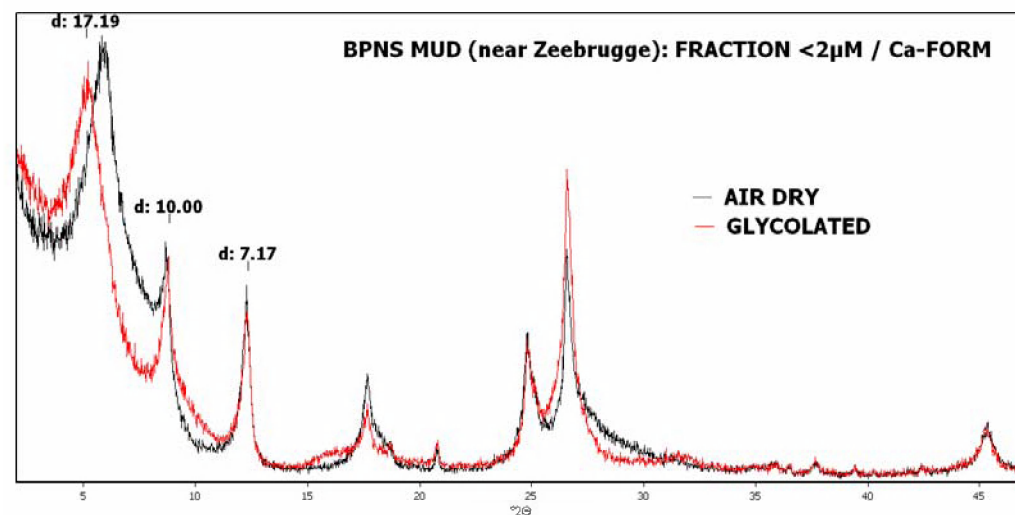
Figure 1. Air-dry and glycolated X-ray diffraction pattern representing a typical BPNS mud sample containing: randomly interstratified mixed-layered illite-smectite, illite, smectite, kaolinite and minor amounts of chlorite and vermiculite.

2.1.2 BPNS suspension samples

Samples

	Description	Location
EZS 83	Centrifuged suspension	Sampling station "700" - near Zeebrugge
EZS 84	Centrifuged suspension	Sampling station "250" - near Scheldt mouth
EZS 85	Centrifuged suspension	Sampling station "TT20" - near Zeebrugge
EZS 86	Centrifuged suspension taken on track	Track between sampling stations "330" and "MC5"
EZS 87	Centrifuged suspension	Sampling station "115b" - near Nieuwpoort
EZS 88	Centrifuged suspension	Sampling station "Birkenfels" N of BPNS
EZS 96	Centrifuged suspension	Sampling station "OE' - near Ostend
EZN 1	Centrifuged suspension	Sampling station "OE' - near Ostend
EZN 2	Centrifuged suspension taken on track	Track between Zeebrugge and Kwintebank
EZN 4	Centrifuged suspension taken on track	Track between sampling stations "315" and "421"
EZN 5	Centrifuged suspension	Hinderbanken
EZN 6	Centrifuged suspension	Hinderbanken
EZN 30	Centrifuged suspension	Sampling station "MOW1" - near Zeebrugge
LGT 47	Centrifuged suspension	East BPNS - 20km offshore Scheldt mouth
LGT25s	Centrifuged suspension	Near sampling station "435" - offshore east BPNS

Quantitative bulk & clay mineralogy

Sample	Qtz	Kspar	Plag	⏐Carb	Pyr	Hal	Gyp	Ana	Am	⏐NC	Kaol	⏐2:1	Smect	Illite	Chl	⏐clay	Total
EZS85	13	2	3	27	0	2	2	0.3	9	58	3	35	21.2	13.4	3	41	100
EZS96	19	2	2	35	0.3	0.8	0.7	0.1	9	69	2	28	17.4	11.0	2	32	100
EZN1	19	3	3	32	0	0.7	0.8	0.2	8	66	3	28	19.1	8.6	4	35	100
EZN2	13	3	2	34	0.1	1	1	0.4	2	56	1	37	19.2	18.0	5	43	100
EZN6	17	2	3	33	0	1	0	0.4	7	63	3	28	18.2	9.8	5	36	100
EZN5	25	3	3	37	0	1	0.7	0.3	8	77	1	21	15.2	5.5	2	24	100
EZN30	16	3	2	31	0.1	1	0	0	9	62	3	31	17.7	13.7	3	37	100
LGT25s	15	2	3	39	0.2	0.9	0	0.7	7	68	4	25	18.8	5.9	4	33	100

Sample	In clay fraction						
	%smect	%illite	%2:1	%kaol	%chl	%S in 2:1	%I in 2:1
EZS85	52.1	33.1	85.2	7.4	7.4	61.2	38.8
EZS96	53.7	33.9	87.7	6.2	6.2	61.3	38.7
EZN1	55.1	24.8	79.8	8.6	11.5	69.0	31.0
EZN2	44.5	41.6	86.1	2.3	11.6	51.7	48.3
EZN6	50.5	27.3	77.8	8.3	13.9	64.9	35.1
EZN5	64.0	23.3	87.3	4.2	8.4	73.3	26.7
EZN30	47.2	36.7	84.0	8.0	8.0	56.2	43.8
LGT25s	57.3	18.2	75.5	12.2	12.2	75.9	24.1

Qualitative detailed clay mineralogy
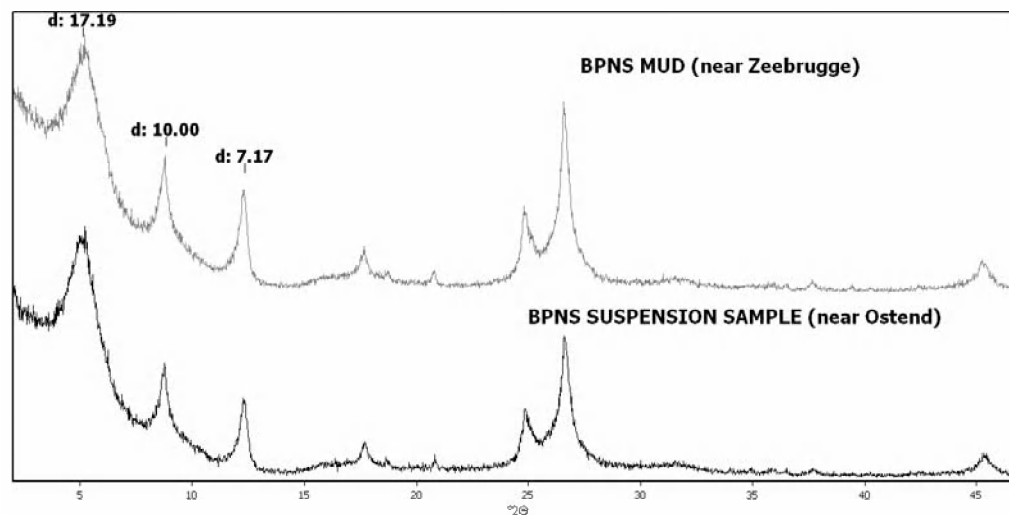
Figure 2. BPNS mud compared to BPNS suspension sample.

Clay mineralogy compared to the clay mineralogy of the BPNS muds

Identical.

Provenance conclusion

Bottom and suspension mud samples on the BPNS have the same origin.

2.2 Characterization of clay mineralogy spatial patterns

2.2.1 Scheldt Estuary Suspension Samples

Samples

	Description	Location
EZN 3	Centrifuged suspension	Scheldt mouth
EZS 12	Dredged mud	Kallo, near Antwerp
LGT45	Dredged mud	Kallo, near Antwerp
EZS 89	Suspension collected on a track	Between Scheldt sampling stations S04-S12
EZS 90	Suspension collected on a track	Between Scheldt sampling stations S18-S22

Quantitative bulk & clay mineralogy

Sample	Qtz	Kspar	Plag	$\Box Carb$	Pyr	Hal	Gyp	Ana	Am	$\Box NC$	Kaol	$\Box 2:1$	Smect	Illite	Chl	$\Box clay$	Total
EZN3	19	7	2	29	0.4	1	0.7	0.3	7	66	4	26			5	35	100
EZS12	32	6	6	17	0.6	0.9	0	0.4	2	64	2	30	22.0	7.8	4	36	100
LGT45	33	7	4	17	0.1	0	0	0.3	1	62	4	33	22.4	11.0	2	39	100
EZS89	27	6	4	27	0	0	0	0.5	0.7	66	3	29	22.2	7.2	4	36	100
EZS90	35	6	5	16	0.5	0.3	0	0.5	2	65	1	31	24.9	6.4	3	35	100

Sample	In clay fraction						
	%smect	%illite	%2:1	%kaol	%chl	%S in 2:1	%I in 2:1
EZN3			74.4	11.4	14.2		
EZS12	61.5	21.7	83.2	5.6	11.2	73.9	26.1
LGT45	56.9	27.9	84.8	10.2	5.1	67.1	32.9
EZS89	60.9	19.9	80.8	8.2	11.0	75.4	24.6
EZS90	70.6	18.1	88.7	2.8	8.5	79.6	20.4

Qualitative detailed clay mineralogy
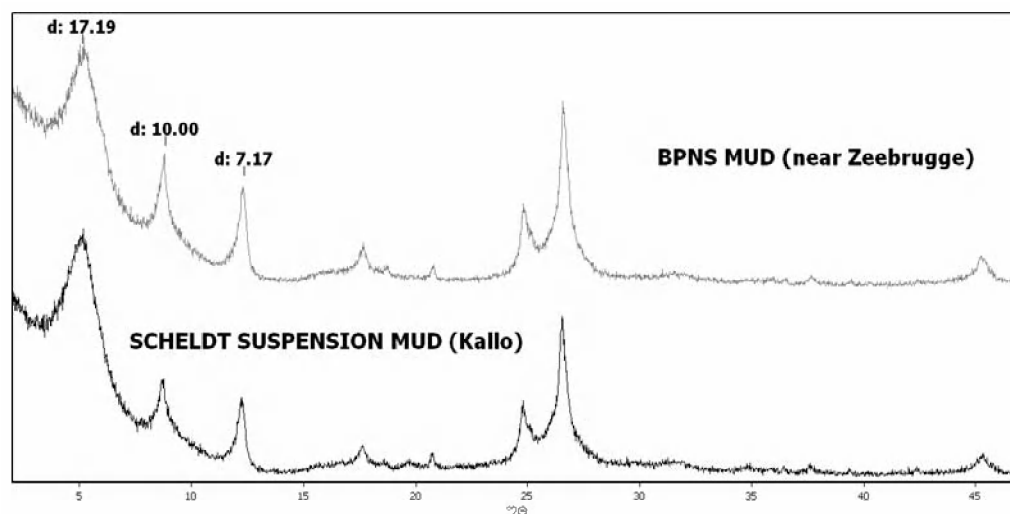
Figure 3. BPNS muds compared to Scheldt suspension sample.

Clay mineralogy compared to the clay mineralogy of the BPNS muds

Very similar, slightly more smectitic.

Provenance conclusion

Strong provenance connection between BPNS muds and Scheldt Estuary suspension samples.

2.2.2 Scheldt estuary bottom samples

Samples

	Description	Location
EZS 29	Bottom sample	Scheldt sampling station S20
EZS 36	Bottom sample	Scheldt sampling station S04
EZS 37	Bottom sample	Scheldt sampling station S07
EZS 38	Bottom sample	Scheldt sampling station S12
EZS 59	Bottom sample	Scheldt sampling station S01
EZS 60	Bottom sample	Scheldt sampling station S15
EZS 61	Bottom sample	Scheldt sampling station S18
EZS 62	Bottom sample	Scheldt sampling station S22
EZS 63	Clay lenses from EZS59	Scheldt sampling station S01
EZS 91	Bottom sample	Scheldt sampling station S18
EZS 93	Scheldt Estuary tidal marsh (18-20cm depth)	Paulina marsh
EZS 94	Scheldt Estuary tidal marsh (27-28cm depth)	Paulina marsh
EZS 95	Scheldt Estuary tidal marsh (41-42cm depth)	Paulina marsh

Quantitative bulk & clay mineralogy

Sample	Qtz	Kspar	Plag	⊡Carb	Pyr	Hal	Gyp	Ana	Am	⊡NC	Kaol	⊡2:1	Smect	Illite	Chl	⊡clay	Total
EZS29	58	5	4	10	0.3	0	0.5	0.3	0.4	78	1	18	14.7	3.5	2	21	100
EZS36	82	5	2	2	0.2	0.6	0.2	0	0.1	92	0.5	8	5.4	3.0	0	9	100
EZS37	81	5	3	3	0	0	0	0	0.0	92	0.7	6	5.8	0.5	0.2	7	100
EZS38	84	5	3	2	0	0	0	0	0.2	94	0.5	5	5.0	-	0.6	6	100
EZS59	75	4	2	6	0.3	0.3	0.5	0	0.1	88	0.2	10	7.0	3.4	0.5	11	100
EZS60	72	6	4	9	0.3	0	0.3	0	0.0	92	0.2	8	3.9	4.3	0.8	9	100
EZS61	71	7	4	9	0	0	0	0	0.0	91	0	8	4.8	3.3	1	9	100
EZS62	77	4	3	5	0	0	0	0	0.0	89	0.4	10	4.6	5.2	1	11	100
EZS63	60	5	3	13	0	0.3	0.5	0	0.3	82	2	14	10.0	4.0	2	18	100
EZS91	79	5	2	2	0.2	0	0.2	0	0.2	89	0.2	10	6.6	3.6	0.4	11	100
EZS93	31	6	5	3	0.5	0	0	0.7	2	47	5	41	29.3	11.8	6	52	100
EZS94	30	6	5	4	0	0	0	0.6	1	46	5	41	27.4	14.0	8	54	100
EZS95	33	6	5	13	0	0	0.4	0.4	0.8	59	5	31	19.2	11.4	6	42	100

Sample	In clay fraction						
	%smect	%illite	%2:1	%kaol	%chl	%S in 2:1	%I in 2:1
EZS29	69.4	16.5	85.8	4.7	9.4	80.8	19.2
EZS36	60.5	33.9	94.4	5.6	0.0	64.1	35.9
EZS37	79.9	7.6	87.5	9.7	2.8	91.3	8.7
EZS38	82.3	-	82.3	8.1	9.7	100.0	-
EZS59	63.0	30.7	93.7	1.8	4.5	67.3	32.7
EZS60	42.2	47.0	89.1	2.2	8.7	47.3	52.7
EZS61	52.2	36.8	89.0	0.0	11.0	58.7	41.3
EZS62	41.2	46.3	87.5	3.6	8.9	47.1	52.9
EZS63	55.3	22.5	77.8	11.1	11.1	71.1	28.9
EZS91	60.7	33.7	94.4	1.9	3.7	64.3	35.7
EZS93	56.2	22.7	78.9	9.6	11.5	71.3	28.7
EZS94	50.3	25.8	76.1	9.2	14.7	66.1	33.9
EZS95	46.2	27.4	73.6	12.0	14.4	62.8	37.2

Qualitative detailed clay mineralogy
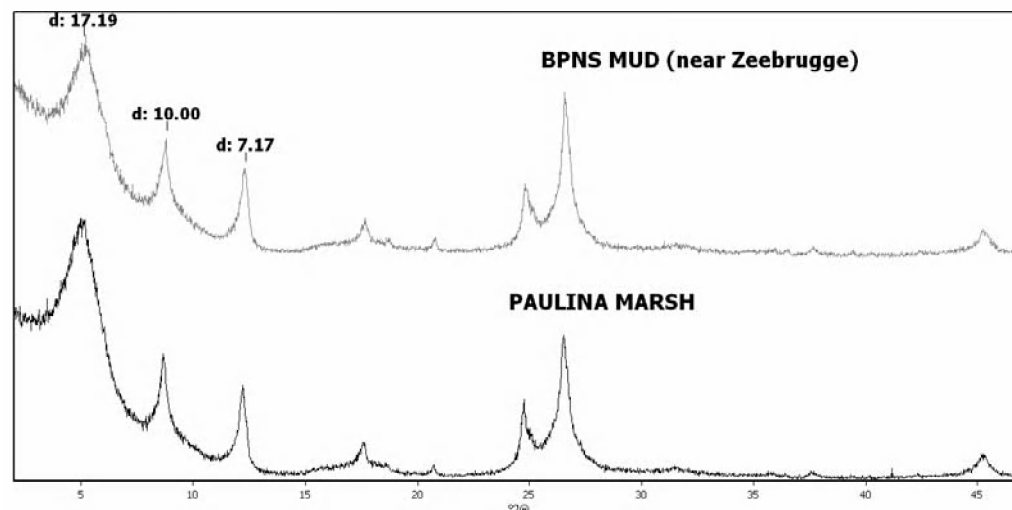
Figure 4. BPNS muds compared to Scheldt suspension sample.

Clay mineralogy compared to the clay mineralogy of the BPNS muds

Most of the bottom samples are sandy and thus have a low clay content, complicating detailed analyses of the clay content, moreover it cannot be excluded that the analyzed clay minerals in fact belong (at least partially) to the original clay mineralogical assemblage of the formations exposed on the Scheldt River floor. However, the samples from the Paulina marsh are clay rich and have a very similar clay mineralogy in comparison to the BPNS muds.

Provenance conclusion

Strong provenance connection between BPNS muds and Scheldt Estuary bottom samples (most clear from Paulina marsh samples).

2.2.3 Scheldt river upstream from Antwerp harbour & the Rupel river

Samples

	Description	Location
EZS 30	Scheldt riverbank sediment	St. Amands
EZS 32	Scheldt riverbank sediment	Antwerp harbour
EZS 33	Scheldt riverbank sediment	Lillo
EZS 34	Scheldt riverbank sediment	Doel
EZS 35	Scheldt riverbank sediment	Hemiksem
EZS 45	Rupel riverbank sediment	Terhagen
EZS 46	Rupel riverbank sediment	Boom
EZS 57	Scheldt riverbank sediment	Hoboken
EZS 58	Scheldt riverbank sediment	Kruibeke
EZN 38	Scheldt riverbank sediment	Rupelmonde
EZN 39	Scheldt riverbank sediment	Steendorp
EZN 40	Scheldt riverbank sediment	Temse
EZN 41	Rupel riverbank sediment	Schelle
EZN 42	Rupel riverbank sediment	Niel
EZN 43	Rupel riverbank sediment	Boom
EZN 44	Rupel riverbank sediment	Rumst

Quantitative bulk & clay mineralogy

Sample	Qtz	Kspar	Plag	$\Sigma Carb$	Pyr	Hal	Gyp	Ana	Am	ΣNC	Kaol	$\Sigma 2{:}1$	Smect	Illite	Chl	$\Sigma clay$	Total
EZS30	52	7	5	11	0.3	0	0	0.1	0.9	77	2	21	11.6	9.3	2	25	100
EZS32	42	6	7	12	0.7	0	0	0.4	1	70	0.9	27	17.2	10.2	2	30	100
EZS33	42	7	6	17	0.4	0	0	0.1	0.3	72	3	21	17.1	3.9	4	28	100
EZS34	27	5	4	18	0.6	0.2	0	0.5	2	57	3	37	24.0	12.7	4	44	100
EZS35	41	7	5	14	0.3	0	0	0.2	0.7	69	4	23	19.8	3.2	5	32	100
EZS45	62	3	3	11	0	0	0	0.1	0.3	80	2	16	7.5	8.4	2	20	99.2
EZS46	61	6	3	7	0.3	0	0	0.2	0.4	78	1	18	13.6	4.5	3	22	100
EZS57	47	7	5	12	0.4	0	0	0.3	0.8	72	2	22	17.6	3.9	4	28	100
EZS58	59	7	6	12	0	0	0	0	0.2	84	0.4	14	10.8	3.6	1	16	100

EZN38	43	6	5	16	0.5	0.2	0	0.3	0.9	72	2	24	18.4	5.3	2	28	100
EZN39	44	7	4	14	0.5	0.2	0	0.2	0.9	70	3	25	21.5	3.0	3	31	100
EZN40	44	6	7	15	0.5	0.2	0	0.3	0.9	73	3	20	18.2	2.1	3	26	100
EZN41	43	9	5	14	0.5	0	0	0.2	0.9	73	2	23	20.5	2.8	3	28	100
EZN42	36	6	5	14	0.6	0.1	0	0.7	9	71	3	29	22.8	6.2	4	36	100
EZN43	61	8	7	10	0.2	0	0	0	0.4	86	0.5	12	11.4	0.3	1	13	100
EZN44	42	6	4	14	0.3	0	0	0.4	0.7	67	2	27	21.0	5.5	3	32	100

| Sample	In clay fraction						
	%smect	%illite	%2:1	%kaol	%chl	%S in 2:1	%I in 2:1
EZS30	46.6	37.3	83.9	8.0	8.0	55.6	44.4
EZS32	56.8	33.6	90.4	3.0	6.6	62.8	37.2
EZS33	61.1	13.9	75.0	10.7	14.3	81.5	18.5
EZS34	55.0	29.0	84.0	6.9	9.2	65.5	34.5
EZS35	61.9	10.0	71.9	12.5	15.6	86.1	13.9
EZS45	37.7	42.2	79.9	10.1	10.1	47.2	52.8
EZS46	61.4	20.5	81.9	4.5	13.6	75.0	25.0
EZS57	63.9	14.3	78.2	7.3	14.5	81.7	18.3
EZS58	68.6	22.5	91.1	2.5	6.3	75.3	24.7
EZN38	66.6	19.0	85.6	7.2	7.2	77.8	22.2
EZN39	70.4	10.0	80.3	9.8	9.8	87.6	12.4
EZN40	69.2	8.0	77.2	11.4	11.4	89.7	10.3
EZN41	72.6	9.7	82.3	7.1	10.6	88.2	11.8
EZN42	63.4	17.2	80.6	8.3	11.1	78.7	21.3
EZN43	86.1	2.6	88.6	3.8	7.6	97.1	2.9
EZN44	66.6	17.5	84.1	6.3	9.5	79.2	20.8

Qualitative detailed clay mineralogy
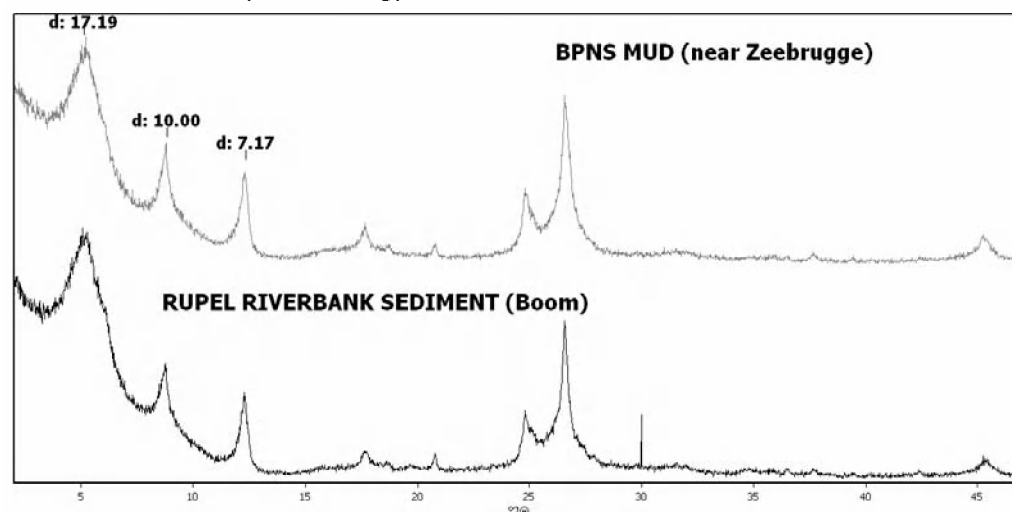
Figure 5. BPNS muds compared to Scheldt suspension sample.

Clay mineralogy compared to the clay mineralogy of the BPNS muds

Similar, but more variable, the samples in and around Antwerp harbour are less smectitic, the other ones more smectitic (the sample in Figure 5 is most similar to BPNS muds, the average sample is slightly more smectitic).

Provenance conclusion

A provenance connection between BPNS muds and Scheldt & Rupel rivers is likely.

2.2.4 English coast

Samples

	Description	Location
EZN 31	Beach sediment	Folkstone
EZN 32	Beach sediment	Bognor Regis
EZN 33	Beach sediment	Worthing
EZN 34	Beach sediment	Brighton
EZN 35	Beach sediment	Beachy Head
EZN 36	Beach sediment	Jury's Gap
EZN 37	Beach sediment	Dymchurch
LGT49	Centrifuged suspension taken on track	Thames Estuary, 50 km offshore
EZS 5	London Clay (outcrop)	unknown (stratigraphic collection)
EZS 9	Kimmeridge Clay (outrcrop)	unknown (stratigraphic collection)
EZS 14	Kimmeridge Shale (outcrop)	unknown (stratigraphic collection)

Quantitative bulk & clay mineralogy

Sample	Qtz	Kspar	Plag	ΣCarb	Pyr	Hal	Gyp	Ana	Am	ΣNC	Kaol	Σ2:1	Smect	Illite	Chl	Σclay	Total
EZN31	33	3	0.2	21	0	0.5	0	0.2	1	59	5	36	17.5	18.3	0	41	100
LGT49	26	6	4	19	0.3	2	0.4	0.7	1	60	5	30	18.4	11.8	5	40	100

Sample	In clay fraction						
	%smect	%illite	%2:1	%kaol	%chl	%S in 2:1	%I in 2:1
EZN31	42.9	44.8	87.7	12.3	0.0	48.9	51.1
LGT49	45.7	29.4	75.1	12.4	12.4	60.9	39.1

Qualitative detailed clay mineralogy
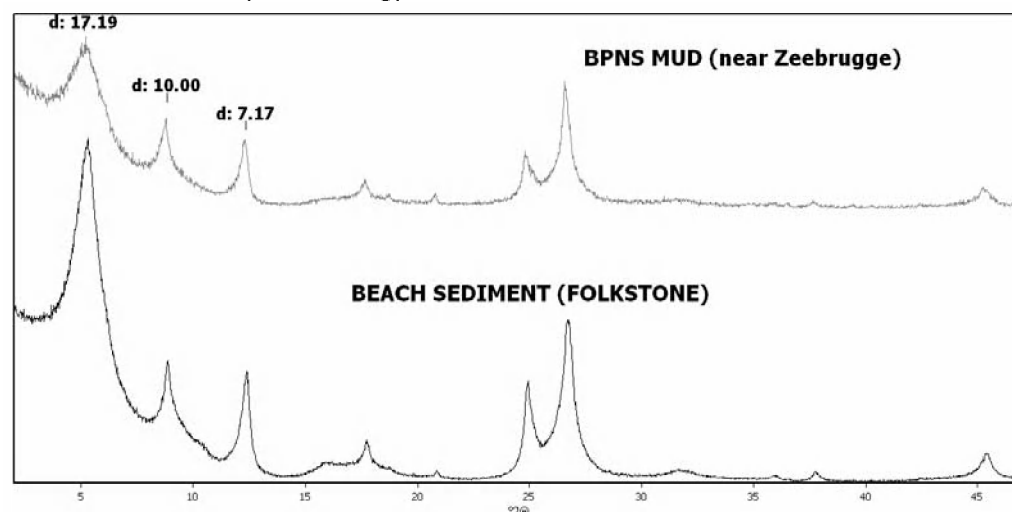
Figure 6. BPNS muds compared to beach sediments from the English coast.

Clay mineralogy compared to the clay mineralogy of the BPNS muds

More smectite and kaolinite, practically no chlorite and vermiculite. The clay mineralogy of the outcrop samples is very different, thus justifying the focus on sampling beach sediments. The Thames suspension sample is clearly richer in kaolinite and chlorite.

Provenance conclusion

Unlikely major source for BPNS muds.

2.2.5 French coast

Samples

	Description	Location
EZN 9	Beach sediment	Bray-Dunes
EZN 10	Beach sediment	Bray-Dunes
EZN 11	Beach sediment	Platier d'Oye
EZN 12	Beach sediment	Sangatte
EZN 14	Beach sediment	Cap Griz Nez
EZN 18	Beach sediment	Canche Estuary, Le Touquet
EZN 19	Marsh clay	Canche Estuary, Le Touquet
EZN 20	Beach sediment	Beck Plage
EZN 21	Tidal flat clay rich sand	Somme Estuary, Le Crotoy
EZN 23	Beach sediment	Ault-Onival
EZN 56	Beach sediment	Calais
EZN 57	Beach sediment	Calais
EZN 13	Weathered shale (outcrop)	Cap Griz Nez
EZN 15	Gray clay (outcrop - Jurassic)	Wimmereux
EZN 16	Brown clay (outcrop - Jurassic)	Wimmereux
EZN 22	Nodular clay rich cohesive sand (outcrop)	Somme Estuary, Le Crotoy
EZS 6	Clay (outcrop)	Cap Griz Nez
EZS 8	Clay (outcrop)	Cap d'Ailly

Quantitative bulk & clay mineralogy

Sample	Qtz	Kspar	Plag	☐Carb	Pyr	Hal	Gyp	Ana	Am	☐NC	Kaol	☐2:1	Smect	Illite	Chl	☐clay	Total
EZN13	56	0	0	26	0.3	0	0	0.3	0.2	83	1	16	7.5	8.1	0	17	100
EZN15	35	3	1	9	0	0	0	0.9	0.8	50	9	39	18.9	19.6	3	51	100
EZN16	19	4	1	12	0	0	0	0.7	1	39	8	50	23.7	26.0	3	61	100
EZN19	22	5	3	39	0	2	0	0.3	0.6	72	4	21	16.9	4.0	4	29	100
EZN20	75	4	2	10	0	0.7	0	0	0.0	92	0.4	5	5.0	-	3	9	100
EZN21	48	4	4	32	0	0.9	0	0	0.1	89	0.5	9	7.1	2.1	2	12	100
EZN22	55	5	4	25	0	0	0	0	0.3	89	0.1	10	5.3	4.4	0.9	11	100
EZN56	42	3	3	34	0	0.5	0	0.2	0.3	83	2	13	11.6	1.5	2	17	100
EZN57	47	3	2	28	0	0	0	0	0.8	81	1	17	10.0	6.5	0.9	18	100

| Sample	In clay fraction						
	%smect	%illite	%2:1	%kaol	%chl	%S in 2:1	%I in 2:1
EZN13	45.4	48.5	94.0	6.0	0.0	48.4	51.6
EZN15	37.4	38.8	76.2	17.8	5.9	49.1	50.9
EZN16	39.0	42.8	81.9	13.2	4.9	47.7	52.3
EZN19	58.5	13.8	72.3	13.8	13.8	80.9	19.1
EZN20	60.9	-	60.9	4.6	34.5	100.0	-
EZN21	60.9	17.7	78.6	4.3	17.1	77.5	22.5
EZN22	49.7	41.0	90.7	0.9	8.4	54.8	45.2
EZN56	67.7	8.9	76.6	11.7	11.7	88.3	11.7
EZN57	54.6	35.1	89.7	5.4	4.9	60.9	39.1

Qualitative detailed clay mineralogy
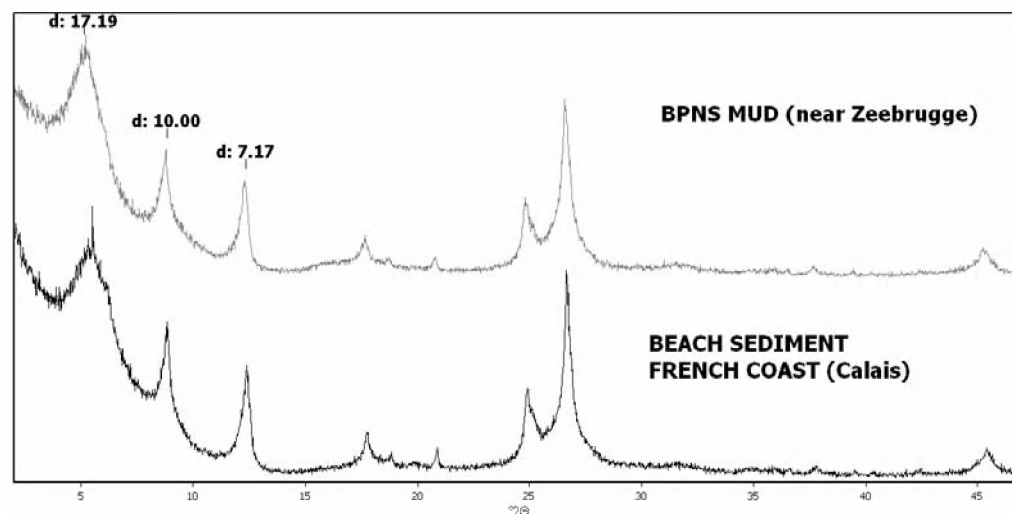
Figure 7. BPNS muds compared to beach sediments from the French coast.

Clay mineralogy compared to the clay mineralogy of the BPNS muds

Beach sediments sampled between the Belgian border almost up to Calais are very similar, from Calais southwards the clay mineral assemblages become slightly different with less smectite. The difference is judged to be significant enough to distinguish them from the BPNS muds.

Provenance conclusion

The largest amount of sediments deposited in the Dover Strait finds its origin south of Calais, therefore the French coast probably is not a major source for the BPNS muds.

2.2.6 Input from the Atlantic Ocean

Samples

	Description	Location
EZN 27	Suspension collected on a track	Acros the Gulf of Biscay - entrance of The Channel
EZN 28	Suspension collected on a track	Entrance of The Channel - middle of The Channel
EZN 29	Suspension collected on a track	Middle of The Channel - past Dover Strait

Qualitative detailed clay mineralogy
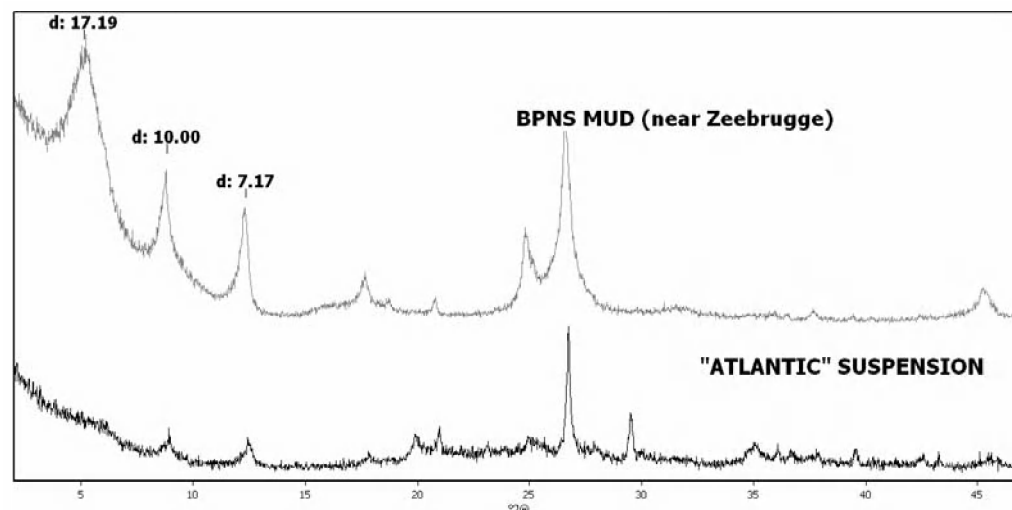
Figure 8. BPNS muds compared to a suspension sample collected in the western part of The Channel.

Clay mineralogy compared to the clay mineralogy of the BPNS muds

Distinctly different, almost no smectite or illite-smectite present.

Provenance conclusion

Unlikely major source for BPNS muds.

2.3 Characterization of Tertiary/Quaternary deposits, exposed on the BPNS

2.3.1 Tertiary deposits exposed on the BPNS seafloor

Samples

Tertiary sediments potentially exposed on the BPNS seafloor range from Early Eocene to Early Oligocene age. To represent this entire interval, 95 samples were taken on land from cores and outcrops in quarries. (Ypresian: 28 samples / Lutetian-Bartonian-Priabonian: 48 samples / Rupelian: 23 samples – *because of its length the sample list is not included here but can be found in the PhD work of E. Zeelmaekers, available end of 2009*).

Quantitative bulk & clay mineralogy

Because of its length the bulk mineralogy results are not included here, but can be found in the PhD work of E. Zeelmaekers, available end of 2009. Clay mineralogical differences between the analyzed Eocene and Oligocene deposits are sufficiently apparent from the qualitative detailed clay mineralogy.

Qualitative detailed clay mineralogy
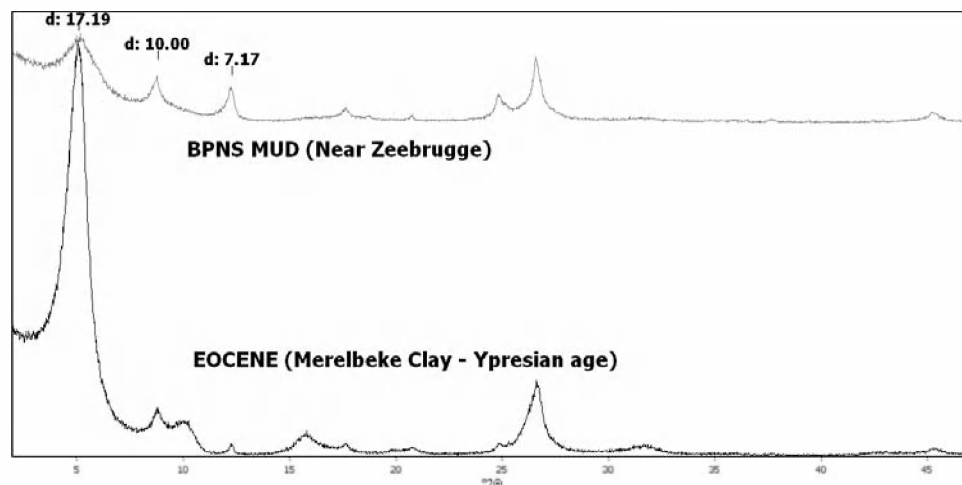
Figure 9. BPNS muds compared to Merelbeke Clay (Eocene).
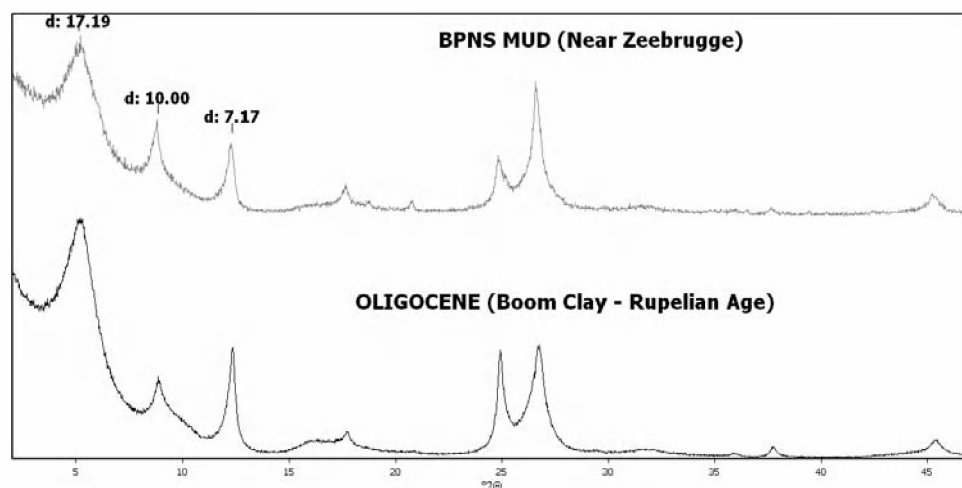
Figure 10. BPNS muds compared to Boom Clay (Oligocene).

Clay mineralogy compared to the clay mineralogy of the BPNS muds

Equivalents of Eocene sediments potentially exposed on the BPNS seafloor are much more smectitic, contain only small amounts of illite and kaolinite and almost no chlorite and vermiculite. Equivalents of Oligocene sediments potentially exposed on the BPNS seafloor contain more kaolinite and smectite and less chlorite and vermiculite.

Provenance conclusion

Erosion of exposed Tertiary deposits is an unlikely major source for the BPNS.

2.3.2 Quaternary deposits exposed on the BPNS seafloor or near coastal area

Samples

	Description: all from LOWER PLEISTOCENE in ROER VALLEY	Location
EZS 51	Reuver Clay	Oebel Quarry
EZS 52	Lower Tegelen Clay	Oebel Quarry
EZS 53	Reuver Clay	Brachterwald - BTA Quarry
EZS 54	Upper Tegelen Clay	Hoherstall Quarry
EZS 55	Upper Tegelen Clay	Oebel Quarry
EZS 56	Clay in Sterksel formation	Oebel Quarry
EZS 71	Reuver Clay	Oebel Quarry
EZS 72	Reuver Clay	Brachterwald - BTA Quarry
EZS 73	Reuver Clay - white layer	Brachterwald - BTA Quarry
EZS 74	Reuver Clay - white layer	Brachterwald - BTA Quarry
EZS 75	Reuver Clay - brown layer	Brachterwald - BTA Quarry
EZS 76	Reuver Clay - white layer	Brachterwald - BTA Quarry
EZS 77	Oebel beds	Brachterwald - BTA Quarry
EZS 78	Lower Reuver Clay	Brachterwald - BTA Quarry
EZS 79	Oebel beds	Hoherstall Quarry
EZS 80	Tegelen Clay	Hoherstall Quarry
EZS 81	Clay in Sterksel formation	Hoherstall Quarry
EZS 82	Tegelen Clay	Maalbeek Quarry

	Description: all from LOWER PLEISTOCENE in CAMPINE BASIN	Location
EZS 47	Rijkevorsel Clay	Merksplas-Beerse
EZS 48	Turnhout Clay	Merksplas-Beerse
EZS 49	Rijkevorsel Clay	Terca Nova Quarry, Beerse
EZS 50	Late Glacial eolian sand	Terca Nova Quarry, Beerse
EZS 64	Beerse sands	Merksplas-Beerse
EZS 65	Rijkevorsel Clay	Merksplas-Beerse
EZS 66	Turnhout Clay	Terca Nova Quarry, Beerse
EZS 67	Late Glacial eolian laminated clay rich/coarse	Westmalle/Brecht
EZS 68	Late Glacial eolian/fluvial with ripple drapes	Westmalle/Brecht
EZS 69	Turnhout Clay	Westmalle/Brecht

EZS 70	Rijkevorsel Clay	Westmalle/Brecht
EZN 58	Periglacial in Beerse sands	Terca Nova Quarry, Beerse
EZN 59	Late Glacial eolian clay rich sand	Terca Nova Quarry, Beerse

	Description: all from WEICHSEL cover sands	Location
EZS 27	Cover sand	Schelle
EZS 28	Cover sand	Schelle
EZS 31	Cover sand	Argex Quarry, Kruibeke
EZS 39	Cover sand	Argex Quarry, Kruibeke
EZS 40	Loam	Bouillon Quarry, Bierbeek

	Description: all from EEMIAN interglacial	Location
EZN 48	Intertidal flats - Leeuwenhof core (7.90m depth)	Between Nieuwpoort and Gistel
EZN 49	Intertidal flats - Leeuwenhof core (8.29m depth)	Between Nieuwpoort and Gistel
EZN 50	Intertidal flats - Leeuwenhof core (9.63m depth)	Between Nieuwpoort and Gistel
EZN 51	Intertidal flats - Leeuwenhof core (10.55m depth)	Between Nieuwpoort and Gistel
EZN 52	Intertidal flats - Leeuwenhof core (11.25m depth)	Between Nieuwpoort and Gistel
EZN 53	Intertidal flats - Leeuwenhof core (11.65m depth)	Between Nieuwpoort and Gistel
EZN 54	Intertidal flats - Leeuwenhof core (12.27m depth)	Between Nieuwpoort and Gistel
EZN 55	Intertidal flats - Leeuwenhof core (12.63m depth)	Between Nieuwpoort and Gistel

	Description: all from HOLOCENE	Location
EZS 16	Salt marsh - Kaaskerke core - (0.96-1.00m depth)	Near Diksmuide
EZS 17	Salt marsh - St. Jozef core (7.35-7.40m depth)	Near Veurne
EZS 18	Salt marsh - Ostend Airport core (0.46-0.50m depth)	Near Ostend
EZS 19	Salt marsh - Kaaskerke core - (1.95-2.00m depth)	Near Diksmuide
EZS 20	Salt marsh - Esen core - (0.78-0.82m depth)	Near Diksmuide
EZS 21	Salt marsh - Veurne core (2.39-2.42m depth)	Veurne
EZS 22	Salt marsh - Knokkebrug core(0.40-0.44m depth)	Near Diksmuide
EZS 23	Salt marsh - St. Jozef core (0.60-0.65m depth)	Near Veurne
EZS 24	Salt marsh - Veurne core (1.11-1.14m depth)	Veurne
EZS 25	Salt marsh - Esen core - (0.94-0.96m depth)	Near Diksmuide
EZS 26	Salt marsh - Veurne core (2.60-2.64m depth)	Veurne
EZN 45	Intertidal flats - Leeuwenhof core (3.65m depth)	Between Nieuwpoort and Gistel

| EZN 46 | Intertidal flats - Leeuwenhof core (2.74m depth) | Between Nieuwpoort and Gistel |
| EZN 47 | Intertidal flats - Leeuwenhof core (7.40m depth) | Between Nieuwpoort and Gistel |

Quantitative bulk & clay mineralogy

Sample	Qtz	Kspar	Plag	ΣCarb	Pyr	Hal	Gyp	Ana	Am	ΣNC	Kaol	Σ2:1	Smect	Illite	Chl	Σclay	Total
EZS51	33	3	0.5	2	0	0	0	0	2	40	6	48	25.5	22.9	5	59	100
EZS52	29	2	2	16	0	0	0	0.5	0.9	50	5	40	19.6	20.8	5	50	100
EZS53	50	4	0	0	0	0	0	0.6	1	56	9	34	14.7	19.5	1	44	100
EZS54	35	4	2	0.5	0	0	0	0.5	1	43	7	43	24.1	18.7	7	57	100
EZS55	47	7	5	0	0	0	0	0	1	60	3	30	16.7	12.9	7	40	100
EZS56	33	4	1	0	0	0	0	0.2	2	40	7	47	16.9	29.6	6	60	100
EZS71	39	4	0	0	0	0.1	0.5	0.8	0.8	45	11	39			5	55	100
EZS72	41	4	0.6	0	0	0	1	0.7	1	49	10	38	13.8	24.4	4	52	100
EZS73	20	3	0	4	0	0	0.9	0.9	1	30	16	50	18.7	31.6	4	70	100
EZS74	38	4	0.4	0	0	0	0	1	1	45	10	42	15.6	26.5	3	55	100
EZS75	50	3	0	1	0	0	0	0.4	1	56	8	33	14.5	18.9	2	43	100
EZS76	57	4	0	0	0	0.1	0	0.9	0.6	63	8	26	12.3	14.1	3	37	100
EZS77	23	4	0.5	1	0	0	0	1	1	31	8	54	30.5	23.5	6	68	100
EZS78	44	5	1	3	0	0	1	0.4	0.5	55	8	32	21.2	11.0	5	45	100
EZS79	36	4	2	0	0	0	0.5	0.5	1	44	9	40	22.8	17.2	7	56	100
EZS80	28	4	3	0	0	0	0	0.9	1	37	5	50			8	63	100
EZS81	45	5	8	0	0	0.4	0	0.3	1	60	4	31	13.3	17.8	5	40	100
EZS82	49	5	5	7	0	0	0	0	0.7	67	2	26			5	33	100

Sample	In clay fraction						
	%smect	%illite	%2:1	%kaol	%chl	%S in 2:1	%I in 2:1
EZS51	42.9	38.6	81.5	10.1	8.4	52.7	47.3
EZS52	38.9	41.3	80.2	9.9	9.9	48.5	51.5
EZS53	33.2	44.2	77.4	20.4	2.3	42.9	57.1
EZS54	42.5	32.9	75.4	12.3	12.3	56.4	43.6
EZS55	42.2	32.6	74.7	7.6	17.7	56.4	43.6
EZS56	28.4	49.8	78.2	11.8	10.1	36.3	63.7
EZS71			70.7	20.1	9.2		
EZS72	26.4	46.8	73.2	19.2	7.7	36.1	63.9

Sample						
EZS73	26.6	44.9	*71.6*	22.8	5.7	37.2	62.8
EZS74	28.2	48.2	*76.4*	18.1	5.4	37.0	63.0
EZS75	33.4	43.6	*77.0*	18.4	4.6	43.3	56.7
EZS76	32.8	37.8	*70.6*	21.4	8.0	46.5	53.5
EZS77	44.9	34.5	*79.4*	11.8	8.8	56.6	43.4
EZS78	46.9	24.4	*71.2*	17.7	11.1	65.8	34.2
EZS79	40.8	30.6	*71.4*	16.1	12.5	57.1	42.9
EZS80			*79.4*	7.9	12.7		
EZS81	33.1	44.5	*77.6*	10.0	12.5	42.7	57.3
EZS82			*79.0*	6.0	15.0		

Sample	Qtz	Kspar	Plag	Σ*Carb*	Pyr	Hal	Gyp	Ana	Am	Σ*NC*	Kaol	Σ*2:1*	*Smect*	*Illite*	Chl	Σ*clay*	Total
EZS47	52	6	3	*0.5*	1	0	0.5	0.2	0.9	*64*	5	*28*	<u>*8.6*</u>	<u>*19.2*</u>	3	*36*	100
EZS48	27	4	2	*0*	0	0	0	0	2	*35*	9	*54*	*22.3*	*32.1*	3	*66*	100
EZS49	23	3	2	*0*	0	0	0	0.5	3	*31*	6	*58*	*23.6*	*34.6*	4	*68*	100
EZS50	70	8	8	*0.4*	0.1	0	0	0.2	0.6	*87*	0.7	*12*	<u>*8.4*</u>	<u>*3.6*</u>	0	*13*	100
EZS64	63	8	6	*0.8*	0	0	0	0.3	0.4	*78*	2	*16*	<u>*8.9*</u>	<u>*7.0*</u>	3	*21*	100
EZS65	25	3	1	*0*	0.2	0	0	0.2	3	*32*	6	*60*	*24.2*	*35.3*	1	*67*	100
EZS66	48	7	5	*1*	0	0.2	1	0.4	1	*64*	3	*29*	<u>*8.9*</u>	<u>*20.2*</u>	4	*36*	100
EZS67	79	0.5	0	*0.5*	0	0	0	0.2	0.7	*81*	3	*15*	<u>*8.5*</u>	<u>*6.6*</u>	0.5	*19*	100
EZS68	86	5	1	*0*	0	0	0	0.2	0.2	*92*	0.9	*7*	<u>*5.3*</u>	<u>*1.3*</u>	0.4	*8*	100
EZS69	28	4	2	*4*	0	0	0.7	0	2	*40*	8	*41*	*-*	*-*	10	*59*	100
EZS70	56	7	5	*0.3*	0	0	0	0.3	1	*70*	2	*24*	<u>*8.4*</u>	<u>*15.1*</u>	5	*31*	100
EZN59	87	5	3	*0*	0	0	0	0	0.1	*95*	0.1	*4*	<u>*4.0*</u>	*-*	0.5	*5*	100

Sample	In clay fraction						
	%smect	%illite	*%2:1*	%kaol	%chl	%S in 2:1	%I in 2:1
EZS47	<u>24.1</u>	<u>53.5</u>	*77.7*	14.0	8.4	<u>31.1</u>	<u>68.9</u>
EZS48	33.6	48.3	*81.9*	13.6	4.5	41.0	59.0
EZS49	34.6	50.7	*85.3*	8.8	5.9	40.6	59.4
EZS50	<u>65.8</u>	<u>28.7</u>	*94.5*	5.5	0.0	<u>69.7</u>	<u>30.3</u>
EZS64	<u>42.4</u>	<u>33.7</u>	*76.1*	9.6	14.4	<u>55.7</u>	<u>44.3</u>
EZS65	36.4	53.1	*89.5*	9.0	1.5	40.7	59.3
EZS66	<u>24.5</u>	<u>56.1</u>	*80.6*	8.3	11.1	<u>30.4</u>	<u>69.6</u>
EZS67	<u>46.0</u>	<u>35.2</u>	*81.2*	16.1	2.7	<u>56.6</u>	<u>43.4</u>
EZS68	66.8	16.8	*83.5*	11.4	5.1	79.9	20.1

Sample						
EZS69	-	-	69.5	13.6	16.9	-
EZS70	27.6	49.5	77.0	6.6	16.4	35.8	64.2
EZN59	88.0	-	88.0	2.0	10.0	100.0	-

Sample	Qtz	Kspar	Plag	⊡Carb	Pyr	Hal	Gyp	Ana	Am	⊡NC	Kaol	⊡2:1	Smect	Illite	Chl	⊡clay	Total
EZS27	84	5	2	0	0	0	0	0	0.2	91	1	8	6.2	1.5	0.2	9	100
EZS28	79	6	4	0	0	0	0	0	0.4	89	0.4	10	8.3	1.4	0.4	11	100
EZS31	58	9	9	9	0	0	0	0.2	0.2	86	1	12	8.6	3.2	1	14	99.1
EZS39	64	10	10	0.5	0	0	0	0	0.6	86	1	13	9.2	4.2	0.2	15	99.4
EZS40	63	8	9	0	0	0	0	0	0.6	81	2	16	11.3	4.9	2	20	100

	In clay fraction						
Sample	%smect	%illite	%2:1	%kaol	%chl	%S in 2:1	%I in 2:1
EZS27	70.1	16.4	86.5	11.2	2.2	81.0	19.0
EZS28	78.6	13.8	92.4	3.8	3.8	85.1	14.9
EZS31	62.0	23.5	85.5	7.2	7.2	72.5	27.5
EZS39	62.8	29.0	91.8	6.8	1.4	68.4	31.6
EZS40	56.0	24.2	80.2	9.9	9.9	69.8	30.2

Sample	Qtz	Kspar	Plag	⊡Carb	Pyr	Hal	Gyp	Ana	Am	⊡NC	Kaol	⊡2:1	Smect	Illite	Chl	⊡clay	Total
EZN48	19	3	3	25	0.2	0.2	0.4	0.4	5	56	3	39	25.1	13.6	4	46	100
EZN49	29	3	2	25	0.3	0	1	0	5	65	3	29	19.1	9.5	3	35	100
EZN50	23	3	4	26	0.1	0.5	2	0.4	1	60	4	34	21.9	11.7	4	42	100
EZN51	29	5	5	25	0.2	0.5	2	0.5	0.8	68	4	26	17.9	7.7	3	33	100
EZN52	24	5	3	24	0	0.6	1	0.4	6	64	4	29	20.3	8.4	2	35	100
EZN53	29	4	3	23	0	1	1	0.2	6	66	2	28	19.4	8.5	3	33	100
EZN54	24	3	4	26	0.7	0	1	0.2	4	63	2	31	18.6	11.9	5	38	100
EZN55	23	3	3	22	0.5	0.5	3	0.3	5	60	3	35	20.2	14.7	2	40	100

	In clay fraction						
Sample	%smect	%illite	%2:1	%kaol	%chl	%S in 2:1	%I in 2:1
EZN48	54.8	29.9	84.7	6.6	8.8	64.7	35.3
EZN49	55.2	27.4	82.7	8.7	8.7	66.8	33.2
EZN50	52.7	28.1	80.8	9.6	9.6	65.2	34.8
EZN51	54.8	23.8	78.5	12.3	9.2	69.7	30.3

EZN52	58.6	24.1	*82.7*	11.5	5.8	70.9	29.1
EZN53	58.9	25.9	*84.8*	6.1	9.1	69.5	30.5
EZN54	49.5	31.8	*81.3*	5.3	13.3	60.9	39.1
EZN55	50.6	36.8	*87.5*	7.5	5.0	57.9	42.1

Sample	Qtz	Kspar	Plag	☐*Carb*	Pyr	Hal	Gyp	Ana	Am	☐*NC*	Kaol	☐*2:1*	*Smect*	*Illite*	Chl	☐*clay*	Total
EZS16	30	5	4	*9*	0	0	0	0.2	2	*50*	2	*46*	*29.0*	*17.2*	0.9	*49*	100
EZS17	44	5	7	*10*	0.4	0	2	0.2	0.9	*69*	2	*27*	*14.9*	*11.7*	2	*31*	100
EZS18	35	4	5	*9*	0	0	0	0.2	1	*54*	1	*40*	*20.7*	*19.1*	4	*45*	100
EZS19	31	5	5	*16*	0.9	0	4	0.5	0.9	*63*	3	*33*	*24.0*	*9.4*	1	*37*	100
EZS20	66	4	4	*8*	0	0	0	0	0.8	*83*	0.5	*15*	*11.0*	*3.8*	1	*16*	100
EZS21	55	6	8	*10*	0.2	0	0	0.5	0.6	*80*	1	*16*	*9.3*	*6.9*	2	*19*	100
EZS22	42	7	7	*3*	0	0	0	0.1	0.9	*60*	4	*32*	*23.0*	*9.0*	3	*39*	100
EZS23	43	5	6	*4*	0	0	0	0.3	1	*59*	4	*31*	*15.9*	*15.2*	5	*40*	100
EZS25	41	7	7	*0*	0	0	0	0.2	1	*56*	4	*37*	*32.6*	*4.3*	2	*43*	100
EZS26	55	7	7	*15*	0.4	0	0	0	0.3	*85*	1	*10*	*4.3*	*6.1*	2	*13*	100
EZN45	63	5	6	*10*	0.4	0	1	0	0.7	*86*	0.5	*12*	*12.0*		0.6	*13*	100
EZN46	24	3	4	*24*	0.2	0	0.8	0.3	7	*63*	3	*33*	*13.2*	*19.4*	3	*39*	100
EZN47	47	7	3	*16*	0.5	0	0.8	0	0.8	*75*	2	*21*	*19.3*	*2.1*	2	*25*	100

Sample	In clay fraction						
	%smect	%illite	*%2:1*	%kaol	%chl	%S in 2:1	%I in 2:1
EZS16	59.1	35.0	*94.1*	4.1	1.8	62.8	37.2
EZS17	48.7	38.2	*86.9*	6.5	6.5	56.1	43.9
EZS18	46.3	42.5	*88.8*	2.2	8.9	52.1	47.9
EZS19	64.1	25.2	*89.3*	8.0	2.7	71.8	28.2
EZS20	67.4	23.4	*90.8*	3.1	6.1	74.2	25.8
EZS21	48.6	35.8	*84.4*	5.2	10.4	57.6	42.4
EZS22	59.1	23.0	*82.1*	10.3	7.7	72.0	28.0
EZS23	39.7	37.9	*77.6*	10.0	12.5	51.2	48.8
EZS25	76.0	10.0	*86.0*	9.3	4.7	88.3	11.7
EZS26	31.9	45.7	*77.6*	7.5	14.9	41.1	58.9
EZN45	91.8		*91.8*	3.7	4.5	100.0	
EZN46	34.2	50.3	*84.5*	7.8	7.8	40.4	59.6
EZN47	76.2	8.1	*84.3*	7.9	7.9	90.4	9.6

Qualitative detailed clay mineralogy
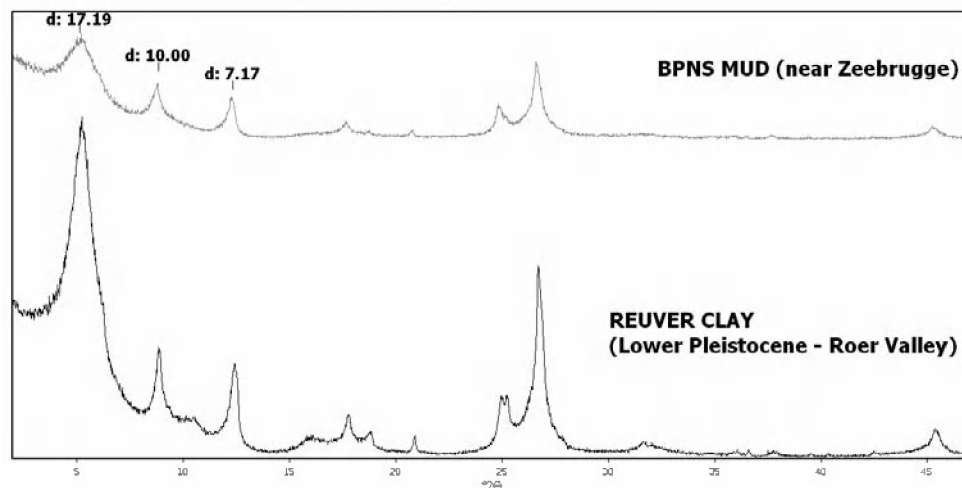
Figure 11. BPNS muds compared to Reuver Clay (Lower Pleistocene).
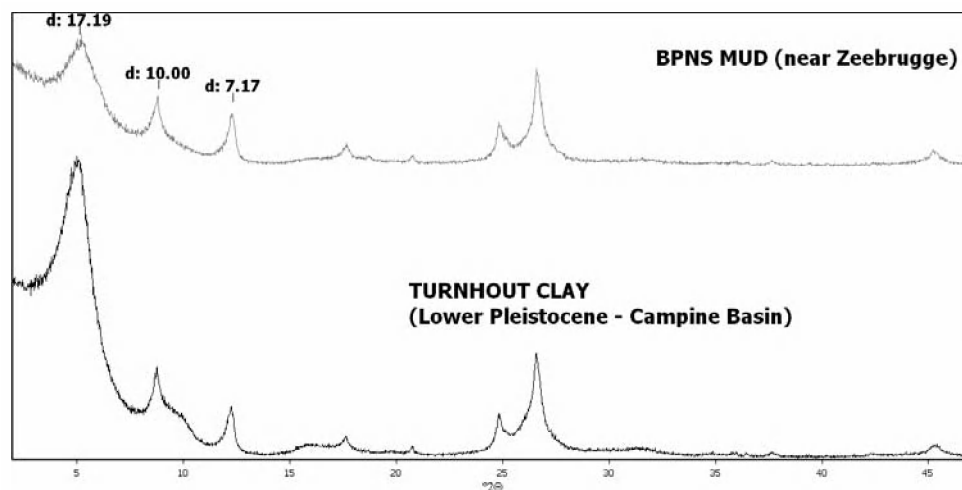

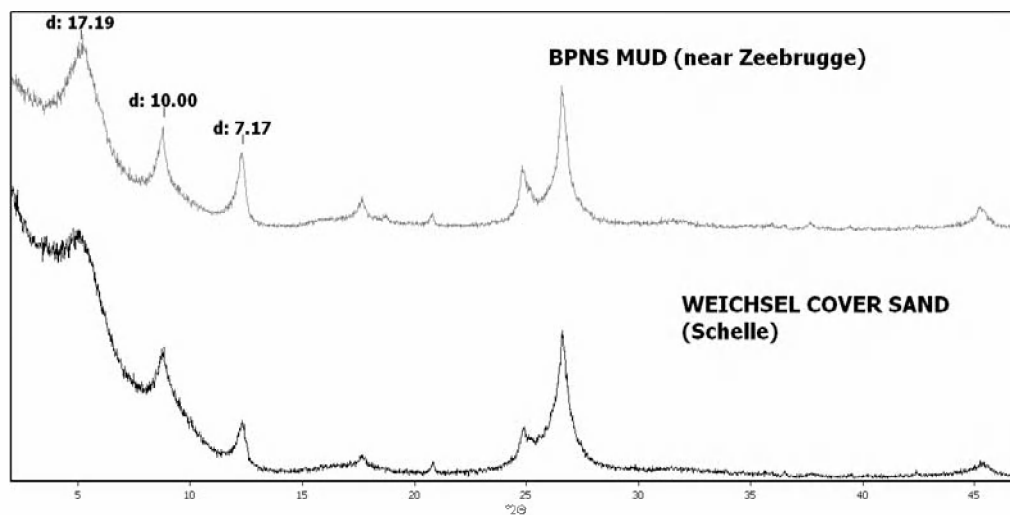Figure 12. BPNS muds compared to Turnhout Clay (Lower Pleistocene).

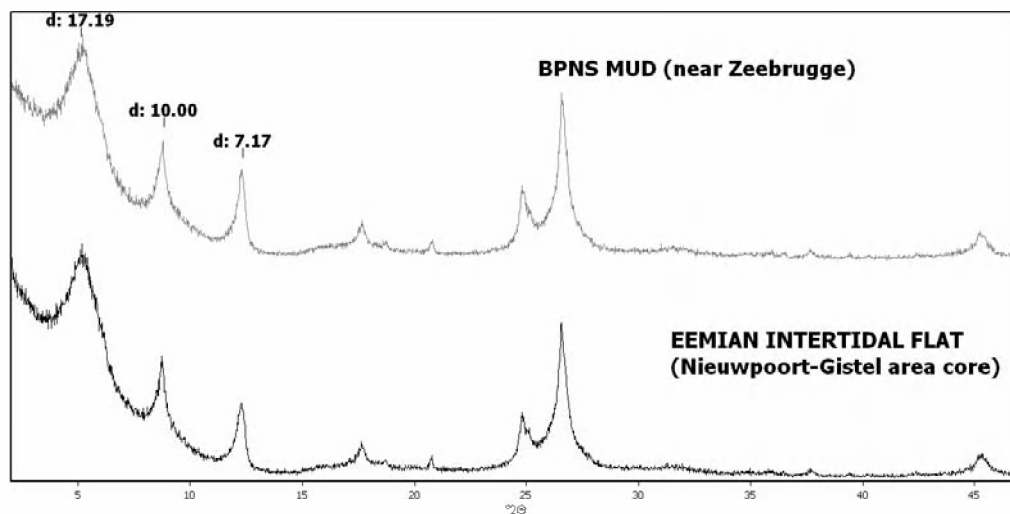Figure 13. BPNS muds compared to cover sand (Weichsel).

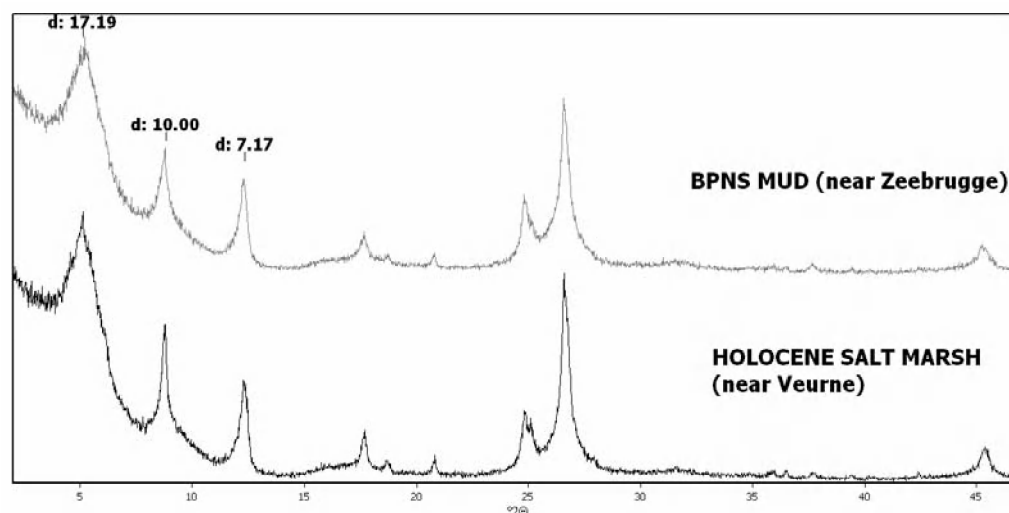Figure 14. BPNS muds compared to Eemian intertidal flat.

Figure 15. BPNS muds compared to Holocene salt marsh.

Clay mineralogy compared to the clay mineralogy of the BPNS muds

The clay mineralogy of the Lower Pleistocene Roer Valley and Campine Basin deposits and the Weichsel cover sands is distinctly different from the BPNS muds. The clay mineralogy of these deposits is very variable, but always shows very different clay assemblages or clay mineral ratios than for the BPNS muds.

The clay mineralogy of the examined Eemian intertidal flats is nearly identical to the BPNS muds, while the clay mineralogy of Holocene salt marshes is very similar.

Provenance conclusion

The Lower Pleistocene and Weichsel deposits are unlikely major sources for the BPNS muds. The Holocene salt marsh and the Eemian intertidal deposits show a strong provenance connection with the BPNS muds, indicating a provenance relation with the Scheldt river system on and off since the Late Pleistocene.

Annex II. Historic Sediments information re-processing: methodologies and final results

J.-S. Houziaux[1], M. Fettweis[2], F. Francken[2], I. Dufour[3], V. Van Lancker[2], S. Jans[2], K. De Cauwer[2].

[1] Royal Belgian Institute of Natural Science (RBINS), Department of Invertebrates, rue Vautier 29, 1000 Brussels, Belgium

[2] Royal Belgian Institute of Natural Science (RBINS), Management Unit of the North Sea Mathematical Models (MUMM), Gulledelle 100, 1200 Brussels, Belgium

1. Material and methods

The "Gilson collection" is a vast and heterogeneous set of biotic and abiotic samples, acquired between 1899 and 1939, mostly within the Belgian part of the North Sea (BPNS), together with paper archives documenting them. The material is disseminated across the RBINS repositories, where it is mixed with other collections on a taxonomical basis. Parts of it have been determined and studied by various researchers (mainly taxonomists) throughout the 20th century; they contributed to further disperse Gilson's material. The virtual historic data-set, represented by this collection, was however a complex puzzle to reconstruct and we forward the reader to the freely available technical reports for details on strategies adopted to overcome this issue (van Loen et al, 2002; Houziaux et al, 2008). Briefly, the main sampling activities of Gilson relatively to invertebrate benthos and sediment took place between 1899 and 1908, although he occasionally continued field work (mainly on commercial fish species) up to 1939. The Gilson's coastal sampling grid (figure 1) was primarily designed on nautical charts, using minutes of latitude and longitude as grid nodes ("exploration réticulaire"). On and around the Westhinder offshore sand bank, a system of virtual "crosses" was set-up, with sampling operations taking place at the cross center, along the virtual arms and, for towed gears, around the cross center ("exploration cruciale"). Few large-scale transects were further drawn starting from the lightship "Wandelaar", in coastal waters ("exploration radiée"), as well as smaller transects visible in the Belgian Western coastal waters (figure 1).

Multiple information sources with varying levels of relevance, adequacy and exhaustivity characterize Gilson's archived material (figure 2). This situation creates a redundancy of information which is most useful to validate the acquired data, but strongly complicates the work. Indeed, the gathered information used to be hand-copied from field log-books to specimen labels, sampling inventories and/or other log-books, a process which has generated accumulation of randomly distributed copying mistakes. These are particularly problematic when geographic coordinates or dates are concerned. The information sources were thus digitized and cross-referenced to determine the intrinsic limitations of the final data-set and enable meaningful data selection, depending on analysis purposes.
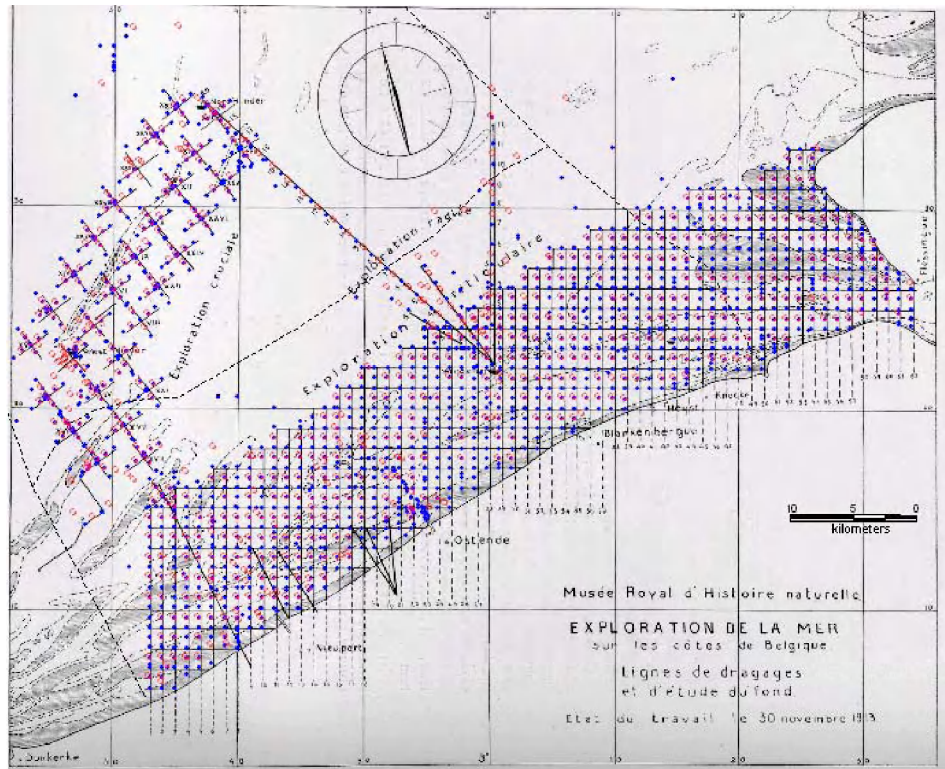
Figure 1. Distribution of Gilson's "ground-collector" (blue dots) and benthic dredge (red open circles; median point of the tow) samples, taken in the BPNS, mostly between 1899 and 1911. See text for details. The data are superimposed on the original map of Gilson's sampling grids in front of the Belgian and Dutch coasts of the southern North Sea (from Gilson, 1914). Dotted line: present limits of the BPNS and territorial waters (12 nautical miles).

In total, Gilson carried out nearly 14,000 sampling operations at sea, listed and summarized in two main general information sources (figure 2). On the one hand, major sampling meta-data were recorded in 5 books under various "explorations", defined on the basis of target compartment (plankton, benthos, fish), surveyed grid and / or survey goals (regular exploration of Belgian waters or ICES surveys). These different "explorations" were highlighted by specific station codes (defining 'station' as one place and one time at which a sample was taken). Sampling date, location (either in the form of verbose description of geographic coordinates), station code and sampling gear were recorded primarily in these books, each sample being represented by one line. On the other hand, individual cards (one card per sampling station) were created by Gilson for every sample in order to summarize all environmental information gathered at that station, including sediment types. Thus, cards of benthic samples, obtained by a dredge towed over a distance of one nautical mile, were in theory filled with additional information about the seafloor collected with the sediment sampler at the start, mid and end points of the tow, but also with water temperature, wind direction and strength, etc (figure 1bis). In practice, these cards were filled with very heterogeneous quality levels and many remained unfilled, yet one card has indeed been created for every sampling station. These two "general" information sources were primarily digitized without validation to form a first data-bank of Gilson's sampling events. The chronological sequence of sampling at sea was then reconstructed on a daily basis to detect errors, such as aberrant positions compared to other successive samples of the day. It also enabled us to link different sampling gears through their position, thus establishing a direct link between their respective information contents (e.g. benthos and sediment).
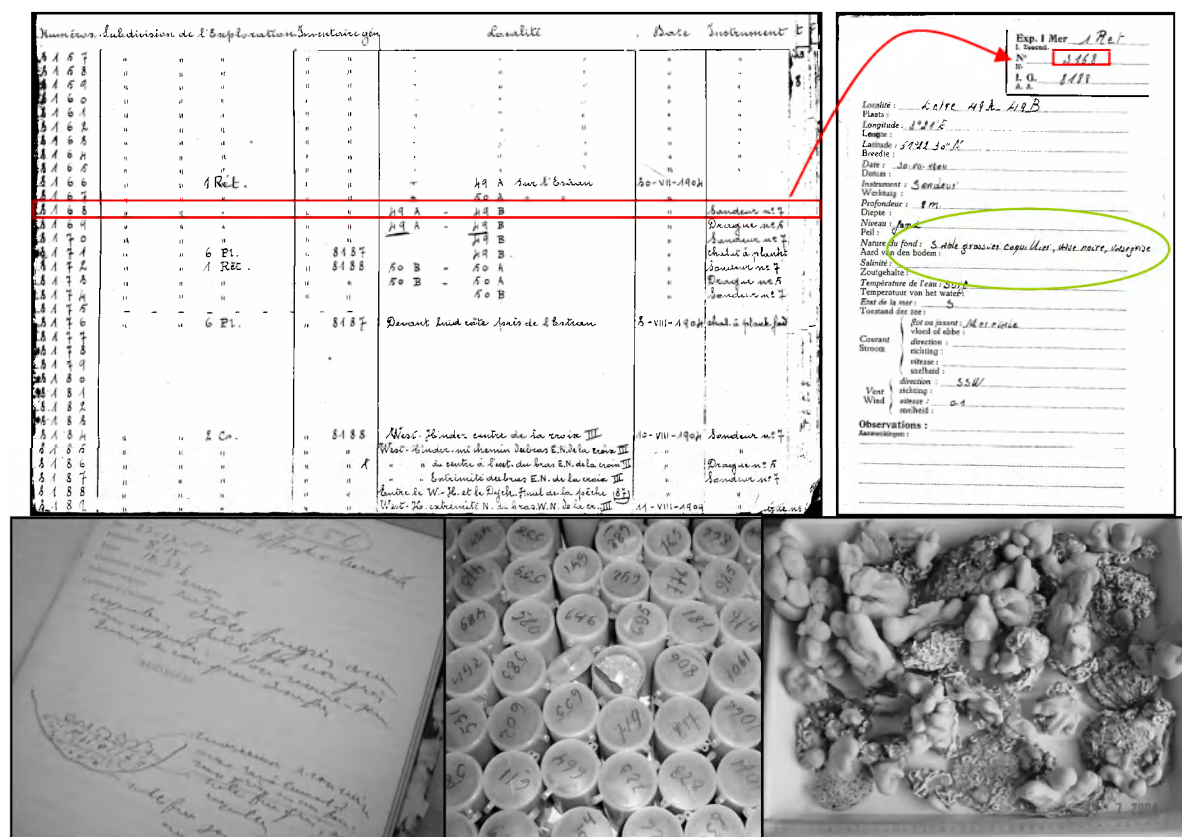
Figure 2: Above: images of a page of a general sampling inventory (left), with the daily sample sequence highlighted in red, and the card corresponding to this station, "3168" (right), both sources providing different levels of details on meta-data. Note the brief sediment description on the card (circled in green). Below: a page of a Gilson's field log-book, with a drawing of the cup content (left), Gilson's sediment sub-samples archived at the RBINS (middle) and stones and oyster shells gathered with the benthic dredge on one station alongside hundreds of colonies of the dead-man fingers *Alcyonium digitatum* (right).

We considered that the detailed analysis of field log-books, written by the hand of Gilson, was necessary information to further validate the historical data-set. 34 field log-books concerning 2195 sediment sampling stations were gathered and their content was fully digitized in a spreadsheet. 1785 of these data were considered valid and useful. In these log-books, we found additional information as compared to the aforementioned general inventories, such as sampling time, field remarks and a much more detailed description of the freshly hauled sediment (table 1). Thus, the sediment descriptions of the cards were much summarized and of a lower 'quality' to infer the seafloor surface composition, compared to those found in the log-books. This fact could prevent further use of the remaining ~ 800 stations, not documented at all in the recovered log-books; these represented a massive data gap in the central coastal grid. A part of these data could however be recovered through an analysis of sampling meta-data.

Table I: Examples of available sediment descriptions (translated from French). The two first records typify the way descriptions were summarized in the cards, while larger amounts of detail were provided in field log-books where available.

Sample code	Sediment description	log-book availability
G2796	Grey mud	No
G2999	Black mud, grey mud, yellow sand	No
GS059	Hard clay, in form of pieces, red and breakable, neritic coarse sand, grey mud, small stones	Yes
G2648	Sandy black mud, pure black mud, grey mud, fine sand, several shells	Yes
G1847	Hard black mud, a bit of grey mud, non muddy fine sand (more than in the previous sample)	Yes
G2670	Coarse sand, a bit neritic, surface grey mud in form of lumps	Yes
G6448	Broken shells	Yes
G3572	Stones, gravel, greyish fine sand, sandy black mud	Yes
G6485	Gravel, pebbles, broken shells, pieces of coal	Yes

Meta-data validation

Meta-data validation focused on sampling date, geographic position and sampling gears, previously to the Q4D project, and are further detailed in Houziaux et al (2008). Dates and geo-positioning were primarily cross-checked using the chronology of sequential sampling, as explained above. Thanks to this procedure, about 500 sediment stations, not covered by the field log-books, could be satisfactorily recovered with their summarized sediment description, raising the initial amount of usable sediment data to about 2,350, or 70 % of the potential data-set.

Geo-positioning accuracy of the sampling stations was a major issue since the expected resolution of the sampling grid is high, suggesting that meaningful interpolation maps could be drawn, based on these data for spatial analysis at sub-regional scale (see figure 1). In the field, sediment samples were not only taken at the nodes (by Gilson with careful positioning), but stations were sampled between them as well; in general at mid-distance along longitude lines. Later on, further samples were collected at or in the vicinity of many previously surveyed stations, but the level of geographic accuracy then decreased, because reference was not made anymore, or imprecisely, to the original grid. Thus, we faced different levels of geographic precision across the whole potential data-set. Furthermore, the geographic position, being primarily determined with reference to land- or seamarks, the proximity of the ship to such reference points will also influence the geographic position accuracy, the exact determination of which calls for tedious station-per-station analysis. In spite of our goal, we decided to create a relative scale of geo-positioning accuracy answering mainly the issue of Gilson's station positioning, relatively to every other. Therefore, stations belonging to the grid were considered as better positioned, than samples collected without reference to it, and offshore stations were considered less well positioned, than stations closer to the shoreline. Thanks to this relative approach, suspect stations can be eliminated from the data-set prior to mapping and interpolating operations, to avoid fuzzy bias arising from poor geo-referencing accuracy, despite the lack of absolute precision figures (figure 3, above). The distribution of years within the interpolation area and the distribution of analyzed samples are shown in figure 3 middle and below, respectively.
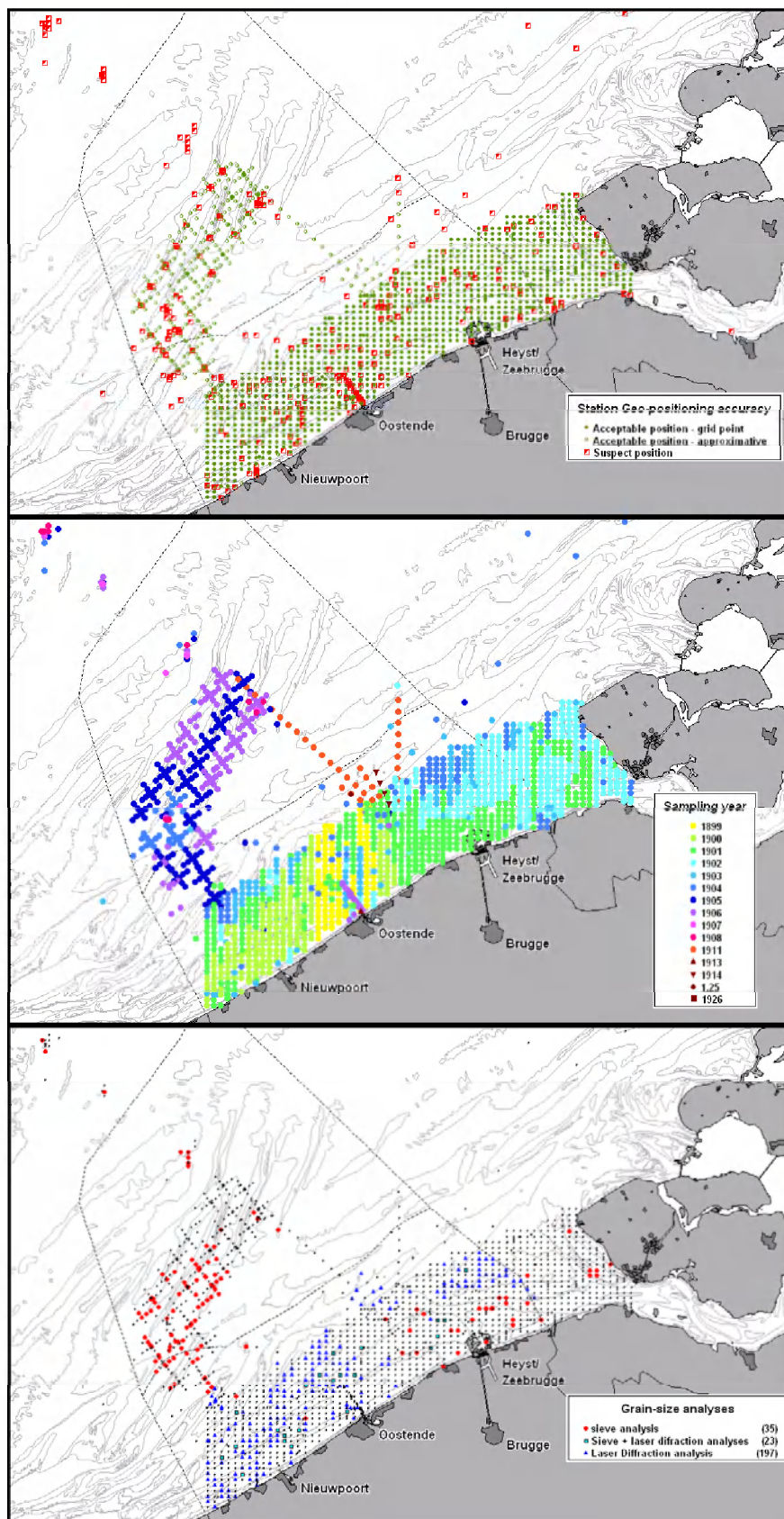
Figure 3. Above: distribution of the three main categories of geo-positioning accuracy (green: acceptable positions; red: suspect positions). Middle: Distribution of sampling years throughout the main sampling area. Below: distribution of sieve and laser diffraction grain-size analysis series. Data are superimposed on the modern coastline, including Zeebrugge harbour (then inexistent).

Sediment descriptions: re-processing

All samples, ranked trustworthy in geo-positioning, that could not be obtained were eliminated from our data-set. This process provided us with an initial data-set of 2354 sediment stations with 'ranked trust' in geographic accuracy.

The sediment descriptions provided in the log-books and station cards, respectively, were further compared to determine to which extent the latter was summarized and valid for our purposes. Sand grain-size estimates were often reproduced in the summarized descriptions, but semi-quantitative indications, on e.g. mud or shell contents were lacking. Thus, these data can be fully used for sand grain-size estimate, but should be avoided when the relative mud or shell content of the surface sediment is being determined tentatively. The quality of the summarized descriptions was thus flagged in our data-sets to enable appropriate station selection or identification at analysis stage. Therefore, the amount of data used to map the relative abundance of surface sediment constituents over the entire sampling grid varies from a constituent to another (i.e. one station may be useful for sand grain-size determination.

Gilson's visual descriptions provide major information on conspicuous sediment constituents: sand grain-size, mud content, shell/shingle content and gravel/pebble content.

For sand, an estimate of the average grain coarseness was generally provided, ranking from "very fine" to "very coarse". A consistent series of sand grain-size categories could thus be defined on the basis of the original descriptions, the accuracy of which can be controlled using Gilson's samples available in the RBINS repositories (see below: control grain-size analyses). Given the fact that these estimates focus on the sand fraction, grain-size analysis results are examined and compared to the original description on the sand fraction solely, i.e. the 63-2000 μm range (but see below for the coarsest fractions). Smaller grains are considered as "mud", coarser grains are considered as "gravel" (Udden-Wentworth scale, Wentworth, 1922).

The mud content of the sediments, which is known to be high in the central and eastern Belgian coastal waters, was also very often visually evaluated by Gilson (e.g. "very muddy sand", "pure mud"). In the descriptions, Gilson seems to make a firm distinction between "clay" (which was generally collected off Belgian waters), "peat" (some occurrences) and "mud". Being determined in the field, "mud" is here defined as an admixture of silts, clay, carbonates and organic matter, most of which should pass through a sieve of 63 μm. The colour of the mud was also provided on most instances ("black", "grey"), as well as information on its consolidation rate (e.g. "fluid", "hard", "in pieces", "pebbles"), which were considered to provide information on the oxygenation, organic matter content and/or vertical position of the described sediment layer. "Black muds" undoubtedly sign occurrence of high organic content, undergoing anoxic decomposition. This information, as well as further details provided by Gilson on this constituent, was used by Fettweis et al (2009) to evaluate the long-term effect of port construction on local sediment composition and processes.

In this contribution, we further refine the determination of the mud content to lower the observed exaggeration effect of the visual (volumetric) estimation of mud content linearly compared to weight-based mud content determination resulting from sieve analysis. The goal is to bring the available historical data into a format enabling more accurate determination of local trends. Control determination of mud content was carried out during the grain-size analysis of Gilson's archived samples (see below), but only few samples with high contents were available. Furthermore, following a standard sieve analysis procedure, the "mud content" is controlled through the "silt content" of the sample after organic matter and carbonates have been removed. It seemed likely that sample analysis without such pre-treatment could provide results closer to the visual aspect of the sample, but results prove hard to interpret.

Shell and shell grit were also very often indicated in these descriptions, sometimes with semi-quantitative information (e.g. "very neritic sand", "mud with lots of black shells"). Gilson thus

imposed a separation between mineral and biogenic nature of the sediment constituents, which poses a problem for long-term trend analyses. Indeed, recent data upon which sedimentary maps are generally drawn, results from mechanical sieving of the sample, thus providing weight-based values for the sediment fraction. Thus, shell fragments smaller than 2 mm would be considered as "coarse sands" in the widely used reference grain-size scale of Udden-Wentworth. Those are excluded from the empirical sand grain-size estimate of Gilson. Therefore, controlling the quality of sand grain-size estimates of Gilson with grain-size analysis of remnant sub-samples was carried out in two ranges: $63\mu m$ – $2000\ \mu m$ and 63-$1000\ \mu m$. We further tested that the proportion of material comprised in the 1000-$2000\ \mu m$ range reflected the semi-quantitative indications provided by Gilson on shell debris content.

When considering sand, mud and shell contents, it proved difficult to accurately evaluate the relative abundance of each constituent in the samples. Therefore, this has not been tempted and we decided to investigate the former distribution of relative content in the considered constituents.

Gilson indicated as well the occurrence of gravels and larger pebbles in his samples. It proved impossible to evaluate "content" for this coarser material. However, gravels and larger pebbles were also collected with larger towed sampling gears such as dredges, "bottom plankton nets" and bottom trawls. These larger fragments are found in the petrography repository of the RBINS, apart from the archived sediment samples, as well as in the invertebrate repositories where they are substratum to colonies of a wide range of sessile taxa. The stones of the petrographic repository have been formerly studied by Verbeek (1956), while those of the biological repositories have been listed during digitization of benthic invertebrate information. The geo-positioning of non-sediment samples, containing such stones was verified to enable their inclusion in our distribution maps for this particular constituent.

Control grain-size analyses

Various series of grain-size analyses have been carried out on Gilson's archived samples. Gilson himself only ordered a hundred grain-size analyses to his brother, Eugene Gilson, at that time chemist at Ghent University. These analyses were reconstructed by van Loen et al (2002) but concern a series of samples collected along a transect line, which could not be individually positioned on the transect line. Vannieuwborg (1982) carried out grain-size analyses on 21 of Gilson's samples, primarily to obtain reference data in areas altered by disposal of material gathered on maintenance dredging in harbours and navigation channels. Verbeek (1956) and Van der Ben (unpublished data, 1960s) carried out limited petrographic investigations on the stones collected by Gilson.

In 2002, a first series of grain-size analyses was carried out using 62 samples selected on the basis of their associated descriptions to evaluate the accuracy of Gilson's sand grain-size estimates (Houziaux and Francken, unpublished data). 5 to 10 samples were selected for every category, which is too low an amount of samples to draw firm conclusions. Overall, we observed a statistically significant gradient of coarseness across the categories ranked as follows: "fine" + "very fine" sands ~ "pure" sands < "relatively fine" sands < "medium" sands < "relatively coarse sands" < "coarse" + "very coarse" sands (non-parametric Kruskal-Walis analysis of variance; $p < 0.001$). However, only differences in the distribution of fractions between "fine" ("very fine") and "coarse" ("very coarse") sands were statistically different when the categories were compared on a pairwise basis (Dunn's test; $p < 0.001$ for "fine" and "coarse" sands). It was thus felt that complementary analyses were necessary.

Subsequently, 27 analyses were carried out in 2005 and 74 in 2006-2007, using the same analytical procedure.

On the other hand, analyses were carried out on more than 200 Gilson's coastal sediment samples with a laser diffraction technique with the specific goal of testing a "habitat suitability" modelling approach to benthic biodiversity prediction, developed for the BPNS (Degraer et al, 2007, 2008; Willems et al, 2008). With this technique, Degraer et al (2008) could demonstrate significant correlation between the median grain-size and the mud content values with the composition of benthic communities in Belgian waters. The motivation for the use of this technique for our purposes was that data are rapidly acquired. Indeed, the labour-intensive sample pre-treatment applied to the sieve analyses is not carried out on the samples used in the developed HSM procedure. The underlying hypothesis for this approach to sediment analysis is that, in absence of heavy seafloor disturbance, similar sediment composition should bear similar benthic communities, even at distant times. Thus, for given values of median grain-size and mud content, the list of species collected by Gilson in a given sediment type should match, that predicted on the basis of recent samples analysis.

For HSM development, the authors used laser diffraction analysis of sediments without pre-treatment of the samples (e.g. to remove carbonates or organic matter). As such, this type of "raw" grain-size determination has the potential to provide grain-size distributions which are more relevant in terms of biological significance. Indeed, sample pre-treatment, applied in our sieve analysis procedure, has removed up to 45 % of the initial sample weight, meaning that the "traditional" sediment analyses do overlook a large part of the fresh sample composition potentially influencing the associated benthic community.

Historical morphologic study of the Grote Rede and the Appelzak gullies.

A direct comparison of bathymetric profiles of 1866 and 1908 was carried out along a transect from Westende to the Dutch border, in the Grote Rede and Appelzak gullies (figure 4). The goal was to investigate occurrence of freshly deposited mud, as compared to nowadays (Fettweis et al, 2009). To that purpose, a transect line was drawn in front of the coast from the Dutch border to west of Oostende, in the middle of de Grote Rede and Appelzak (figure 4). Depths recoded on both maps, along the transect and in its direct vicinity, were reported along the line axis. Gilson's data on mud content were superimposed on the map to identify areas of high mud content.
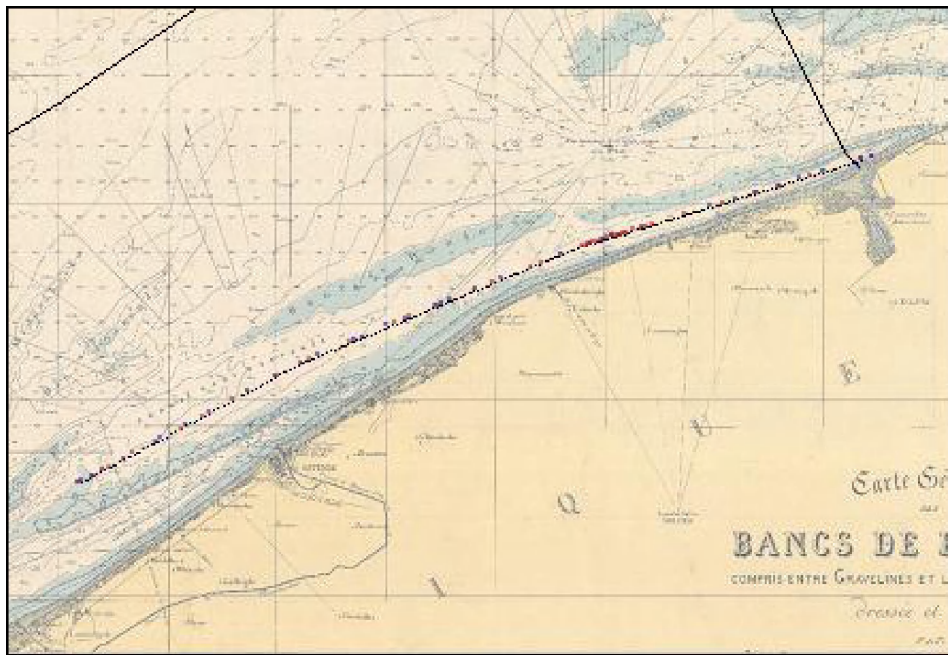

Figure 4: Transect along the Grote rede and Appelzak gullies, together with stations at which depths were recorded, respectively by Stessels (1866; blue dots) and Urbain (1911; red dots). Background: bathymetric chart of Stessels (1866).

Statistical analyses

Results from grain-size analyses were compared to a description-based ordination of samples for every sediment constituent, using a combination of univariate and multivariate techniques. For sand grain-size, multivariate ordination of samples was carried out through Euclidean distance calculation and Multidimensional Scaling ordination ("Primer-E v6" software package), as well as Principal Factor Analysis, both yielding very similar results; the latter providing insights in the contribution of individual fractions to the overall ordination pattern. These were analysed on the whole distribution range of the sandy fractions (from 63 to $<2000\mu$m), as well as on the restricted range 63-1000 μm, to detect any effect by fossil and sub-fossil shell remains and small stones on possible mismatch between measured average grain-size and Gilson's visual estimate of sand coarseness, which excluded such features.

The distribution of mean and median grain-sizes among Gilson's categories was tested using non-parametric univariate statistics (Kruskal-Wallis analysis of variance and Dunn's test on pairwise comparisons). Sediment parameters were calculated for the full distributions, since multivariate analyses evidenced no significant difference between the full and cut ranges on matching Gilson's sand categories (see results). Graphical (Folk and Ward), as well as statistical moment parameters were calculated. The assemblage of graphical values for mean grain-size, median grain-size, sorting and skewness was further tested with multivariate analysis to track any detectable patterns among Gilson's sediment categories.

2. Results and discussion

2.1 Sand grain-size parameters

The mean and median grain-sizes, obtained for the range 63-2000 μm in every Gilson's estimate categories, show a significant trend (Kruskal-Wallis analysis of variance: p < 0.001) to coarsening from "fine" to "coarse" sands (figure 5). On pairwise comparisons (Dunn's test), "pure" sands can be considered as a synonym for "fine" sands. The average grain-size for sands described as "very fine" or "very coarse" did not differ from regular values of "fine" and "coarse" samples. The intermediate categories "rather fine", "medium" and "rather coarse" show on average a trend to coarsening, but the pairwise separation of close categories is never significant (Dunn's test: p > 0.05). On the contrary, "fine" and "coarse" sands are clearly distinct sediment types (p < 0.001), with non-overlapping distributions. Their mean and median grain-size ranges classify as "fine sand" (125-250 μm) and "medium sand" (250-500 μm) in the nowadays acknowledged Udden-Wentworth scale. The small range, separating Gilson's extreme categories, explains that the "intermediate" categories are hardly separated, despite a significant overall trend.

a   b
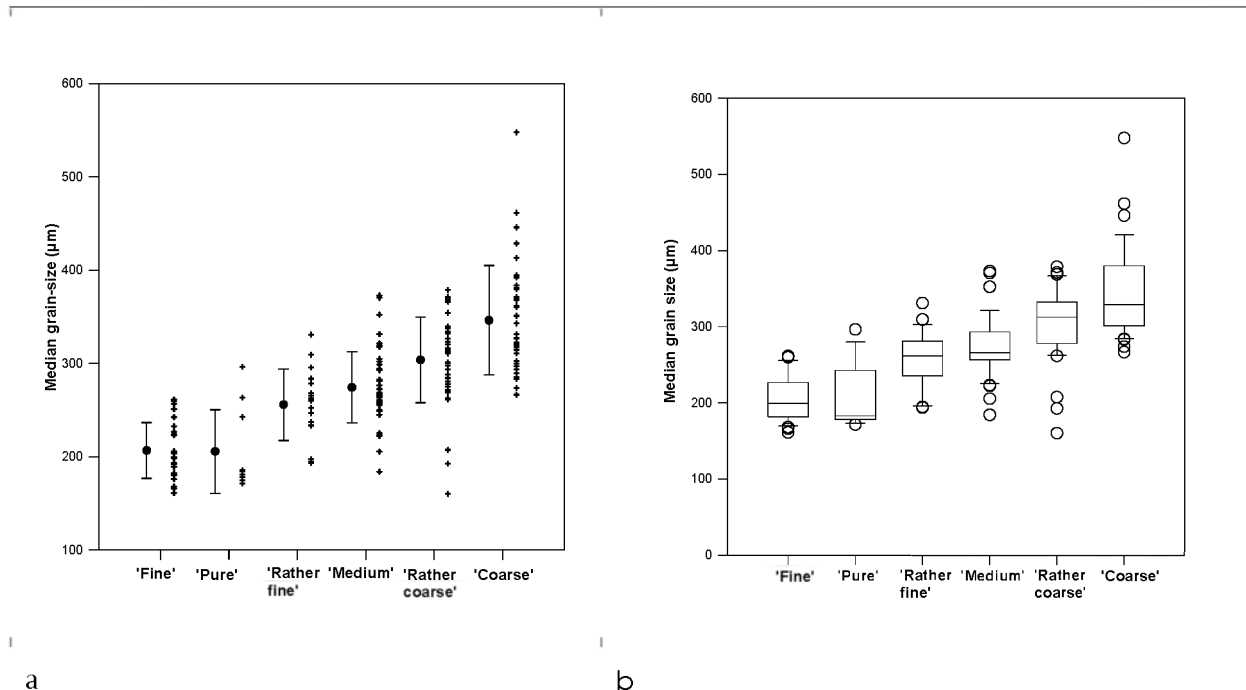
Figure 5 : a.. Distribution, mean and standard deviation of median grain-sizes across Gilson's sand categories. b. Box-plot of the same data.

The findings, arising from univariate non-parametric statistics, are confirmed by multivariate analyses applied to standardized cumulative data (figure 6a: MDS ordination of Euclidean distances; range: 63-2000 μm). The grain-size distributions of fine and coarse sands are well distinct (ANOSIM permutation test on "fine" and "coarse" grain-size distributions: p < 0.001), but other intermediate categories form an indistinct cloud. PCA analysis provides a similar data distribution, further showing that the 200-250 μm interval acts as a pivot fraction, with smaller grains being typical of "fine" sands, while coarser grains dominate in "coarse" sands. No difference appeared in the results when working on the 63-1000 μm range, indicating that the distributions of contemporary data do not need to be 'cut' under the range 63-2000 μm for long-term comparison purposes.

Further multivariate analysis of 4 calculated parameters (Folk and Ward graphical mean, median, sorting and skewness, fraction 63-2000 μm; figure 5b.) indicate that the samples are differentiated mainly through the mean and median grain-size, while sorting and skewness vary much in every category and independently from median parameters.
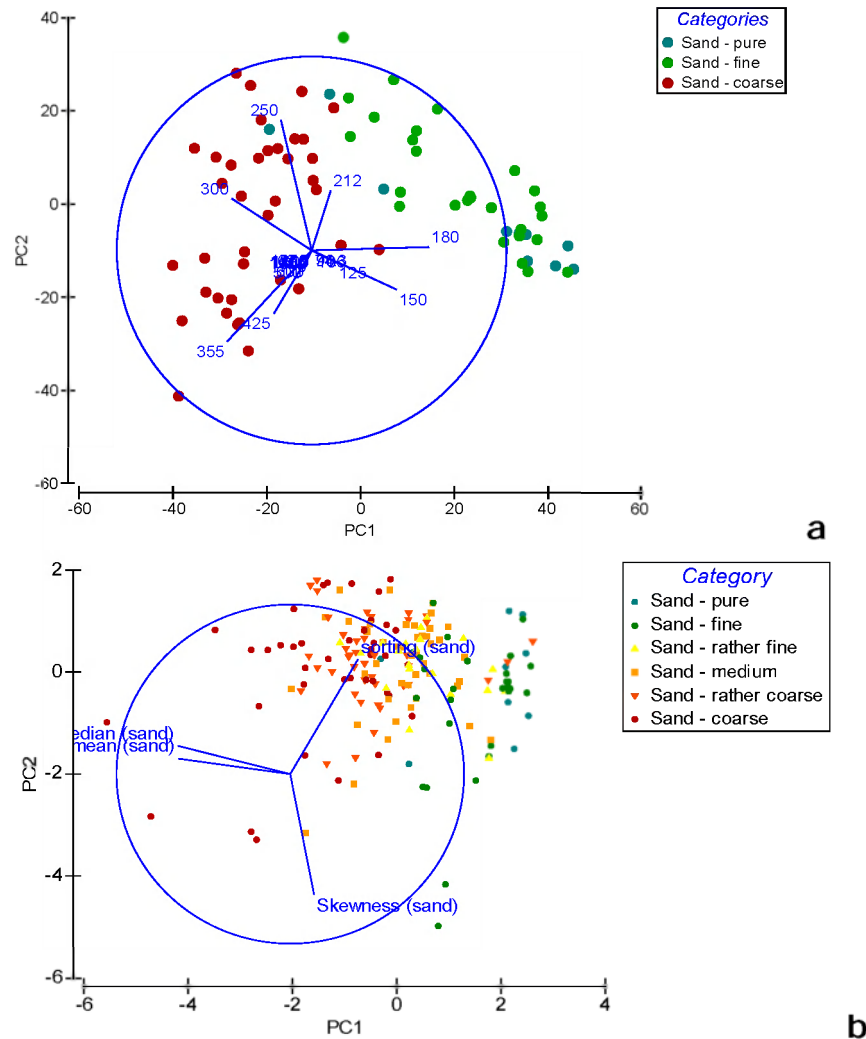

Figure 6.a. Multivariate ordination (Multidimensional Scaling - MDS) of samples according to Gilson's sand grain-size categories (Euclidean distances, calculated on the standardized cumulative grain-size distributions), with only "fine", "pure", and "coarse" categories represented. b. PCA of average grain-size parameters (Folk & Ward, 63-2000 μm fraction: median, mean, sorting, skewness).

The mean and median of "fine"+"pure" and "coarse" can thus be assigned a mean value, with 99% confidence interval:

"Fine" sand: 192.0 μm < Mean < 227.6 μm; 190.7 μm < Median < 222.7 μm

"Coarse" sand: 319.4 μm < Mean < 364.0 μm; 321.1 μm < Median < 371.4 μm

For long-term analysis, thus, a selection of areas of interest with relative large amounts of samples is made to analyse long-term changes in the local sand grain-size median and mean. In areas where the sand median grain-size was historically homogeneous, a departure of the mean value from the confidence interval should be indicative of long-term trends. This assumption should now be tested. Target areas for specific long-term analyses can thus be identified, based on thematic maps Figure 7). Unfortunately, no or too few recent samples are available to

evaluate changes in the selected areas. However, a future sampling campaign could target these areas, specifically.
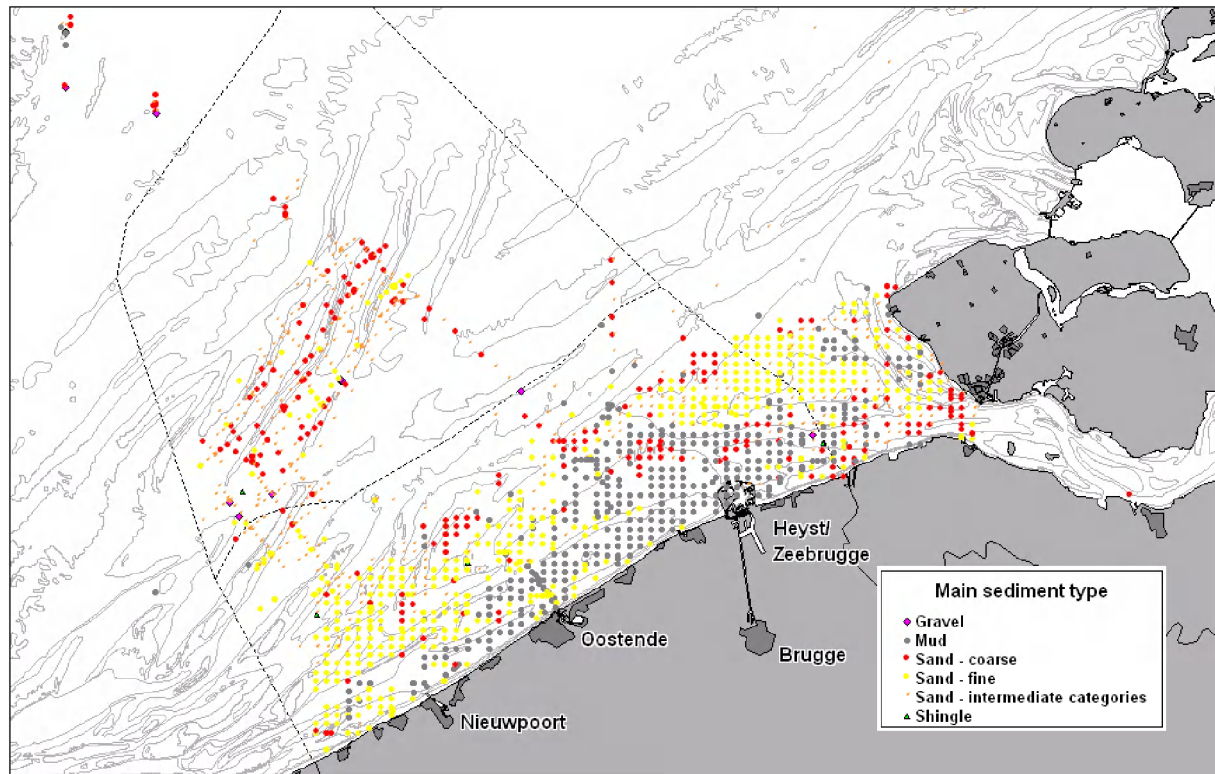
Figure 7. Map of the distribution of Gilson's "fine" and "coarse" sands, in front of the Belgian and Dutch coasts; stations described as mainly gravels, mud or shingle (which generally lack sand grain-size information) are also indicated.

2.2 Mud content

A first analysis of the geographic distribution of mud content, according to Gilson's visual descriptions was carried out by Fettweis et al (2009) with the aim of relating long-term changes in the distribution of fine sediments to increased anthropogenic pressure (e.g. construction of Zeebrugge harbour and the artificially deepened navigation channels). For that purpose, the sediment descriptions of Gilson were screened and reclassified under 14 distinct categories between 0 and 100% mud, however without support of grain-size analyses. At that stage, the linear "mud content" scale, derived from Gilson's visual sample examination appeared to exaggerate the values in the middle part of the scale. Although the geographic distribution of relative mud contents (relatively to every other sample) was usefully mapped, it proved difficult to carry out long-term analysis, because the real values are not known in the historic data-set.

The discrepancy between estimated and measured values arises from two major causes: (1) the description-based "mud content" is based on volumetric ratios, while weight is considered in sieve analysis; and (2) a bias is expected on the definition of "mud", since it is impossible to state that Gilson's "mud" effectively corresponds to material $< 63 \ \mu$m. However, the fine tuning of Gilson's descriptions, often including detailed information, such as composition of various layers, should lead to a straightforward correlation between volumetric estimate and measured weight content.

On the other hand, fresh mud contains significant amounts of material, other than silts and clays, i.e. along the Belgian coast mainly carbonates (up to about 40 %) and organic matter (up to 8 %). Fettweis et al (2007) indicate that SPM concentrations of carbonates are in the range of 34 – 58 %, while organic carbon only constitutes 2 to maximum 10 % w/w. Similar carbonate

contents were measured by various authors (e.g. Gullentops et al, 1978) in sedimentary mud. On pre-treatment for sieve analyses of Gilson's sample, we noted that up to 45% of the initial weight could be removed prior to sieving. Fettweis et al (2009) showed that a very limited portion of this SPM tends to deposit and accumulate in the long run, while a large part of surface muddy sediments are of 'ancient' origin (so-called "Holocene" muds). The accumulation of muddy sediments in de Grote Rede, during the period 1860-1910, demonstrates that a significant amount of SPM deposited on the seafloor and accumulated in the meantime in this area. The process was intense enough to prevent the development of benthic communities, as shown by the lack of macrobenthic specimens which characterizes this area.

Gilson's visual estimates of fresh samples included more material than the effectively measured "silt" contents, derived from sieving procedure. The exaggeration of estimated contents relatively to measured values in the mid part of the scale is coherent. Although absolute long-term trends in "mud content" cannot be determined, historic and recent distributions of relative mud content can be compared to identify trends in geographic spreading. This observation can probably be extended to a wide range of historic sediment descriptions reported in various sources, such as nautical charts, as proposed by Hamilton (1999) for more recent Australian chart data.

Unfortunately, only few of the Gilson's samples archived in the RBINS have large mud contents. In total, 23 samples have been analyzed with the two distinct methods: laser diffraction, without sample pre-treatment and sieve analysis with pre-treatment for carbonates and organic matter. Only few of these samples display mud contents higher than 10% w/w. We can expect these methods to provide very different results, because of the difference in treatment and the intrinsic methodological bias (ref: laser diffraction analysis provides coarser distributions than sieve analysis, e.g. ref). Therefore, the 23 samples analyzed with both techniques are first compared (figure 8).

In general, the laser analysis provided higher mud percentages than the sieve analysis, which can be considered as a direct effect of differential pre-treatments, however they are strongly correlated. Laser data thus should better match Gilson's visual (volumetric) estimates of "fresh" mud content. The higher mud percentages obtained with laser diffraction method can be seen when mud content is compared to the initially determined mud content categories derived from Gilson's descriptions (14 categories; see Fettweis et al, 2009) for all samples analyzed (figure 9). Categories "0" to "2" contain up to maximum 10% silt with both techniques, while category 3 displays some higher values with the laser only. Categories 4 and 5 display up to 40% silt. Category 6 has too little data – 1 result per technique and the result is to consider inconclusive. Category 9 bears only 1 result either, in relatively good agreement with expectations: > 50 %. Category 11 bears 1 result per technique and provides contents above 50%. Category 12 bears about 90% silt with both techniques, but only one result is available per technique.
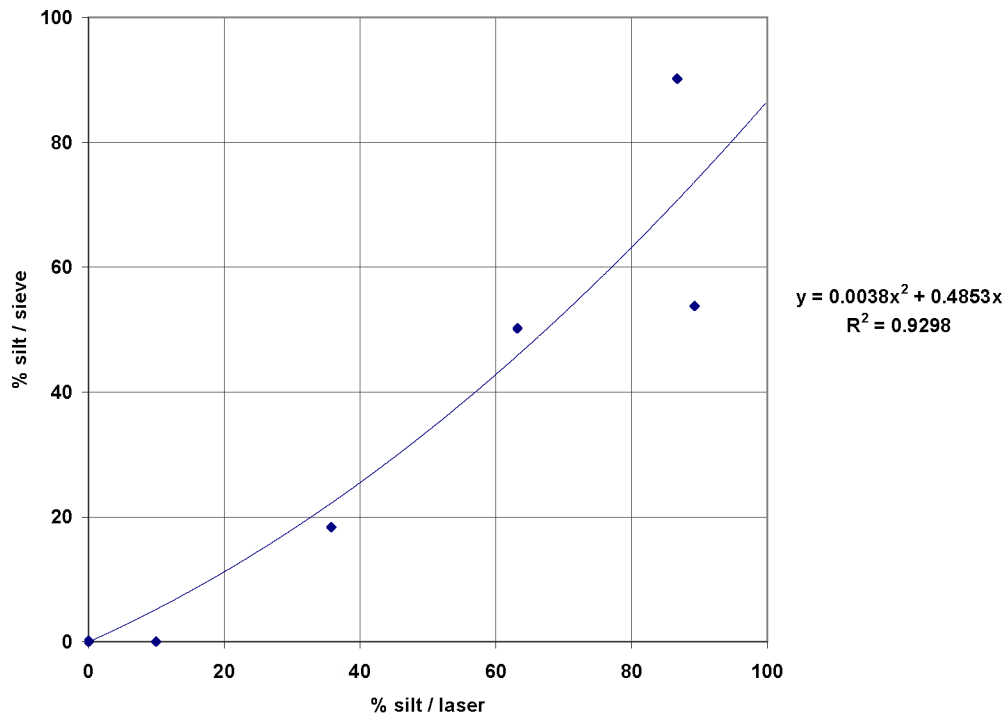
Figure 8. Correlation plot of % silt, obtained from sieve analysis (with pre-treatment for organic matter and carbonates) and laser diffraction analysis (no pre-treatment) of 23 samples analyzed with both techniques. Note that most values are regrouped within very small contents.
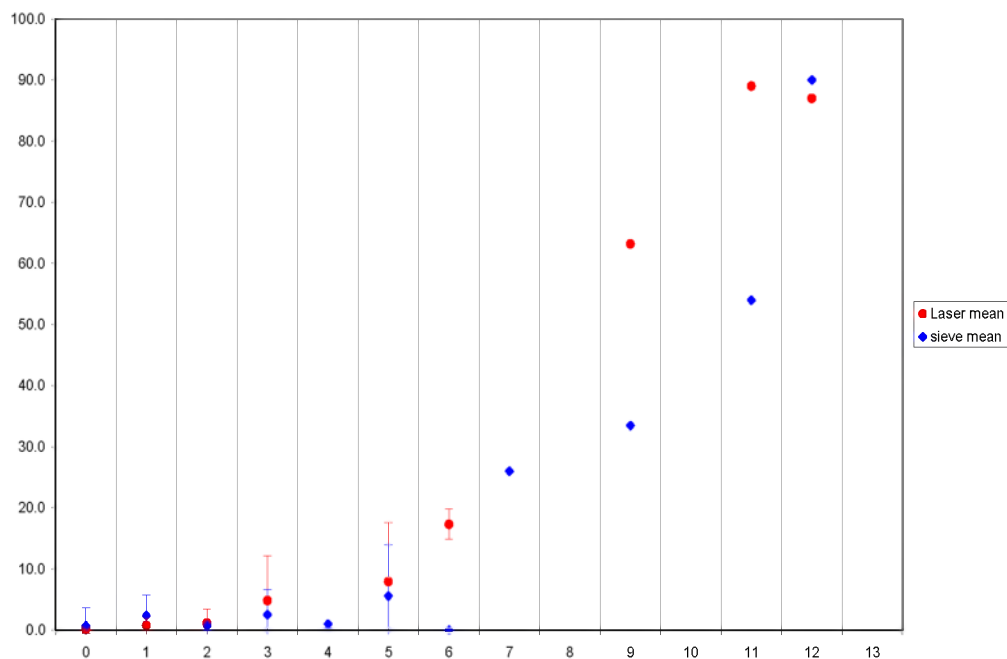

Figure 9: Average and standard deviation of measured mud contents within the 14 initially defined mud content categories. Red dots: laser diffraction analysis; blue dots: standard sieving procedure.

Ideally, sieve data should be recalculated first, on the basis of overall sample weight, rather than on the carbonate- and O.M.- free sample weight. Given the fact that sieve and laser diffraction are highly correlated, calculating average mud contents of categories using both sieve and laser diffraction data is acceptable for our purposes. The categories of smaller contents were thus

regrouped within a scale reduced to 12 categories, and a theoretical (polynomial) relationship between category increment and expected mud content was calculated (figure 10).
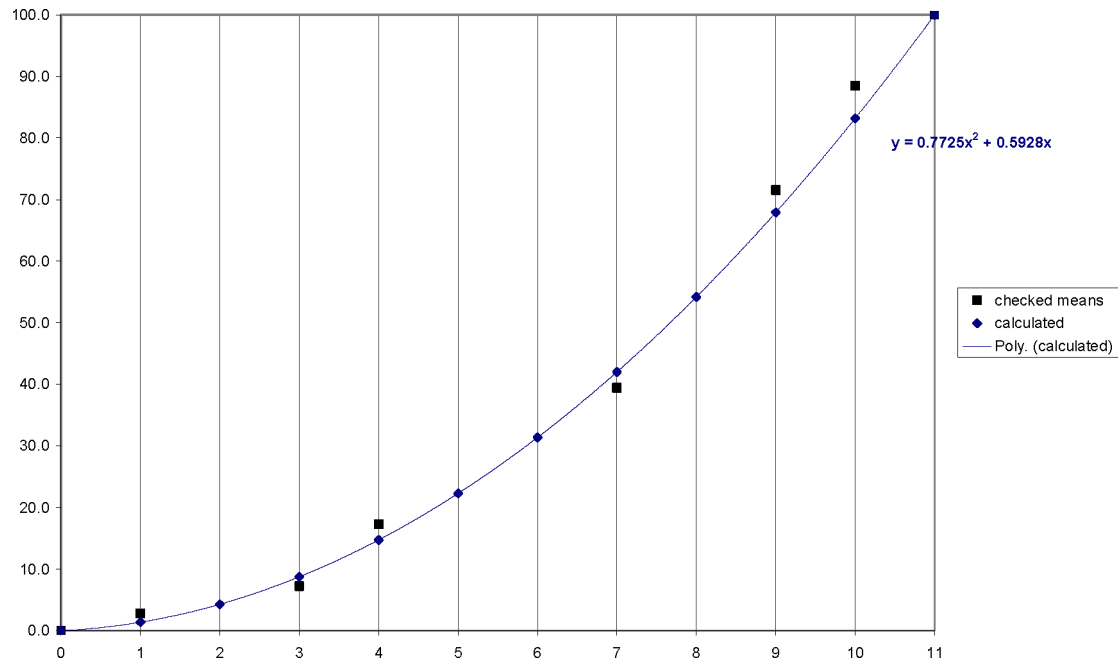
Figure 10: Measured (black dots) and calculated (blue dots and line) mud content (%) of the 12 final categories of description-derived mud contents.

The polynomial relationship very well approximates the measured average mud content. Using this relationship, the new mud contents were assigned to the empirical categories and the interpolation map of mud content across Gilson's sampling grid was redrawn. Raw interpolation results were manually corrected for sample-free areas and local morphological features, such as large sand banks, which are mainly composed of sands (figure 11).

The data clearly point at maximum mud content in the surface sediment West of Oostende (eastern end of the Westdiep gully and a patch further west), East to Oostende in the whole Grote Rede area up to Blankenberge, and further seawards of the "Wenduyne" sand bank, off the latter locality and Zeebrugge. In these areas, mud content is such that sand grain-size was never estimated by Gilson (see figure 7). The Stroombank and the Wenduyne banks appear to form boundaries between distinct muddy areas.

The historical data of Gilson, combined with analysis of bathymetric changes between 1866 and 1911 (Fettweis, 2009; see figure 12) indicated that the area seemed favourable to tidal mud deposition during the past 40 years, since depth decreased in the interval. Gilson's "soft" muds (interpreted as freshly deposited) were reported in the western part, while "hard" muds (interpreted as consolidated ancient mud) were reported in the eastern part, probably indicating different sediment dynamics. Much less shallowing was noticed for the eastern Westdiep and the Zeebrugge muddy areas when nautical charts were compared; no change was detected at the mud patches of the western West Diep and seawards of the Wenduyne sand bank.
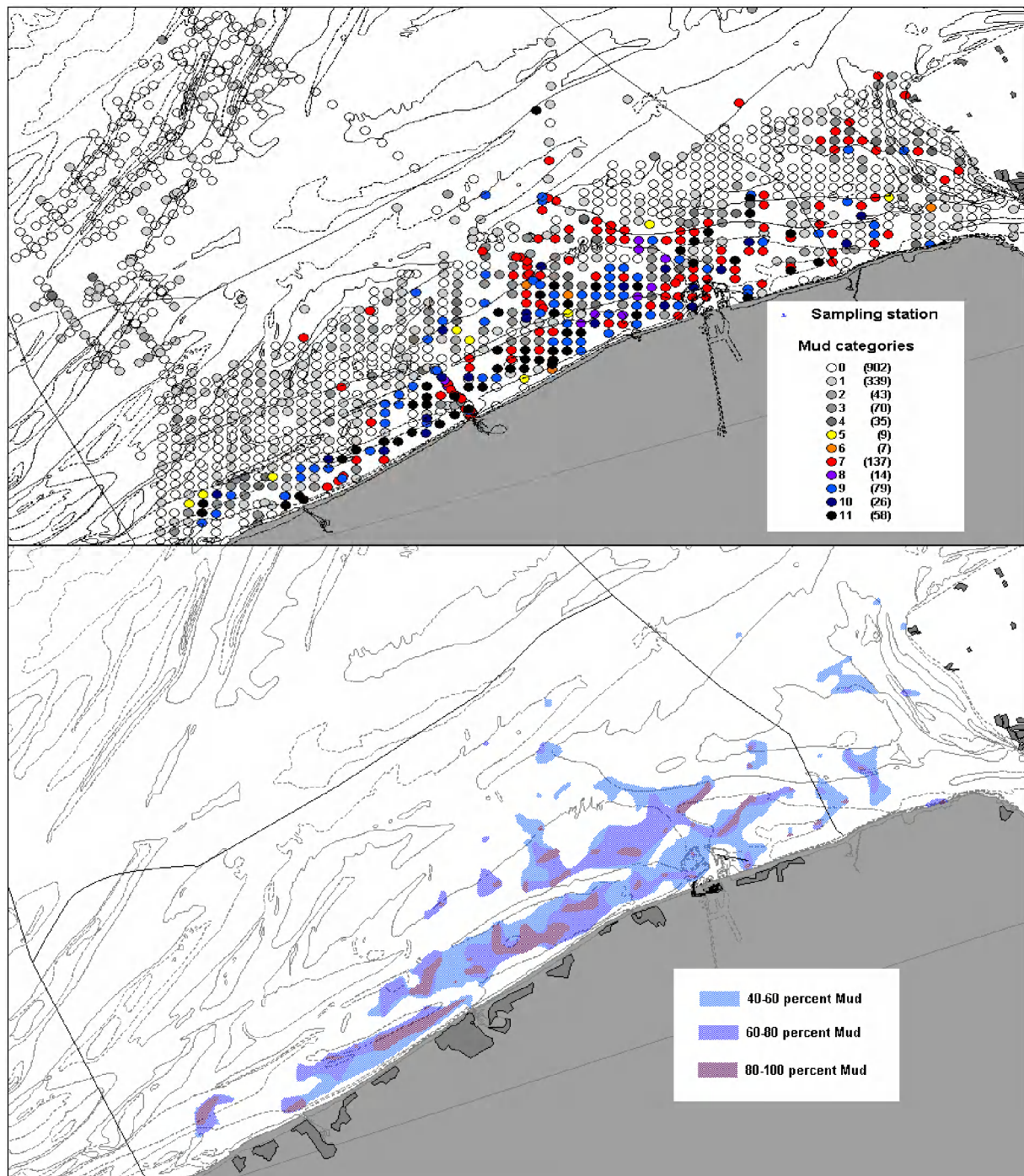
Figure 11. Above: distribution of the 12 empirical mud content categories, derived from fresh sediment descriptions and grain-size analysis of Gilson's archived samples, period 1899-1913. Below: distribution of corresponding high mud content classes (interpolation map (Inverse Distance Weighting, search radius 2km, grid resolution 0.5 km) manually adjusted for sand bank crests).
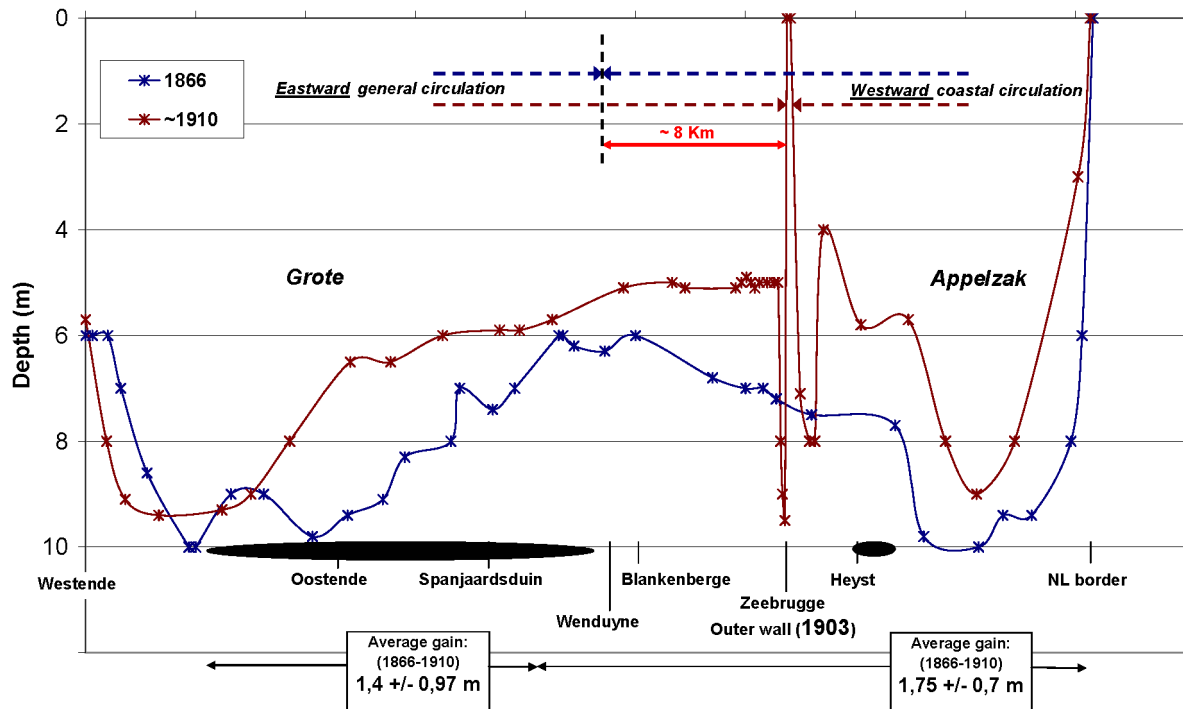
Figure 12: Bathymetric profiles in the Grote Rede and Appelzak gully (transect between Westende and the Dutch border), recorded by Stessels (1866; blue) and Urbain (1911 – with measurements up to 1908; red). Upper arrows indicate the theoretical meeting point of general North-eastward and coastal (Appelzak) westward residual circulations in both periods (see text). The black-filled areas at the basis of the figure represent the areas where pure mud samples were gathered, in the vicinity of the transect of Gilson (1900s). Average seafloor rising trends (decreased depth) were calculated.

2.3 Shell / shingle content

The shell/shingle content of Gilson's description appeared much less well-defined than sand grain-size and mud content. Semi-quantitative indications were less numerous, which makes it difficult to create a meaningful relative content scale as done for muds. On the other hand, as far as we know, the shell/shingle content at the BPNS was so far only studied and mapped by Gullentops et al (1978), in the framework of a large-scale and multidisciplinary sampling of the Southern Bight of the North Sea. Therefore, limited analyses were carried out on this parameter. As stated in results obtained for sand on grain-size analysis, the interval 1000-2000 μm does not significantly alter the overall sand grain-size distribution pattern, and it accordingly proved uncorrelated to the estimated relative amounts of shells and shell debris. Heterogeneity in the distribution of these coarser constituents in the original sample could explain the mismatch. We consider that "high" (up to 100% of the sample) and "medium" contents have the potential to provide information on the distribution of areas likely to constitute a distinct biotope as compared to pure clean sands. The map of medium and high shell / shingle contents of Houziaux et al (2008) is thus reproduced in figure 13. Gilson's values, however, do not match the map of shell content by Gullentops et al (1978). When the maps are superimposed in a GIS, this discrepancy appears to arise from differences in the scale at which sampling was operated. Indeed, Gilson's data are much more detailed and show that the distribution of shell content is more heterogeneous, than suggested by Gullentops et al (1978).
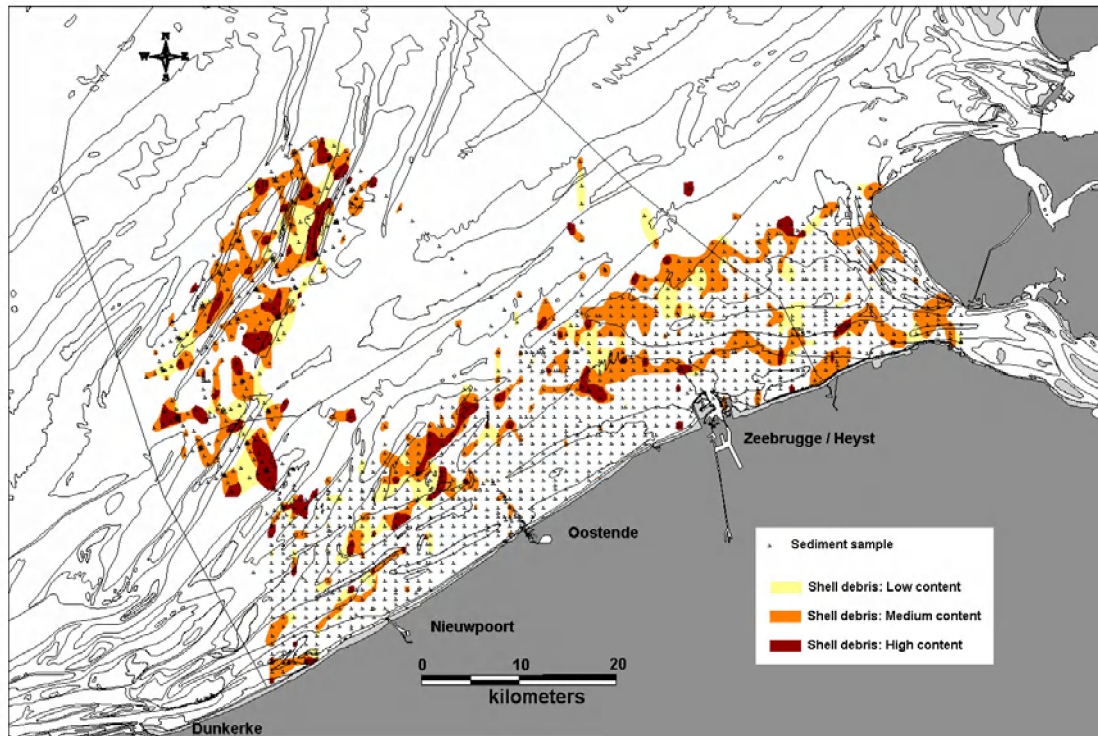
Figure 13. Distribution of Gilson's shell and shingle content estimates (reproduced from Houziaux et al, 2008). (correlation old coastline??)

2.4 "Gravel" content

The map of gravel content of Houziaux et al (2008) is reproduced in figure 14.
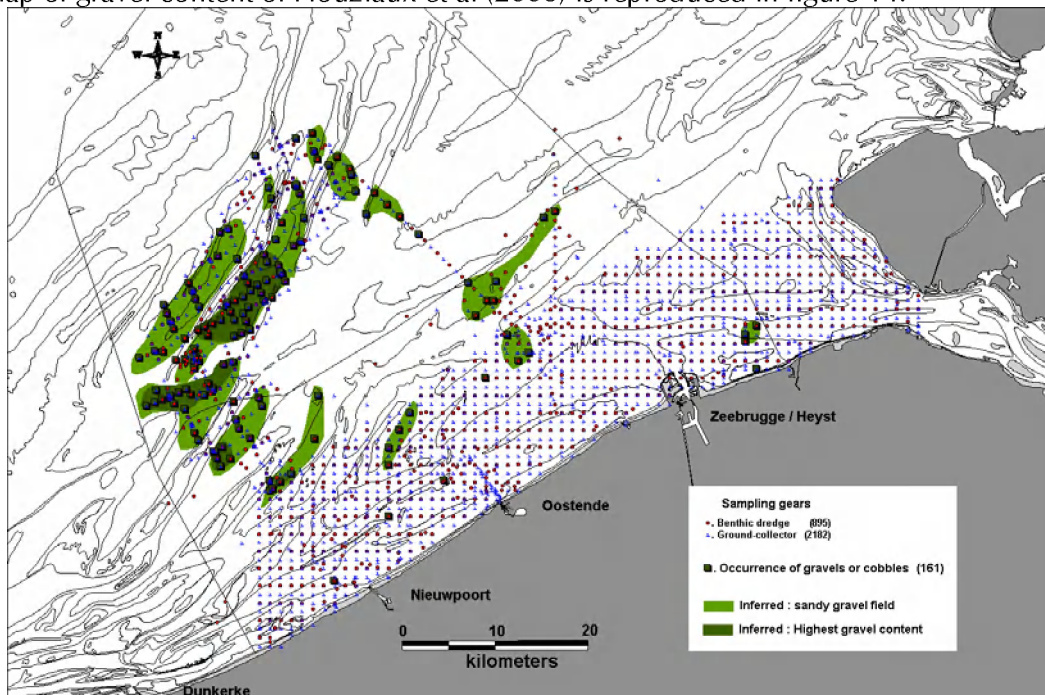

Figure 14. Distribution of 'gravel' and larger cobbles in the surface sediment, based on Gilson's visual sediment descriptions and occurrence of cobbles in towed gears (dredges and trawls). For the latter, the median position of the tow was used for mapping purposes. Gravel grounds were inferred and drawn manually (green). Areas where all samples gathered gravels or cobbles are highlighted in dark green. Reproduced from Houziaux et al, 2008.

See Houziaux, 2008 for discussion on the Westhinder gravel grounds

2.5 Final 'baseline' integrated sediment type map in favour of long-term analysis

The high level of heterogeneity of the seafloor from one area to another is obvious when the data, derived from visual sediment descriptions, are integrated in a simplified map (figure 15), while sedimentologically distinct "units" clearly and consistently appear. Benthic habitat features, here considered, vary, but are consistently mixed from area to area; this suggests that a patchwork of specifically associated benthic communities must exist throughout the sampling grid, if sediment composition is the main driver to benthic community structuring (Degraer et al, 2008). And indeed, the bivalve *Donax* is found consistently in the fines sands in the early 20th century. However, it seems that siltations rates and SPM concentration in the water column are much important drivers than mud content of the sediment, although the latter is an important parameter (see macrobenthos results section).

The distribution of "coarse" sands closely matches the distribution of medium shell contents, except on the Vlakte van de Raan where clean fine sands dominate largely and homogeneously. It seems likely that "coarse sands" are sands mixed up with consistent amounts of moderately fine shell debris, while areas with high content in shells coincide with larger amounts of shells or large shell fragments. These thus probably are indicative of zones bearing or formerly bearing intense benthic activity and productivity, a hypothesis to test against the benthic content of Gilson's dredge samples collected in these surroundings. In the Westhinder area, this is demonstrated to be the case with the former occurrence of wild beds of the European flat oyster (Houziaux and Kerckhof, in prep), but the area also used to host some other typical species, such as the bivalves *Aequipecten opercularis* and *Striarca lactea*, little encountered in more recent samples obtained in the Westhinder area (Houziaux, unpublished data). Baseline analyses of the Gilson's macrobenthos data with respect to the determined sediment composition are expected to provide insights into the factors structuring the communities by then, i.e. at a time of much reduced levels of ecosystem exploitation and degradation. This analysis is likely to provide key arguments to support a particular hypothesis on long-term human footprint.
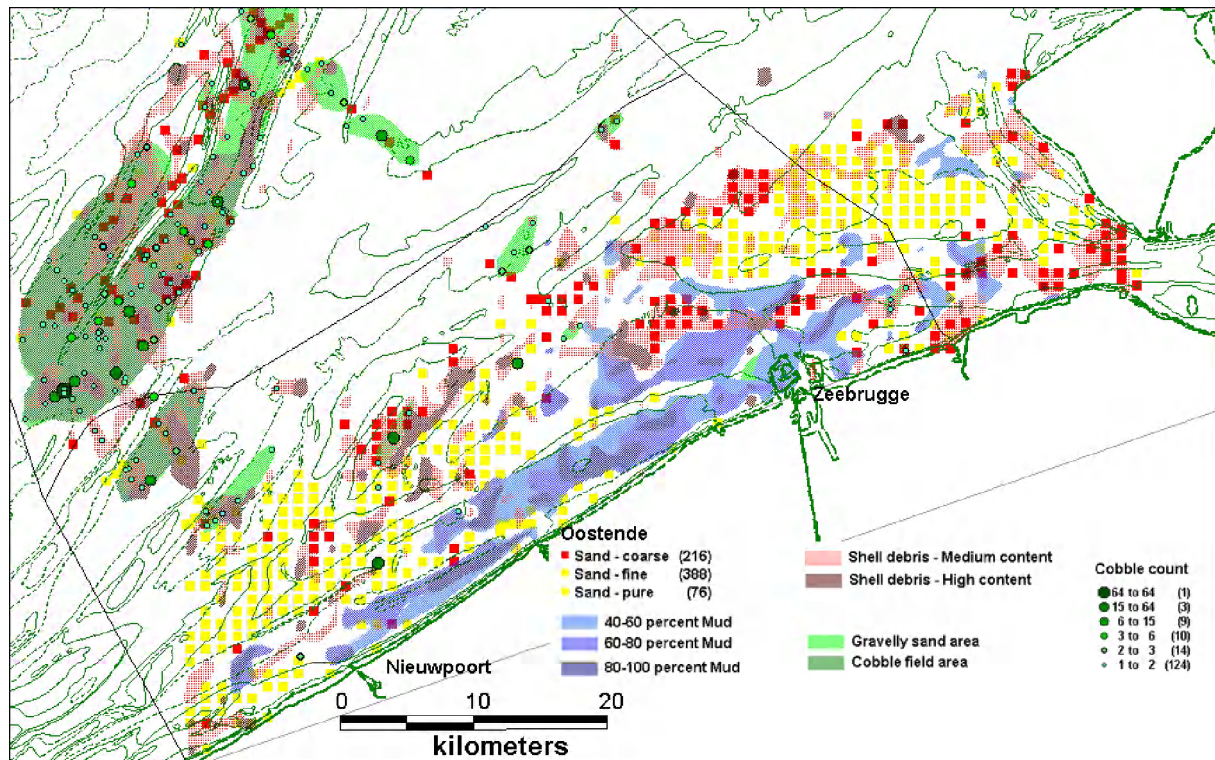
Figure 15. Integrated sediment type map of Gilson's validated historic information on the seafloor of the Belgian part of the North Sea, period 1899-1914; cobbles collected at gravel stations are highlighted also.

3. Conclusion

The main strength of the Gilson's collection lies in the fact that the sediment and benthos data were acquired sequentially through standardized sampling and sample processing within high resolution sampling grids. Although data "quality" cannot compare with contemporary technologies, the data distribution is regular and could be well controlled; this provides a consistent snapshot of the period 1899-1913. The visual descriptions of freshly hauled sediments, provided by Gilson, are accurate within certain limits which could be successfully defined. They can thus be used to reconstruct the former distribution of certain sediment constituents and features and to investigate long-term trends in surface sediments and benthos. The case-study of the Grote Rede area shows that significant changes in physiographic conditions can be detected, in agreement with changes detected in biological data (see macrobenthos result section). There is room for an extended set of analyses on long-term trends in seafloor composition in Quest4D phase II, in particular related to benthos data-set, using this reconstructed historic data-set, of which reliability is here demonstrated. The data upon which analyses were carried out, are transferred to the Belgian marine Data Center where they will be freely accessible.

Bibliography

Degraer, S. , Wittoeck, J., Appeltans, W., Cooreman, K., Deprez, T., Hillewaert, H., Hostens, K., Mes, J., Van den Berghe, E. and Vincx, M. (2007) Macrobenthic atlas of the Belgian part of the North Sea. Belgian Science Policy, Brussels, belgium. 164 pp.

Degraer, S., E. Verfaillie, W. Willems, E. Adriaens, M. Vincx & V. Van Lancker, 2008. Habitat suitability modelling as a mapping tool for macrobenthic communities: An example from the Belgian part of the North Sea. Continental Shelf Research, 28(3):369-379. doi: 10.1016/j.csr.2007.09.001.

Fettweis M, Houziaux J-S, Du Four I, Van Lancker V, Baeteman C, Mathys M, Van den Eynde D, Francken F, Wartel S., in press. Long-term influence of maritime access works on the distribution of cohesive sediment: Analysis of historical and recent data from the Belgian nearshore area (southern North Sea). Geo-Marine Letters.

Gullentops, F., Moens, M., Ringelé, A. & Sengier, R., 1978. Geologische kenmerken van de suspensie en de sedimenten. In: Project Zee / Projet Mer, Volume 4: Sedimentologie. (Nihoul, J.C.J. & Gullentops, F., Eds.), Brussels, Science Policy Office, 137 p.

Houziaux, J.-S., Kerckhof, F., Degrendele, K., Roche, M. and Norro A., 2008. "The Hinder banks : yet an important region for the Belgian marine biodiversity?" ('HINDERS'). Belgian Science Policy Office, Final report. 123 pp. + 131 pp. Annexes.

Stessels, LT., 1866. Carte générale des Bancs de Flandre d'après les ordres du Ministre des affaires étrangères, Antwerpen. Herdruk: Hydrografische Dienst, Ministerie van de Vlaamse Gemeenschap

Urbain, 1911. Carte "Mer du Nord, Dunkerke - Flessingue". Royaume de Belgique, Service des Ponts et Chaussées, report n 687. (soundings of 1908, including updates from11/05/1911).

van Loen, H., Houziaux, J.-S. and Van Goethem, J., 2002. The collection of Gustave Gilson as a reference framework for the Belgian marine fauna : feasibility study. OSTC-project MN/36/94, final report. 62 p.

Van Mierlo, C.-J., 1899. La carte lithologique de la partie méridionale de la mer du Nord. Bulletin de la Société Belge de Geologie, Paléontologie et Hydrologie, XII, 2nde série (tome III) : p. 219 – 265.

Verbeek, T., 1954. Gesteenten uit de zuidelijke Noordzee. Thesis Licentiaat Aard- en Delfstofkundige Wetenschappen, RUG. 85 p.

Annex III. Historical Benthos composition and distribution: preliminary results

Houziaux[1(*)] J.-S., Mallaerts, T.[2], Van Eegroo, J.[2*], Smistek, K.[2]!, Emery, C.[2], Gallina, F.[1*], van Loen H.[1*], Caers M.[1*] and Bruyndoncx L.[1*]

Royal Belgian Institute of Natural Sciences
  [1]Department of Invertebrates
  [2]Department Information Technologies
Rue Vautier 29
B-1000 BRUSSELS / Belgium

1. Data acquisition: general results

During the Quest4D project, the historic data acquisition from the RBINS collections focused on Bivalvia, Amphipods and Polychaeta, because these contain the bulk of Gilson's soft bottom macrobenthos. This task, completed thanks to a close cooperation with the project "DIGIT05" (Belspo, digitalization of national Museum collections; this project provided encoders and the in-house 'Darwin' database facility to gather new data between 2007 and early 2009), has enabled to fullfil the bulk of the overall macrobenthos data-set, resulting from Gilson's sampling programmes, the reconstruction of which has been initiated during the "Hinders" project (Houziaux et al, 2008).

In total (including Gilson and other benthos collectors), the merged raw data-set provides information on 870 taxa, of which 708 are determined at Species level, 96 at Genus level and 35 at Family level. 240 taxa were added to the previous species list, during the Quest4D project. The resulting data-base contains a total of 28,150 'records'[1], of which more than 10,500 'records' were added during Quest4D phase I.

With 24,475 'records', Gilson's data thus represents 87 % of the collection of regional marine invertebrates of the RBINS, confirming the importance of this data-set for marine biodiversity studies. The overall data-set, which can be considered as representative of the Belgian marine invertebrate fauna, is dominated by molluscs (mainly bivalves and gastropods), arthropoda (mainly crustaceans), annelids (polychaetes), bryozoans and cnidarians (mainly hydrozoans), as shown in figure 1.

From the bulk of invertebrate data, a selection of data relevant to Quest4D objectives was achieved. To do so, few data parameters were examined (figure 1):

1. Representation of taxa in different sampling methods, used by Gilson;

2. "Freshness" of collected material; and

3. Status of specimen on collection (alive or as skeletic parts)

---

[1] A 'record' is defined as occurrence of specimens of a species at a given station, with unique specimen parameters. It happens that specimens, with identical states, are spread in different jars, each of which is considered as a separate 'record', as well at the encoding stage.

The benthic dredge, which was operated at the BPNS within a grid and sequentially with sediment sampling (Gilson's 'ground-collector', see sediment section), represents more than 60% of the bulk data-set. Our initial expectation that soft-bottom macrobenthic invertebrates should be best represented in Gilson's sediment samples was wrong, since only few hundred of 'records' were obtained. It seems that the plan of Gilson was to rely on dredge data for conspicuous species, which led him to discard specimens collected with sediments. Gilson's programme represents a transition from 'old fashioned' dredge sampling (to obtain basic information) to 'modern' quantitative sampling. However, notes on species collected with the ground-collector are available in Gilson's paper archive; the usefulness of which yet remains to be investigated, because the specimens were quickly identified onboard, often at taxonomic levels, higher than species or genus. These data remain available for any further control of results. To analyze the benthic species composition at the BPNS, we thus focus subsequent analyses on the dredge data.
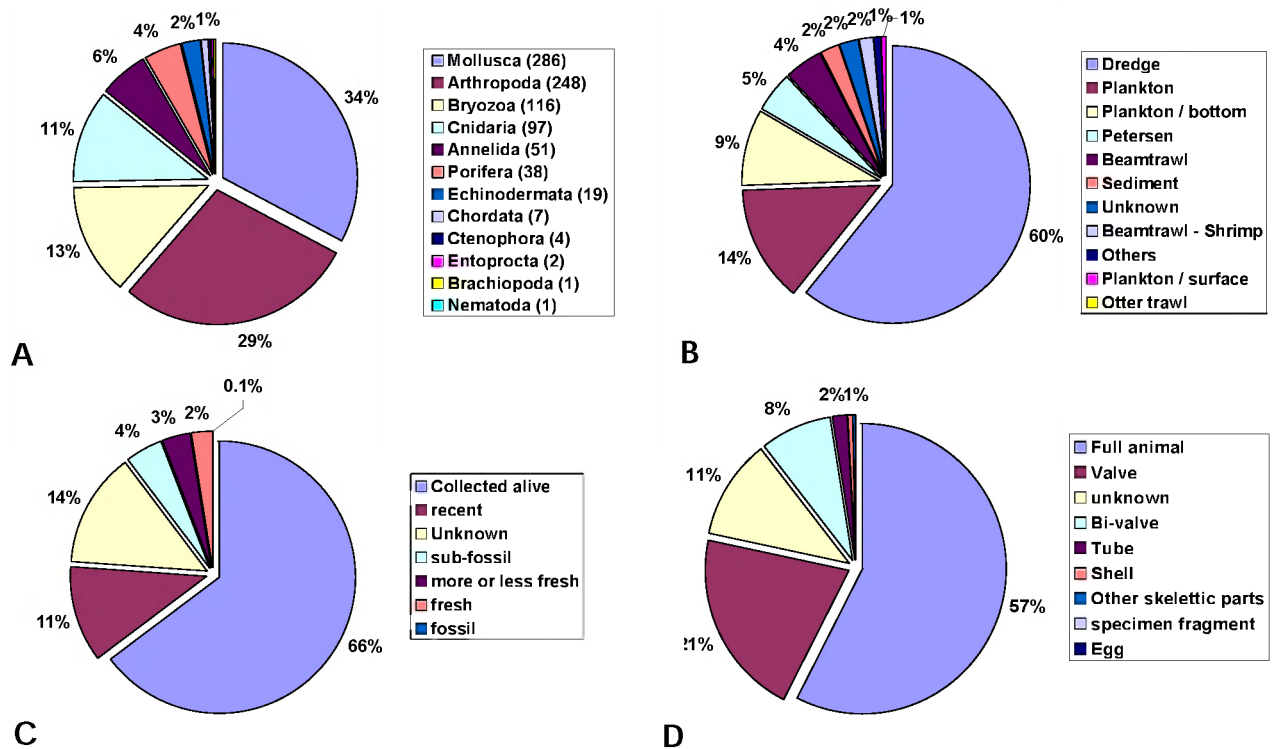

Figure 1: General figures from the bulk of data, gathered from the historic collection of invertebrates of G. Gilson (relative proportions of 'records' from the bulk data-set). A. Species richness of the represented phyla. B. Relative importance of sampling methods. C. Relative abundance of specimen's "freshness" levels in the collections. D. Relative abundance of specimen states in the collection.

For subsequent analysis, we focus on specimens collected alive. However, for dry samples of molluscs or tube worms, the status of the animal at sampling was not recorded. To overcome this problem preventing determining whether shells represent old loose valves or specimens collected alive, but stored dry, the "specimen status" and the "freshness level" (figure 1) were determined on encoding in the "Darwin" database of RBINS collections. However, this information is lacking for taxa encoded prior to 2004, which results in about 10% of taxa flagged with 'unknown' states and excluded from the data-set. Such is the case for most dry gastropod shells, a part of the bivalves and some tube-building polychaetes. For the bulk of bivalves in particular, only "collected alive" and "fresh" + "Bi-valve" (dry valves still attached one to another) states are retained to analyse the living benthos composition. Assuming that the transport of such empty 'bi-valves' by tidal currents must rapidly lead to a breaking of the

ligaments holding the valves together, 'fresh bi-valves" specimens are thus indeed considered as indicative of either alive specimens, stored dry or specimens which died out shortly before sampling.

The recording of these collection parameters enables to determine whether the distribution of empty valves and shells is representative of the species distribution through time or not (e.g. hydrodynamics and human activities are suspected to disperse these items after death). Thus, we expect that skeletic parts of species not collected alive, at all, can be mapped to determine their former distribution in the area, which potentially provides information on the environmental history of the area and some "average" picture of the long-term trends in the species distribution.

2. Baseline maps of macrobenthic biodiversity: overall patterns in the distribution of benthic species within Gilson's grids

Prior to data preparation for long-term analysis in coastal waters (The Hinders area was poorly sampled in recent time, apart from Houziaux et al, 2008), overall maps were created for the distribution of species richness and overall specimen abundance (figure 1).

For these, all 'species' collected alive are taken into account at accurately geo-referenced sampling stations (suspect stations eliminated from the data-set to avoid interpolation bias). Strikingly, overall species richness and specimen abundance show drastically differing patterns. In agreement with formerly obtained results (Houziaux et al, 2008), the Westhinder area hosts highest levels of benthic species richness, especially in the western and eastern gullies south to the kink area of the Westhinder sandbank and the scarp in the gullies; here maximum amounts of cobbles were gathered, as well. These stations thus appear as the core of the pebble community of gravels at the BPNS. High levels of richness are also found in the northern (Northern tip of 'Westhinder', and around 'Oosthinder') and southern (the Buyten ratel – Oostdijck gully) adjacent areas.

Although much lower amounts of samples are available from these areas, the gullies located south to Thornton, Goote and Akkaert banks appear as also bearing some high values, comparable to what is measured along the westernmost part of the coastal waters. To the East, some high values of species richness are also found along the Dutch coast of Walcheren (Deurloo and West-Kapelle channels).
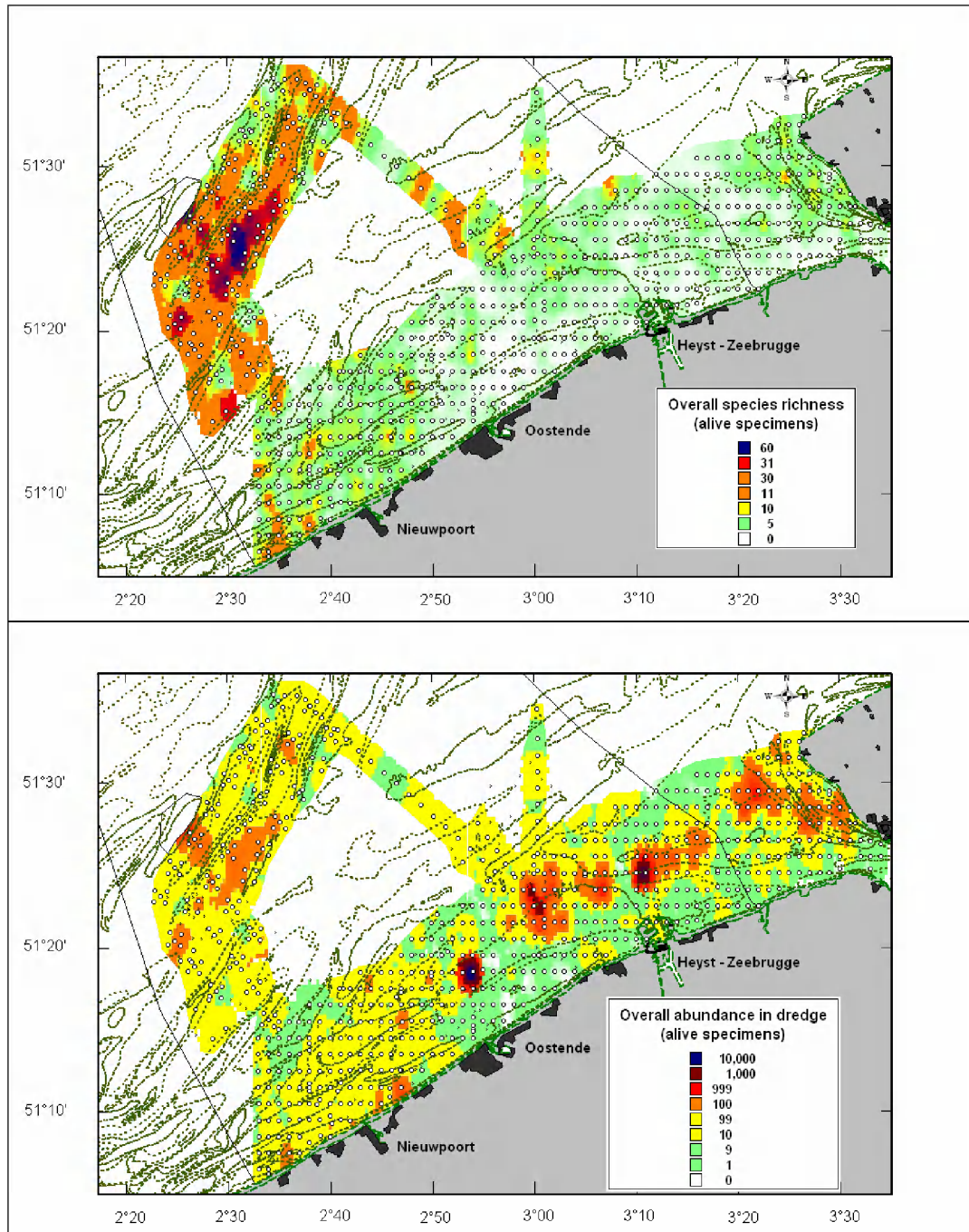
Figure 2: Total species richness (above) and total specimen abundance (below) at accurately geo-positioned dredge stations (suspect stations eliminated), for the period **1899-1908** (very few stations up to 1914). Background: present-day bathymetry and coastline. (Interpolation maps: Inverse Distance Weighting, Search radius = 2km, cell size 0.5 km)

Maximum amounts of benthic specimens were gathered at 4 distinct patches at some 8-12 km off the coast from Oostende to the Dutch coast of Walcheren. Of these, two brought more than 10,000 living animals and can be viewed as "hot-spots" of benthic productivity. However, these much higher values can be induced by e.g. a particularly high recruitment during one year. More similar stations with high overall abundances can be found geographically close to these two extremes, in the patch extending from Bredene to the Dutch border. This area clearly bears very high densities of few macrobenthic species in the surface seafloor, indicative of high biomasses and secondary production. The patches appear to be numerically dominated by the bivalve *Abra alba*, a deposit-feeder.

A separate, similar large patch occurs along the Dutch coasts, and is centered upon the species-rich stations. To the West of Oostende, only few coastal stations bear more than hundred individuals, amongst which the areas of highest species richness along the Westhinder sand bank.

By contrast, extremely low amounts of animals were gathered at all in coastal waters between Oostende and Blankenberghe, landward of the Wenduyne bank.

Noticeably, the interpolation maps evidence the fact that distributional patterns of benthos are consistent with the general distribution of sand banks in the Western part of the sampling grid, providing further evidence that coastal and offshore sand banks have remained stable during the 20th century.

Bibliography

Houziaux, J.-S., Kerckhof, F., Degrendele, K., Roche, M. and Norro A., 2008. "The Hinder banks : yet an important region for the Belgian marine biodiversity?" ('HINDERS'). Belgian Science Policy Office, Final report. 123 pp. + 131 pp. Annexes.

Wentworth, C. K., 1922. A scale of grade and class terms for clastic sediments; *Journal of Geology*, 30: 377-392.

Annex IV. SediCURVE@SEA v.1 database:

development of a multitemporal, multilayer sediment parameter database, in support of Environmental Assessments at Sea

Vera Van Lancker

Royal Belgian Institute of Natural Science (RBINS), Management Unit of the North Sea Mathematical Models (MUMM), Gulledelle 100, 1200 Brussels, Belgium

Details: SediCURVE@SEA v1.0
Version: March 2009
Size reference: 9927 distribution records
Content: Full distribution curves of grain-size data
Temporal coverage: 1899-2008
Geographical cover: Belgian part of the North Sea, mainly
Datum: WGS84
Timestamp : UTC, where known (yyyy-mm-dd hh:mm:ss)
Access : since the database compiles data from various sources, release of data will depend on the data-originator

Abstract

For the comparison of long-term changes in sediment distributions, a new sediment database was constructed containing cumulative distribution curve information of sediment samples. In total, 9927 samples were compiled from various institutes, with major contributions from ILVO (ILVO BIOLMON database, K. Hostens), UG-MARBIOL (MACRODAT database, M. Vincx), UG-RCMG/MUMM (Belspo Marebasse project, Van Lancker et al., 2007), UG-RCMG Msc theses, and Fund for Sand Extraction. The SediCURVE@SEA database spans the period 1971-2008 and also contains data from recently re-analysed sediment samples from the Gilson collection (1899-1914, Houziaux et al. 2008). The spatial distribution of the sample locations is given in Fig. 1.

Procedures

The original data were cleaned, homogenized and standardized in one database (following IDOD structure, www.mumm.ac.be/datacentre) further enabling easy data analysis and parameter calculation in a uniform way (Microsoft Visual Foxpro). Calculation of parameters was performed on both the bulk sample, as well as on the sand fraction only. The data are further treated in GIS.

The following parameters are calculated and optionally stored in other databases:
- Lithological fractions (percentages), following the Wentworth scale (Wentworth, 1922):
  - Clay ($< 8 \mu$m)
  - Silt (8-63 μm)
  - Sand: very fine (63-125 μm), fine (125-250 μm), medium (250-500 μm), coarse (500-1000 μm) and very coarse (1000-2000 μm)
  - Gravel ($> 2000 \mu$m)
- Percentiles
  - D5, 10, 16, 20, 25, 30, 35, 40, 50, 60, 65, 70, 75, 80, 84, 90, 95

- Sediment parameters following the graphical method of Folk & Ward (1957)
  - o Mean grain-size
  - o Sorting, *measure of uniformity of the grain-size distribution*
  - o Skewness, *measure of asymmetry of the grain-size distribution*
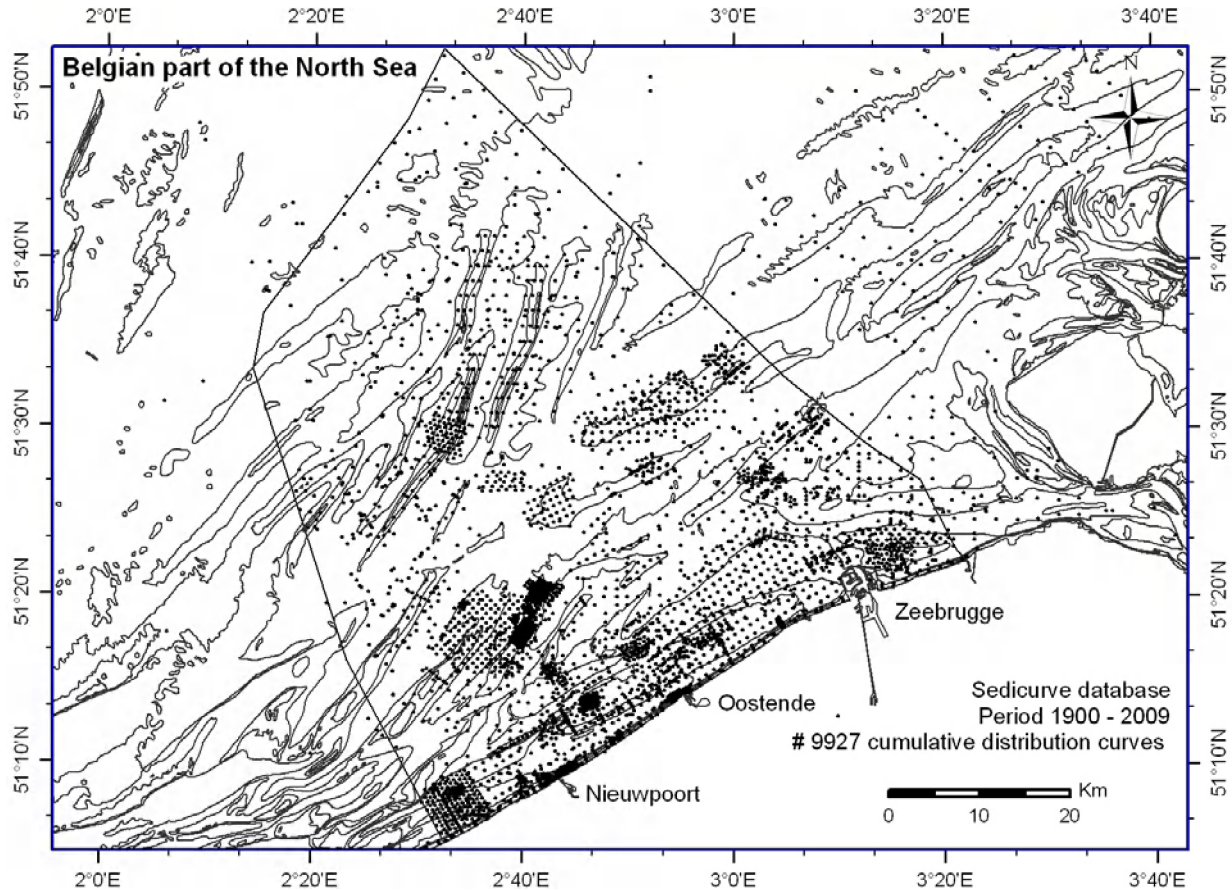 - o Kurtosis, *measure of the steepness of the grain-size distribution*

Figure 1.   Spatial distribution of sediment samples for which cumulative distribution curves have been compiled.

Multilayer

Results are incorporated from both surficial sediments, as well as from subsurface sediment layers. Distinction is to be made between active layers and buffer layers, a process which needs further development and validation.

Applications

These relate to seabed nature mapping, long-term time series analysis, seabed mobility studies, habitat suitability modelling, improved bedmodels for sediment transport modelling, and grain-size trend analyses.

Data bias

Since the database compiles data from various sources, inaccuracies arise from the use of various methodologies (e.g. sieve versus laser analysis; various size classes of the sieves used) and/or (pre-)treatment of the sediment samples. Another important aspect is whether or not shell fractions have been removed and are regarded as gravel or not.

Sources of data (cumulative distribution curves)
Baeye, M. (2008). Staalnames Wandelaar. UG-RCMG.

Belgische Geologische Dienst, 1991. Geologie van het Belgisch continentaal plat. Fase 5. Eerste fase van de kartering der oppervlakkige sedimenten. Granulometrische analysen. Ref. KWA/88 – 1.2.2.b. Deel 2A: Sedimentologische steekkaarten. NCP0719. 91.00037 (1988)

Deleu, S. (2001). Zeebodemmobiliteitsstudie van de Hinderbanken regio. Thesis submitted to obtain the degree of Master in Geology. Unpublished Msc Thesis, Gent (B): Universiteit Gent (Renard Centre of Marine Geology), 135 pp.

Charlet, F. (2001). Etude de la dynamique sédimentaire et morphologique d'un haut-fond marin: Le Paardenmarkt, Mer du Nord méridionale. Apports d'une étude couplée: granulométrie / outils acoustiques/ modélisation des courants. Unpublished Msc Thesis, Gent (B): Universiteit Gent (Renard Centre of Marine Geology), 74 pp.

Degraer, S., Van Lancker, V., Moerkerke, G., Vincx, M., Jacobs, P. & Henriet, J. (2002). Intensive evaluation of the evolution of a protected benthic habitat: HABITAT. Final report. Federal Office for Scientific, Technical and Cultural Affairs (OSTC), Ministry of the Flemish Community (WWK). Universiteit Gent, Gent, 124 p

Degraer, S., Van Lancker, V., Moerkerke, G., Van Hoey, G., Vanstaen, K., Vincx, M. & Henriet, J.-P. (2003). Evaluation of the ecological value of the foreshore: habitat-model and macrobenthic side-scan sonar interpretation: extension along the Belgian Coastal Zone. Final report. Ministry of the Flemish Community, Environment and Infrastructure Department. Waterways and Marine Affairs Administration, Coastal Waterways, 63 p.

Deleu, S. (2002). Tide-topography interaction near the kink in the Westhinder sandbank (Southern North Sea). Thesis submitted to obtain the degree of Master in Science in Advanced Studies in Marine and Lacustrine Sciences. Unpublished Msc Thesis, Gent (B): Universiteit Gent (Renard Centre of Marine Geology), 43 pp.

Federal Public Service Economy, Self-Employed, SME's and Energy, Fund for Sand Extraction. Sediment grain-size data in the marine aggregate concession zones. (1999-2001)

GILSON database: Houziaux, J.-S., Kerckhof, F., Degrendele, K., Roche, M., Norro A., 2008. "The Hinder banks : yet an important region for the Belgian marine biodiversity?" ('HINDERS'). Belgian Science Policy Office, Final report. 123 pp. + 131 pp. Annexes. (1899-1914)

ILVO-BIOLMON. version 2008. ILVO macrofauna data: macrofauna monitoring on the Belgian Part of the North Sea since 1979 (Responsible: K. Hostens). Sediment parameters. (http://www.vliz.be/imis/imis.php?module=dataset&dasid=1043) (1978-2007)

MUMM SEBAB/MOMO projecten: Fettweis, M., Francken, F., Pison, V. & Van den Eynde, D. 2003. Bepaling van de Sedimentbalans voor de Belgische Kustwateren (SEBAB-III). Activiteitsrapport 2: Naar een 3D model van het BCP en de sedimentologische analyse van bodemstalen. BMM-rapport SEBAB/3/MF/200304/NL/AR/2. (2000-2005)

Papili, S. (2008). Staalnames Wandelaar. UG-RCMG/Belgische Marine.

Tytgat, J., 1989. Dynamics of gravel in the superficial sediments of the Flemish Banks, southern North Sea. In: J.P. Henriet and G. De Moor (Editors), The Quaternary and Tertiary Geology of the Southern Bight, North Sea. Ministry of Economic Affairs, Belgian Geological Survey, Gent, pp. 217-228.

UG-MARBIOL-MACRODAT, version 2009. MACRODAT compiles data gathered in the framework of different research projects and PhD studies. Next to macrobenthic densities and species richness values, also sedimentological data are integrated in the database, (Responsible: M. Vincx) (http://www.vliz.be/imis/imis.php?module=dataset&dasid=633) (1994-2008)

UG-RCMG/MUMM Marebasse datasets (Belspo PODOII): Van Lancker, V., Du Four, I., Verfaillie, E., Deleu, S., Schelfaut, K., Fettweis, M., Van den Eynde, D., Francken, F., Monbaliu, J., Giardino, A., Portilla, J., Lanckneus, J., Moerkerke, G., Degraer, S., 2007. Management, research and budgetting of aggregates in shelf seas related to end-users (Marebasse). Final Scientific Report. Belgian Science Policy, 125pp. (2002-2006)

Van Lancker, V. (1999). Sediment and morphodynamics of a siliciclastic near coastal area, in relation to hydrodynamical and meteorological conditions: Belgian continental shelf. Unpublished Ph.D. Thesis, Universiteit Gent, Gent, 194 pp. (1995-1999)

Van Nieuwenhove, B. (2003). Akoestische en sedimentolgische karakterisering van zand-slib mengsels in de Belgische kustnabije zone. Thesis to obtain the degree of Master in Geology. Unpublished Msc Thesis, Gent (B): Universiteit Gent (Renard Centre of Marine Geology), 127 pp.

Verbeeck, P. (2004). Akoestische en sedimentologische karakterisering van een oude munitiedumpplaats: de Paardenmarkt, Belgisch continentaal plat. Thesis submitted to obtain the degree of Master in Geography. Unpublished Msc Thesis, Gent (B): Universiteit Gent (Renard Centre of Marine Geology), 103 pp.

Verfaillie, E. (2002). Evaluation of sonar techniques for the descrimination of macrobenthic communities. Thesis submitted to obtain the degree of Master in Science in Advanced Studies in Marine and Lacustrine Sciences. Unpublished Msc Thesis, Gent (B): Universiteit Gent (Renard Centre of Marine Geology/Section Marine Biology), 26 pp.

VITO Stranddatabase (Dr. Bart Deronde) (2000).

References

Folk, R.L. and Ward, W.C., 1957. Brazos River Bar: A study in the significance of grain size parameters. Journal of Sedimentary Petrology, 27(1): 3-26.

Houziaux, J.-S., Kerckhof, F., Degrendele, K., Roche, M., Norro A., 2008. "The Hinder banks : yet an important region for the Belgian marine biodiversity?" ('HINDERS'). Belgian Science Policy Office, Final report. 123 pp. + 131 pp. Annexes.

Van Lancker, V., Du Four, I., Verfaillie, E., Deleu, S., Schelfaut, K., Fettweis, M., Van den Eynde, D., Francken, F., Monbaliu, J., Giardino, A., Portilla, J., Lanckneus, J., Moerkerke, G., Degraer, S., 2007. Management, research and budgetting of aggregates in shelf seas related to end-users (Marebasse). Final Scientific Report. Belgian Science Policy, 125pp.

Wentworth, C.H., 1922. A scale of grade and class terms of clastic sediments. Journal of Geology 30, 377-392.

Annex V. A large-scale idealized sediment transport model

Toon Verwaest

Flanders Hydraulics

A simple semi-empirical model, able to represent the essence of coastal mud dynamics on a time scale of years, was built, based on a mass balance and on the present state of knowledge on large scale mud processes in the Belgian coastal zone (plus the mouth of the Schelde river).

From in-situ and remote sensing measurements it is known that a turbidity maximum is formed between Oostende and the mouth of the Schelde, with Zeebrugge in the centre. From the same measurements it is observed that SPM concentrations further off-shore than ca. 20 km are very small, in comparison with the SPM concentrations in the coastal water. See Fettweis et al, 2009 (submitted to Marine Geology, Special Issue Tidalites 2008). Therefore, for the idealised modelling the geographical domain being the BCP plus the mouth of the Schelde is represented by three boxes: 1) the eastern coastal waters (the turbidity maximum area), 2) the western coastal waters, 3) the off-shore zone. This is illustrated by the Figure xx below.
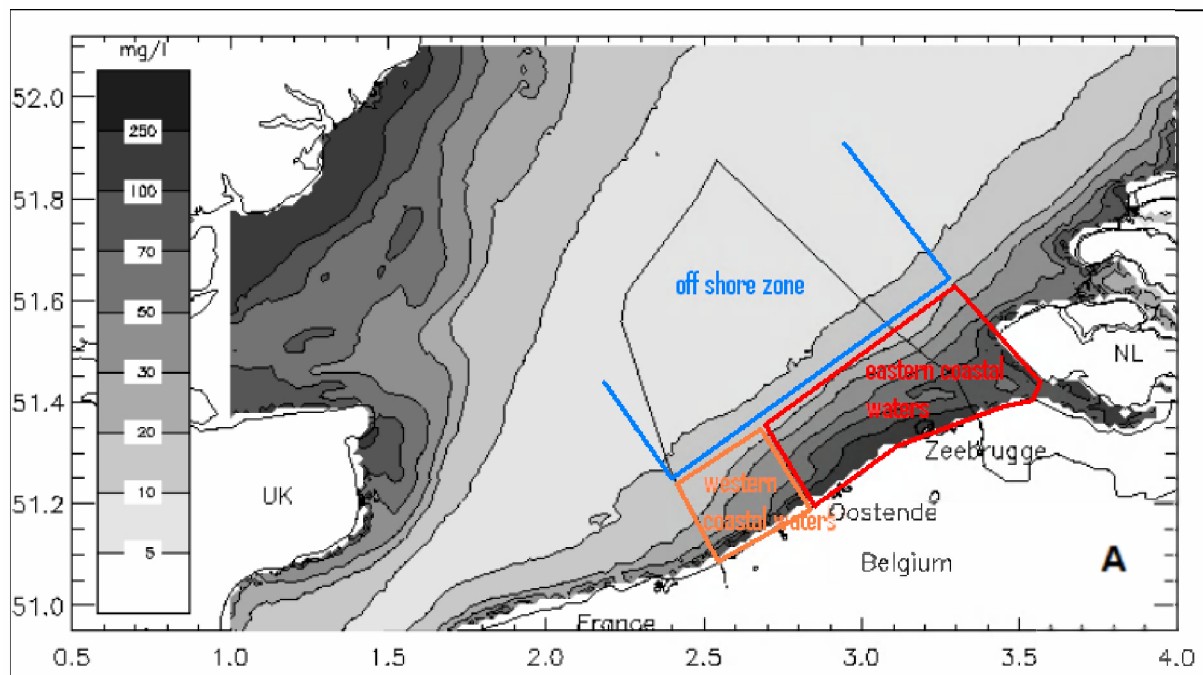

Figure 1. Subdivision of the geographical domain in three zones on the basis of the state of knowledge on the averaged SPM concentration, namely from Fettweis et al, 2009 (submitted to Marine Geology, Special Issue Tidalites 2008)

An idealised model has been set up describing the mud sediment balance on a time scale of years for the eastern coastal waters, it is the coastal turbidity maximum area. The result is shown in the Figure below.
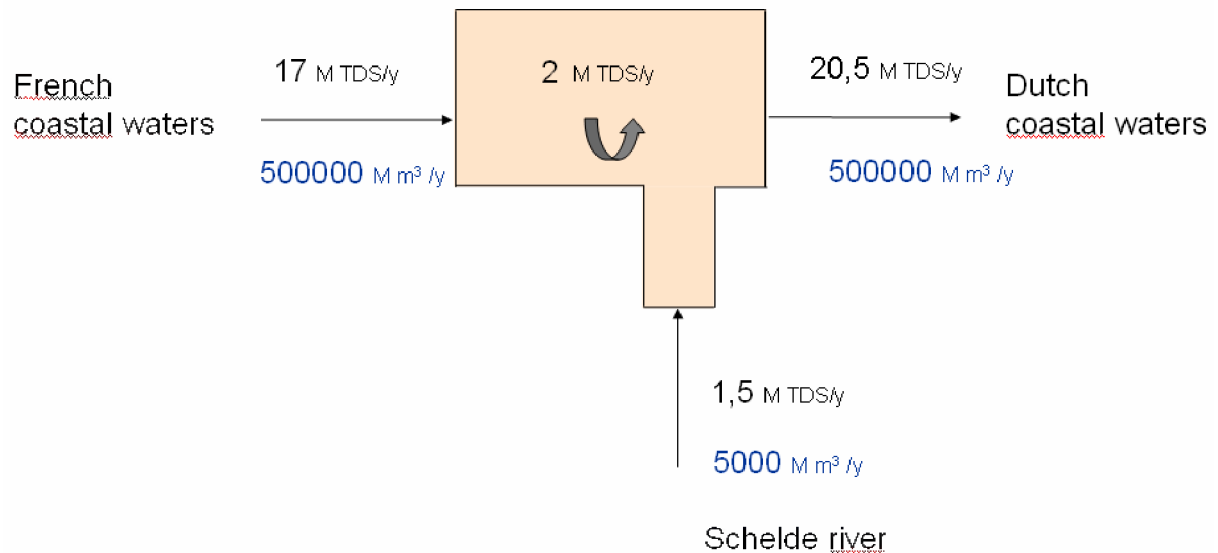

Figure 2. Idealised model describing the mud sediment balance on a time scale of years for the eastern coastal waters (it is the coastal turbidity maximum area).

The residual hydraulic flow along the Belgian coastal waters is directed from SW to NE (from French coastal waters to Dutch coastal waters). This residual hydraulic flow amounts to 500000 M m3 per year order of magnitude and is caused mainly by the tidal flood volume being larger than the tidal ebb volume. This is a factor 100 larger than the river Schelde input, so the hydraulic flow from the Schelde can be neglected, for the scale considered.

The average input of mud from French coastal waters is relatively accurately quantified as 17 M TDS per year, from a combination of measurements (remote sensing as well as in situ sampling) and process modelling (see Fettweis et al, 2007) [Fettweis, M., Nechad, B., Van den Eynde, D. 2007. An estimate of the suspended particulate matter (SPM) transport in the southern North Sea using SeaWiFS images, in-situ measurements and numerical model results. Continental Shelf Research, 27, 1568-1583.].

The average input of mud from the Schelde river of 1,5 M TDS per year is a very rough preliminar estimation based on a few years of monitoring of the suspended sediments at the landward end of the Schelde estuary, in several tributaries, also taking into account the results of process modelling exercises (cfr. supra "Mud transport model Scheldt estuary"). In 1999 monitoring of suspended sediment transport started in several tributaries of the Schelde-estuary. At present the measurement techniques are still in development but approximately 40% of the total discharge is monitored quasi continuously. Measurements are performed at inward locations situated at the limit of the tidally influence area. See Figure below.
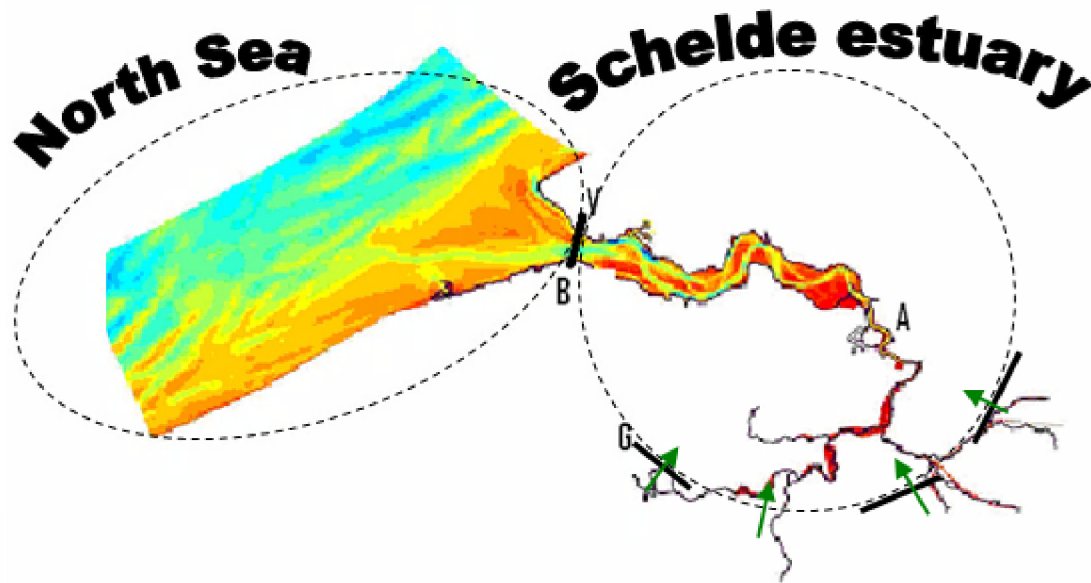
Figure 3. Measurements of sediment input are located at the landward end of the Schelde estuary, at the limit of the tidally influenced area (green arrows). At present approximately 40% of the total discharge is monitored.

Structural erosion of the sea bottom takes place especially in the area in and around the access channels towards the coastal harbour of Zeebrugge and the Schelde estuary. Deepening of the navigation channels results in erosion of the neighbouring sea bottom because the channel slopes are gradually flattening towards an equilibrium profile, with an average slope of 1/200. The surface area of this erosion zone is ca. 80 km^2. See the Figure below.
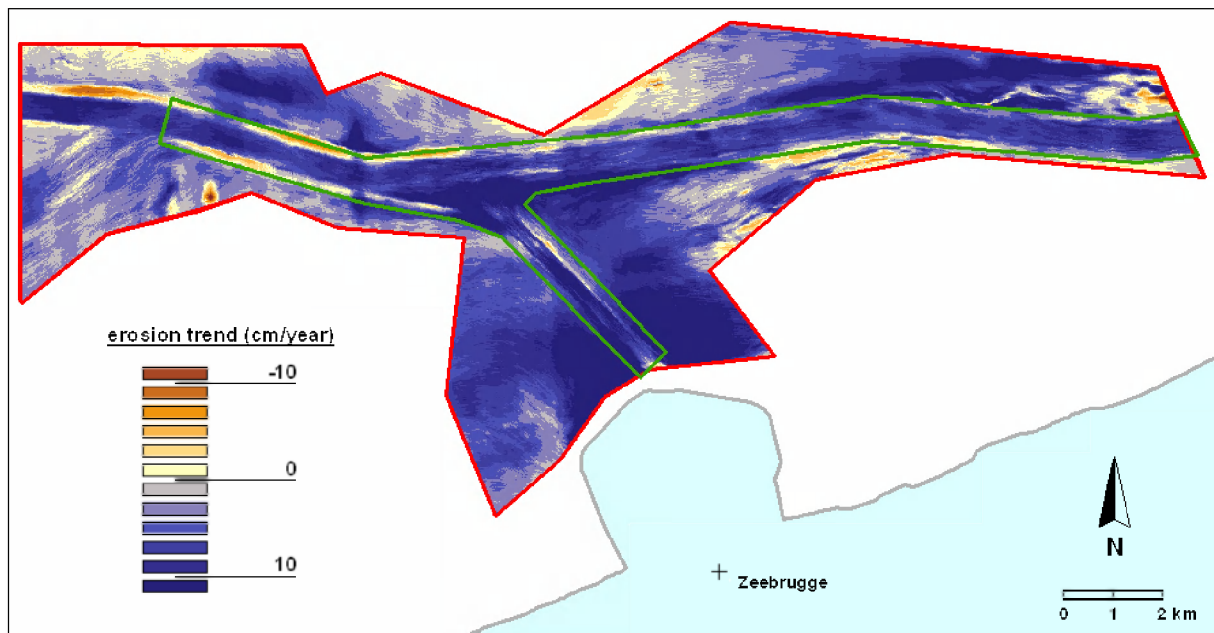

Figure 4. Erosion of the sea bottom in and around the access channels towards the coastal harbour of Zeebrugge and the Schelde estuary. Trend calculation for the period 1987-2003.

Multiplying the erosion trend with the mud percentage of the sea bottom sediment (see Van Lancker et al, 2007 : de MAREBASSE DVD), this is executed in GIS with a pixel size of 250 m x 250 m, a yearly local mud source of ca. 2 M TDS is calculated. The mud content is relatively high, because this area was part of the coastal plain a few thousands years ago (Holocene back-barrier deposits). The resulting mud flux is shown in the Figure below.
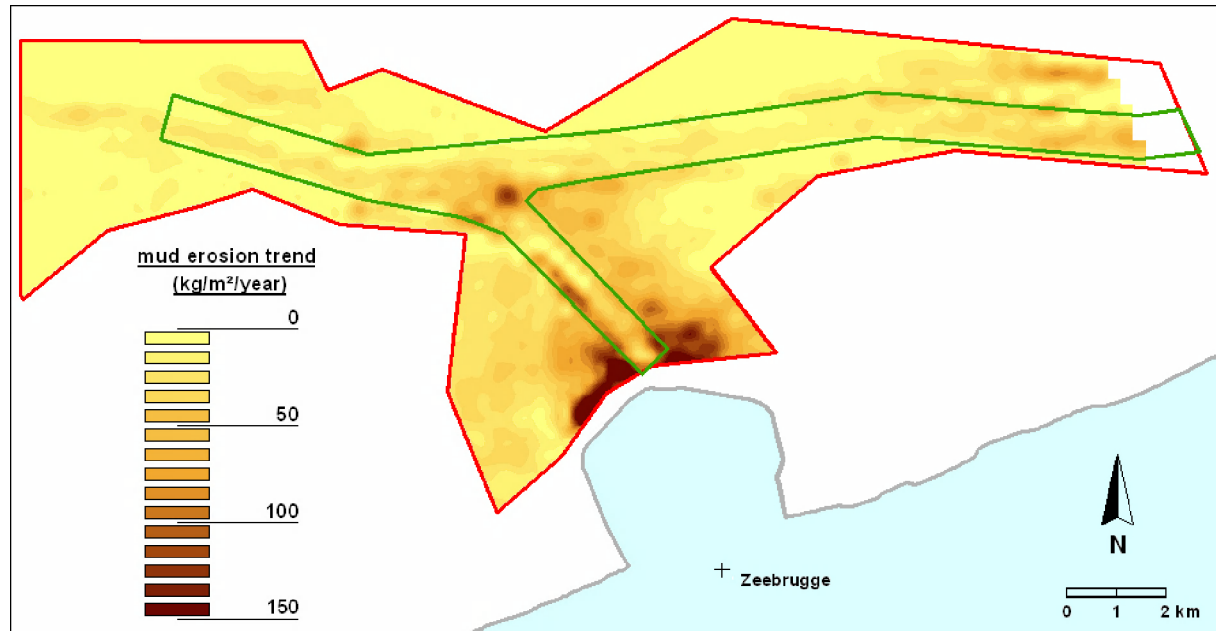

Figure 5. Mud source due to erosion of the sea bottom in and around the access channels towards the coastal harbour of Zeebrugge and the Schelde estuary. A multiplication of morphological trends and sea bottom sediment composition in GIS (raster size 250 m x 250 m).

Because in the remaining part of the eastern coastal waters the erosion and sedimentation areas are relatively small and more or less compensating (as a rough estimation +- 1 MTDS per year, based on the morphological trend results given in the task 1.1.3 "long-term bathymetry changes", cfr. infra) the output of mud towards the Dutch coastal waters is determined by summation of the different mud sources described before as 20,5 M TDS per year.

From this idealised model one can estimate the contributions of local erosion and mud input from the Schelde river, to the yearly averaged turbidity increase in the eastern coastal waters. One finds a turbidity increase of 12 % (= 2 / 17) due to local erosion and a turbidity increase of 9 % (= 1,5 / 17) due to the Schelde mud input, both compared to the turbidity in the surrounding coastal waters. From observations the yearly averaged turbidity in the eastern coastal waters is about a factor 2 higher than in the surrounding coastal waters. The idealised model presented doesn't take into account the dynamics on shorter time scales than years. It is concluded that the effect of these processes, such as erosion and deposition of fresh mud on a tidal, lunar, storm and seasonal time scale, as well as dredging and dumping are the dominant processes in forming the turbidity maximum in the eastern coastal waters.

Annex VI: Storm influence on SPM concentrations in a coastal turbidity maximum area (southern North Sea) with high anthropogenic impact

Michael Fettweis[1], Frederic Francken[1], Dries Van den Eynde[1], Toon Verwaest[2], Job Janssens[2], Vera Van Lancker[3,1]

[1]Royal Belgian Institute of Natural Science, Management Unit of the North Sea Mathematical Models, Gulledelle 100, 1200 Brussels, Belgium

[2]Flanders Hydraulics Research, Antwerp, Belgium

[3]Ghent University, Renard Centre of Marine Geology (RCMG), Krijgslaan 281, S8, 9000 Gent, Belgium

Introduction

Waves have an important impact on cohesive sediment processes on continental shelves (e.g. Green et al., 1995; Cacchione et al., 1999; Traykovski et al., 2007; Shi et al., 2008). During these events high concentrated mud suspensions (HCMS) have been measured, which can be formed by settling of suspended matter or fluidization of cohesive sediment beds (Maa and Mehta, 1987; van Kessel and Kranenburg, 1998; Li and Mehta, 2000). Fluidization or liquefaction of mud layers occurs if the stress caused by wave pressure exceeds the yield stress of the sediments. The high concentrated mud suspensions (HCMS) and fluid mud deposits are easily transported and may result in very high sediment fluxes. The cohesive sediment processes associated with storms are not well documented in the Belgian coastal area; the results presented here are an attempt to assess, based on field measurements and numerical model results, the hydrodynamics, sediment dynamics and bed erosion processes during extreme meteorological events.

Data collection was conducted between April 2005 and February 2007 using a tripod deployed at MOW1 and near Blankenberge (Fig. 2.1). Both sites are characterised by the occurrence of near-bed Holocene medium-consolidated mud, albeit covered with an ephemeral slightly muddy fine sand layer with a median grain size of about 170 μm. The thickness of the sand layer increases towards the shore. The water depth is 9 m MLLWS at the MOW1 site and about 5 m MLLWS at the Blankenberge site. The tripod measuring system was developed to monitor SPM concentration and current velocity. Mounted instruments include a SonTek 3 MHz ADP, a SonTek 5 MHz ADV Ocean, a Sea-Bird SBE37 CT system, two OBS, two SonTek Hydra systems for data storage and batteries and a LISST 100C. The high frequency ADV measurements have been used to calculate shear stress (Andersen et al., 2007). Three periods have been selected for further analysis to assess storm influences. Field calibration of the OBS sensors have been carried out during 5 tidal cycles between April 2005 and May 2006 at site MOW1.

Results

The data of SPM concentration, water depth, ADV current velocity and bottom shear stress collected at MOW1 in autumn 2005 are presented in Fig 1. Spring tide occurred around December 1 (day 10), neap tide around November 26 (day 5). The measuring period was characterised by 2 days of calm weather followed by a WNW storm with wind velocities of more than 16 m/s (7 Bf) and significant wave heights of up to 3.5 m in the coastal zone. The water was pushed up against the coast and low water levels raised with almost 2 m. The SPM concentrations follow a quarter-diurnal (ebb-flood) signal. Although the currents are flood dominated, no significant difference in magnitude between ebb and flood SPM concentration peaks occurs. A significant increase in SPM concentration occurred almost immediately after the beginning of the WNW storm (day 3-4). The SPM concentration measured at 0.3 meter above

bottom (mab) increases to 1-3 g l⁻¹, whereas at 1.9 mab the SPM concentrations remain less than 0.5 g l⁻¹. The sudden increase in SPM concentration at the onset of the storm was induced by the exceptional meteorological conditions and partly because the storm occurred after a calm period and around neap tide. Neap tidal conditions and calm periods favour the deposition of fluffy layers, as has been observed from bottom samples and from model simulations (Fettweis and Van den Eynde, 2003). After the WNW storm the SPM concentration decreased in magnitude, however both OBS's still measured very high peak concentrations (0.3 mab: up to 3 g l⁻¹, 1.9 mab: up to 1 g l⁻¹) until the end of the deployment (1 week after the storm). The high minima in SPM concentration measured by the OBS1 (0.5-1 g l⁻¹), indicates that a HCMS or fluid mud layer was formed. It is only days after the storm that the SPM concentrations, measured by both OBS's, show again similar minima and that the near bed high SPM concentrations have disappeared.
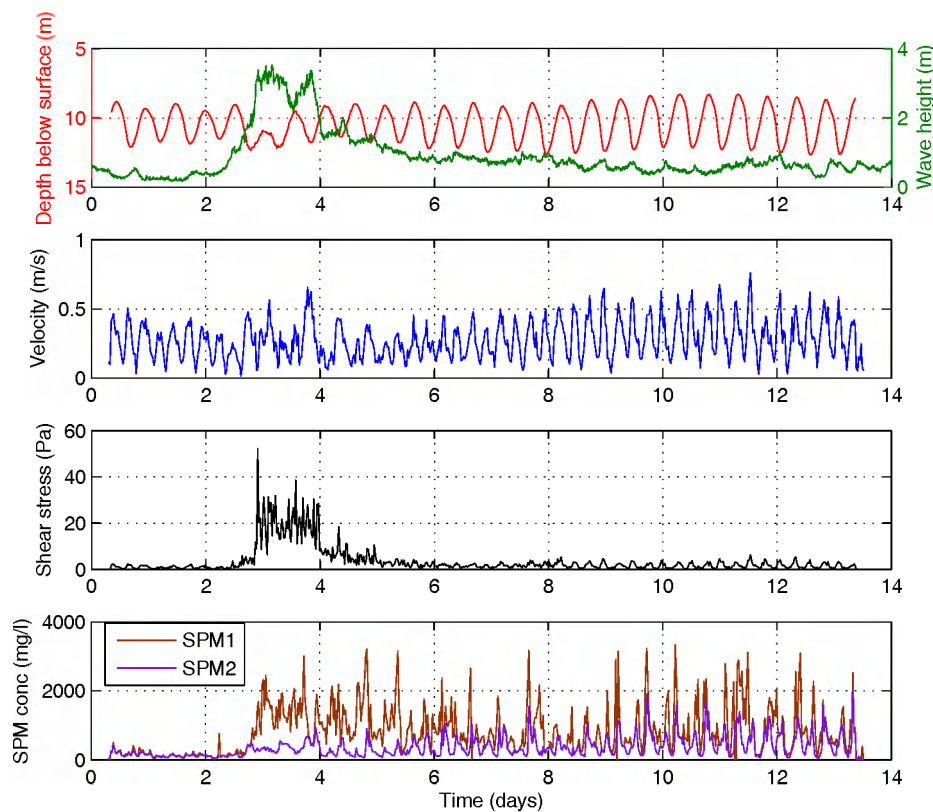

Figure 1: MOW1 site, tripod measurements of 22 November – 5 December 2005. From up to down: depth below water surface (m) and significant wave heights; ADV current velocity (m/s); shear stress (Pa) derived from the ADV and SPM concentration at 0.3 mab (SPM1) and 1.9 mab (SPM2).

The data from 7-18 November 2006 and 24 December 2006 – 8 January 2007 collected at the Blankenberge site have been analysed. In Fig. 2 the data from November are presented. On 12-13 November, a NW storm generated significant wave heights of about 2.7 m. The second half of December was characterized by low wind speeds from mainly W-SW. The highest SPM concentrations during the November 12 storm have been registered only about one day after the storm by the OBS at 0.2 mab and about two days after by the OBS at 2 mab (Fig. 2). The OBS at 0.2 mab data has very high minima in SPM concentrations (>0.8 g l⁻¹). The OBS at 2 mab has measured only during a short period after the storm an increase in SPM concentration. This indicates that vertical mixing was limited. Similar data have been collected during the storm of December 31. During this storm the increase in SPM concentration occurred during ebb indicating that the suspended matter has mainly been transported from the NE, i.e. from the

mouth of the Westerschelde estuary and in the direction of the wind-driven and the ebb current. Local resuspension of mud layers was at that time of minor importance.

The following conclusions can be drawn from the three measurement periods:

1. There is a dominant quarter-diurnal (ebb-flood) signal in the SPM concentration time-series. The spring-neap tidal signal can be identified clearly during calm meteorological conditions;
2. The data from LISST 100C prove that the suspended particles are flocs: the biggest particles have been measured during slack water and low current velocities and the smallest during peak current velocities;
3. Considerable variations in SPM concentrations exist during a tidal cycle: maximum concentrations were sometimes up to 50 times higher than the minimum concentrations;
4. The very high SPM concentrations measured near the bed are related to storm periods; our data prove that HCMS occur near the bottom in the coastal turbidity maximum of the Belgian-Dutch nearshore zone; and
5. Wind-driven advection can have a significant influence on SPM concentration.

Discussion

The formation of HCMS in wave-dominated areas is well documented (de Wit and Kranenburg, 1997; Winterwerp, 1999; Li and Mehta, 2000). The occurrence of fluid mud or HCMS on many continental shelves is associated with wave or current-driven sediment gravity flows off high-load rivers (Wright and Friedrichs, 2006). However, the origin of the suspended matter in the southern North Sea and in the Belgian-Dutch nearshore zone has been mainly ascribed to the inflow of fine-grained sediments through the Dover Strait (Gerritsen et al., 2000), as no high-load rivers exist in the area. This SPM flux amounts to about 34×10^6 t per year, from which about 50% is transported along the continental side (i.e. France-Belgian-Dutch nearshore area), see Fettweis et al. (2007a). Due to the high tidal energy permanent layers of freshly deposited to very soft consolidated cohesive sediments occur in the Belgian-Dutch nearshore area only in some protected hydrodynamic environment such as ports, navigation channels and disposal grounds of dredged material. However, thin fluffy layers, temporarily present, do occur over large areas.
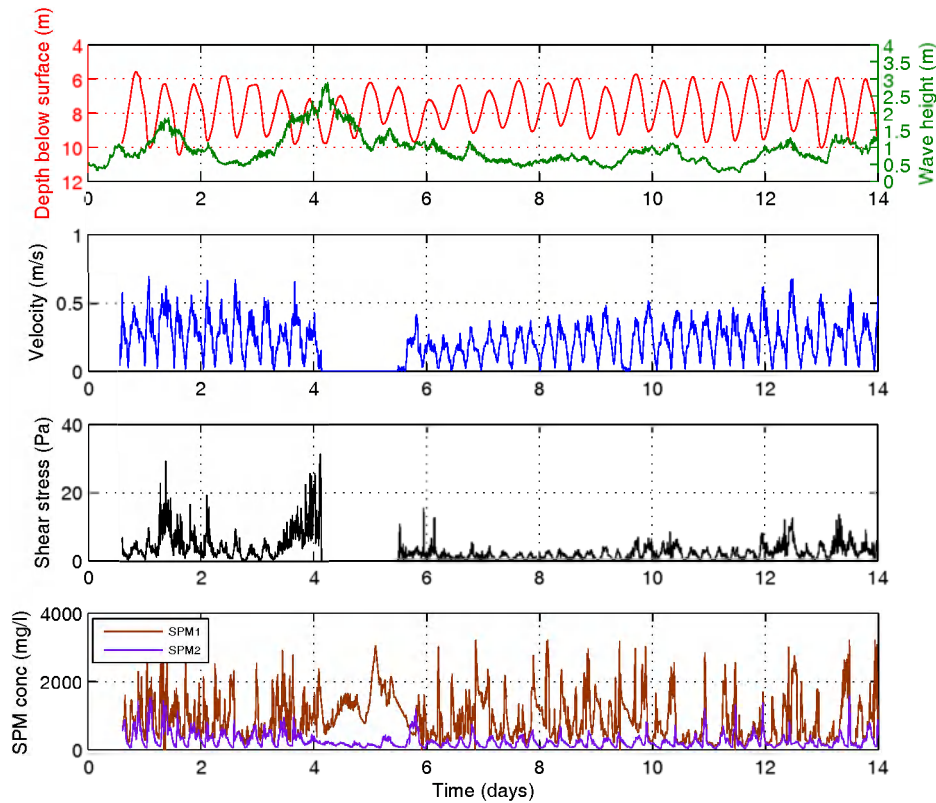
Figure 2: Blankenberge site, 7-20 November 2006. From up to down: depth below water surface (m) and significant wave heights; ADV current velocity (m/s); shear stress (Pa) derived from the ADV; and SPM concentration at 0.2 mab (SPM1) and 2.2 mab (SPM2).

The fluctuation of SPM concentration with time is complex and it is not always straightforward to identify the origin of some of the variations. A low correlation was found between tidal amplitude and tide-averaged SPM concentration, this points to the fact that the neap-spring tidal signal is overprinted by other processes, such as high wave conditions and wind-induced long- and cross-shore advection.

Using SeaWiFS images the average mass of SPM over the period 1997-2004 in the turbidity maximum area has been calculated as about 1×10^6 t. Variations of the order of 30% occur between spring and neap tides, as also of the order of 40-60% in-between seasons. Based on the tripod measurements, the SPM mass during storm conditions has been estimated as $3\text{-}5\times10^6$ t in the same area. An important amount of fine-grained matter has thus to be resuspended, eroded or transported during a storm. Below, some points are discussed in more detail to better identify the possible sources of fine-grained sediments and the processes that result in the significant increase in SPM concentration during storms.

SPM transport and wind-driven advection

The effect of winds on SPM concentration is variable and depends also on the wind direction and the availability of muddy sediments. Along- or cross-shore advection, enhanced during winds from the SW/NE or NW/SE, respectively, transports water masses with low SPM concentration and higher salinity to the measurement location. During periods with high salinity variations during a tide, a negative correlation between salinity and SPM concentration exists, see Fig. 3. High salinities and low(er) SPM concentrations are associated with flooding and low salinities and high(er) SPM concentrations with ebbing tide. The data show that during the first 3 weeks of January 2007, SW winds prevailed resulting in advection of high salinity and low

turbid water from the English Channel towards the southern North Sea. At the end of January, the wind direction changed towards S-SE and low salinity, high turbidity water originating from the Schelde estuary dominated the signal.
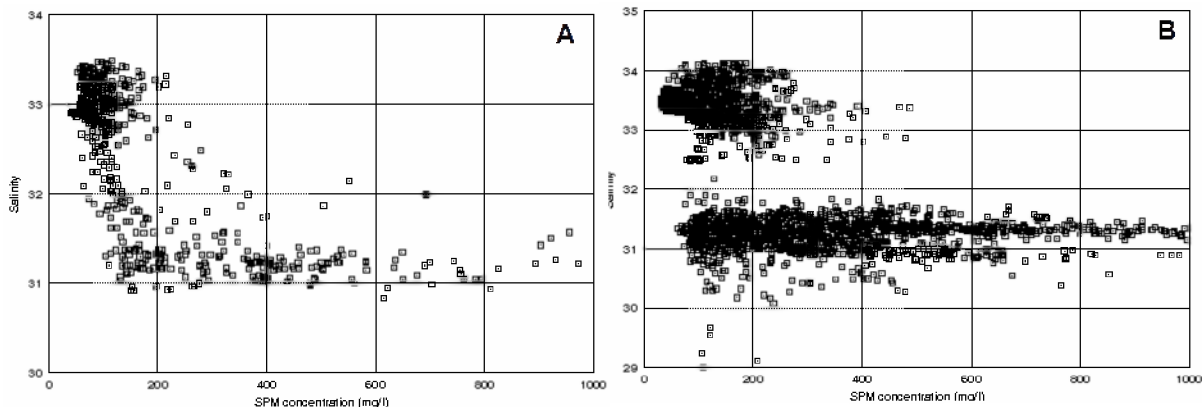
Figure 3: SPM concentration (2 mab) as a function of salinity. The effect of alongshore advection of high saline and low turbid water is shown at the Blankenberge site. (A) Negative correlation between salinity and SPM concentration during prevailing SW winds (5-7 January). (B) Two successive periods are shown; the first is characterised by high salinity and low SPM concentration (16-22 January) and the second by low salinity and high SPM concentration (22-31 January). The sudden decrease in salinity was induced by a change in wind direction from SW to SE.

Holocene mud as SPM source

The largest reservoir of fine-grained sediments in the nearshore area consists of the medium-consolidated Holocene mud (bulk density > 1500 kg m^{-3}). The area where these mud deposits occur in the first meter of the seabed is ~ 744 km^2 (Fettweis et al, 2007b). Erosion behaviour measurements confirm that consolidated cohesive bed layers are difficult to erode by only fluid-transmitted stress. The maximum bottom shear stress during calm periods and during spring tide is about 4 Pa (see Fig. 1-2). The sediments of the mud fields can thus not be eroded under calm meteorological conditions. Near bed shear stresses derived from the ADV data amount up to 40 Pa (average is 12 Pa) during storm conditions. These values indicate that erosion of Holocene mud by fluid-transmitted shear stress can occur and that SPM could have been released into the water column from the Holocene mud fields under storm conditions. Using the Ariathurai-Partheniades formulation (Ariathurai, 1974) for erosion of cohesive sediments, a mean bed shear stress of 12 Pa, a critical erosion shear stress of 10 Pa and an erosion rate of 0.5 g m^{-2} s^{-1} the mass of Holocene mud that can be eroded amounts to 864 t km^{-2} day^{-1}. If all the Holocene mud would outcrop then about 0.6×10^6 t per day could have been eroded by horizontal tidally- and wave-induced shear stress during the storm. This is a maximum estimate as large parts of the Holocene mud fields are probably covered by thin layers of sandy sediments. Most probably, erosion of Holocene mud by entrainment represents only a minor source of suspended sediments during storms.

Still, in literature, it is well documented that a cohesive mud bed may be eroded and fluidised by waves (Maa and Mehta, 1987; De Wit and Kranenburg, 1997; Li and Mehta, 2000; Silva-Jacinto and Le Hir, 2001). The effect of water waves on a cohesive, deformable bed can be described by a pressure wave, inducing normal and shear stresses in the bed. These stresses modify the strength of the bed and thus also the erodibility of the sediments. Silva Jacinto and Le Hir (2001) explain the observed liquefaction and failure of consolidated mud layers along sandy layers by waves due to pumping effects. Mud pebbles are an indication of this type of erosion, they have been observed regularly in the area of investigation (Fettweis et al., 2007b). However, due to insufficient data availability, the mass of mud pebbles or of suspended matter originating from wave induced bed failure cannot be quantified yet.

Mixed sediments as SPM source

Other important erosion mechanisms are due to the mutual interaction of cohesive and non-cohesive sediments (Le Hir et al., 2007): one can distinguish between sand grains moving on a cohesive substrate and erosion of mixed sediments. Thin sand layers on top of Holocene mud layers and mixed sediments have often been observed in the turbidity maximum area. Williamson and Torfs (1996) were the first to show that the addition of mud to a sandy bed increases the sediment shear strength. Van Ledden et al. (2004) argue that a transition in erosion behaviour can be expected when the bed changes between cohesive and non-cohesive properties, and when the network structure is formed by another sediment fraction. Mixed sediments could therefore act as a reservoir for fine-grained material that is only resuspendable under more extreme meteorological conditions. However, on the basis of existing data, we cannot quantify the amount of fine sediments that is released as SPM due to the erosion of mixed sediments.

Freshly deposited mud as SPM source

The movement of recently deposited sediment in the wave boundary layer exposes fine-grained sediment to resuspension when shear stresses become sufficiently high. These resuspended sediments are then transported further by waves and currents. Results from a hydrodynamic numerical model indicate that, under normal conditions, the bed shear stress in the navigation channels and at location MOW1 or Blankenberge is lower than 4 Pa. The critical erosion shear stresses of in-situ samples in the navigation channels and around Zeebrugge and the disposal ground of Oostende are, below the fluffy surface layer, generally higher than 4 Pa. The deposits of fresh mud below the fluffy layer in these areas forms thus a reservoir of SPM that will only be resuspended during periods with high shear stresses e.g. caused by storms. The fluffy surface layer having thicknesses of a few centimetres and a $\tau_{e,crit}$ of <1 up to ~4 Pa, will be fully resuspended during periods with higher stresses (storms, spring tides).

The total surface of the area where freshly deposited mud is found is not precisely known. The surface of the navigation channels, where mud is dredged, equals to ±15 km². Mud with similar erosion behaviour has also been sampled near the disposal ground of dredged material near Oostende and around Zeebrugge. Based on bed samples, the surface of these deposits has been estimated as 30 km². The bulk density of these sediments amounts to 1200-1400 kg/m³. If we assume a thickness of 20 cm very soft mud in these areas, then the total mass of mud available for resuspension equals 1.8-3.6×10⁶ t. This is of the same order of magnitude as what has been estimated to be in suspension during storms. The MOW1 and the Blankenberge site are both situated in the vicinity of the navigation channel towards Zeebrugge (Pas van het Zand) and the Westerschelde (Scheur). The data suggest that an important part of the HCMS, measured at both sites, could have been resuspended from the very soft mud deposits in the navigation channels and adjacent areas.

Conclusion

Measurements have been collected at two locations in the vicinity of the port of Zeebrugge and its navigation channels. Between autumn 2005 and winter 2007, three stormy periods have been selected with similar wave conditions. The data have shown that during or after a storm, the SPM concentration increases significantly and that HCMS have been formed. SPM concentration is clearly related to high wave and wind activity. The wind direction and the advection of water masses, the previous history and availability of fine-grained sediments in fluffy layers, the very soft mud deposits around navigation channels, and the erosion of medium-consolidated mud, of Holocene age, influence the SPM signal. The data suggest that for the generation of very high SPM concentrations near the bed, significant amounts of fine-grained

sediments have to be resuspended and/or eroded. The navigation channels and other areas with soft mud have been found to be the major source of fine-grained sediments during storms. This result is important, as it suggest that the deepening of the navigation channels has made available fine-grained matter that contributes significantly to the formation of high concentration mud suspensions. This suggests that HCMS were probably less frequent in the past, when anthropogenic activities were limited.

References

Andersen, T. J., Fredsoe, J., Pejrup, M. 2007. In situ estimation of erosion and deposition thresholds by Acoustic Doppler Velocimeter (ADV). Estuarine, Coastal and Shelf Science, 75, 327-336.

Ariathurai, C. R. 1974. A finite element model for sediment transport in estuaries. University of California, Davis.

Cacchione, D.A., Wiberg, P.L., Lynch, J.F., Irish, J.D., Traykovski, P. 1999. Estimates of suspended-sediment flux and bedform activity on the inner portion of the Eel continental shelf. Marine Geology, 154, 83-97.

de Wit, P.J., Kranenburg, C. 1997. The wave-induced liquefaction of cohesive sediment beds. Estuarine, Coastal and Shelf Science, 45, 261-271.

Eisma, D. 1981. Supply and deposition of suspended matter in the North Sea. In: Holocene Marine Sedimentation in the North Sea Basin. (Nio, D.D., Shuttenhelm, R.T.E., van Weering, T.C.E., eds.). IAS Special Publication, 5, Blackwell Scientific, 415-428.

Fettweis, M., Van den Eynde, D. 2003. The mud deposits and the high turbidity in the Belgian-Dutch coastal zone, Southern bight of the North Sea. Continental Shelf Research, 23, 669-691.

Fettweis, M., Nechad, B., Van den Eynde, D. 2007a. An estimate of the suspended particulate matter (SPM) transport in the southern North Sea using SeaWiFS images, in situ measurements and numerical model results. Continental Shelf Research, 27, 1568-1583.

Fettweis, M., Du Four, I., Zeelmaekers, E., Baeteman, C., Francken, F., Houziaux, J.-S., Mathys, M., Nechad, B., Pison, V., Vandenberghe, N., Van den Eynde, D., Van Lancker, V., Wartel, S. 2007b. Mud Origin, Characterisation and Human Activities (MOCHA). Belgian Science Policy, EV/35, 59pp. Available at http://www.belspo.be/belspo/home/publ/pub_ostc/EV/rappEV35_en.pdf

Gerritsen, H., Boon, J.G., van der Kaaij, T., Vos, R.J. 2001. Integrated modelling of suspended matter in the North Sea. Estuarine, Coastal and Shelf Science, 53, 581-594.

Green, M.O., Vincent, C.E., McCave, I.N., Dickson, R.R., Rees, J.M., Pearson, N.D. 1995. Storm sediment transport: observations from the British North Sea shelf. Continental Shelf Research, 15, 889-912.

Günther, H., Rosenthal, W., 1985. The hybrid parametrical (HYPAS) wave model. In: Ocean wave modelling, Swamp group. Plenum Press, New York, 211-214.

Koutitas, C.G., 1988. Mathematical Models in Coastal Engineering. Pentech Press, London, UK, 156pp.

Lafite, R., Shimwell, S., Grochowski, N., Dupont, J.-P., Nash, L., Salomon, J.-C., Cabioch, L., Collins, M., Gao, S. 2000. Suspended particulate matter fluxes through the Strait of Dover, English Channel: observations and modelling. Oceanologica Acta, 23, 687-700.

Lauwaert, B., Bekaert, K., Berteloot, M., De Brauwer, D., Fettweis, M., Hillewaert, H., Hoffman, S., Hostens, K., Mergaert, K., Moulaert, I., Parmentier, K., Vanhoey, G. & Verstraeten, J. 2008. Synthesis report on the effects of dredged material disposal on the marine environment (lecensing period 2006-'08). BMM, ILVO, AK & AMT rapport, BL/2008/01, 109pp.

Le Bot, S., Van Lancker, V., Deleu, S., de Batist, M., Henriet, J.-P., Haegeman, W. 2005. Geological and geotechnical properties of Eocene and Quarternary deposits on the Belgian continental shelf: synthesis in the context of offshore wind farming. Netherlands Journal of Geosiences, 84, 147-160.

Le Hir, P., Monbet, Y., Orvain, F. 2007. Sediment erodability in sediment transport modelling: Can we account for biota effects? Continental Shelf Research, 27, 1116-1142.

Li, Y., Mehta, A.J. 2000. Fluid mud in the wave-dominated environment revisited. In: Coastal and Estuarine Fine Sediment Dynamics. (McAnally, W.H., Mehta, A.J., eds.), Proceedings in Marine Science, 3, 79-93.

Luyten, P. J., Jones, J. E., Proctor, R., Tabor, A., Tett, P., Wild-Allen, K. 1999. COHERENS A Coupled Hydrodynamical-Ecological Model for Regional and Shelf Seas: User Documentation. MUMM report, Brussels. 911pp. [Available at http://www.mumm.ac.be/coherens].

Maa, P.-Y., Mehta, A. J. 1987. Mud erosion by waves: a laboratory study. Continental Shelf Research, 7, 1269-1284.

Nikora, V.I., Goring, D.G., 1998. ADV measurements of turbulence: can we improve their interpretation? Journal of Hydraulic Engineering, 124, 630-634.

Pison, V., Ozer, J. 2003. Operational products and services for the Belgian coastal waters. In: Building the European capacity in operational modeling, Proc. 3rd Int. Conf. on EuroGOOS (Dahlin, H., Flemming, N.C., Nittis, K., Petersson, S.E., eds.). Elsevier Oceanography Series 69, 503-509.

Pope, N. D., Widdows, J., Brinsley, M. D. 2006. Estimation of bed shear stress using the turbulent kinetic energy approach - A comparison of annular flume and field data. Continental Shelf Research, 26, 959-970.

Shi, J.Z., Gu, W.-J., Wang, D.-Z. 2008. Wind wave-forced fine sediment erosion during slack water periods in Hangzhou Bay, China. Environmental Geology, 55, 629-638.

Silva-Jacinto, R. Le Hir, P. 2001. Response of stratified muddy beds to water waves. In: Coastal and Estuarine Fine Sediment Processes (McAnally, W.H., Mahta, A.J., eds.). Proceedings in Marine Science, 3, 95-108.

Stapleton, R.L., Huntley, D.A., 1995. Seabed stress determination using the inertia dissipation method and the turbulent kinetic energy method. Earth Surface Processes and Landforms 20, 807-815.

Thompson, C.E.L., Amos, C.L., Jones, T.E.R., Chaplin, J. 2003. The Manifestation of Fluid-transmitted Bed Shear Stress in a Smooth Annular Flume - A Comparison of Methods. Journal of Coastal Research, 19, 1094-1103.

Traykovski, P., Wiberg, P.L., Geyer, W.R. 2007. Observations and modeling of wave-supported sediment gravity flows on the Po prodelta and comparison to prior observations from the Eel shelf. Continental Shelf Research, 27, 375-399.

Van Alphen, J.S.L.J. 1990. A mud balance for Belgian-Dutch coastal waters between 1969 and 1986. Netherlands Journal of Sea Research, 25, 19-30.

Van den Eynde, D., 1992. mu-WAVE: An operational wave forecasting system for the Belgian coast, 3rd Int. Workshop on Wave Hindcasting and Forecasting, Montréal, Canada, 313-324.

van Ledden, M., van Kesteren, W.G.M., Winterwerp, J. 2004. A conceptual framework for the erosion behaviour of sand-mud mixtures. Continental Shelf Research, 24, 1-11.

van Kessel, T., Kranenburg, C. 1998. Wave-induced liquefaction and flow of subaqueous mud layers. Coastal Engineering, 34, 109-127.

Verney, R., Deloffre, J., Brun-Cottan, J. C., Lafite, R. 2007. The effect of wave-induced turbulence on intertidal mudflats: Impact of boat traffic and wind. Continental Shelf Research, 27, 594-612.

Voulgaris, G., Trowbridge, J.H., 1998. Evaluation of the Acoustic Doppler Velocimeter (ADV) for Turbulence Measurements. Journal of Atmospheric and Oceanic Technology, 15, 272-289.

Williamson, H., Torfs, H. 1996. Erosion of mud/sand mixtures. Coastal Engineering, 29, 1-25.

Winterwerp, J. 1999. On the dynamics of high-concentrated mud suspensions. TU Delft, Delft. 172pp.

Wright, L.D., Friedrichs, C.T. 2006. Gravity-driven sediment transport on continental shelves: A status report. Continental Shelf Research, 26, 2092-2107.